THE INFLUENCE OF *APOE* GENOTYPE ON NEURONAL PLASTICITY: IMPLICATIONS FOR ALZHEIMER'S DISEASE AND RECOVERY AFTER HEAD INJURY

Fiona White B.Sc. (Hons)

A thesis submitted for the degree of Doctor of Philosophy to the Faculty of Medicine, University of Glasgow

Department of Neuropathology, Institute of Neurological Sciences, Southern General Hospital, Glasgow
and Wellcome Surgical Institute and Hugh Fraser Neuroscience Laboratories, University of Glasgow, Garscube Estate, Bearsden Road Glasgow, G61 1QH

Contents

List of tables

List of figures

Abbreviations

ABC	avidin biotin complex
AD	Alzheimer's disease
ANOVA	analysis of variance
APOE	apolipoprotein E gene
apoE	apolipoprotein E protein
apoJ	apolipoprotein J
APP	amyloid precursor protein
Aβ	amyloid protein
BSA	bovine serum albumin
CNS	central nervous system
CSF	cerebrospinal fluid
DAB	diaminobenzadine
DNA	deoxyribonucleic acid
ECL	entorhinal cortex lesion
ELISA	enzyme linked immunosorbent assay
GAP-43	growth-associated protein
GFAP	glial fibrillary acid protein
GFP	green fluorescent protein
HDL	high-density lipoprotein
HSPG	heparin sulphate proteoglycan
HSV	herpes simplex virus
ICP	infected cell protein
IML	inner molecular layer
LDL	low-density lipoprotein
LRP	low-density lipoprotein receptor related protein
MAP-2	microtubule-associated protein 2
MML	middle molecular layer
MND	Motor Neurone disease
mrf-1	microglial response factor-1
MRI	magnetic resonance imaging

MS	Multiple Sclerosis
NLS	nuclear localisation signal
NMDA	N-methyl-D-aspartate
NSE	neuron specific enolase
OML	outer molecular layer
PAGE	polyacrylamide gel electrophoresis
PBS	phosphate buffered saline
PCR	polymerase chain reaction
PD	Parkinson's disease
PDGF	platelet derived growth factor
PGK	phosphoglycerate kinase
PNS	peripheral nervous system
PVDF	polyvinylidene flouride membrane
RAP	receptor-associated protein
ROD	relative optical density
S.E.M	standard error of the mean
SDS	sodium dodecyl sulphate
TBARS	thiobarbituric-reactive oxygen species
TBS	Tris buffered saline
TLE	temporal lobe epilepsy
VLDL	very low-density lipoprotein

Declaration

I declare that this thesis comprises my own original work, unless otherwise acknowledged and has not previously been submitted for a degree in any other format.

Fiona White November 2001

Acknowledgements

I would like to thank everyone at the Wellcome Surgical Institute for their help and support over the last three years. In particular I would like to thank my supervisor Dr Karen Horsburgh for her unrelenting support, scientific guidance and shoulder to cry on, on days when things weren't going right. Somehow we both managed to stay sane throughout the entire three years. I also wish to thank Dr James Nicoll, who was a co-supervisor and provided scientific support from time to time and to his technician Janice Stewart for carrying out all of the PCR analysis. I wish also to acknowledge Prof David Graham and Prof James McCulloch who offered their pearls of wisdom when required. I would like to thank all of my friends and fellow students at the Wellcome Surgical Institute for keeping me calm especially towards the end when I thought I was actually going to have a nervous breakdown whilst trying to write this thesis. These people include, Eileen McCracken, Jill Fowler, Louise Marks, Deborah Bingham, Barry McColl, Dan Cuthill and David McCaig.

I wish to thank my family, in particular my mum, dad, gran and sister who have supported and encouraged me throughout a very long seven years at university. I'm sure they thought I was going to be a student for the rest of my life. I can assure you now categorically, that I am not going to be taking any more degrees. Well, not any time soon anyway! Finally I would especially like to thank my long-suffering housemaid, Alan, (I also call him husband) for putting up with me through these very trying three years. Things have been tough, especially when I have had to work long hours. He had to learn how to use many technical pieces of equipment such as the vacuum cleaner and washing machine through necessity, otherwise the house would have fallen to bits. He and my family have supported me emotionally (and financially) and in thanks for all they have done, I dedicate this thesis to them.

Summary

Apolipoprotein E (*APOE*: gene, apoE: protein) is a lipid transport protein which has a well-characterised role in response to peripheral nerve injury. It has been demonstrated that the *APOE* ε4 allele of the gene is a major risk factor for Alzheimer's disease and is associated with a poor outcome after brain injury. The mechanisms underlying this are unclear but may involve a role for apoE in neuronal repair processes. This thesis investigated the role of apoE in repair processes after brain injury and determined whether this effect was *APOE* genotype dependent. In order to address this, models of synaptic plasticity (*in vitro* and *in vivo*) were validated. Using these models the role of apoE could be defined. The influence of *APOE* genotype was determined using two different lines (human promoter and GFAP promoter) of genetically modified mice (*APOE* knockout, human ε3 and ε4 alleles). The main studies and results are as follows:

(1) Investigation of ApoE in Relation to Degeneration/ Regeneration Using a Mouse Model of Entorhinal Cortex Lesion

An *in vivo* model of hippocampal plasticity was characterised in C57BL/6J mice (the background strain of genetically modified mice used in this thesis). A lesion of the entorhinal cortex (ECL) was induced by stereotactic injection of ibotenic acid. Specific markers (synaptophysin, GAP-43 and MAP-2) were used to define the temporal profile of degeneration and regeneration post-ECL. In the molecular layers of the dentate gyrus, synaptic decline and fibre degeneration occurred up to 28 days post-ECL, but at 90 days post-ECL, synaptogenesis and fibre sprouting were observed. Alterations in apoE paralleled degeneration and regeneration post-ECL. ApoE was upregulated within the neuropil and reactive astrocytes at day 7 post-ECL, with a further increase in the neuropil of the outer molecular layer at day 90 post-ECL. This pattern of upregulation was similar to alterations observed for apoJ. There were minimal alterations in LRP (apoE receptor) with an increase in LRP immunoreactivity on reactive astrocytes at day 7 post-ECL. Degeneration products identified by silver staining were maximal 3 days post-ECL and absent by day 90 post-ECL. This study demonstrated the utility of the entorhinal cortex lesion as a reproducible model of hippocampal plasticity. The results also supported a role for apoE in neuronal repair processes after brain injury.

(2) Analysis of *APOE* Genotype Influence on CNS Plasticity in Transgenic Mice Expressing Human *APOE* ε3 and ε4 Alleles (under a human promoter sequence) Following Entorhinal Cortex Lesion

The entorhinal cortex was lesioned in *APOE* transgenic mice, which express human *APOE* alleles (ε3, ε4) in astrocytes and neurons. This study assessed *APOE* genotype influence on the long-term response to brain injury. Specific markers (synaptophysin, GAP-43 and MAP-2) were used to define the temporal profile of degeneration and regeneration post-ECL. Initially *APOE*ε3 mice exhibited more extensive degeneration than ε4 mice. However, with longer recovery the *APOE*ε4 mice demonstrated an impaired reparative capacity. There were no significant differences in the extent of apoE, apoJ and LRP immunoreactivity between *APOE*ε3 and ε4 mice. There was also no significant difference in the deposition and clearance of degeneration products between *APOE*ε3 and ε4 mice. *APOE*ε4 mice displayed a deficit in MAP-2 immunoreactivity compared to *APOE*ε3 mice that paralleled the deficit in reparative capacity. The dendrites in the molecular layer of *APOE*ε4 mice were disorganised and disarrayed. This study indicated that the ε4 allele was associated with impaired neuronal repair. The underlying mechanism may involve apoE isoform differences in interactions with cytoskeletal proteins.

(3) Analysis of *APOE* Genotype Influence on CNS Plasticity in *APOE* Knockouts and Transgenic Mice Expressing Human *APOEε3* and ε4 Alleles (GFAP Promoter) Following Entorhinal Cortex Lesion

The entorhinal cortex was lesioned in *APOE* knockout, ε3 and ε4 transgenic mice (expressing human *APOE* in astrocytes) and the influence of *APOE* genotype on the long-term response to brain injury was assessed. In this study it was shown that mice expressing the *APOE*ε4 allele displayed impaired neuronal sprouting capabilities compared to *APOE* knockout and ε3 mice, however there was no difference in synaptic density between *APOE* knockout, ε3 and ε4 mice at any time-point. Alterations in apoE and apoJ paralleled regeneration but there was no significant difference between *APOE*ε3 and ε4 mice. Similarly, there were no significant differences in alterations in LRP, MAPs or extent of degeneration product clearance. This study indicated that neuronal repair mechanisms were impaired in *APOE*ε4

mice compared to *APOE* knockout and ε3 mice. There were no significant differences in dendritic structure unlike that shown in the previous transgenic line and this suggests that the underlying mechanisms may not be directly related to cytoskeletal interactions in this particular line of transgenic (astrocytic expression).

(4) *APOE* Genotype Influence in the CNS of Aged *APOE* Knockout, ε3 and ε4 Transgenic Mice (GFAP Promoter)

The ageing process is now thought of as a form of chronic brain injury and *APOE* genotype may influence age-related neurodegeneration. *APOE* genotype effect on ageing was analysed using specific markers (synaptophysin, GAP-43 and MAP-2) to define the temporal profile of synapse and fibre density in *APOE* knockout, ε3 and ε4, young (3 months) and aged (1 year) transgenic mice. There was no statistically significant difference in synaptic density between *APOE* knockout, ε3 and ε4 mice at any age. Fibre density was found to be significantly less in *APOE*ε4 mice compared to *APOE* knockout and ε3 transgenic mice at 3 months, but was not significantly different at 1 year of age. This was paralleled by a reduction in IML width in *APOE* ε4 mice by 1 year, compared to *APOE* knockout and ε3 transgenic mice. ApoE immunoreactivity was similar between the genotypes at 3 months of age. At 1 year, apoE neuropil immunoreactivity was increased, but to a greater extent in *APOE* ε4 mice. There were no significant differences in MAP-2 and apoJ immunoreactivity between the genotypes at any time. This study has shown that *APOE* genotype has no demonstrable influence on ageing in the brain of these transgenic mice.

(5) An *In Vitro* Organotypic Hippocampal Slice Model to Study *APOE* Genotype Influence on Neuronal Plasticity and Analysis of Herpes Simplex Virus as a Vector for *APOE* Delivery

(a) Characterisation of plasticity responses in hippocampal slices derived from C57BL/6J mice

An *in vitro* organotypic hippocampal slice culture method was characterised in C57BL/6J slices. The slices were cultured for a period of 7 or 18 days and the synaptic and sprouting response was assessed using specific markers (synaptophysin and GAP-43). At day 18 *in vitro*, synaptophysin and GAP-43 immunoreactivity increased within the molecular layers of the dentate gyrus compared with

immunoreactivity in 7 day slices. ApoE immunoreactivity was increased within the neuropil of the hippocampal molecular layers at day 7 *in vitro*, but was reduced by day 18 *in vitro*. This study validated the use of *in vitro* hippocampal mouse slices to study apoE and *APOE* genotype in neuronal plasticity.

(b) Influence of *APOE* genotype on neuronal plasticity *in vitro*

Hippocampal slices were cultured from male *APOE* knockout, ε3 and ε4 transgenic mice and maintained in culture for a period of 7 or 18 days. The synaptic and sprouting response was assessed using specific markers (synaptophysin and GAP-43). Synaptophysin and GAP-43 immunoreactivity was similar in all slices cultured for 7 days. At day 18 *in vitro*, sprouting and reactive synaptogenesis had occurred in all slices, marked by an increase in GAP-43 and synaptophysin immunoreactivity. However, the sprouting response was significantly poorer in *APOE*ε4 slices compared to *APOE* knockout and ε3 slices. No apoE immunoreactivity was present in *APOE* knockout slices. ApoE immunoreactivity was elevated in *APOE*ε3 and ε4 slices within the neuropil and reactive astrocytes at day 7. However, there was significantly greater apoE immunoreactivity in *APOE*ε3 slices. ApoE immunoreactivity was reduced at day 18 *in vitro* but there was no difference between genotypes. This study supported the previous *in vivo* study and indicated the ε4 allele is associated with impaired neuronal repair mechanisms.

(c) Herpes simplex virus as a vector for gene delivery

The previous studies in this thesis indicate that *APOE* genotype influences repair processes, the ε4 allele being associated with a poor capacity for repair. The next aim was to determine whether, the poor response associated with the ε4 allele could be ameliorated by increasing the levels of apoE or changing the genotype present. This study examined the uptake and expression of a modified Herpes Simplex viral vector in the organotypic hippocampal slice preparation. The Herpes Simplex virus mutant employed in this study is non-virulent due to lack of the ICP34.5 protein. The virus was applied directly to the slice as a single dose on day 1 *in vitro* at a concentration of 10^5 or 10^6 virus particles with a Green Fluorescent Protein (GFP) reporter gene. The virus, was found to be expressed within the molecular layer of the dentate gyrus and was cellular in nature. Expression was sustained until day 18 *in vitro*. Data from

this study suggest that this Herpes Simplex virus may be useful as a vector for *APOE* gene delivery in this *in vitro* model. This is an area for future development.

(6) *APOE* Genotype Influence on Apolipoprotein E Interaction with Microtubules

Although previous studies indicated that there were apoE isoform differences in neuronal repair i.e. differences in MAP-2 immunoreactivity, the mechanisms underlying this were unclear. In this study, the influence of apoE E3 and E4 on microtubules was assessed. Tubulin immunohistochemistry was performed on sections from 0 day control and 90 day survival mice, in the two different lines of *APOE* transgenic mice (human and GFAP promoter). There was a deficit in tubulin immunoreactivity in the molecular layers of *APOE*ε4 mice in both lines of mice, indicative of an effect on microtubule proteins. The next aim was to determine the effect of binding of apoE E3 and E4 to microtubules and their effect on microtubule structure. ApoE E3 and E4 protein was isolated from the HDL fraction of human plasma, donated by ε3 and ε4 homozygotes and used to assess isoform binding to microtubules. At apoE concentrations of 5μg/ml and 20μg/ml it was found that the apoE E4 isoform was more greatly associated with microtubules compared with apoE E3 protein. Additionally, microtubules incubated with apoE E4 protein were irregularly shaped compared to those incubated with apoE E3 protein. These data suggests that although apoE E4 was more greatly associated with microtubules, it did have a detrimental effect on microtubule structure.

These studies illustrate the utility of animal models to study apoE and *APOE* genotype influence in long-term outcome after brain injury. Together, the results of these studies indicate that the *APOE* ε4 allele is associated with impaired neuronal repair processes and that differences in cytoskeletal interactions may underlie this.

Chapter I

Introduction

1.1 Brain Repair

The capacity of the human brain to repair itself is truly remarkable. The degree of plasticity within the human brain following brain injury has been shown to be extensive where neuronal cells are capable of sprouting in an attempt at repair. Exploitation of this endogenous capability of the brain to repair itself could have significant implications for recovery from neurodegenerative disease and brain injury. In recent years much speculation has been made on the usefulness of growth factors and other such compounds in the treatment of neurodegenerative disorders such as Alzheimer's disease (AD). However the ability of each individual brain to repair may be genetically linked and may depend on several factors. One such factor, apolipoprotein E, is discussed in this thesis and its function in brain plasticity elucidated.

1.2 Apolipoproteins

Apolipoproteins were first identified in the 1970's as constituents of lipid complexes in plasma including apoAI, apoAII, apoAIV, apoCI, apoCII, apoCIII, apoB, apoD, apoE and apoJ (Boyles *et al*, 1985). These proteins are produced by the liver and secreted into the bloodstream. In more recent years novel members of this family have been identified but are present at very low concentrations within plasma (Beffert *et al*, 1998). All members of this protein family have been found to be associated with most classes of lipid, including very low density lipoprotein (VLDL), low density lipoprotein (LDL), high density lipoprotein (HDL) and cholesterol. This led to the discovery that the primary function of these proteins within plasma was to direct lipid metabolism (Mahley *et al*, 1988). In the central nervous system (CNS), the presence of apolipoproteins has now been identified within many cell types in the brain and also within cerebrospinal fluid (CSF).

1.2.1 Apolipoprotein E

A subset of apolipoproteins are expressed in the CNS and apolipoprotein E (apoE) is the most abundantly expressed apolipoprotein. ApoE was first identified in 1973 as a plasma constituent and it was here that its function in lipid metabolism and cholesterol homeostasis was first determined (Mahley *et al*, 1988). ApoE also performs lipid metabolism duties within the CNS and in recent years analysis of the function of apoE (apoE denotes protein, *APOE* denotes gene) within the nervous system, has revealed that this protein may be involved in more complex functions within the CNS. ApoE is present in human plasma and CSF as an integral component of lipoproteins (VLDL and HDL)(Danik and Poirier *et al*, 1998). Lipoprotein particles consist of a neutral lipid core mainly composed of triglycerides and cholesterol surrounded by polar molecules that stabilise the complex. The polar outer coat is composed of phospholipids and apolipoproteins. The apolipoproteins protrude from the surface (Figure 1.1) and direct transport and binding. CNS apoE is structurally different to peripheral apoE in that it is differentially sialylated. ApoE is capable of interacting with a host of other brain proteins including amyloid protein and several microtubule associated proteins (Strittmatter *et al*, 1994) and it also interacts with a number of receptors, mainly of the endocytic class (Beffert *et al*, 1998). In human brain, it is widely accepted that apoE is synthesised within most subtypes of glial cell including astrocytes, microglia and oligodendrocytes (Boyles *et al*, 1985; Mahley *et al*, 1987; Stone *et al*, 1995). Endogenous synthesis of apoE within neurons has been shown using *in situ* hybridisation (Xu *et al*, 1999). In the peripheral nervous system apoE is localised mainly to Schwann cells.

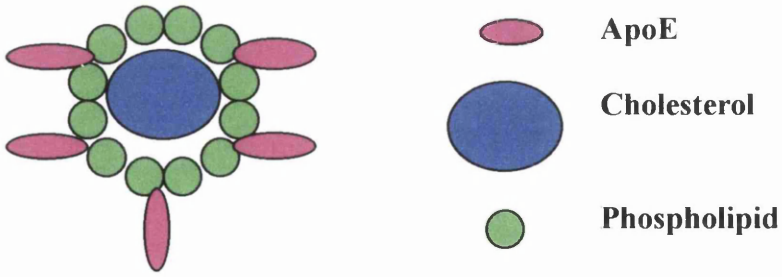

Figure 1.1 Diagram illustrating the basic components of a lipoprotein particle

1.2.2 ApoE structure and genetic polymorphisms

Human apoE exists as a single glycosylated 34 kDa polypeptide containing 299 amino acids and is encoded by a four exon gene on the long arm of chromosome 19 (Poirier *et al*, 1995). Biochemical studies have revealed apoE contains two folded structural domains, an amino terminal and a carboxyl terminal. The protein contains five α helices where four of these are arranged into a four helix bundle (Weisgraber and Dong, 1996) (Figure 1.2). The amino terminal contains the regions that mediate receptor binding and the carboxyl terminal is involved in ligand binding.

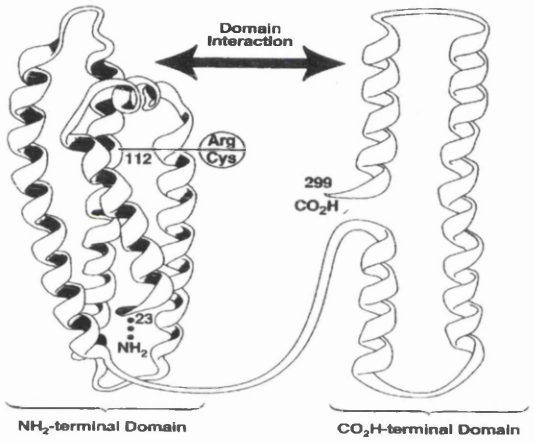

Figure 1.2 Diagram illustrating the structure of apoE. ApoE is composed of 5 helices, four of which are arranged into a bundle (Weisgraber *et al*, 1997)

Three major alleles of *APOE* exist within the human population at varying frequencies, ε2(8%) ε3(77%) and ε4(15%), as a result of multiple alleles at a single genetic locus and differ by a single amino acid substitution at positions 112 and 158 within the protein. The E2 isoform of the protein contains two cysteine residues at positions 112 and 158 of the amino acid sequence. The E3 isoform contains cysteine at position 112 and arginine at position 158, whereas the E4 isoform contains arginine residues at both positions (Weisgraber *et al*, 1981). The E2 and E3 isoforms of the protein exist as dimers under normal physiological conditions, whereas E4 exists in a monomeric state. This genetic polymorphism gives rise to three common homozygous phenotypes (ε2/2, ε3/3 and ε4/4) and three heterozygous phenotypes (ε2/3, ε3/4 and ε2/4), (Roses *et al*, 1997) which arise at varying frequencies within the general population. (Table 1)

Genotype	% within the General Population
ε3/ε3	60
ε3/ε4	21
ε3/ε2	11
ε2/ε4	5
ε2/ε2	<0.5
ε4/ε4	2

Table 1. Table illustrating the % of the general population expressing each of the six *APOE* genotypes (Western hemisphere).

Molecular analysis of the gene highlighted that the ε2 and ε3 genotypes arose from the ancestral ε4 allele and that the ε3 allele increased in frequency (Fullerton *et al*, 2000). This divergence of genotypes occurred within the last 200,000 years. Statistically significant differences in allele frequency across populations of the world have been identified (Davignon *et al*, 1988). A vast array of population based studies have been carried out and the prevalence of each *APOE* genotype established for each population. In general, the ε3 allele is the most common studied to date in all populations ranging in frequency from 0.536 to 0.911 (Kamboh *et al*, 1995). The ε2 allele is the least common. The ε4 allele frequency ranges from 0.052 in Sardinians to 0.407 in Pygmies (Zekraoui *et al*, 1997) within the world's populations and is negatively correlated with ε3 allele frequencies in African and European populations (Corbo and Scacchi, 1999). The *APOE*ε3 allele is now increasing in frequency within Europe with a relative decline in ε4 allele frequency. Allelic heterogeneity is absent in all other animal species studied to date with the exception of primates.

1.2.3 Apolipoprotein J

Another member of the apolipoprotein family, apoJ, is present within the CNS. This apolipoprotein is thought to perform similar plasticity promoting effects in the CNS to apoE and its expression after injury is also considered in this thesis. Apolipoprotein J (apoJ) is a 499 amino acid, 70kDa protein associated with high density lipoporteins (HDL) (Pasinetti *et al* 1994; Shanmugaratnam *et al*, 1997; Calero *et al*, 1999). Structurally apoJ is comprised of two disulfide-linked subunits, apoJα and β, and is also known by a range of other names including clusterin and sulphated glycoprotein-2 (De Silva *et al*, 1990; Stuart *et al*, 1992). The gene for apoJ is located on chromosome 8 in the human genome and the sequence has been highly conserved throughout evolution (Jordan-Starck *et al*, 1992). ApoJ has a common two allele polymorphism designated APOJ*1 and APOJ*2 with frequencies of 0.76 and 0.24 respectively, however these polymorphisms are only present in Black African and Black American populations and is monomorphic in all other populations (Kamboh *et al*, 1991). The gene for this protein was first identified in reproductive organs as a gene involved with apoptosis (Michel *et al*, 1992). More recently the role of apoJ within the CNS has been investigated. ApoJ synthesis is similar to apoE in the CNS, in that it is expressed in most classes of glial cell and neuronal cells (Danik *et al*, 1993; Pasinetti *et al*, 1994). Under normal conditions apoJ is widely distributed throughout the human brain and plays a role in lipid transport and neurotransmitter secretion. ApoJ also protects membrane integrity by closely associating with the membrane surface and is believed to perform extracellularly what heat-shock protein performs intracellularly in protecting membrane proteins from protease attack while folding occurs (Jordan-Starck *et al* 1992). ApoJ has been found to bind amyloid avidly *in vivo* and *in vitro* (Strittmatter *et al*, 1993; Zlokovic *et al*, 1994) and is believed to aid in cross blood-brain barrier transport of soluble amyloid.

1.3 Apolipoprotein Receptors in the CNS

1.3.1 Receptor classification

ApoE has a wide and diverse set of functions within the CNS, however, equally important are the receptors which mediate its effects including the entry of lipid bound apolipoproteins into cells requiring the material they are chaperoning. There is a whole family of receptors for apolipoproteins in the peripheral system yet only a subset are expressed within the brain. In addition to the low density receptor related protein (LRP), the main receptor for apoE in the brain, several other receptors including the low density lipoprotein receptor (LDL), the very low density lipoprotein receptor (VLDL), gp330/megalin receptor (main apoJ receptor) and the apolipoprotein E receptor 2 are also expressed (Beffert *et al*, 1998). These receptors all share structural homology and their functional behaviour is similar in that they are all receptors of an endocytic class (Brown *et al*, 1986; Stockinger *et al*, 1998). Receptors of the LDL receptor family can be divided according to their extracellular domains. The LDL and VLDL are low molecular weight receptors. In contrast, the high molecular weight receptors such as LRP and gp330 are composed of a cluster of ligand binding repeats, followed by homology domains. The extracellular parts of these receptors appear as multiple copies of the LDL receptor. The high molecular weight receptors are thought to be older in evolutionary terms (Willnow *et al*, 1999).

1.3.2 Low density lipoprotein receptor-related protein (LRP)

In the brain LRP is expressed in neurons (dendrosomatic localisation) and reactive astrocytes, with the most dense staining noted on neurons of the hippocampus (Rebeck *et al*, 1993, Bu *et al*, 1994). The VLDL receptor is localised to microglia and neurons as identified in AD brain and control autopsy tissue (Christie *et al*, 1997) and the LDLr has a diffuse neuropil stain (mainly present on astrocyte bodies and processes)(Lopes *et al*, 1994; Page *et al*, 1998; Beffert *et al*, 1998) with a particularly dense labelling of white matter (Pitas *et al*, 1987; Rebeck *et al*, 1993). There is a vast array of data on each receptor type and its functions, however in recent years the association between apoE and the LRP receptor suggest the receptor itself may be implicated in Alzheimer's disease (AD). The LRP receptor is the largest endocytic

endocytic receptor identified to date at approximately 600 kDa, with a 515kDa extracellular domain and an 85kDa membrane anchor (Willnow *et al*, 1999).

1.3.2.1 Ligand binding of the lipoprotein receptor related protein (LRP)

On binding with the apoE-lipid complex, the LRP receptor is internalised in coated pits and transported to lysosomes, where the ligand is dissociated from the receptor (Herz *et al*, 1990; Rebeck *et al*, 1993; Stockinger *et al*, 1998; Cooper and Howell, 1999). In this way the receptor and indeed apoE may be recycled to the cell surface for reutilisation, whilst successfully delivering lipid and cholesterol to the cell. The destiny of apoE once internalised, is the subject of some debate and will be discussed later in connection with endocytosis. This receptor is particularly remarkable because of its ability to bind multiple ligands including amyloid, amyloid precursor protein (APP) and several viruses (25 ligands in total to date) (Strickland *et al*, 1995; Kuonnas *et al*, 1995). Therefore, it has been found to be involved in a plethora of processes, which include direction of lipid metabolism within the CNS, developmental processes and recycling of lipid and cholesterol for the construction of cellular elements in neurite outgrowth.

1.3.2.2 Heparin sulphate proteoglycan

The LRP receptor is generally closely associated with a protein called heparin sulphate proteoglycan (HSPG). Combined the LRP and HSPG mediate the effects of apoE in the CNS due to their astrocytic and neuronal localisation. The HSPG functions in the intial capture of lipid particles from the environment, however it is also heavily involved in the uptake process (Mahley and Ji, 1999). The HSPG is capable of functioning as a receptor by itself and can bind a similar range of ligands to the LRP itself (Ji *et al*, 1998). Also associated with this receptor is the aptly named, Receptor Associated Protein (RAP) which interacts closely with the binding domain of the receptor to regulate binding ligands (Willnow *et al*, 1996; Umans *et al*, 1999). In several cases, this protein has been shown to competitively inhibit the binding of many ligands (Williams *et al*, 1997). RAP controls the folding of the LRP protein soon after it is manufactured by the endoplasmic reticulum. It associates with the newly synthesized protein to prevent premature ligand association (Willnow, 1998).

1.3.3 Receptors for apoJ in the brain

ApoJ uptake is mediated primarily by a 600 kDa protein (megalin). This was first identified in Heymann nephritis which is a rat model of glomerulonephritis (Zheng *et al*, 1994; Kuonnas *et al*, 1996). This receptor was found to be concentrated within coated pits and therefore it also functions via endocytosis. The gp330 receptor has multiple ligands including lipoproteins, blood clotting factors and plasminogen, among others, and like the LRP receptor, gp330 associates with RAP protein intracellularly (Zheng *et al*, 1994; Panckhurst *et al*, 1998; Niemeier *et al*, 1999). Very few studies have focused on this receptor past basic localisation studies (Kuonnas *et al*, 1994) and little is known at present of its endogenous function. However, its function in early development is evidently crucial as gp330 knockout mice die perinatally and exhibit defective forebrain development (Willnow *et al*, 1996). Gp330 is expressed in abundance in renal tissues, retina, thyroid, inner ear and also within the ependymal cells and choroid plexus of the brain (Beffert *et al*, 1998). No study has clearly oulined which cell types in the brain actually express the gp330 receptor and a study by Page *et al* (1998) failed to detect mRNA for this receptor anywhere within the rodent brain.

1.4 Alzheimer's Disease

1.4.1 History and statistics

Alzheimer's disease (AD) was first discovered in 1906 by Bavarian neurologist Alois Alzheimer who described the symptoms in a female patient known as Auguste D. He observed that the patient exhibited many of the standard features of senile dementia but that there were some unusual developments. He witnessed that the disease usually manifested itself in the seventh or eighth decade of life, however it also very often appeared earlier in life. Patients suffered from cognitive decline, altered behaviour and memory impairments in the early stages but later they also displayed motor deficits that were similar to those observed in Parkinson's disease. No further progress was made in the field until the 1960s when Michael Kidd and Robert Terry described the structural neuronal changes associated with senile plaque formation and neurofibrillary tangles. In the 1970s it was discovered that a certain population of neurons within the brain were selectively vulnerable to degeneration in this disease and were the cholinergic neurons of forebrain nuclei. Now it is realised that cholinergic neurons are not solely affected and that there is widespread cell death throughout the brain regardless of neurotransmitter expression in AD. Only in the last 20 years, Glenners group was able to clone and sequence the protein present within senile plaques and this protein is now known as β-amyloid. Extensive work has since been carried out on this protein and its various isoforms and its function in the normal and diseased state established. Production and deposition of β-amyloid is believed to be central to the pathogenesis of AD. β-amyloid protein (and associated processing proteins i.e. presenilins) is now a target for drug development in therapies for AD. Senile plaques in the brains of AD sufferers are composed of β-amyloid, a protein cleaved from the amyloid precursor protein.

AD is the most common neurodegenerative disorder, affecting approximately 10% of individuals under the age of 65 and a total of up to 40% of individuals under the age of 80 years (Gelman *et al*,1989). As a whole it affects 2.5% of the worlds population. Approximately 20% of patients in psychiatric institutions are suffering from AD and

this combined with the care of elderly individuals diagnosed with the disease, is an important economic concern for governments around the world.

AD is classified into two clinical categories, familial and sporadic late-onset disease. Familial AD is inherited through the parent lineage (Selkoe, 2001) and sporadic arises randomly within the human population, although it has now become clear that this form may too have a genetic component (Saunders *et al*, 1993). Early AD dementia manifests itself clinically as small, momentary lapses in memory. This progresses to large voids in memory where sentences become difficult to complete because the original reason for the sentence being constructed is lost. In the final stages of the disease the individual is unable to perform simple everyday tasks and autonomic regulation fails (Soininen and Reikkinen, 1996). Cognitive abilties in AD patients are now tracked clinically worldwide using mental score testing of various forms. Definitive diagnosis of this disease can only be made microscopically on postmortem analysis.

1.4.2 Neuropathology of Alzheimer's disease

The neuropathological features of AD are well characterised and consist of essentially three major components: brain atrophy (neurodegeneration), amyloid plaque formation and neurofibrillary tangles.

1.4.2.1 Brain atrophy

Alzheimer's disease pathology displays a characteristic extensive synaptic decline and neuronal cell death in defined regions of the cortex (entorhinal cortex) and limbic system (hippocampus) which can strikingly lead to a loss of up to 50% of the brains total mass (Hyman *et al*, 1986; Braak and Braak, 1991; Masliah *et al*, 1993). Cellular loss ultimately leads to atrophy within defined regions of the brain, notably the cortex and limbic structures. Associated with this is an increase in ventricular volume with a parallel increase in cerebrospinal fluid (CSF) volume (Graham and Hume, 1990). Sulci become more exaggerated due to loss of tissue mass of the cortical gyri. Recent studies have shown that AD neurodegeneration changes originate in layer II of the entorhinal cortex spreading to the hippocampus via the perforant pathway (Braak and Braak, 1991; Masliah *et al*, 1994; Gomez-Isla *et al*, 1996). This then leads to

complete disconnection of the perforant pathway and continued degeneration of intra and extra-hippocampal pathways eventually leads to the isolation of the hippocampus from the rest of the brain. This explains the associated loss of cognitive functions (Hyman *et al*, 1986). In the present day, non-invasive imaging technology such as MRI (magnetic resonance imaging) and CT scanning (computerised tomography) are used to measure brain atrophy and ventricular enlargement, and magnetic resonance imaging now has the resolution to detect single senile plaques in any region of the brain. Neurodegeneration combined with the accumulation of intra and extracellular amyloid plaque deposits, formation of neurofibrillary tangles (Terry and Wisniewski, 1970; Arriagada *et al*, 1992; Yamaguchi *et al*, 1988) and a decrease in specific transmitters (Perry *et al*, 1977) creates a profound effect on the brain manifesting itself classically, as chronic memory loss and progressive cognitive decline (Hyman *et al*, 1986).

1.4.2.2 Amyloid plaques

Amyloid plaques are located extracellulary within most regions of the AD brain but are greater in density within the limbic system and association cortex (Weisgraber *et al*, 1994; Selkoe, 2001). Little was known about senile plaques beyond the original identification histologically, almost one hundred years ago, until the 1980's. Glenner (1984) dissected out plaques from vascular tissue, cloned and sequenced the protein. This then led to the cloning of amyloid precursor protein (APP). Senile plaques are composed of amyloid protein. Amyloid β protein (Aβ) exists in varying amino acid lengths (Aβ 1-40/ Aβ 1-42/43) (Borchelt *et al*, 1996). Amyloid β protein is a cleavage product of the larger amyloid precursor protein (APP). This protein is an axonally transported, transmembrane cell surface glycoprotein that performs a putative role in maintaining axon terminals and is synthesised by most cell types (Mattson *et al*, 1993; Mucke *et al*, 1994). Under normal physiological conditions APP is cleaved to produce soluble forms of β amyloid protein intracellularly which are then released extracellularly. Insoluble isoforms of the amyloid protein aggregate into plaques that cannot be degraded or released extracellularly. The processing of APP into Aβ protein occurs in the brain under normal physiological conditions. At present it is unclear how senile plaques are formed in AD although common hypotheses at

present are that plaques are due to overproduction of Aβ or reduced metabolism and clearance from neurons.

1.4.2.3 Neurofibrillary tangles

Neuronal structure is supported by the cytoskeleton comprised of a network of microtubules, neurofilaments and intermediate filaments. Under normal physiological conditions these elements maintain cellular structure and aid in vital cellular mechanisms such as axonal transport. Neurofibrillary tangles are a common pathology found in AD and are present within the neuronal cytoplasm within brain regions typically affected by AD i.e. limbic system and entorhinal cortex. How tangles are formed is the subject of much debate, however the present prevailing hypothesis is that they are formed by the hyperphosphorylation of the microtubule associated protein tau by protein kinases. Tau is a protein involved in microtubule assembly and stabilization. Hyperphosphorylation of this protein results in tau protein adopting a paired helical filament (PHF) formation intracellularly (Terry and Wisnieski, 1970; Masliah *et al*, 1989; Arriagada *et al*, 1992).

1.4.3 Genes and Alzheimer's Disease

It became apparent that AD could be passed on genetically through the parent lineage and several groups became heavily involved in scanning the human genome in search of genes involved in the development of AD. A host of gene sites were found to be associated with AD including genes on chromosome 14, 1 and 21 (Selkoe, 2001). With the advancement of sequencing and cloning technology, these sites were found to encode presenilin 1, presenilin 2 and amyloid precursor protein. Mutations on chromosome 21 encoding APP can result in abnormal cleavage sites in the APP structure (Clarke and Goate, 1993). This ultimately leads to the formation of a form of amyloid (Aβ1-42/43) which forms aggregates more readily than the form produced in normal brain. Amyloid protein 1-42/43 is toxic to neurons and is likely to aid in the generation of free radicals and aggregation finally leads to upsets in ionic homeostasis (Shoji *et al*, 1992; Games *et al*, 1995). Many APP mutations can lower the age of onset to approximately 30 years of age (Roses *et al*, 1997). Subsequently, mutations in genes encoding presenilin 1 and 2 were identified. These mutations, similar to the mutations in APP are causative for AD. There is now evidence to indicate that mutations in presenilins are associated with increased production of Aβ1-42/43. Although it had been identified that mutations in genes encoding APP, presenilin 1and 2 were causative for familial AD, this still did not account for a considerable number of familial AD cases and indicated that other genes may be involved. This led to the linkage to chromosome 19, and a gene encoding *APOE*.

1.4.4 *APOE* Genotype and Alzheimer's Disease

1.4.4.1 APOE genotype and risk of AD

A study of autopsy tissue from patients suffering from sporadic late-onset AD highlighted an over-representation of the *APOE*ε4 allele in these subjects (Saunders *et al*, 1993), where subjects possessing an ε4 allele were not only more likely to develop AD but had an earlier age of onset. An increasing body of evidence has highlighted the *APOE*ε4 allele as a major risk factor for sporadic and familial late-onset AD, associated with a marked over-representation of the *APOE*ε4 allele in the AD population (0.52) compared with a control population (0.14) (Roses *et al*, 1995). Approximately 64% of sporadic and 80% of familial late-onset AD possess the ε4 genotype compared with 30% of controls (Corder *et al*, 1993; Roses *et al*, 1996). This allele not only increases the susceptibility but also lowers the age of onset by 6-8 years per inherited allele, in an allele dose dependent manner. Multiple population-based studies have confirmed these findings.

1.4.4.2 APOE genotype and amyloid

Amyloid plaques and neurofibrillary tangles are the classic neuropathological hallmarks of AD. The interaction of apoE with amyloid and microtubule associated proteins may be central to the development of these phenomenon and may occur in an isoform specific manner. In normal individuals, the binding of apoE to amyloid is thought to aid its proteolytic degradation and improve its solubility, however in AD a breakdown in this process is thought to occur (Russo *et al*, 1998). Aβ1-42/43 levels are increased in the brain in AD in an isoform specific manner such that levels are greatest in individuals within an *APOE*ε4 genotype (Masliah *et al*, 1998). Increased plaque density has been shown to occur in the cortex and hippocampus of subjects with AD carrying one or two copies of the ε4 allele compared to ε3 (Schmechel *et al*, 1993; Rebeck *et al*, 1993; Hyman *et al*, 1995; Beffert *et al*, 1996). Amyloid plaques are strongly apoE immunoreactive (Kida *et al*, 1995; Sheng *et al*, 1996). *In vitro* data has shown that apoE E4 (delipidated) binds amyloid protein more readily, whereas apoE E3/E2 interacts less avidly and forms a less stable complex (Strittmatter *et al*, 1993). Other groups dispute this finding (Aleshkov *et al*, 1997). In the presence of apoE E4 protein, amyloid formed complex networks that had the classical appearance

of amyloid plaques. In the presence of apoE E3, the networks are less complex (Ma *et al*, 1994; Sanan *et al*, 1996). It has been suggested that these dense networks formed with apoE E4 are not easily broken down and removed in the clearance process and thus could explain the greater plaque load in *APOE*ε4 carriers. Under conditions of lipidation however the biochemical properties of apoE alter to the extent that apoE E4 binds less avidly to amyloid compared to apoE E3 (LaDu *et al*, 1994; Hardy *et al*, 1998). ApoE can be attached along the length of amyloid fibrils or incorporated into the structure (Ma *et al*, 1994). It has also been shown that binding of amyloid to apoE can alter the interactions of apoE with its main receptors (Guillaume *et al*, 1996). ApoE is complexed to HDL under normal physiological conditions and HDL is also capable of forming an association with, and inhibits, the formation of amyloid fibrils (Oleson and Dago, 2000).

1.4.4.3 APOE genotype and neurofibrillary tangles

In AD, apoE immunoreactive neurons also contain neurofibrillary tangles. These tangles most often occur within the neuronal cytoplasm and are composed of hyperphosphorylated tau (Weisgraber *et al*, 1994). *In vitro* studies have shown that apoE E3 binds avidly to the microtubule associated protein tau whereas apoE E4 does not (Strittmatter *et al*, 1994). It is suggested that the binding of apoE to tau protects this protein from hyperphosphorylation and therefore defends its structure and prevents the formation of neurofibrillary tangles and dystrophic neurites (Weisgraber *et al*, 1994). AD patients with the ε4 genotype have been shown to have a greater number of neurofibrillary tangles compared to ε3 patients (Schmechel *et al*, 1993). Other groups dispute an *APOE* genotype influence on tangle density (Olichney *et al*, 1996; Gomez-Isla *et al*, 1996).

1.4.4.4 APOE genotype and neurodegeneration in AD

Several MRI studies have highlighted a significantly greater reduction in the volume of specific brain regions including the hippocampus and entorhinal cortex of heterozygous ε4 AD patients compared with controls (30% loss compared with 25% in controls)(Lehtovirta *et al*, 1995). Atrophy of these regions is more significant in ε4

homozygous AD patients (40%). In a similar study of non-demented ε4 individuals hippocampal atrophy was also significantly greater when compared with control groups (Crook *et al*, 1986; Bigler *et al*, 2000). A few studies have focused on white matter changes in relation to *APOE* genotype and reported more severe deep white matter lesions in ε4 carriers (Bronge *et al*, 1998), whilst other groups dispute this (Schmidt *et al*, 1996; Czech *et al*, 1994). A multitude of studies have shown that ε4 AD patients perform poorly in cognitive tests compared to controls. More interestingly, middle-aged, non-demented *APOE*ε4 individuals also display a deficit in cognitive capabiltites compared to non ε4 control subjects (Flory *et al*, 2000). Positron emission tomography (PET) images show a state of hypometabolism in the brains of clinically diagnosed AD patients (Mielke *et al*, 1998). Progeny of AD patients also display altered glucose metabolism (Small *et al*, 1996). Non-demented ε3/ε4 heterozygotes of approximately 50 years of age display glucose hypometabolism when compared to ε3/ε3 siblings (Reiman *et al*, 1996). The PET images from ε3/ε4 and ε4/ε4 non-aged individuals resembled that observed in AD sufferers (Roses, 1997). The authors suggested that this measure could act as a predictor of AD since it was approximately 20 years before onset that these metabolic abnormalities manifested.

1.4.4.5 APOE genotype and brain levels of apoE

Cholinergic dysfunction in AD patients is shown to be directly related to *APOE*ε4 genotype where reduction in choline acetyl transferase (chAT) activity was proportional to the ε4 allele copy number (Poirier *et al*, 1994; Soininen *et al*, 1995). Associated with this is a parallel decrease (40-50%) in choline levels (Nitsch *et al*, 1992). These alterations in neurotransmitter may be related to apoE levels in the brain. The level of apoE in the brain has been the subject of much debate. The levels of apoE in the CSF of AD patients, is significantly lower (3.4mg/L) compared to control subjects (4.5mg/L) (Hesse *et al*, 2000). Total apoE content of brain homogenate has also been shown to be lower in the post-mortem tissue of AD patients (100ng/mg protein) compared with control tissue (150ng/mg protein) (Bertrand *et al*, 1995). Some studies dispute this and suggest apoE levels are actually elevated or unaffected in the AD brain and that levels only appear to be reduced

because of a dilution effect, due to an equivalent increase in CSF volume (Terrisse *et al*, 1998). Reduced levels of apoE results in deficient phospholipid delivery to cells (Wurtman *et al*, 1992). This data has significant implications for therapy development where the *APOE*ε4 genotype of patients undergoing drug therapy has to be taken into account. This led to the observation that *APOE* ε4 AD sufferers responded poorly when treated with cholinomimetic drugs such as tacrine (Poirier *et al*, 1995; Farlow *et al*, 1998; Poirier and Sevigny, 1998).

1.4.4.6 LRP receptor and Alzheimer's disease

Initial interest in this receptor in AD came about with the initial observation, that apoE and LRP are co-localized in senile plaques (Rebeck *et al*, 1993; Poirier *et al*, 1995; Hyman *et al*, 2000) and acts as a receptor for APP (Trommsdorff *et al*, 1998; Van Uden *et al*, 2000). LRP binds amyloid protein efficiently and internalizes it for degradation intracellularly and inhibition of this pathway with the addition of the 39kDa RAP manifests as an aggregation of β amyloid protein extracellularly (van Uden *et al*, 2000; Hyman *et al*, 2000; Rebeck *et al*, 2001). Furthermore, recent reports have shown a genetic linkage between LRP and AD (Kang *et al*, 1997; Lendon *et al*, 1997). Several mutations of the LRP receptor have been studied to determine if deficient expression or function of the LRP receptor is central to AD pathology. Most recently, studies have demonstrated a linkage of late-onset AD to the LRP-1 gene on chromosome 12 and to date approximately 48 polymorphisms of this gene have been identified (Zuliani and Hobbs, 1994). Where functional defects in the LDL receptor would manifest themselves as familial lipid traits such as hypercholesterolaemia, the LRP gene is so large that point mutations may not manifest themselves clinically (van Leuven *et al*, 1998). Several groups have examined the 5' region of the LRP gene where a tetranucleotide repeat polymorphism occurs. Recently, two studies identified a polymorphism of a silent mutation in exon 3 of the LRP receptor (C766T) which was found to be weakly associated with late-onset AD (Hollenbach *et al*, 1998; Beffert *et al*, 1999). As of yet, no clear association has been established between any of the polymorphisms and AD (Chung *et al*, 1996; Clatworthy *et al*, 1997). However, a site nearby the locus of the LRP gene on chromosome 12 is currently under scrutiny, a site which is believed to code for α2-

macroglobulin. α2- macroglobulin is a ligand for the LRP receptor, is a proteinase inhibitor and in a recent study was genetically linked to AD (Moestrup *et al*, 1994). The study of the mechanics of this receptor and its role in disease and injury is made especially difficult as LRP knockout animals cannot be engineered. The LRP gene is crucial for foetal development and knockout animals die shortly after birth (Herz *et al*, 1992). Recently a colony of mice have been engineered with exogenous Lox P sites inserted into their genome that allows conditional inactivation after birth. (Mahley and Ji, 1999). The engineering of LDL and VLDL receptor knockout mice has been much more successful and has outlined other signalling functions which they may be involved in (Ishibashi *et al*, 1994; Trommsdorf *et a*l, 1999; Umans *et al*, 1999). Mice lacking the RAP protein have also revealed that absence of this protein has significant effects on LRP localisation within the brain (Umans *et al*, 1999).

1.4.4.7 Apolipoprotein J and Alzheimer's disease

Many studies have suggested a role for apoJ in AD pathology. ApoJ is expressed at high levels in many pathological conditions and acts as an inducer of apoptosis. For that reason it is normally expressed in conditions involving transformation of cells such as gliomas and Scrapie (Beffert *et al*, 1998). However, it is also associated with AD and functions in a neuroprotectant capacity (Giannakopoulos *et al*, 1998). Probing of post-mortem AD hippocampal tissue revealed increased apoJ mRNA expression (May *et al*, 1990). ApoJ immunoreactivity has been observed in senile plaques in the cortex and hippocampus of Alzheimer brain tissue and is also upregulated in neurons and reactive astrocytes (Kida *et al*, 1995; Harr *et al*, 1996; Lidstrom *et al*, 1997). In human AD postmortem tissue, ε4 subjects show low brain levels of apoE where apoE levels decrease with increasing number of *APOE*ε4 alleles. In contrast, hippocampal apoJ protein levels increase with increasing *APOE*ε4 allele number (60% compared to non-demented control subjects) suggesting a compensatory role of apoJ in tissue with low apoE levels (Bertrand *et al*, 1998).

1.5 Human Brain Injury

1.5.1 Etiology and statistics

Head injury is the most frequent cause of mortality in individuals aged up to 45 years of age. Approximately 1 in 300 families in the UK have a member permanently disabled by a head injury as the result of violence (5%), fall (35%), or road traffic accident (53%) (Graham and Gennarelli, 1997). 400 patients per 100,000 of the population are admitted to hospital every year with a head injury. A survey of 1,000 patients admitted to hospital following a head injury found 31% died within 6 months, 30% recovered, 20% were moderately disabled, 16% were severely disabled and 3% were vegetative. Regardless of the initial injury, it is evident that recovery of physical and cognitive abilities, varies from individual to individual. Some of this may be due to environmental factors, such as standard of post-injury rehabilitation. However, it is becoming more evident that some individuals may be genetically predisposed to a poor recovery following brain injury and the mechanisms involved may be closely related to mechanisms previously studied in AD.

1.5.2 Neuropathology of acute human brain injury

Acute brain injury can be divided into categories such as: ischaemic injury as the result of cerebrovascular incident or cardiac arrest and traumatic brain injury, the result of a missile and non-missile head injury (Graham *et al*, 2000). Each year thousands of humans suffer from one of these injury types and, although differing in their origin, these injuries follow common pathways in secondary damage after the event and in subsequent recovery over long periods of time. Ischaemic injury occurs when cerebral blood flow is severely reduced as the result of a stroke, or cardiac arrest that in turn reduces oxygen supply to the brain. This leads to ischaemic cell death where cells are classically pyknotic in appearance and intensely eosinophilic. Macroscopically, brain swelling and atrophy are visible where the ventricles become enlarged and midline shift, due to raised intracranial pressure, is evident (Forbes *et al*, 1993). The neuropathology of traumatic brain injury is less well defined and consists of many components (Graham *et al*, 1995; Samatovicz 2000). Brain pathology after head injury may be classified in two ways: (1) focal, with injury categorised as skull fractures, intracranial haemorrhage and contusions and (2) diffuse, where injury is

categorised into ischaemic brain injury, diffuse axonal injury and brain swelling (Gentleman *et al*, 1995, Graham et al, 1995) (Tables 2 and 3).

Focal	Diffuse
Skull fracture	Diffuse axonal injury
Contusions	Ischaemic brain injury
Intracranial haemorrhage	Brain swelling
Raised ICP	Infection

Table 2 Categories of brain injury.

Primary	Secondary
Lesions	Haemorrhage
	Ischaemic brain damage
Fracture	
	Brain Swelling
Diffuse axonal injury	Raised ICP
	Infection

Table 3 Classification of brain pathology.

Focal injury is most likely to be sustained by physical contact as the result of a fall while diffuse injury is associated with acceleration/deceleration, the type of injury sustained from a road traffic accident (Gennarelli *et al*, 1982). Within these categories primary and secondary pathology has been identified, the primary events being diffuse axonal injury and skull fracture (Polvishock and Christman, 1995). The secondary events being processes that do not manifest themselves clinically, until a period of time after the initial injury. These include ischaemia, brain swelling and raised intracranial pressure. Secondary damage evolves over a period of hours, days and even a few weeks following the initial injury.

The secondary damage associated with primary events in common with diffuse and focal injury are very often neurochemically driven, caused by fluctuations in ion homeostasis (Ca^{2+} most importantly), cerebral metabolism and breakdown in the blood-brain barrier (Graham and Gennarelli, 1997; Maxwell *et al*, 1997). This inevitably leads to breakdown in cytoskeletal elements, primarily microtubules. However, of emerging importance are the events that occur months and years following the initial injury. Regardless of the original brain injury source, individuals who are not dead or vegetative generally follow a process of recovery that can include regaining speech skills, learning how to walk again, or even recovering lost cognitive capabilities. Recovering these skills requires alterations in the brain to allow the formation of new connections and the repair of injured processes, but to achieve this certain proteins within the brain must be activated to aid this process.

1.5.3 *APOE* genotype and acute brain injury: outcome and recovery

1.5.3.1 Traumatic brain injury

The relationship between AD and head injury was made by initial observations in the brain tissue of boxers who suffered from being 'punch drunk' or *dementia pugilistica* (Corsellis *et al*, 1973; Roberts *et al*, 1990). The brains of these individuals displayed some of the common neuropathological features associated with AD, including neurofibrillary tangles and Aβ–containing plaques. Subsequent epidemiological studies revealed a significant association between head trauma and a risk of developing AD neurodegenerative-like symptoms. Further investigation showed the presence of Aβ deposits in a large proportion of head trauma victims on postmortem examination following short survival periods after the initial injury (Roberts *et al*, 1990; 1994). With the association between head injury with AD pathology it was examined whether brain pathology after injury was influenced by susceptibility factors for AD such *APOE* genotype. It was found that a history of previous head injury in *APOE*ε4 survival patients conferred a ten times greater chance of developing AD later in life (Mortimer *et al*, 1991; Mayeux *et al*, 1993). It was determined that *APOE*ε4 individuals who died following a head injury were significantly more likely to display Aβ aggregation (odds ratio of 0.78) than non ε4 individuals (odds ratio of 0.15) (Nicoll *et al*, 1995; Horsburgh *et al*, 2000). This indicated for the first time that

genotype could modulate the brain's response to injury. Amyloid deposition has been shown as early as 4 hours after injury and these deposits are strongly apoE immunoreactive. It was suggested that the amyloid deposits pre-dated the head injury because the mean age of the ε4+ group was 52 years, whilst it was 28 years for the ε4- group. However, the criteria for inclusion into the study required death within 30 days after the initial injury. This lends to the possibility that the older victims in the non-ε4 group did not die so rapidly after the injury (within 30 days) or alternatively, the plaques could develop at an earlier age in individuals possessing an ε4 genotype (Roses *et al*, 1997). The issue of whether amyloid deposits were present in head injury victims before the injury in that study remains largely unresolved.

Genetic possession of the *APOE* ε4 allele has now been shown to have great implications for outcome after traumatic brain injury and further studies have outlined an association between the ε4 allele and poor recovery from closed head injury (Plassman *et al*, 2000). A higher proportion of *APOE*ε4 individuals were found not to recover consciousness compared with individuals not possessing an ε4 allele. Furthermore, 57% of patients with an *APOE*ε4 allele had a poor outcome according to the Glasgow Outcome Scale, scored as either dead, vegetative, or severely disabled compared with 27% in non ε4 carriers (Teasdale *et al*, 1997). Similar studies also highlighted a poor outcome in individuals carrying an ε4 allele following traumatic brain injury and was associated with a greater incidence of prolonged unconsciousness (Friedman *et al*, 1999), a higher incidence of death (Roses *et al*, 1995) and poorer response to rehabilitation (Lichtman *et al*, 2000). More recently, the presence of neurofibrillary tangles has been elucidated in young individuals following repetitive head injury (Geddes *et al*, 1999). The relationship between repetitive head injury and *APOE* genotype was explored in professional boxers and it was shown that those possessing an *APOE*ε4 genotype displayed greater scores in a clinical scale of chronic traumatic brain injury (Jordan *et al*, 1997). To the present date, no study has defined the events that occur at longer survival periods following traumatic brain injury or looked at *APOE* genotype influence on long-term recovery.

1.5.3.2 Intracerebral haemorrhage, stroke and cardiopulmonary bypass

APOE genotype has been linked to CNS disorders such as cerebrovascular disease and stroke. The possession of an *APOE*ε4 allele has long been associated with atherosclerosis (Hixson *et al*, 1991) and elevated cholesterol levels (Davignon *et al*, 1988). This, combined with the presence of amyloid laden cerebral blood vessels, warranted the investigation of *APOE* genotype in cerebrovascular disease (Namba *et al*, 1991). Work by Schmechel (1993) and others revealed that the *APOE*ε4 allele was linked to vascular amyloid deposition in a population of AD subjects in a dose dependent manner (Greenberg *et al*, 1995). Subsequent studies have revealed that the E4 isoform modulates the severity of cerebral amyloid angiopathy (CAA) by promoting the aggregation of Aβ40 around cerebral blood vessels (Alonzo *et al*, 1998). Rather unexpectedly, it was found that inheritance of the *APOE*ε2 allele posed greater risk for blood vessel rupture, this allele had previously been thought of as neuroprotective in its role in AD (Nicoll *et al*, 1997).

The *APOE*ε4 allele association with a poor outcome following spontaneous intracerebral haemorrhage (Alberts *et al*, 1995; McCarron *et al*, 1998; 1999) was then identified, an effect which could not be solely explained by larger hematoma volumes and more severe oedema in *APOE*ε4 individuals (Sorbi *et al*, 1995). Although there is no clear association between *APOE* genotype and the occurrence of intracranial haemorrhage, an apparent link was established between recovery and *APOE* genotype. In a prospective series of patients with nonaneurysmal intracerebral haemorrhage, mortality rate was significantly greater for individuals genotypically ε4 and patients without an *APOE*ε4 displayed more improved physical and cognitive abilities when compared with control groups (McCarron *et al*, 1998). The *APOE*ε2 allele has been shown to be beneficial in intracerebral haemorrhage (more favourable outcome) (Nicoll *et al*, 1996, 1997). To date no clear association of the *APOE*ε4 allele with risk of ischaemic stroke has been determined, however, patients with an *APOE*ε4 allele are significantly more likely to be functionally and cognitively impaired (McCarron *et al*, 2000). Several groups have actually determined a more favourable outcome from ischaemic stroke in *APOE*ε4 individuals (McCarron *et al*, 1998). Additionally *APOE* genotype is also implicated in acute brain injury associated with

with cardiopulmonary bypass (Newman *et al*, 1995). Individuals with an *APOE*ε4 genotype displayed impaired cognitive capabilities compared with a non-ε4 control group following surgery (Tardiff *et al*, 1997). These studies all suggest that the influence of apoE on recovery from head trauma may depend on the type of insult incurred. Neuronal apoE immunoreactivity is increased in the human brain following episodes of global ischaemia due to cardiac arrest, where apoE immunoreactivity was associated with ischaemic neurons in the vulnerable pyramidal layers of the hippocampus (Horsburgh *et al*, 1999). Upregulation of apoE immunoreactivity also occurs in the brains of individuals suffering from hypoglycemia and epilepsy.

1.6 Animal Models of Brain Injury

1.6.1 Animal models that mimic some of the neuropathological events of human brain injury

Several different animal models have been developed which mimic some of the neuropathological events that occur in human brain injury. These models include the fluid percussion model (Lindgren and Rinder, 1966), the cortical impact model (Dixon *et al*, 1991), closed head injury (CHI) (Chen *et al*, 1997), stretch models of axonal injury (i.e. optic stretch) (Gennarelli *et al*, 1989), glutamate/excitotoxicity, subdural haematoma, focal ischaemia (Tamura *et al*, 1981; Longa *et al*, 1989; Macrae *et al*, 1993) and global ischaemia (Horsburgh *et al*, 1997; Li *et al*, 1998). These models have been employed primarily in rodents (although higher species have been used) to study various components contributing to human brain injury. Using these models, the acute (immediate) and chronic (long-term) responses to injury may be assessed. By modulating animal survival, the long-term response of the brain to injury may be studied and one of the main events, which occur weeks or months after injury, is brain plasticity. The contents of this thesis describe the entorhinal cortex lesion model of brain injury, which is perhaps, the best characterised model in terms of stimulation of plasticity mechanisms. Removal of afferent input into the hippocampus stimulates a dramatic plasticity response that is unparalleled in any other region of the brain.

1.6.2 Hippocampal structure and pathways

The hippocampal formation consists of the hippocampus, dentate gyrus and the parahippocampal gyrus. In synergy these structures perform valuable functions in learning and memory. The formation of new memories requires dendritic remodelling and the formation of new synapses to take place within defined regions of the hippocampus. This process is termed plasticity and many studies employ the hippocampus as a model of CNS plasticity, because of this natural ability to remodel. The hippocampus is comprised of highly intricate but well organised circuits, which have been relatively well preserved throughout evolution and therefore basic hippocampal circuitry is structurally homologous in humans and other mammalian species (Barr and Kiernan, 1993). The human hippocampus is proportionally smaller

to the size of the entire brain compared with rodent brain, however the entorhinal cortex is geographically closer. The hippocampal formation has four main sources of afferent fibres originating in the cortex; the septal nuclei, the contralateral hippocampus and the reticular formation and is supplied with blood from the anterior choroidal artery. The largest afferent input into the hippocampus is from the entorhinal cortex where 80-90% of the fibres from layers II and III of this region project to the molecular layers of the dentate gyrus. Fibres from the entorhinal cortex project through the underlying white matter and terminate within the outer two thirds of the dentate molecular layer. A proportion of these fibres also project to the stratum lacunosum moleculare (Figure 1.5).

The hippocampus proper is composed primarily of 3 layers. The pyramidal cell layer (subdivided into the CA1, CA2, CA3 and CA4), the molecular layers (subdivided into inner, middle and outer) and the polymorphic cell layer. The molecular layers of the dentate gyrus are composed of the dendritic processes of granule cells. The granule cells are the dominant cells of the dentate gyrus, giving it the characteristic 'V' shape (Figures 1.3 and 1.4)

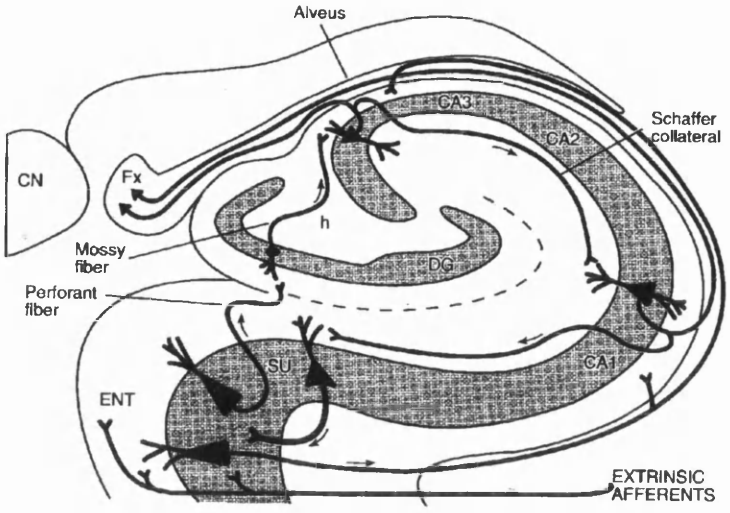

Figure 1.3 Diagram derived from The Human Nervous System by Barr and Keirnan, 1993. The diagram illustrates the structure of the human hippocampus and highlights the intrinsic and extrinsic circuits of the hippocampus.

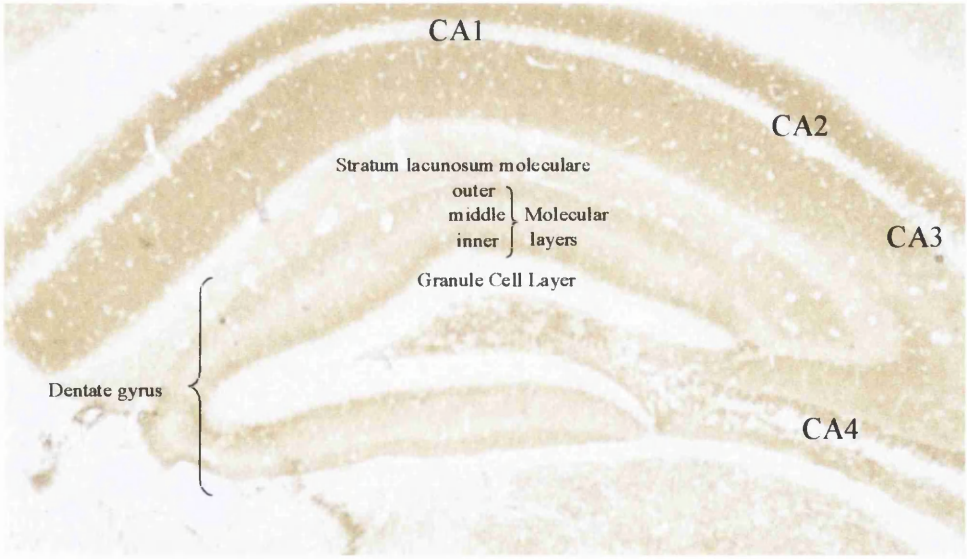

Figure 1.4 Illustrative example of basic hippocampal structure in a synaptophysin immunostained coronal section of a mouse brain. CA1, 2, 3, 4 are the pyramidal cell layers and within the dentate gyrus are the molecular cell layers labelled inner, middle and outer. The molecular layers are the main regions of interest in this thesis.

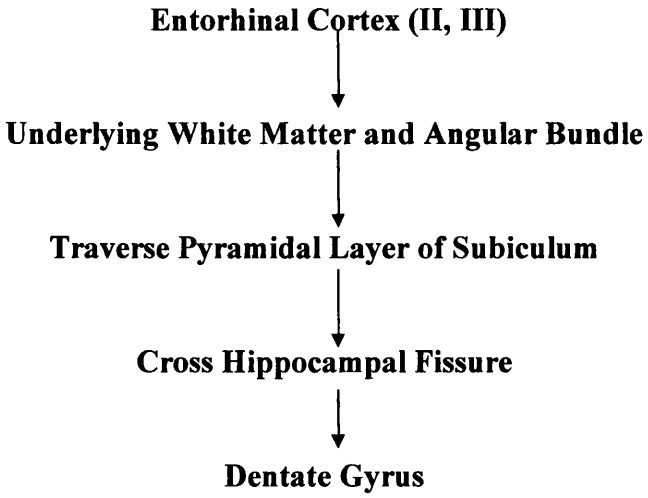

Figure 1.5 Diagram illustrating the perforant pathway route from the entorhinal cortex to the dentate gyrus.

Intrahippocampal circuitry connections are also shown in the diagram below and highlight the feedback nature of these pathways (Figure 1.6). With the development of electrophysiological techniques and the use of rodent brain, our knowledge of hippocampal circuitry has undoubtedly increased, something that could not be achieved using human subjects.

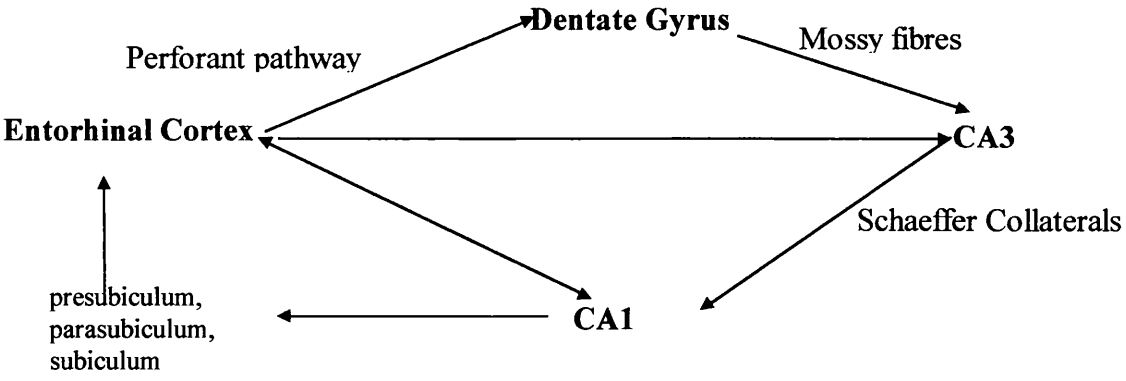

Figure 1.6 Intrahippocampal pathways

The entorhinal cortex receives input from the neocortex of the temporal lobe and communicates with sensory areas of the cortex in association with this. In this way the hippocampus is kept informed of all sensations and higher brain activities. In this capacity it is believed to function in the storage of short-term memories.

1.6.3 Entorhinal cortex lesion as a model of brain plasticity

The process of neurodegeneration occurs in many human diseases, after brain injury and also as an integral part of the ageing process. However, there is some suggestion that the human brain is capable of repair and regeneration to a limited extent. This has been shown in studies of AD where aberrant sprouting and reactive synaptogenesis has been identified within the hippocampus at chronic stages of the disease (Masliah *et al*, 1991, 1992). These phenomena have also been shown following head injury (Grady *et al*, 1989). The entorhinal cortex lesion (ECL) is well characterised and allows the study of plasticity within the mature CNS. This model is believed to mimic neurodegenerative events characteristic of AD and human head injury (Poirier, 1994; Poirier *et al*, 1995; Danik and Poirier, 1997; Masliah *et al*, 1996).

Many protocols have been employed to lesion the entorhinal cortex including chemical (Cho and Jaffard, 1995) and physical disconnection of the cortical region (Masliah *et al*, 1995) which projects to the hippocampus (see Hippocampal Pathways). The mode of lesioning used determines the extent to which neurodegeneration occurs within the hippocampus. The most common method used at present is aspiration, where the entorhinal region is removed by suction and many studies have shown that this leads to degeneration within the outer molecular layer of the dentate gyrus (Masliah *et al*, 1991). The chemical method (achieved by administering toxic agent) (Cho and Jaffard, 1995; Scharfman *et al*, 1998), electrolytic lesion (achieved by injecting small pulses of electricity) (Poirier *et al*, 1990; Hardman *et al*, 1997; Anderson *et al*, 1998; Terrisse *et al*, 1999) and cutting (using a fine blade) (Ramirez *et al*, 1996; Haas *et al*, 1997) all lead to extensive neurodegeneration within the middle and outer molecular layers of the dentate gyrus. These layers are composed of the dendritic branches from the granule cells (Figure 1.7). Loss of afferent input onto these cells, results in the breakdown of these branches with an associated loss of synapses. This animal model was first characterised in the 1960s where tract tracing methods were used to identify the projections of the neurons in the entorhinal cortex of the rat and were further mapped to define precise projection patterns into the hippocampus (Steward, 1976). To confirm these findings the investigators damaged these cells, which resulted in loss of fibre definition (60%) in the dentate molecular layers in a time-dependent manner

(over a period of 14 days) (Cotman *et al*, 1976; Steward and Vinsant, 1983). Evidence for post-lesion sprouting and reactive synaptogensis was initially obtained from electron microscopy studies focusing on synapse replacement on denervated neurons in the septal nuclei (Raisman *et al*, 1969). This led to the analysis of sprouting in the hippocampus following ECL. Light microscope studies revealed proliferation of presynaptic processes from other neighbouring afferent fibre systems. The creation of new synaptic contacts was termed reactive synaptogenesis (Cotler and Nadler, 1978; Steward *et al*, 1988) and the proliferation of fibres called sprouting (Steward and Vinsant, 1983). Steward and Vinsant (1976) were the first investigators to identify the origin of the cells producing the proliferation response and describe a time-course for the reinnervation process. Since that discovery, a host of studies have employed the ECL to assess CNS plasticity and cellular response to lesions of this kind. Masliah *et al* (1991) validated an entorhinal cortex lesion model in rat and identified specific markers of neurodegeneration and reinnervation, using immunohistochemical markers such as synaptophysin and GAP-43. Synaptophysin is a synaptic vesicle marker that allows the analysis of synaptic loss and gain. GAP-43 on the other hand is the marker of a presynaptic membrane protein involved in neurotransmission (Van Lookeren Campagne *et al*, 1990; Lin *et al*, 1992; Stroemer *et al,* 1993). This protein is predominately found in the membrane of growth cones and therefore this antibody is valuable in identifying not only fibre degeneration but also sprouting. Masliahs group noted a significant decrease in both markers by day 7 post-lesion, however GAP-43 and synaptophysin levels returned towards control levels by day 30 post-lesion. To substantiate this finding, several studies have shown that, following ECL rats display deficits in memory and learning, which is reduced following a suitable period of survival to allow fibre sprouting to occur (Ramirez *et al*, 1996; Hardman *et al*, 1997; Anderson *et al*, 1998).

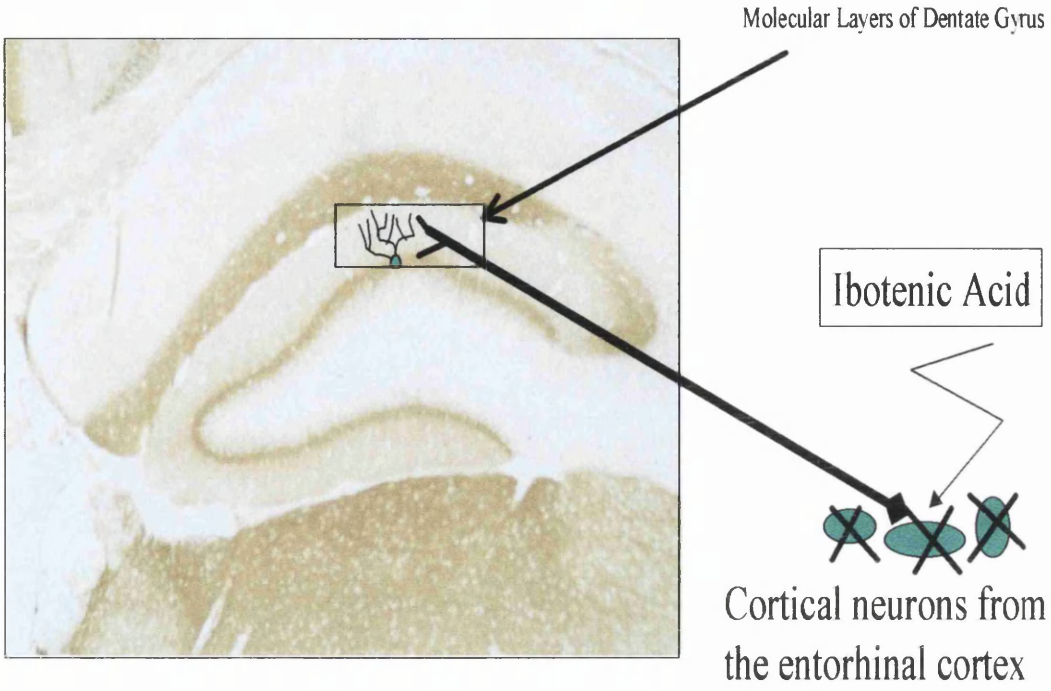

Figure 1.7 Lesioning the entorhinal cortex. The perforant pathway connecting the cortex to the hippocampus can be disconnected via different means i.e electrolytically, chemically or aspiratively. Lesioning in the studies included in this thesis are achieved chemically. This results in degeneration within the molecular layers of the dentate gyrus (shown on the diagram). The molecular layers are comprised of the dendritic branches of the granule cell layers.

On loss of afferent input to the hippocampus, several other extra and intra hippocampal fibre systems have been shown to sprout to compensate (Frotscher *et al*, 1997). These fibre systems have mainly been identified in animal lesion models, primarily the entorhinal cortex lesion (Steward and Vinsant, 1983; Steward *etal*, 1988; Masliah *et al*, 1991). Sprouting has been identified from three main fibre pathways (Deller *et al*, 1996; Frotscher *et al*, 1997). These are cholinergic fibres from the septal nuclei (Deller *et al*, 1999), crossed temperodentate projections from the contralateral hippocampus (Steward and Vinsant, 1983; Deller and Frotscher, 1997) and commissural-associational fibre projections from the pyramidal layers of the ipsilateral hippocampus (Deller *et al*, 1996; Deller and Frotscher, 1997). Although some groups would argue there is no change in cholinergic markers following entorhinal cortex lesion (Aubert *et al*, 1994; Henderson *et al*, 1998), compensatory

sprouting from each of these pathways has been demonstrated in animal models of injury. Only projections from the septal nuclei have been clearly shown in human brain. In animal models, projections from the commissural-associational fibres have been shown to extend up to 10's of μm into the molecular layers of the dentate gyrus (Steward and Vinsant, 1983; Steward *et al*, 1988) and can be assessed by measuring increases in the width of the inner molecular layer (Anderson *et al*, 1998).

1.6.4 Organotypic hippocampal slice culture: an *in vitro* model of hippocampal plasticity

The ability to maintain a brain slice is an important tool for studying whole brain circuits, which is more physiologically relevant than single cells in culture (Gahwiler, 1983, 1984). In recent years brain slices and in particular hippocampal slices have become attractive to electrophysiologists, pharmacologists and biologists because the method allows manipulation of the system (drug addition to culture medium) and easy access for analysis of current physiological state (electrophysiology). To culture CNS tissue from any region successfully, all that is required is sufficient oxygen supply, balanced culture medium, and a stable environmental temperature of 36-37^{0}C. Conditions being exact, the explant will maintain tissue organisation and cellular connections that resemble the original *in situ* conditions (Stoppini *et al*, 1991; Gahwiler *et al*, 1997). In the case of hippocampal slices, there are essentially two methods that can be used to maintain survival for a period of days, up to months. The tissue is normally sectioned at 100-400μm whilst being maintained in a balanced salt solution sufficiently supplied with oxygen. The tissue then has to be attached to a substrate that will allow maintenance for long periods. In the roller-tube method, slices are embedded in a collagen matrix and exposed to continuous changing of the liquid to gas interface. In the membrane culture method (interface method), slices are placed on a semi-permeable membrane balanced over the culture medium. This allows diffusion of nutrients across the membrane without complete submersion in the culture medium. Oxygen is received from above the slice and kept completely stationary throughout the entire culture period. Tissue for culturing is normally obtained from postnatal animals (<10 days old), as adult tissue generally does not survive well due to impaired plasticity capabilities (Stoppini *et al*, 1991). Many of the mechanisms involved in plasticity (GAP-43 expression) may be common to both neonatal tissue and adult tissue and is therefore still relevant in these types of studies.

To allow culturing of hippocampal slices, they require to be dissected from the surrounding tissue. This results in removal of the cortical input into the hippocampus in a similar manner to that observed in the previously described entorhinal cortex lesion (Heimrich and Frotscher, 1990), causing degeneration within the dentate gyrus of the hippocampus. Sprouting in hippocampal slices occurs mainly from unlesioned intrahippocampal fibre systems (Stoppini *et al*, 1997; Stoppini *et al*, 1993). Co-culturing the slices with pieces of entorhinal cortex tissue can eliminate this sprouting response. In hippocampal slices, survival of neuronal and glial cells is extremely high and the morphological appearance of these cells is virtually as found *in situ,* including dendritic structure. Immediately following culture the synaptic density decreases due to the deafferentation, however, as found *in vivo*, reactive synaptogenesis occurs (Frotscher and Gahwiler, 1988). Synaptic density tends to remain low in distal dendrites due to the lack of extrahippocampal fibre pathways. Therefore, it is evident that slices retain a certain capacity for short and long-term plasticity alterations.

The uses for organotypic hippocampal slice culture are wide and varied. Electrophysiologists have long been interested in this application as means of recording from established neuronal circuitry and this has been particularly useful in the study of long-term potentiation (LTP) and in the study of epilepsy. However, this culture system is especially relevant for investigations which require the long-term survival of the tissue for studies involving chronic administration of drugs (Teter *et al*, 1999), analysis of synaptogenesis and sprouting (Stoppini *et al*, 1993), gene expression and the long-term influences of ischaemia or hypoxia (Lake *et al*, 1999). This technology combined with the protein analysis systems such as immunohistochemistry and Western blotting allows the analysis of behaviour of cells and networks in a more physiologically relevant environment.

1.7 Assessment of ApoE Function and Genotype Influence in Animal Models of Brain Injury

1.7.1 Human studies versus animal studies

The initial studies linking *APOE* genotype to AD and head injury were pioneering studies and catalysed a vast field of research, which resulted in *APOE* genotype being linked to many other human disorders. However, the majority of these studies were human neuropathological or clinical studies. The use of animal models has allowed investigators to answer basic fundamental questions, such as cellular localisation of apoE before and after brain injury (Poirier *et al*, 1998). It was not only enough to investigate this in normal rodent brain, as they express an apoE isoform structurally similar to the human E4 isoform, but systems had to be developed which allowed the behaviour of human apoE and its isoforms to be assessed under conditions of brain injury. Subsequently, several populations of transgenic mice were engineered which expressed the human apoE isoforms. *APOE* knockout mice were developed which addressed the most fundamental question of the primary role of apoE in the CNS.

1.7.2 Genetic engineering of transgenic mice

Transgenic animals are manufactured by a generally common method, using embryonic stem cell technology in which the endogenous mouse target gene is deleted and the human DNA encoding the appropriate gene sequence inserted by micro-injection (Gordon *et al*, 1980; Xu *et al*, 1996). Human genomic DNA fragments are isolated and purified (from homozygous carriers for the *APOE*ε2, ε3 and ε4 alleles), digested, cloned into a vector and transfected into a cell line. Following this, the cell lines are screened for presence of the target DNA. Initially, the endogenous gene (*APOE*) is disrupted by gene targeting in the host mouse (Piedrahita *et al*, 1992). Following restriction digestion the purified DNA is micro-injected into the pronucleus of single cell embryos, where one parent is a knockout transgenic (Figure 1.8). This produces transgenic offspring possessing the target DNA human sequences (Figure 1.9). The animals can then be backbred with knockout animals, to produce heterozygotes, or can be further bred to homozygosity. The presence, integrity and copy number of the inserted gene is analysed using polymerase chain reaction (PCR)

and Southern blotting. Protein expression levels can then be checked using enzyme linked immunosorbent assay (ELISA) or Western blotting.

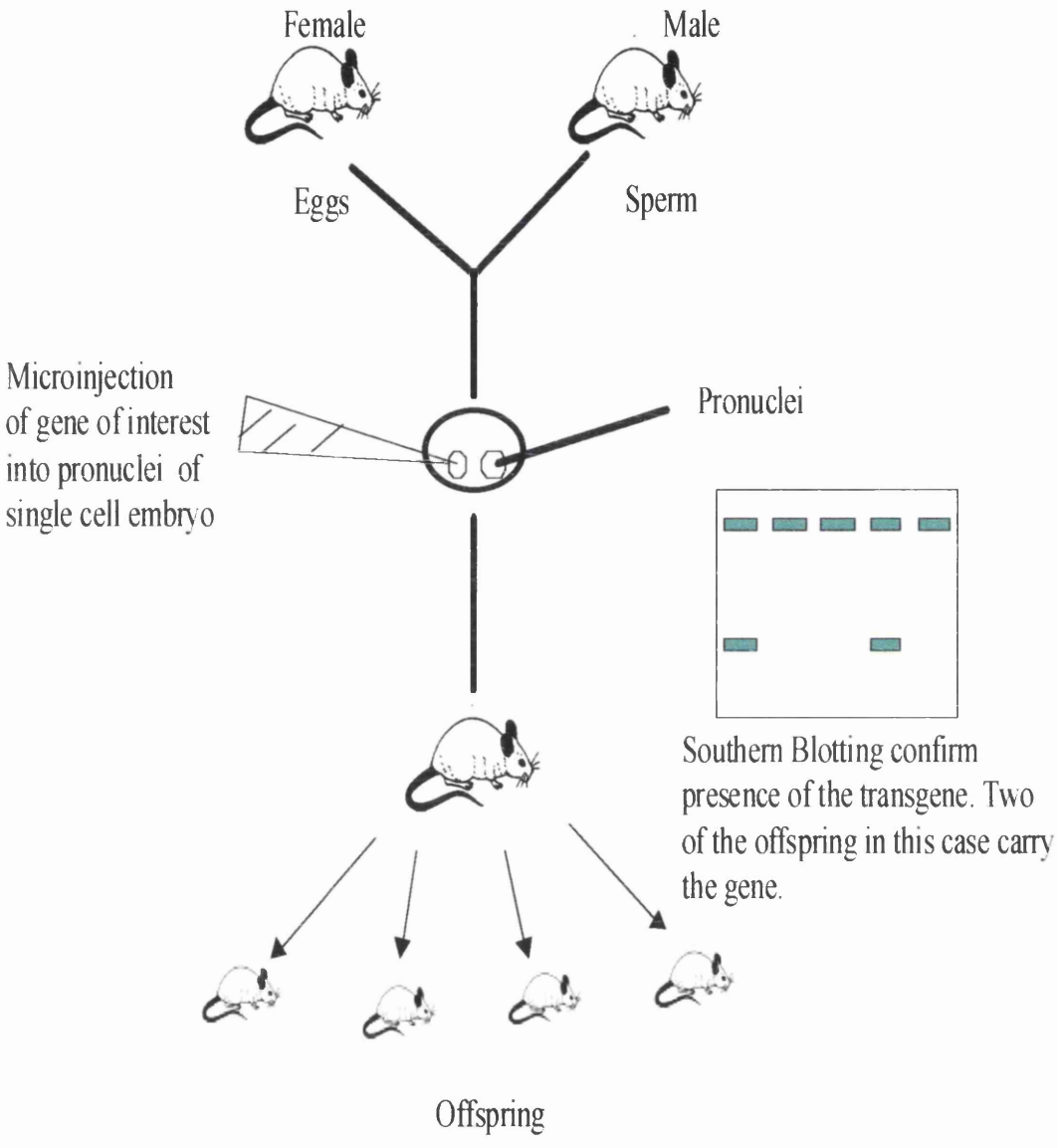

Figure 1.8 Diagram illustrating the standard procedure for generating transgenic mice regardless of the gene of interest.

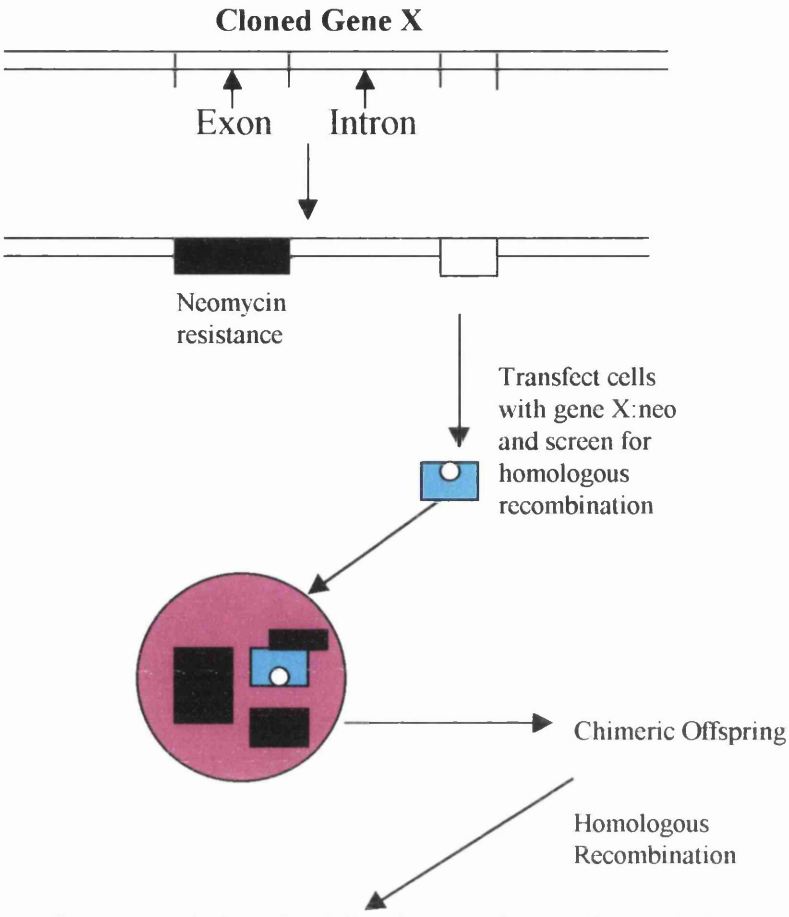

To check for germline transmission the following test is usually carried out.

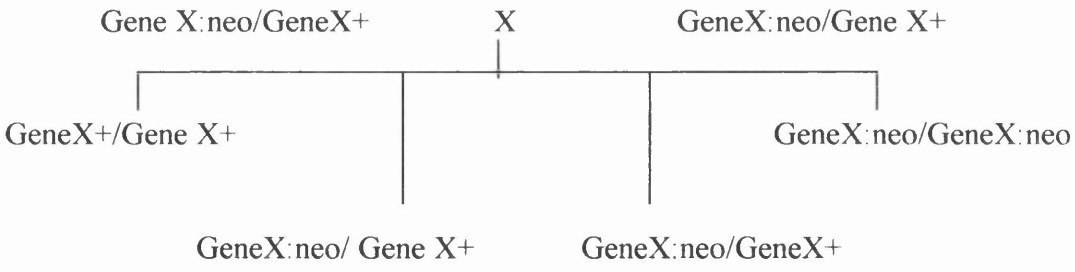

Figure 1.9 To produce knock-out and transgenic animals before transgene introduction the gene is replaced with a gene for neomycin resistance.

1.7.3 *APOE* knockout mice advanced the understanding of basic apoE function in the central nervous system

The development of *APOE* knockout or deficient mice has allowed understanding of the basic function of apoE. Several groups have produced *APOE* knockout mice of which some, but not all, display functional or anatomical deficits. The initial findings in *APOE* knockout mice were of abnormalities in the lipid distribution vascularly. *APOE* knockout mice exhibit an hypercholesterolaemic phenotype where cholesterol levels are six times higher (577-900mg/dl) compared to wild-type mice (80-114mg/dl)(Zhang *et al*, 1992; Hayek *et al*, 1998), and arterial lesions develop within the proximal aortas by 3 months of age (Reddick *et al*, 1994). Under normal physiological conditions, some *APOE*-deficient mice also display peripheral nerve structural defects where the myelin of myelinated axons appears electron dense and disordered when compared to the peripheral nerves of wild type animals using electron microscopy (Fullerton *et al*, 1998). In parallel with this, slight motor deficits have been detected in these mice (Chen *et al*, 1997). Within the brain of *APOE* deficient mice, alterations in phospholipid metabolism have been identified where levels of membrane phophatidylcholine are significantly lower than in littermate controls (Mato *et al*, 1999; Lomnitski *et al*, 1999). A similar study also highlighted a derangement in the transbilayer distribution of cholesterol in brain synaptic plasma membranes (Veinbergs *et al*, 1999; Igbavboa *et al*, 1999). In specific brain regions synaptic densities of cholinergic, noradrenergic and serotonergic projections are significantly lower than control animals. Dopaminergic neuron density is relatively unaffected in these animals (Chapman and Michaelson, 1998). In some studies of *APOE* knockouts a reduction in forebrain cholinergic neurons is associated with spatial learning deficits when tested in the Morris water-maze (Gordon *et al*, 1995; Krzywkoski *et al*, 1997; Masliah *et al*, 1997). Some groups however, have found there is no cholinergic deficit in *APOE* deficient mice (Anderson *et al*, 1998; Bronfman *et al*, 2000). Aged *APOE* deficient mice display even greater spatial learning problems that are associated with a breakdown in dendritic structure (Masliah *et al*, 1995). In addition to this *APOE* deficient mice were also shown to have abnormal presynaptic terminals, with reduced numbers of synaptic vesicles. The microtubule protecting effects of apoE are also highlighted, as in the brains of *APOE* deficient mice the microtubule associated protein tau is hyperphosphorylated, which

contributes to the abnormal dendritic structural changes (Genis *et al*, 1995; 1999). Immune responses are also altered in *APOE* knockout mice, suggesting a putative role of apoE in cell mediated immunity (Laskowitz *et al*, 2000). The behavioural alterations observed in knockout mice could also be linked to hormonal dysfunction due to the disruptions in the hypothalamic-pituitary system. This may also lead to metabolic abnormalities (Raber *et al*, 2000).

1.7.4 *APOE* transgenic mouse populations and different promoter systems

1.7.4.1 Expression of human APOE alleles under the endogenous human promoter sequence

There are several populations of *APOE* transgenic mice that have been engineered. The first strain to discuss are the human *APOE*ε3 and ε4 transgenic mice manufactured by Xu *et al* (1996) and developed by Glaxo Research and Development. Deletion of the gene was achieved in this case, by removing the *APOE* genes exon and intron 3 and replacing them with the neomycin resistance gene. Following homologous recombination, the normal and the modified alleles are inherited. The knockout males from this stage are used to fertilise cells from C57BL/6 female mice. The human *APOE* genomic DNA (28-30kb) was selected from a restriction digest and then injected into the pronucleus of a fertilised embryo. The founder mice are then backbred to *APOE* knockout animals to create animals heterozygous for the human *APOE* genes. Control animals for studies employing these transgenics, include littermate *APOE* knockout controls and wildtype C57BL/6J mice. The *APOE* DNA sequence is inserted in its entirety into the genome including the downstream promoter sequences in the creation of these transgenics. This has vital implications for the cellular localisation of apoE. *APOE* expression in these transgenic lines has been shown in glial cells throughout the brain, but neuronal apoE has also been identified. This corresponds with the endogenous pattern of expression in human brain, while rodent *APOE* expression is strictly glial in nature. This has been shown by Xu *et al* (1998) using high stringency *in situ* hybridisation that indicated neuronal synthesis of apoE. At the present time, these transgenics reflect most accurately *APOE* expression and levels in human brain. Similar study in humans also

suggests neuronal synthesis of apoE under normal physiological conditions (Han *et al*, 1994, Xu *et al*, 1999).

1.7.4.2 Expression of human APOE alleles under a GFAP promoter

A similar set of transgenic mice engineered by Holtzman *et al* (Sun *et al*, 1998) at the University of Washington, express the human apoE isoforms. However, their promoter sequence is an exogenous astrocyte-specific glial fibrillary acid protein (GFAP) promoter which, dictates that apoE expression is strictly astrocytic (Sun *et al*, 1998; Holtzman *et al*, 1999). Following the production of GFAP ε3 and ε4 mice, they were bred with *APOE* knockout mice and back-crossed onto a C57BL/6J background. These animals were heterozygous for the *APOE*ε3 or ε4 transgenes and expression was determined to be present in astrocytes and neuropil throughout the brain.. This pattern of expression is similar to that found in transgenics produced by a group at Duke University in which the *APOE* gene is under the control of the endogenous mouse promoter. The levels of apoE in these line of mice are comparable to that in human brain.

1.7.4.3 Expression of APOE alleles under a neuronal promoter system

The third population of transgenic mice were generated by Tesseur *et al* (2000) at the Flemish Institute for Biotechnology, Belgium. These mice were manufactured originally to investigate axonal degeneration and over-express the *APOE*ε4 allele. Downstream of the gene, a number of regulatory sequences including the Thy1, platelet derived growth factor (PDGF), glial fibrillary acid protein (GFAP) or the phosphoglycerate kinase (PGK) promoters were inserted so apoE was expressed neuronally in Thy1, PDGF and PGK mice and astrocytically under the GFAP promoter. These mice were aged and the brain and spinal cord examined then compared in neuron and astrocyte expressing animals. Mice expressing neuronal apoE developed severe axonal degeneration and axonal transport was impaired with a suggestion of hyperphosphorylation of tau. Levels of apoE in these mice are high compared to human brain levels. Another colony of neuronally expressing mice was generated by the Gladstone Institute, where the *APOE* gene is under a neuron specific

enolase (NSE) promoter (Buttini *et al*, 1999), however, these mice express similar apoE levels to those in human brain.

1.7.5 ApoE and the brains response to injury

1.7.5.1 ApoE response to acute brain injury in normal rodent brain

The data from the clinical studies indicated *APOE* alleles had a major role in head injury and AD, but very little was known of what apoE was doing in the brain. Initially, the response of apoE to brain injury was assessed in rodents following global ischaemia. ApoE in rodent brain is localised to glia, not neurons and therefore is different to humans. However, the initial studies in rats were undertaken to determine cellular localisation and alterations after injury. A global ischaemic insult in rodents results in widespread ischaemic cell death within regions such as the caudate and specific layers of the hippocampus. In rats, exposed to 15 mins occlusion, apoE immunoreactivity was increased at 24 hrs reperfusion within astrocytes and neuropil and by 72 hours neuronal cell bodies are intensely stained within the CA1 layer of the hippocampus (Kida *et al*, 1995, Horsburgh *et al*, 1996). In contrast, at 72 hours apoE immunoreactivity in astrocytes had decreased. The results indicated apoE is transported to neurons from astrocytes in response to injury. Similar increases in apoE have been shown in gerbil brain using *in situ* hybridisation techniques following global ischaemia (Hall *et al*, 1995; Ali *et al*, 1996) Intraneuronal accumulation of apoE was found to occur within 30 mins in a rat model of subdural haematoma (Horsburgh *et al*, 1997).

1.7.5.2 ApoE response to entorhinal cortex lesion

Before the production of this thesis, a few authors described the response of apoE to lesioning in the rat. Poirier *et al* (1991) first characterised the apoE response in rat brain following entorhinal cortex lesion using *in situ* hybridisation. *APOE* mRNA was increased 7 fold within the hippocampus and expression peaked by day 6 post-ECL. ApoE immunoreactivity was largely restricted to cells expressing GFAP mRNA and immunoreactivity decreased towards baseline levels by day 30 post-ECL. This study however did not include markers of sprouting, although the authors did suggest the study displayed a similar time scale to apoE expression following sciatic nerve transection and linked this event to remodelling events within the hippocampus.

Subsequent studies have also shown increased apoE expression (Zarow *et al*, 1998; Anderson *et al*, 1998). ApoJ immunoreactivity has also been shown to increase within the neuropil and glial cells of the dentate molecular layers (Johnson *et al*, 1996). Prior to the production of this thesis, no other studies have investigated the influence of *APOE* genotype on long-term neuronal plasticity.

1.7.5.3 APOE deficient mice and acute brain injury

The primary function of apoE in the brain could be elucidated using *APOE* deficient mice to establish the brain response to injury in the absence of apoE. Exposure of *APOE* deficient mice to a period of global ischaemia, produced significantly greater ischaemic neuronal damage when compared to wild type littermate controls (Horsburgh *et al*, 1999; Sheng *et al*, 1999). This difference is not attributable to cerebral blood flow, as blood flow measurements are comparable in *APOE* knockout mice and wild-type mice (Bart *etal*, 1998). One study highlighted the protective effects of apoE in brain injury, by infusing apoE intraventricularly following a period of global ischaemia (Horsburgh *etal*, 2000). Infusion of the exogenous apoE significantly reduced the amount of ischaemic neuronal damage in *APOE* knockout and wild-type mice. ApoE deficient mice also display an increased susceptibility to focal cerebral ischaemia. Knockout mice sustain larger infarcts compared to wild-type mice, with a mortality rate in *APOE* deficient mice of 40%, compared with 0% in wild-type mice following a period of focal ischaemia (Laskowitz *et al*, 1997). Exposure to closed head injury results in widespread neuronal cell death bilaterally which is accentuated in *APOE* deficient mice (Genis *et al*, 2000). In conjunction with this, these mice also display marked motor deficits, cognitive deficits (Chen *et al*, 1997) and decreased antioxidant activity (Lomnitski *et al*, 1997) following closed head injury, which are significantly more severe than that found in control animals. Even milder traumatic brain injury, such as concussive-like injury, renders widespread hippocampal damage in *APOE* deficient mice (Han *et al*, 2000).

1.7.5.4 APOE genotype and acute brain injury in transgenic animal models

Studies in *APOE* knockout mice illustrated that apoE was neuroprotective. The next step was to determine *APOE* genotype influence on human disease. This could be addressed, as transgenic animals had been developed expressing human isoforms of apoE. It has shown that following a period of global ischaemia, *APOE*ε4 mice exhibit significantly greater hippocampal neuronal cell damage when compared to *APOE*ε3 mice exposed to the same episode (Horsburgh *et al*, 1999). The same is true of transgenic mice of the same line exposed to focal cerebral ischaemia (Sheng *et al*, 1998). After 24 hours of recovery, infarct volume was found to be significantly larger in the *APOE*ε4 group compared to the *APOE*ε3 group. Lesion associated paralysis was also less severe in *APOE*ε3 mice, probably as a result of the reduced infarct volume. Following exposure to closed injury, *APOE*ε4 mice displayed a mortality rate of 50% following the injury, where only 25% died in the *APOE*ε3 group. On examination 1 hour after the injury all mouse groups (ε4, ε3, knockout and littermate controls) displayed similar severity of injury. Following 11 days of survival, the *APOE*ε3 mice had significantly smaller lesion sizes and they also exhibited significantly smaller neurological scores, compared with the other three groups who all displayed similar scores (Sabo *et al*, 2000). Altogether, these studies showed that the *APOE*ε4 allele was associated with a poor response to acute brain injury.

1.8 The Role of ApoE and Influence of *APOE* genotype on Plasticity

1.8.1 Mechanism of lipid redistribution in CNS plasticity

Neurons have a unique structure, in which the axon terminals may be at a distance of a metre or more from the cell soma and therefore not only the anterograde transport of lipids is important, but also other means of delivery (Vance *et al*, 2000). Cells do not need to acquire all their lipid material from the cell body, as lipid and cholesterol may be taken up from the environment (Fazio *et al*, 2000) via endocytic receptor pathways. Endocytic receptors such as the LRP receptor have been shown to be localised dendrosomatically and axonally (Beffert *et al*, 1998; Page *et al*, 1998). Electron microscopy revealed dense LRP receptor localisation in regions of high synaptic density. Many studies highlight a role of apoE (and possibly apoJ) in lipid mobilisation for the growth and repair of neurons following injury (Ignatius *et al*, 1987; Poirier *et al*, 1998; Beffert *et al*, 1998).

The human, and rodent brain retain an amazing ability to maintain neuronal integrity under normal physiological conditions, but are also capable of repair and compensation under conditions of severe stress (Masliah *et al*, 1991; Lie *et al*, 1999; Steward and Vinsant, 1976; Arendt *et al*, 1997). Loss of neuronal input into discrete regions of the brain is one of the classic hallmarks of many neurodegenerative disorders, such as AD and these neurodegenerative events are also common to head injury (Grady *et al*, 1989). The major constituents of the neuronal structure are lipid, cholesterol and water. Combined, these elements form the membranous compartments of the nuclear envelope, mitochondria, endoplasmic reticulum, Golgi apparatus and the lipid bilayer, which encase the cellular elements. The axon also requires lipid for the maintenance of myelin structure and function. As neurodegeneration occurs, the cellular structure is degraded releasing vast amounts of lipid and cholesterol debris into the extracellular environment (Poirier *et al*, 1993; Posse de Chaves *et al*, 1997). This material is recyclable and may be scavenged for reutilisation in the construction of new cellular components (Fazio *et al*, 2000), primarily cell membrane. It is in this role as a lipid scavenger in which apoE (and possibly apoJ) are thought to excel (Poirier *et al*, 1993). Although the peripheral nervous system (PNS) has been shown to be capable of regeneration to a limited extent, the CNS is not capable of

regeneration *per se* but rather a process of compensatory sprouting in response to denervation. This manifests as dendritic proliferation and sprouting of unlesioned fibre pathways (Steward and Vinsant, 1967; Deller and Frotscher, 1997). Growth of a neurite occurs at the tip of the fibre at a region called the growth cone (Vance *et al*, 2000). The progression of a growth cone can occur at a rate of up to 1mm/day and therefore extension of the plasma membrane demands an assiduous supply of membrane materials. Electron microscopy studies have shown that lipid is supplied to membranes by vesicles, which fuse with the membranes and deliver the lipid encased for incorporation into the structure (Posse de Chaves *et al*, 1997). The source of the lipids for this purpose may come from essentially two places. The cell body, axon and dendrites of neuronal cells, all contain the apparatus to manufacture proteins that are then transported throughout the cell via fast and slow anterograde and retrograde transport (Alvarez *et al*, 2000). Of more importance is the exogenous lipid sources, which are transported from other neighbouring cells and from the extracellular environment. Mahley *et al* (1987) first suggested that when a nerve degenerated, lipid debris from the membranes is scavenged from the environment, assembled into lipoprotein packages and delivered to other cells, which are active in the process of sprouting (Vance *et al*, 2000), and that apoE is heavily involved in this process. Evidence confirming this has shown that axonal degeneration products are not cleared in *APOE* knockout mice following injury (Fagan *et al*, 1998).

1.8.2 ApoE and lipid scavenging

The main hypothesis and one which has prevailed for some time is that on injury, apoE protein levels are increased as cells such as astrocytes, microglia and Schwann cells upregulate the production and secretion of apoE (Boyles *et al*, 1985; Stone *et al*, 1997; Ignatius *et al*, 1987). Once trafficked through the extracellular matrix, the apoE-lipid complex binds to receptors of the LDL receptor family, which are present throughout the nervous system and most importantly are present on neurons (and at the tips of growth cones) (Ignatius *et al*, 1987; Fagan *et al*, 1996; Narita *et al*, 1997). The complex is then internalised via clathrin-coated pits and the lipid and lipoproteins cleaved (Poirier *et al*, 1993). Lipid is then freely available for incorporation into cellular elements (Figure 1.10). The internalised receptor is then thought to be recycled to the cell surface. The destiny of apoE following this process is the subject

of some debate. Under normal physiological conditions, the interaction of apoE with the microtubule-associated proteins is believed to promote cytoskeletal stabilization (Roses *et al*, 1996). However, under conditions of injury when the process of neurite outgrowth is required, the interaction of apoE with microtubules is essential for extension of neurite processes (Johnson and Jope, 1992; Pitas *et al*, 1998). This requires escape of apoE from endosomes and this process will be discussed in the final conclusions (DeMattos *et al*, 1999). A similar process of lipid scavenging is believed to be performed by apoJ because of its upregulation following brain injury (Tornqvist *et al*, 1996), axonal injury (Tao *et al*, 1999) and in AD (Bertrand *et al*, 1995). However, the pathways and mechanisms involved have not been clearly demonstrated and are confounded by reports that the apoJ receptor, gp330, is very poorly expressed or indeed even absent from the human and rat brain (Page *et al*, 1998; Han *et al*, 2001).

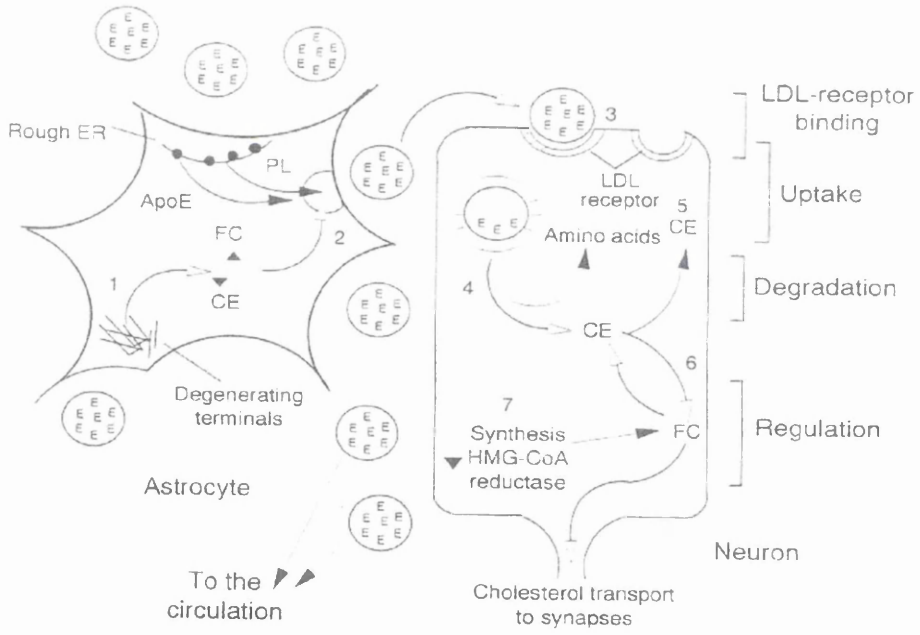

Figure 1.10 Derived from Poirier (1994). Diagram illustrating the movement of apoE from cell to cell and the process of lipid scavenging from the local environment. Lipid is transported back to neurons and endocytosed via receptor mediate mechanisms. In this way essential cholesterol and lipid can be reutilised for the reconstruction of cellular elements.

1.8.3 A role for apoE in regeneration was established initially within the peripheral nervous system

It is widely accepted, that nerve fibres of the peripheral nervous system (PNS) display an amazing ability to regenerate following injury. After peripheral nerve injury, lipid and cholesterol materials are released from degenerating axons. ApoE is believed to bind to the debris in the extracellular space and transport it to macrophages and Schwann cells. Cholesterol from the breakdown of the material can be stored as cholesteryl ester for future utilisation (Poirier *et al*, 1993). The lipid material can also be sequestered and used in the reconstruction of various axonal components. ApoE is secreted from the macrophage, complexed to an endogenous lipid source and transported primarily to the growth cone of the axon engaged in regeneration (Ignatius *et al*, 1987). At the cell surface, the apoE-lipid-complex is internalised via receptors of the LDL family. Axons express the LDL receptor along their length and increased expression coincides with axonal regeneration and remyelination (Boyles *et al*, 1989).

Initial studies looking at peripheral nerve regeneration, revealed that apoE was increased by approximately 200% following optic nerve and sciatic nerve crush and that this event paralleled extension and reconnection of the nerve endings (Figure 1.11). Increases were so marked, that after 3 weeks the apoE protein levels account for 5% of the total protein concentrations in the nerves (from 0.2%) (Ignatius *et al*, 1986). Much of the secreted apoE was associated with lipid and these complexes were internalised by receptor mediated endocytosis. Subsequent studies have shown dense expression of the LDL receptor on the tips of regenerating nerve fibres. The delivery of lipids and cholesterol aid in axonal elongation and may even be involved in the remyelination process (Vance *et al*, 2000). Regeneration was also investigated in dorsal root ganglion cells in culture, incubated with lipidated (βVLDL) apoE, and was found to increase neurite outgrowth and branching (Handelmann *et al*, 1992, Nathan *et al*, 1994). Lipid free apoE reduced neurite branching, but neurite extension directed away from the cell body was increased. This was thought to occur because apoE reduces the adhesiveness of neurites to the extracellular matrix. In the case of PNS injury macrophages enter the wound site and synthesise huge quantities of apoE.

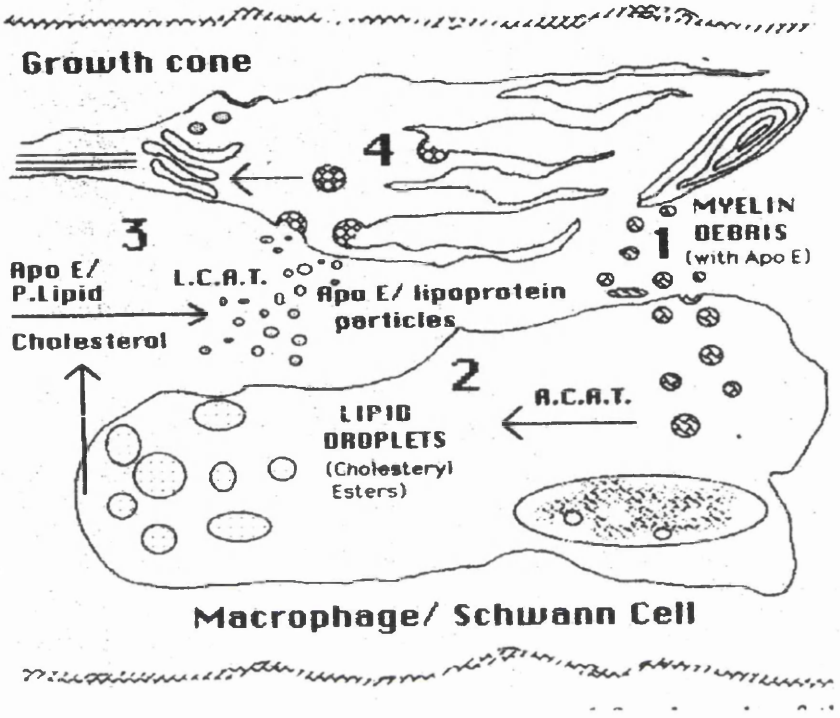

Figure 1.11 Diagram derived from Ignatius *et al* (1987) illustrating the transport of apoE to regenerating axons and the timecourse of events involved in regeneration and remyelination. The relative thickness of the lines indicates the size of the event.

This event parallels myelin reabsorption by Schwann cells as axons death progresses (Ignatius *et al*, 1987). 14-21 days after the injury, the process of remyelination begins to occur and apoE and apoAI are present within the extracellular matrix and found to be associated with large quantities of lipid and cholesterol-like lipids (Boyles *et al*, 1989). Ignatius *et al* (1987) used the injured rat sciatic nerve model to determine if neurites are capable of internalising apoE from the environment. They used pheochromocytoma (PC12) cells, which may be stimulated to produce growth cones. ApoE labelled with fluorescent dye is endocytosed by the growth cones in a rapid manner, suggesting the internalisation was via lipoprotein receptors and not by axonal transport. ApoJ too, is upregulated within astrocytes in axotomised processes, however its link with regeneration is less well defined and many researchers believe it may actually be more involved in the cell death process (Tornqvist *et al*, 1996; Tao *et al*, 1999).

Work by Bellosta *et al* (1995) highlighted that the regeneration promoting effects of apoE are genotype specific. They demonstrated, that in the presence of very low density lipoproteins, apoE E3 and E4 have differential effects on the ability to promote neurite outgrowth. When added to the culture medium of dorsal root ganglion cells, apoE3, combined with β-VLDL, decreased branching but stimulated neurite extension. Cells treated with apoE E4 displayed limited neurite outgrowth. Interestingly, apoE added alone to the culture medium had no effect on outgrowth. These results suggested that the apoE E4 isoform conferred a poor ability for PNS regeneration.

1.8.4 *In vitro* evidence for a role of apoE in CNS plasticity

Data from studies in the PNS suggesting a detrimental effect of the apoE E4 isoform on plasticity lead to interest in the role of apoE in CNS plasticity and whether there was an *APOE* genotype effect. The preliminary studies investigating this were carried out *in vitro* using cell lines derived from the CNS, as opposed to the peripheral nature of the dorsal root ganglia (DRG) in the initial studies. Pitas *et al* (1997) cultured cells from a murine neuroblastoma cell line (Neuro-2a) transfected to secrete apoE E3 or E4 and, when an exogenous lipid source was added to the culture medium, the apoE

E3 expressing cells produced neurite outgrowth whilst outgrowth was inhibited in apoE E4 expressing cells. It was also found, that this effect could be attenuated using blocking agents of the LRP receptor mediated uptake. In contrast, DeMattos (1998) suggested that addition of exogenous lipid sources inhibited the inherent outgrowth promoting effects of apoE E3 from transfected cells and that apoE E3 and VLDL could work independently. In a similar study using untransfected Neuro-2a cells (cells do not produce apoE endogenously) it was found that addition of exogenous apoE E3, combined with βVLDL, promoted neurite outgrowth whereas addition of apoE E4 inhibited it (Fagan *et al*, 1995; Holtzman *et al*, 1995). When examined more closely it was found that cells incubated with apoE E4 possessed microtubular abnormalities, which may contribute to the observed difference in sprouting. Hippocampal neurons harvested from C57BL/6J mice were also shown to produce extensive neurite outgrowth when grown on a monolayer of astrocytes, cultured from transgenic mice expressing *APOE*ε3 under a GFAP promoter sequence (Sun *et al*, 1998). Outgrowth was inhibited in neurons grown in the presence of apoE E4 secreting astrocytes. Questions have arisen as to whether the βVLDL lipid source employed in the majority of these studies is physiologically relevant, as apoE is found endogenously attached to high density-like (HDL) lipoproteins within the CNS. For this reason Fagan *et al* (1996) carried out a study in which apoE E3 and apoE E4 enriched HDL was incubated with a neuronal cell line (GT1-1 trk9) and again it was found that apoE E3 enhanced neurite outgrowth where apoE E4 did not. This effect was blocked by an LRP-receptor blocker, indicating that it was a receptor-mediated event.

1.8.4.1 LRP receptor function in neurite outgrowth

The LRP receptor mediates apoE-dependent neurite outgrowth, a phenomenon which has been identified in a host of *in vitro* studies (Narita *et al*, 1997). ApoE E3 promotes neurite extension in a population of nervous system-derived neuronal cell line, an effect which is abolished by the addition of RAP, LRP antibody or lactoferrin to the culture medium (Fagan *et al*, 1996; Williams *et al*, 1998). It is completely feasible that the isoform-specific effect differences are due to differential interactions of each apoE isoform at the receptor interface. The single amino acid changes in apoE

structure for each isoform, is in the LDL/LRP receptor-binding domain and therefore it is possible that this would confer binding differences (Mahley *et al*, 1988). However, biochemical studies have revealed that iodinated apoE E3 and E4 have similar binding affinities, with apoE E2 displaying the greatest affinity (Weisgraber *et al*, 1993). Ji *et al* (1998) analysed uptake of ^{125}I-VLDL enriched apoE E2, E3 and E4 and discovered a 2-3 fold greater accumulation of apoE E3 (and E2 although to a lesser extent) than E4 in Neuro-2A cells following 2 hours of incubation, a response which was not mediated by either the LDL or LRP receptor since the response persisted in cells deficient in both these receptors. The differential accumulation was enforced by heparan sulphate proteoglycan (HSPG), a protein closely associated with LRP at the membrane surface and responsible for the sequestration of apoE-enriched lipoproteins before internalisation by the HSPG-LRP pathway (Mahley *et al*, 1994). On treatment with heparinase, differential accumulation is abolished and thus it is evident that the intracellular levels of apoE rely heavily on the presence of the receptor associated HSPG (Bellosta *et al*, 1995). Indeed, some studies have shown that HSPG is capable of apoE-complex internalisation in the absence of either the LDL or LRP receptors (Mahley *et al*, 1995). Following the publication of these studies, there has been very little literature focussing on the biochemistry of the HSPG-LRP pathway. Such work may hold the key to *APOE* genotype influence on cell function.

1.8.5 *APOE* genotype may influence plasticity in Alzheimer's disease

In the last 10 years interest in brain plasticity has increased, with the initial realisation that long-term potentiation was a basic synaptic plastic mechanism that was primarily involved in the acquisition of memory (Gomez-Fernandez, 2000). Neurogenesis does not occur in the adult mature brain, however, processes of compensatory growth and repair are initiated in an endogenous attempt to reduce functional deficit. Neuroplasticity is a natural ability of the nervous system to reorganise and alter its function in response to environmental changes. Sprouting in the brains of patients with temporal lobe epilepsy (TLE) are the best documented cases of plasticity in the adult brain. Using a range of markers such as Growth Associated Protein-43 (GAP-43) and 5' nucleotidase, which is a marker of spontaneous synaptic turnover, plasticity has been shown in the dentate molecular layers of the hippocampus (Pollard

et al, 1994; Lie *et al*, 1999). Neurodegeneration is extensive in AD, resulting in the loss of cortical input into the molecular layers of the hippocampus. Several intrahippocampal fibre systems are capable of reinnervating the denervated molecular layers, including those from the contralateral hippocampus, commissural-associational fibres from the CA3 pyramidal layer/hilus region and cholinergic fibres from the septum, as identified in rat models. In AD postmortem tissue, mechanisms of compensatory growth have been shown especially within the hippocampus, using antibodies such as GAP-43 (Masliah *et al*, 1991 and 1992; Bogdanovic *et al*, 2000). The sprouting observed in these AD cases tends to be aberrant with respect to their localisation and neurotransmitter composition, however the intensity of dendritic changes is apoE genotype dependent. The brains of Down's syndrome patients with marked dementia related neuronal loss, also exhibit neuronal sprouting (Ohara *et al*, 1999). Data from a study by Arendt *et al* (1997) suggested that plastic remodelling is severely impaired in *APOE* ε4 carriers. The ε4 allele dose was also shown to have significant effects on the severity of the initial degeneration, degeneration which was not restricted to cholinergic neurons, suggesting a more widespread effect of apoE.

1.8.6 *APOE* genotype and brain plasticity after head injury

Cortical plasticity in humans after brain injury has been documented (Robertson and Murre, 1999). Following unilateral perinatal brain injury, the brain switches its functions to the healthy cortex, this results in ipsilateral motor control using ipsilateral corticospinal projections and the contralateral cerebellum. Patients with this disorder produce mirror limb movements (Nirkko *et al*, 1997). The hippocampus of patients who have undergone uncal herniation due to raised intracranial pressure, display sprouting within the termination field of the entorhinal cortex (Grady *et al*, 1989). Reorganisation of the CNS is crucial if lost modalities such as speech and motor functions are to be returned after injury. Several studies have shown synaptic change, tracked electrophysiolgically, could contribute to functional recovery after traumatic brain injury and stroke (Lee and van Donkelaar, 1995; Ivanco and Greenough, 2000; Kempermann *et al*, 2000). The first study suggesting *APOE* genotype may modulate long-term plasticity after traumatic brain injury was carried out by studying clinical outcome, 6 months after traumatic brain injury. *APOE*ε3 and ε4 head injured

individuals over a range of ages were recruited and assessed over a period of 6 months following a traumatic brain injury. Initially, it appeared there was no genotype effect on outcome, however when the groups were broken down into age categories, it was found that the *APOE*ε3 <15 years group exhibited significantly better clinical outcome compared to *APOE*ε4 carriers when controlled for severity of initial injury (Teasdale *et al*, 2000). This would suggest that the differences in outcome may be more related to genotype effects on plasticity and not age related effects, such as amyloid deposition.

1.8.7 A role for apoE in plasticity mechanisms in other human diseases

The vital role of apoE in the transport of lipids and cholesterol and the isoform specific differences in this role has implications for many other human diseases and disorders, particularly those which are primarily neurodegenerative disorders. Although a topic of some debate, it appears that multiple sclerosis (MS) may have a significant genetic component. Studies in the past have failed to detect any *APOE* genotype influence, until recently, with the advancement of MRI technology (Weatherby *et al*, 2000). A recent study of 83 MS patients revealed subjects with an ε3/ε4 genotype showed a greater T2-LL than patients with the ε2/ε3 genotype, supporting speculation on an *APOE* genotype influence on MS severity (Fazekas *et al*, 2000). The authors suggest this may be attributed to more extensive destruction or less efficient repair. It has also been shown that the frequency of the *APOE*ε4 allele is significantly higher in MS patients compared with a control group ($P<0.05$) and the rate of progression was significantly greater in *APOE*ε4 individuals (Hogh *et al*, 2000). Conversely, a study by Carlin *et al* (2000) highlighted that remyelination was defective in patients genotypically *APOE*ε2. ApoE immunoreactivity was increased within demyelinated regions localised to macrophages and astrocytes. More severe white matter degeneration has been shown in AD associated with the *APOE*ε4 allele (Bronge *et al*, 1999). In subsequent studies the *APOE*ε4 genotype has been linked to several other neurodegenerative conditions, such as AIDS related neuropathy, diabetic neuropathy and motor neuron disease (MND) (Bedlack *et al*, 2000). Possession of an *APOE*ε4 allele in patients with MND results in rapid deterioration and a significantly lower age of onset. Average survival, from the onset of the disease

to death, was not found to be statistically different in ε4 individuals however, in clinical, terms this equates to a mean survival time of 36 months compared to 49 months. The data concerning Huntington's disease is less well defined but highlights, in contrast, a more rapid progression of the disease in *APOE*ε2 carriers and this was particularly noted in females (Kehoe *et al*, 1999). The reason for this adverse effect of ε2 is unknown although may be related to estrogen levels. Parkinson's disease (PD) is one of the most common neurodegenerative disorders manifesting itself in 1% of Western populations and therefore is a major economic burden. Several authors have investigated whether the *APOE*ε4 allele is associated with PD and Parkinson's related dementia, considering that PD dementia possesses many of the neuropathological features of AD. PD patients show a trend for greater ε4 allele frequency than control subjects, however dementia was not significantly greater in those individuals (Inzelberg *et al*, 1998; Oliveri *et al*, 1999). More recently it has been suggested that individuals have an increased susceptibility to sporadic PD when an *APOE*ε4 genotype is combined with a polymorphism of allele 1 of the alpha-synuclein promoter (Kruger *et al*, 1999). The *APOE*ε4 allele has also been shown to predispose patients to a greater degree of dopaminergic drug induced hallucinations (Inzelberg *et al*, 2000).

Aims of Thesis

The *APOE*ε4 allele confers an increased risk for the development of AD and more exaggerated neuropathology (plaque load and tangle density), when compared with individuals not in possession of an *APOE* ε4 allele. The *APOE* ε4 allele has also been shown to be associated with a poor outcome following brain injury. The introduction of this thesis, has highlighted a role for apoE in the modulation of the brains response to acute injury. However, there is evidence that apoE may play a role in long-term recovery and repair processes.

The aims of this thesis are to:

1. Establish a model of entorhinal cortex lesion using C57BL/6J wild-type mice and characterise the acute and chronic cellular and protein alterations following the injury (Chapter III).
2. Analyse *APOE* genotype influence on CNS plasticity, in a line of *APOE* transgenic mice, expressing human *APOE*ε3 or ε4 alleles under the endogenous human promoter sequence following entorhinal cortex lesion (Chapter IV).
3. Analyse *APOE* genotype influence on CNS plasticity, in a line of *APOE* knockout and transgenic mice, expressing human *APOE*ε3 or ε4 alleles under a GFAP promoter sequence following entorhinal cortex lesion (Chapter V).
4. Analyse *APOE* genotype influence on ageing in the brains, of a line of *APOE* knockout and transgenic mice expressing human *APOE*ε3 or ε4 alleles under a GFAP promoter sequence (Chapter VI).
5. Establish an organotypic hippocampal slice culturing model and use this to characterise the sprouting response in hippocampal slices derived from C57BL/6J and *APOE* transgenic mice and analyse Herpes Simplex Virus as a potential vector for apoE gene delivery (Chapter VII).
6. Analyse microtubular binding of apoE E3 and apoE E4 protein and determine if there is an isoform specific difference (Chapter VIII).

Chapter II

Materials and Methods

2.1 Mice

2.1.1 Wild type C57 BL/6J mice

Male C57BL/6J mice were obtained from Harlan Olac and maintained in an animal unit at the University of Glasgow.

2.1.2 *APOE* transgenic mice on a human promoter

APOE ε3 and ε4 heterozygous transgenic mice were generated as previously described (Xu *et al*, 1996). Briefly, the coding and promoter sequences of human *APOE* were inserted into the genome of apoE knockout mice. The mice were backcrossed at least six times to C57BL/6J mice in the USA, before transportation to the UK and further backcrossing at GlaxoWellcome. In the present study, *APOE* ε3-437 and *APOE* ε4-81 lines were used which carry two copies of the appropriate gene. These lines were selected as they were best matched for apoE levels. The mice were obtained from GlaxoWellcome and maintained in an animal facility at the University of Glasgow.

2.1.3 *APOE* transgenic mice on a GFAP Promoter.

*APOE*ε3 and ε4 heterozygous transgenic mice were generated as previously described (Sun *et al*, 1998). Briefly, the coding sequences of human *APOE* were inserted into the genome of B6/CBA mice. An exogenous glial promoter sequence was attached to the *APOE* DNA sequences, so expression is driven astrocytically. Integration of the transgene was determined by PCR and Southern blotting analysis. The mice were imported from Dr D. Holtzman, maintained and bred in an animal unit at the University of Glasgow. These mice were also employed in the *in vitro* studies used as 7 day neonates.

2.2 *APOE* Genotyping

2.2.1 Restriction Digest of Mouse Tissue

The genotype of transgenic animals was confirmed by PCR analysis (Nicoll *et al*, 1995). Tail tip samples (carried out by Dr K. Horsburgh) were collected from each transgenic mouse aseptically and placed in DNA/RNA free tubes filled with sterile ethanol. The genotypes were then analysed at the Southern General Hospital (by Janice Stewart). DNA was isolated in an enzyme digest mix containing proteinase K overnight at 56^0C. The samples were then incubated at 95^0C for 10 mins to inactivate the proteinase K. 0.8µl of the target DNA was then added to 14.2µl master mix (containing deoxynucleotide bases, primers L3 and R3+ and Amplitaq Gold polymerase) (see appendix) and transferred to a thermal cycler (Techne GENIUS). Briefly the cycler progressed through a series of temperatures, 35^0C (to denature the target DNA), 95^0C (to anneal the primers) and 65^0C (for new DNA synthesis). To the final PCR product, restriction enzyme was added (Hha1) and incubated overnight at 37^0C. This restriction enzyme cleaves at 'GCGC' sites on the DNA sequence (i.e. arginine residues) and therefore at positions 112 and 158 where the residue substitutions occur that are responsible for apoE isoform structural differences.

2.2.2 PCR Gel Electrophoresis

To 15µl of PCR product, 4µl of loading gel was added before loading the samples onto a gel for electrophoretic separation. A Hinf 1 marker was also loaded onto the gel as a DNA ladder. The gel was run at 200 volts for 40 mins. The electrode assembly was removed from the tank and carefully prised from between the glass plates. The gels were then incubated in ethidium bromide solution (10mg/ml) for 4 mins, the bands visualised on a ultra violet light box and photographic images collected (Figure 2.1).

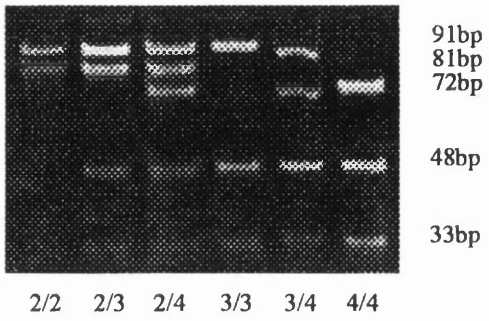

Figure 2.1 PCR analysis of *APOE* genotype from human brain tissue

2.3 Entorhinal Cortex Lesion

2.3.1 Surgery

All animals employed in these studies were approximately 12 weeks of age at the time of procedure and weighed approximately 25-30g in weight. Animals were fed on the same diet and housed under identical conditions. Anaesthesia was induced by a combination of 3% halothane in 70% N_2O/ 30% O_2. The animals were fixed in a Kopf stereotaxic frame, with anaesthesia maintained at the above levels. Each animal was ventilated mechanically throughout the entire procedure. Body temperature was monitored by a rectal probe and regulated by a heat lamp to 37^0C.

All surgical procedures were carried out under sterile conditions. A rostrocaudal incision was made above the right eye extending to the ear, revealing the cranium. The skull overlying lambda was drilled away, with the aid of an operating microscope, to expose the occipital lobe and the dura removed. Ibotenic acid (8)(α-amino-3-hydroxy-5-isoazoleacetic acid (Sigma)) (10mg/ml in phosphate buffered saline (PBS)) was injected using a Hamilton syringe. Co-ordinates for the injection site were determined from Bregma (AP 4.72mm; L 4.75mm; A 17^0 from vertical). The needle was lowered vertically 1.5mm through the cortex to the entorhinal region. A total volume of 0.5μl of ibotenic acid was injected at a rate of 0.1μl/ min. The needle was left in place for a further 5 mins to allow diffusion through the tissue. Following the procedure the wound was sutured and 0.5ml of saline administered subcutaneously, to

keep the animal hydrated throughout the recovery period. The animals recovered from anaesthesia in an incubator for 2 hours, and returned to the animal unit. Control animals (0 days) underwent an identical procedure but were terminated immediately after the surgery.

2.3.2 Processing of Tissue

Following the appropriate survival period, the animals were perfused transcardially under halothane anaesthesia with heparinised saline (10mls), followed by buffered 4% paraformaldehyde (20mls). The brains were post-fixed in the skull for 24 hours, to prevent artefacts due to mechanical damage, removed and post-fixed for a further 2 hours and processed for paraffin embedding. The brain was cut into two 3mm coronal blocks containing the occipital cortex for lesion assessment and the other, at the level of the lateral habenula, for visualisation of the hippocampus. The blocks were placed into plastic cassettes, dehydrated through a graded series of alcohols and cleared in xylene. This processing had been optimised previously. Following submersion of the cassettes in liquid paraffin for 24 hours at 60^0C, the blocks were embedded in paraffin and left to harden at 4^0C. 6μm coronal sections were cut on a microtome and collected onto polylysine coated slides.

2.3.3 Assessment of Lesion

2.3.3.1 Haematoxylin and Eosin Staining

Sections from the occipital cortex containing the entorhinal region were stained with haematoxylin and eosin to confirm correct needle placement and the presence of the lesion. Briefly, sections were dewaxed in histoclear, dehydrated in absolute alcohol and rinsed in water, before submersion in haematoxylin for a period of between 1-10 mins. The sections were then rinsed in water and differentiated in acidic methylated alcohol (1% HCl). Following another rinse in water the sections were placed in Scot's tap water substitute (STWS) for 1 min, rinsed again and placed in eosin (aqueous) for 3mins. After a final wash in water the sections were dehydrated through a graded series of alcohols, cleared in histoclear and coverslips mounted with histomount.

2.3.4 Immunohistochemistry

2.3.4.1 Single Labelling Immunohistochemistry

Paraffin sections were placed in an oven at 60^0C for 15 mins, dewaxed in histoclear for 30 mins and dehydrated in absolute alcohol (2x10 mins). Endogenous peroxidase was eliminated by incubating the sections with 3% H_2O_2 in methanol for 30 mins. Sections were washed in PBS (phosphate buffered saline), non-specific binding reduced using blocking agent (10% normal serum/ 2% bovine serum albumin (BSA) in PBS) for 1 hour and primary antibody was applied overnight at 4^0C. Concentrations of antibodies applied are shown in Table 4. Sections were then incubated in biotinylated secondary antibody (1:100) for 1 hour and processed with a Vectastain ABC (avidin biotin complex) standard kit. Diaminobenzadine (DAB)(Vector) was employed as the chromagen in the visualisation step (Figure 2.2). The reaction was allowed to proceed for exactly 3 mins and the reaction stopped by submerging the sections in distilled water. The sections were then thoroughly washed in water before being dehydrated through a graded series of alcohols, cleared in histoclear and coverslipped. Negative controls were generated by omission of primary antibody (Figure 2.3). Optimal working dilutions were determined for each antibody.

2.3.4.2 Double Labelling Immunohistochemistry

The same basic method as above was applied. Following the DAB stage from the first antibody, blocking solution is then applied and the next primary antibody applied. The procedure continues by addition of the appropriate secondary antibody for the second primary antibody and ABC application for 1 hour. SG was employed as the second chromagen and the sections were incubated in this for exactly 3 mins. SG appears grey in colour microscopically.

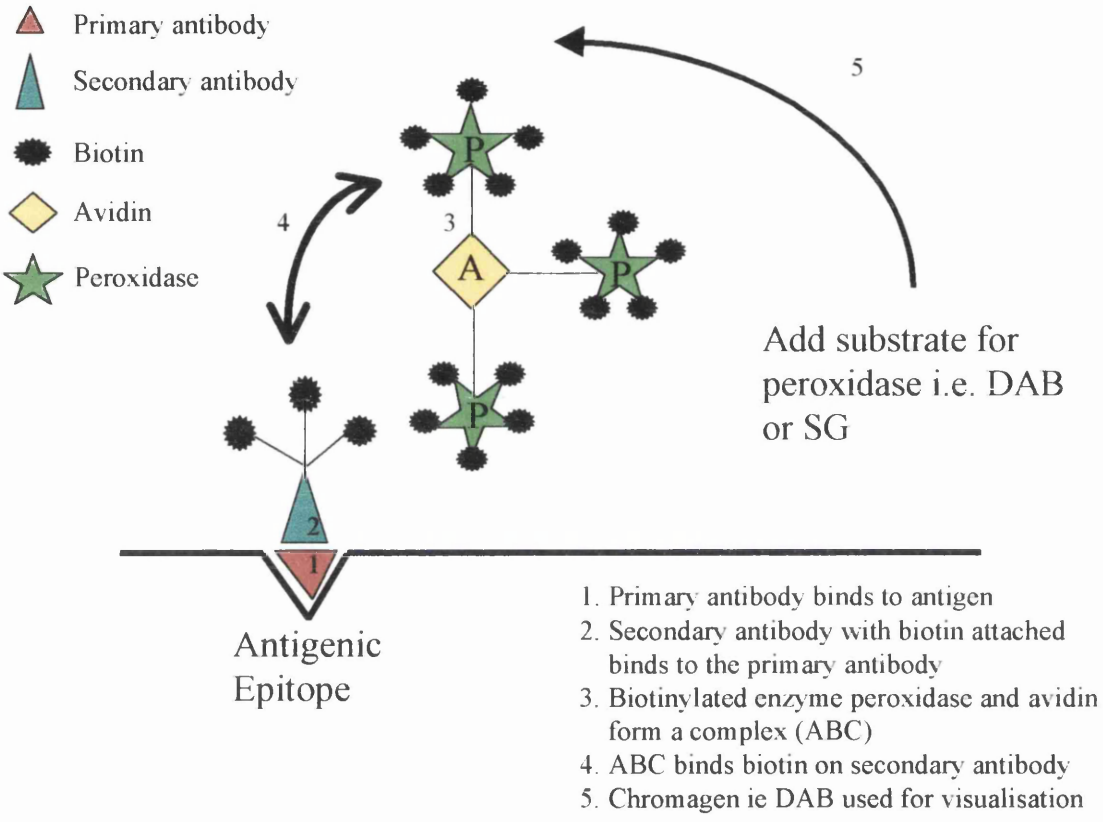

Figure 2.2 Diagram illustrating the chemical interactions involved in immunohistochemistry.

Antibody	Conc^{n} used for Immunohistochemistry	1. Primary antibody 2. Blocking serum 3. Secondary antibody	Source of primary antibody
Synaptophysin	1:200	1. Mouse monoclonal 2. Normal horse serum 3. Anti-mouse (horse)	Sigma
GAP-43	1:500	1. Mouse monoclonal 2. Normal horse serum 3. Anti-mouse (horse)	Sigma
MAP-2	1:750	1. Mouse monoclonal 2. Normal horse serum 3. Anti-mouse (horse)	Sigma
ApoE	1:5000	1. Goat polyclonal 2. Normal horse serum 3. Anti- goat (horse)	Chemicon
ApoJ	1:50	1. Goat polyclonal 2. Normal horse serum 3. Anti- goat (horse)	Chemicon
GFAP	1:1000	1. Mouse monoclonal 2. Normal horse serum 3. Anti-mouse (horse)	Sigma
LRP (Lipoprotein receptor-related protein)	1:1000	1. Rabbit polyclonal 2. Normal goat serum 3. Anti-rabbit (goat)	Gift:Dr D Strickland
LRP	1:1000	1. Rabbit polyclonal 2. Normal goat serum 3. Anti-rabbit (goat)	Gift : Dr J Herz
Tubulin	1:500	1. Mouse monoclonal 2. Normal horse serum 3. Anti-mouse (horse)	Sigma
mrf-1 (microglial response factor)	1:20	1. Rabbit polyclonal 2. Normal goat serum 3. Anti-rabbit (goat)	Gift : Dr S. Tanaka

Table 4 Data table illustrating information on the antibodies used in all studies.

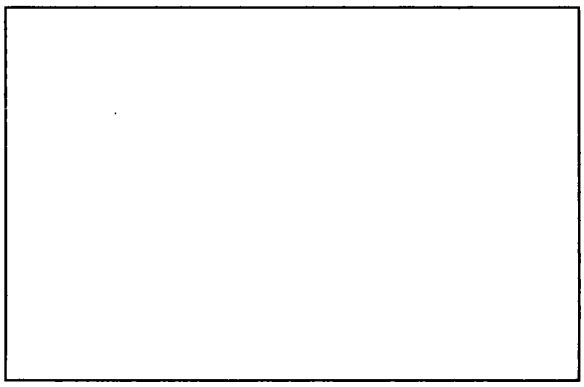

Figure 2.3 Illustrative example of a negative control for immunohistochemical staining. This was achieved by omission of the primary antibody acting as a control for non-specific staining.

2.3.4.3 Quantification of Immunohistochemistry

Multiple controls were carried out to ensure consistency of optical density measurement. Immunohistochemistry for each antibody was carried out on all sections in a series batch simultaneously to eliminate differences in the immunohistochemistry process. Relative optical density (ROD) values for immunostaining were measured using an M4 image analysis system (MCID) connected to a microscope. All measurements for a single antibody series were rigorously recorded in the dark, on the same day and at the same microscope light intensity, to eliminate light variation effects. Optical density readings were taken from the inner, middle and outer molecular layers (IML, MML, OML) of the dentate gyrus of both the ipsilateral and contralateral hippocampus using a $1cm^2$ sampling box. The box was placed randomly, six times within each layer (IML, MML and OML) and an average taken for each layer. The averages from each subject entered into a statistical program (Graphpad Prism) for analysis.

Density measurements were also taken from subcortical white matter regions to act as a control for intensity of immunohistochemical staining. ANOVA was also carried out on contralateral readings to ensure that staining was of an identical intensity in every section of a series.

2.3.5 Statistical Analysis

2.3.5.1 C57BL/6J mice

One way ANOVA was carried out on the contralateral hippocampal readings and the ipsilateral and contralateral readings were compared using a Student's paired *t*-test. All data is represented graphically as the mean +/- standard error of the mean (S.E.M.).

2.3.5.2 APOE transgenic mice (human promoter)

One way ANOVA was carried out on the contralateral optical density readings and the percentage difference between the ipsilateral and contralateral readings was compared using a Student's unpaired *t*-test. Bonferroni correction for multiple comparisons was carried out where necessary and is specified in the legend to specific graphs. All data is represented graphically as the mean +/- S.E.M.

2.3.5.3 *APOE transgenic mice (GFAP promoter)*

ANOVAR was carried out on the groups and the genotypes compared using a posthoc Student's unpaired *t*-test with Bonferroni correction for multiple comparisons. All data is represented graphically as the mean +/- S.E.M

2.3.5.4 Ageing study

ANOVAR was carried out on the data at 3 months of age and then at 1 year. The genotypes in each group were then compared using a Student's unpaired *t*-test with Bonferroni correction for multiple comparison. All data is represented graphically as the mean +/- S.E.M.

2.3.6 Quantification of IML Width

The width of the inner molecular layer was measured in GAP-43 immunostained sections to give an indication of the sprouting index. Expansion of this layer is indicative of sprouting from the commissural-associational fibre pathway, an important source for reinnervation of the molecular layers (Anderson *et al*, 1998). The MCID analyser was calibrated to measure distance in millimetres using a stage graticule and measurements were taken from the ipsilateral and contralateral IML of 0 day control animals and 90 day survival animals. ANOVAR was carried out on the

contralateral readings to ensure no significant variance in width. In C57BL/6J mice the ipsilateral and contralateral IML width at day 90 post-ECL was compared using a Student's unpaired *t*-test. The width of the IML in knockout and *APOE* ε3 and ε4 transgenic mice was compared using a Student's unpaired *t*-test with Bonferroni correction for multiple comparisons.

2.3.7 Western Blotting

2.3.7.1 Tissue Collection

The entorhinal cortex was lesioned in male C57BL/6J mice and the animals allowed to survive for periods of 0, 7 and 28 days (n= 5 per timepoint). The animals were culled by anaesthetic overdose and the brains removed. The ipsilateral and contralateral hippocampus was dissected out from each brain and rapidly frozen in liquid nitrogen.

2.3.7.2 Tissue Homogenisation and Protein Assay

The hippocampal tissue was weighed and a 5X volume of homogenisation buffer added to the eppendorf. Hippocampal homogenates were produced by homogenisation of the tissue with a polytron in a buffer (2.5mM Tris-HCl: pH6/ 3mM $MgCl_2$/ 100mM NaCl). The samples were centrifuged for 15 mins (10,000 rpm) in a bench top centrifuge and the supernatant removed for protein assay. The protein content was determined using Bio-Rad protein assay reagent. Briefly, light absorbancy measurements from bovine serum albumin standards were determined in a spectrophotometer at a wavelength of 595nm (Table 5). The homogenate samples were then loaded into the spectrophotometer and absorbancy readings taken from these. Using linear regression analysis, the protein concentrations of each sample were determined (Figure 2.4). Appropriate volumes of H_2O and Laemelli buffer were then added to the correct volume of homogenate to gain the appropriate protein concentration (10μg/ml).

2.3.7.3 Sodium Dodecyl Sulphate-Polyacrylamide Gel Electrophoresis (SDS-PAGE)

All gel apparatus was washed and cleaned in ethanol before construction. Spacers were placed between the glass plates and a tight seal was ensured before

commencement. Resolving gel (10%) was poured gently between the glass plates and a thin layer of 0.1% SDS added on top before setting. After leaving to set for 1 hour, the SDS was poured off and the stacking gel poured between the plates. The combs were carefully added making sure no air bubbles formed between the teeth and gel. The stacker was allowed to set for $1^1/_2$ hours, the combs were removed and the wells rinsed with running buffer. Finally the reservoir was connected and filled with running buffer. The samples were boiled for 5mins and immediately placed on ice. 10µg of protein was then loaded into the wells using a Hamilton syringe and separated overnight at 12mA. A prestained molecular weight marker was included onto each gel for identification of protein bands. Cross gel controls were introduced due to multiple gel running.

Table 5 Standard Curve Generation from BSA Samples

Volume BSA (µl)	Volume Water (µl)
0	800
1	799
2	798
5	795
10	790
15	785

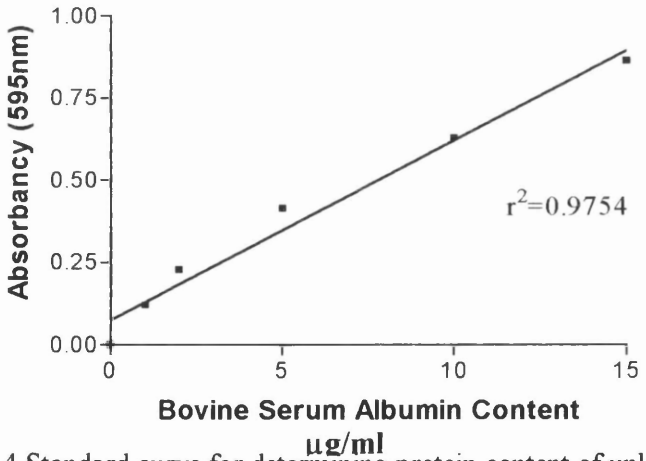

Figure 2.4 Standard curve for determining protein content of unknown samples.

2.3.7.4 Protein Transfer

Following electrophoresis, the gels were removed from between the plates and the stacking gel discarded. The gels were floated in transfer buffer (see appendix for

recipe) and the polyvinylidene flouride membrane (PVDF) (Amersham Pharmacia) placed in methanol, whilst transfer apparatus was assembled. The membrane was finally equilibriated in water and sandwiched in the apparatus (Mesh, Sponge, Card, Gel, PVDF membrane, Card, Sponge, Mesh). The apparatus was submerged into the buffer filled transfer tank ensuring the gel was nearest the negative electrode. Proteins were then transferred for 3 hours at 75volts.

2.3.7.5 Immunoblotting

Following transfer, the blots were placed overnight in blocking solution consisting of Tris-buffered saline containing 3% non-fat dried milk to reduce non-specific binding before incubation in primary antibody for 1 hour at 4^0C (Table 6). The blots were then rinsed in T-TBS (6x5mins) (0.2% tween/ TBS) before incubation in secondary antibody (horseradish peroxidase conjugated anti-mouse (Promega) and anti-goat (SAPU) 1:1000 in 3% non-fat dried milk/TBS) for 1 hour on a shaker. After vigorous washing in TBS (6x5mins), the blots were then developed using ECL chemiluminescence detection and exposed to Fuji-RX film.

Antibody	Concentration Used	Purchased
Synaptophysin	1:100,000	Sigma
GAP-43	1:5000	Sigma
ApoE	1:1000	Chemicon
Tubulin	1:1000	Sigma

Table 6 Illustrating information on the antibody concentrations for immunoblotting.

2.3.7.6 Semi-Quantification of Protein Levels and Statistical Analysis

Protein bands were assessed as relative optical density values using an M4 image analysis system (MCID). ANOVAR was carried out on the readings from the contralateral hippocampus. The ipsilateral and contralateral density readings were then compared using a Student's paired *t*-test. In determining apoE protein expression, the protein bands were compared in *APOE*ε3 and ε4 transgenic mice using a Student's unpaired *t*-test.

2.3.7.7 Reprobing of Western Blots

Following immunohistochemistry for a single antibody the membranes were stripped using stripping agent (100mM mercaptoethanol/ 2% SDS/ 625mM Tris-HCl pH6.7 in water). The membranes were agitated in this solution for 30 mins at 50^0C, following which they were placed in blocker to begin the immunoblotting steps again for a different antibody.

2.3.8 Silver Staining

2.3.8.1 Fink-Heimer Silver Staining of Degenerating Terminals

Fink-Heimer (Fink and Heimer, 1967) silver staining was employed to determine the degeneration product clearance within the lesioned hippocampus. This stain allows specific labelling of degenerating axon terminals. Paraffin sections awere initially dewaxed and dehydrated before pretreatment with 0.1% potassium permangate ($KMnO_4$) to produce a distinctive brown hue, following which they were incubated in decolourizing solution (1% hydroquinone/ 1% oxalic acid) until colourless in appearance. The tissue was then processed through a series of silver impregnation steps (0.5% uranyl nitrate ($UO_2(NO_3)_2$/ 2.5% $AgNO_3$) in which silver particles were deposited onto the tissue. Following a third impregnation step in ammonical silver nitrate, reducing agent (10% formalin/ 1% citric acid/ 95% alcohol) was then used to develop these silver particles. The sections were then dehydrated through a graded series of alcohols, cleared in histoclear and coverslips mounted.

2.3.8.2 Semi-Quantification of Silver Staining

Levels of silver labelled degeneration products within the hippocampus were assessed semi-quantitatively using a scoring method (0= no staining, 1= minimal, 2= moderate and 3= extensive) and differences between *APOE*ε3 and ε4 mice compared using a Mann-Whitney test for comparing non-parametric data. The data is represented graphically using the median +/- standard deviation (S.D.)

2.4 Organotypic Hippocampal Slice Culture

2.4.1 Preparation of Hippocampal Slices

2.4.1.1 Preparation of Cell Wells

All procedures are carried out under aseptic conditions, in a culture cabinet, unless otherwise stated. Cell culture dishes were prepared approximately an hour before culturing the hippocampal slices to allow the medium to attain the correct temperature. Briefly, membrane inserts (0.4μm pore size, Becton Dickinson) were inserted into the culture dish wells using only four wells per plate to avoid contamination. 1ml of culture medium consisting of 96% minimum essential medium with balanced salt solution (GIBCO), 6.5mg/ml glucose, penicillin/streptomycin (50 U/ml), glutamax (0.5%) and the serum substitute TCM (final concentration 2%; ICN Biomedicals) was added to each cell well between the insert and culture well (derived from that of Teter *et al*, 1999). This interface method was derived from that of Stoppini *et al* (1991), in which the slice is not bathed in medium but forms an interface with the membrane insert which being in contact with the culture medium allows diffusion of nutrients. The prepared plates were then transferred to an incubator to equilibriate to the desired temperature before culturing commenced (5% CO_2/ 37^0C).

2.4.1.2 Tissue Harvesting

Mice were derived from a breeding colony of C57BL/6J or GFAP transgenic mice (knockout v ε3 v ε4) maintained in an animal unit in the University of Glasgow. Male, 7 day old neonatal mouse pups were anaesthetised by intra-peritoneal injection of euthatal and their brains removed rapidly using curved forceps. Tail tips were collected from the pups for *APOE* genotyping. The cerebellum and forebrain were removed and the brain adhered, forebrain down, onto a vibratome stage and fixed into a vibraslicer. The tissue was then submerged in ice cold Geys balanced salt solution (Life Technologies) for slides and oxygenated using a pipe connected to an oxygen cylinder. The reduced temperature and oxygenation kept the slices living until fully cultured. 300μm hippocampal slices were collected into a petri dish on ice, containing ice cold, oxygenated Geys solution. Approximately 8 slices were collected from each brain.

2.4.1.3 Culturing of Hippocampal Slices

The excised hippocampi were then transported to the clean hood and placed onto a black surface in the petri dish for visualisation. A sterile spatula was then used to retrieve a slice from the petri dish and placed into a cell well by washing it off with a drop of Geys salt solution using a Pasteur pipette. The slice was then orientated within the cell well and the excess Geys medium surrounding the slice removed using a pipette. Two slices were placed in each cell well. The plates were then returned to the incubator. The medium was changed every 3 DIV (days *in vitro*) for the desired culture period. Cultures were maintained for 7 or 18 DIV in C57BL/6J studies (n=5/timepoint) and in transgenic studies (n=8/timepoint).

Following the desired culture period, the medium was removed and the slices submersion fixed in 4% paraformaldehyde for 2 hours, at which point the slices float from their membrane. The fixative was then removed, phosphate buffer added and the tissue stored at 4^0C.

2.4.2 Hippocampal Slice Immunohistochemistry

2.4.2.1 Immunohistochemistry

The slices were transferred into a 24 welled culture dish (1 slice/ well) and permeabilised by submersion in PBS containing 0.2% Triton X-100 for 1 hour. Non-specific binding was eliminated by applying blocking solution (10% normal serum/ 2% BSA in PBS) and the tissue was incubated overnight in primary antibody (made in blocking serum) (Table 7). Following 3X5 min rinses in PBS, biotinylated secondary antibody was applied for 1 hour and processed with a Vectastain ABC standard kit. Diaminobenzadine was employed as the chromagen in the visualisation step. The slices were then dehydrated through a graded series of alcohols (30 mins in each of 70%, 90%, 100% X2), cleared in histoclear for 10 mins, mounted onto slides and coverslipped.

Antibody	Concentration Used	1. Primary antibody 2. Blocking serum 3. Secondary antibody	Primary antibody supplied
Synaptophysin	1:2000	1. Mouse monoclonal 2. Normal horse serum 3. Anti-mouse	Sigma
GAP-43	1:2000	1.Mouse monoclonal 2. Normal horse serum 3. Anti-mouse	Sigma
MAP-2	1:5000	1. Mouse monoclonal 2. Normal horse serum 3. Anti-mouse	Sigma
ApoE	1:1000	1.Goat polyclonal 2. Normal horse serum 3. Anti-goat	Chemicon
ApoJ	1:1000	1. Goat polyclonal 2. Normal horse serum 3. Anti-goat	Chemicon

Table 7 Table showing concentration of antibodies used in hippocampal slices

2.4.2.2 Quantification of Immunohistochemistry and Statistical Analysis

Relative optical density (ROD) values for immunostaining were measured using an image analyser (MCID) connected to a microscope. All controls were applied as for immunohistochemistry on sections. Optical density readings were collected from the dentate molecular layers and from CA1 pyramidal cell layer to ensure consistency of immunostaining. Ten readings were collected randomly across the expanse of the molecular layer using a $1cm^2$ sampling box, and an average of the ten readings taken. In C57BL6 derived tissue, optical density readings were compared in the 7 and 18 day slices using a Student's unpaired *t*-test. In the tissue derived from the transgenic mouse lines, optical density measurements were compared in *APOE* ε3, ε4 and knock-out animals also using ANOVAR with a posthoc Student's unpaired *t*-test with Bonferroni correction for multiple comparisons.

2.4.3 Herpes Simplex Virus 1716 as a Viral Vector

2.4.3.1 Production of Genetically Modified Herpes Simplex Virus 1716

The genetically modified virus employed in this study was produced in the laboratory of Prof Moira Brown (Southern General Hospital). Briefly the virus was made by targeting the ICP34.5 protein which is a specific determinant of virulence. ICP34.5 null mutants are avirulent unlike the wildtype virus and may only replicate in cells actively undergoing proliferation/ differentiation. The virus employed in this study possesses a green fluorescent protein (GFP) reporter gene that results in the expression of GFP if the virus is replicated within the cell. Other reporter genes have also been used, including luciferase and β-galactosidase, although not employed in this study.

2.4.3.2 Addition of Herpes Simplex Virus 1716 to Hippocampal Slice Preparations

Hippocampal slices were prepared from C57BL/6J wild-type mice and *APOE*ε3 transgenic mice as previously described and transported to the Neurovirology Unit at the Southern General Hospital. All virus handling was carried out within a category 2 culture hood. Following virus use, all instruments were submerged in detergent and the culture hood exposed to U.V. radiation for at least half an hour to exterminate any stray virus particles. 10^6 and 10^5 virus particles were diluted in culture medium and added directly onto the slices as a single dose of 10μl of the mixture pipetted directly onto the surface of the slices. The slices were then returned to an incubator and maintained for a period of 3, 7, 12 or 18 DIV with changing of the medium every 3 DIV. Control cases received no infection by HSV1716 virus. GFP labelled wild-type virus was also employed.

2.4.3.3 Fluorescence Microscopy

Following the appropriate survival period, the slices were submersion fixed in 4% paraformaldehyde for 2 hours. The slices were mounted onto glass slides and coverslipped, submerged in hardening medium or the slices were removed unfixed, attached to the membrane and visualised without the addition of a coverslip. A fluorescence microscope was used to visualise the GFP and the image captured using a camera attached to the microscope.

2.5 Microtubule Binding

2.5.1 Preparation of Lipidated ApoE

Human plasma samples were obtained from human *APOE* ε3/3 and ε4/4 donors, pooled and processed to isolate high density lipoprotein (HDL) with the appropriate apoE isoform attached (in collaboration with Dr Muriel Caslake, Dept of Pathological Biochemistry, Glasgow Royal Infirmary). To obtain HDL bound apoE, the plasma samples were cushioned with potassium bromide (KBr) solution (density 1.063g/ml) and centrifuged overnight at 39,000 rpm at 15^{0}C. The intermediate and low-density lipoprotein component (IDL, LDL) were discarded (1.006-1.063g/ml) KBr added again and centrifuged for a further 36 hours to give HDL at a density of 1.063-1.21g/ml. All samples were then dialysed and concentrated. The apoE concentration of each of these samples was confirmed using an ELISA and the HDL and cholesterol concentrations.

2.5.2 Microtubule Associated Protein Assay

2.5.2.1 Microtubule Assembly

Tubulin protein is reconstituted in 210μl of tubulin dilution buffer containing GTP solution (5mg/ml), divided into 10μl aliquots and stored at –70^{0}C for future use. An aliquot of this tubulin was thawed out and transferred to ice adding 2.5μl of microtubule cushion buffer and incubated at 35^{0}C for exactly 20 mins. 180μl of tubulin dilution buffer and 40μM of taxol (stabilises microtubules) were mixed together and incubated at 35^{0}C. 180μl of this solution was then added to the polymerised tubulin and mixed thoroughly but gently. The microtubules were now at a concentration of 1x10^{12}/ml and 5-10μm in length.

2.5.2.2 Microtubule Binding Activity

A preliminary experiment to determine if a protein of interest shows microtubule binding activity is described (Table 8).

Eppendorf	Protein	Microtubules (μl)	TDB/taxol solution (μl)
1	MAP-2 (4μl)	20	26
2	BSA (1.5μl)	20	28.5
3	0	20	30
4	MAP-2 (4μl)	0	46
5	BSA (1.5μl)	0	48.5
6	Test Protein (ApoE):5μg/ml/20μg/ml	20	50μl final volume

Table 8 Initial test for microtubule binding activity

These reactions were then left at room temperature for 20 mins to attain equilibrium. 100μl of cushion buffer was placed in eight ultracentrifuge tubes at room temperature and 20μM taxol added to each tube. The reaction product was carefully pipetted on top of the corresponding cushion. This mixture was then centrifuged at 48,000 rpm (100,000 xg) at room temperature for 20 mins.

The supernatant was removed and a volume of 50μl removed, equal to the original reaction volume. To this, an equal volume of 2xSDS gel loading buffer was added (100mM Tris pH 6.8, 5% SDS, 10% beta-mercaptoethanol, 20% glycerol, 0.2% bromophenol blue). The pellet fraction can then simply be resuspended in 1xSDS sample buffer. The supernatant and pellet fractions were then separated on an SDS-PAGE gel (see Western Blotting protocol), transferred and visualised using a polyclonal antibody to apoE (1:1000) (with goat HRP secondary 1:1000) and detected using an enhanced chemiluminescence detection system (ECL). The presence of microtubules in the pellet fraction and absence in the supernatant was confirmed using tubulin immunohistochemistry (1:1000).

2.5.2.3 Analysis of Microtubular Binding

Multiple microtubule preparations containing either apoE E3/HDL or apoE E4/HDL at concentrations of 5μg/ml and 20μg/ml were then run on a gel as described and apoE immunohistochemistry performed. For analysis purposes it was initially determined whether apoE was present in the supernatant or pellet fraction. Any protein that is microtubule bound should be present within the pellet fraction. Any unbound protein remains within the supernatant fraction. Protein bands were then analysed as relative optical density values using a $1cm^2$ sampling box. Optical density values from the pellet fraction were then compared between apoE E3 and apoE E4 containing samples using a Student's unpaired *t*-test.

2.5.3 Fluorescent Microtubule Binding

2.5.3.1 Preparation of Taxol Stabilized Fluorescent Microtubules

The correct fluorescence intensity of the microtubule assemblies should be determined before beginning this experiment. All components of this kit were stored at -70^0C. To obtain fluorescent microtubules with a final labelling stoichiometry of 0.33 labels per tubulin heterodimer, one aliquot of rhodamine labelled tubulin (2μl) was thawed and placed on ice and was diluted in 4μl of unlabelled tubulin. This solution was divided into 2μl aliquots and frozen for future use. 20μl of microtubule cushion buffer and 40μl of general tubulin buffer were then added together to produce a solution called polymerisation buffer and this solution was placed on ice. 2μl of the polymerisation buffer was then added to the 0.33 tubulin and incubated at 35^0C for 20 mins. While the tubulin was polymerising 500μl of general tubulin buffer was placed at 35^0C and after 15 mins at this temperature 5μl of taxol was added (20μM). This solution was stored at room temperature and labelled taxol/microtubule buffer. The polymerised tubulin was removed from the incubator and immediately had 100μl of taxol/microtubule buffer added mixing thoroughly but gently, using a Pasteur pipette. This preparation should now contain a population of taxol stabilized microtubules that average 6.5μm in length at a concentration of $7x10^{10}$/ml. The microtubules can then be visualised microscopically by diluting 1μl of the microtubule preparation in 10μl of taxol/microtubule buffer containing 20μl of antifade solution. This preparation is then smeared onto a slide, coverslipped and visualised using fluorescence microscopy.

2.5.3.2 Addition of Lipidated Human ApoE E3 and E4 to Microtubule Preparations

After preparing a population of stabilised microtubules, the solution was split so the apoE isoforms were being tested in a homogenous population of microtubules. This solution was incubated with HDL lipidated apoE E3 or E4 derived from human CSF samples at a concentration of 5μg/ml or 30μg/ml for 20 mins at room temperature to allow binding to occur.

2.5.3.3 Immunohistochemistry on Microtubule Preparations

An apoE polyclonal antibody was added to the mixture at a concentration of 1:100 and incubated for 30 mins and the goat secondary antibody applied for 30 mins proceeding this (1:100). Avidin D fluorescein was then added to the preparation for 30 mins at a concentration of 1:100. To visualise microscopically 1μl of this final solution was dissolved in 10μl of taxol/microtubule buffer and 10μl of antifade and smeared onto a microscopy slide. The microtubules appear red (rhodamine) and the bound apoE appears green (fluorescein).

2.5.3.4 Confocal Image Analysis

Microtubules with bound apoE were analysed qualitatively using confocal microscopy.

Chapter III

Investigation of ApoE in Relation to Degeneration/ Regeneration Using a Mouse Model of Entorhinal Cortex Lesion

3.1 Introduction

ApoE has been shown to play a role in acute brain injury in humans and in animal models of brain injury (Horsburgh *et al*, 1996, 1999). However, the role of this protein in chronic brain injury is less well understood. At the outset of this thesis, no models of chronic brain injury had been established. However, in rats, the entorhinal cortex lesion model was well characterised as a model of degeneration and regeneration (Cotman *et al*, 1975, 1976; Steward and Vinsant, 1983). It was realised that following a suitable recovery period, certain fibre systems were capable of sprouting to compensate for the primary deafferentation (Steward and Vinsant *et al*, 1976, 1983). The hypothesis in this study was that apoE would be upregulated post-ECL and be associated with the plasticity response at long-term survival periods.

3.2 Aims

(1) to establish a model of hippocampal degeneration and regeneration by entorhinal cortex lesion (ECL)

(2) to define temporal alterations in apoE and related proteins after ECL

3.3 Materials and Methods

3.3.1 Entorhinal cortex lesion

The entorhinal cortex was lesioned using male C57BL/6J mice (12 weeks old, weighing approximately 30g) (as described in chapter II). The mice were allowed to survive of 1, 3, 7, 28 or 90 days (n=8 per timepoint). Control animals underwent an identical procedure but were terminated immediately after the procedure. Sections from the entorhinal cortex were histologically stained using haematoxylin and eosin to confirm lesion placement. Immunohistochemistry for synaptophysin, GAP-43, apoE, apoJ, LRP, MAP-2, GFAP and mrf-1 was performed on hippocampal sections. Double labelling was also performed to determine cellular localisation of apoE and apoJ. Fink Heimer silver staining was carried out to assess terminal degeneration products and to determine a time-course for clearance. IML width was measured in GAP-43 sections and analysed as outlined in chapter II.

In a separate group, mice underwent ECL to generate tissue for Western blotting (n=5/ timepoint). Following the appropriate survival periods of 0, 7 and 28 days the ipsilateral and contralateral hippocampus were harvested and frozen in liquid nitrogen. 10μg of protein was separated by gel electrophoresis and immunoblotting for synaptophysin, GAP-43 and apoE was carried out.

3.3.2 Quantification of immunohistochemistry and statistical analysis

Relative optical density values for immunostaining were collected from the inner, middle and outer molecular layers from both the ipsilateral and contralateral hippocampus using an M4 image analysis system connected to a microscope. Six optical density readings were collected from each layer using a $1cm^2$ sampling box and an average taken. One way analysis of variance (ANOVA) was carried out on the contralateral hippocampal readings and the ipsilateral and contralateral readings compared using a Student's paired *t*-test. Readings were taken from a reference area to ensure consistency of staining. Western blots were also analysed by collecting optical density measurements. Data is represented graphically using the mean +/– S.E.M. (standard error of the mean).

3.4 Results

3.4.1 Characterisation of a mouse model of entorhinal cortex lesion

3.4.1.1 Setting up the model: technical considerations

The C57BL/6J mouse strain was chosen because it is the background strain of the transgenic lines to be employed in the following studies. Primarily, the method to lesion the cortex was considered. In rats, a number of methods were available including aspiration and electrolysis. Pilot studies were initially carried out to determine the stereotaxic placement of the injection. Precise stereotaxic co-ordinates were determined from the mouse brain atlas and transposed onto the surface of the skull. The final location for the injection was chosen on the basis that it was a site which would not incorporate the hippocampus itself when the lesion was fully developed and the entorhinal cortex is at its largest in size in a coronal view. The concentration of ibotenic acid employed was determined from a study by Cho and Jaffard (1995). Differing amounts of ibotenic acid were injected into the brain (0.5μl and 1μl) to produce the optimal lesion.

Concentration curves were generated for all antibodies employed in this study and the dilution chosen which optimally displayed the protein alterations. Synaptophysin (a synaptic vesicle marker) and GAP-43 (presynaptic membrane protein also found on growth cones) were chosen to assess the temporal profile of degeneration and regeneration because they would most accurately highlight not only synaptic loss and fibre degeneration respectively, but also synaptogenesis and fibre sprouting. These antibodies had been employed and validated in previous rat studies of CNS plasticity. When the pilot tissue was stained with these antibodies they accurately reflected degeneration and reinnervation within the molecular layers of the dentate gyrus. The MAP-2 antibody was chosen to highlight cytoskeletal changes and was included because it would be relevant in the future studies of apoE genotype and mictrotubule interaction.

3.4.1.2 Lesion assessment

Haematoxylin and eosin staining was used to assess lesion placement within the entorhinal cortex. The lesion appeared as an area of pallor, engulfing the entire entorhinal region in which all cell types were pyknotic in appearance (Figure 3.1).

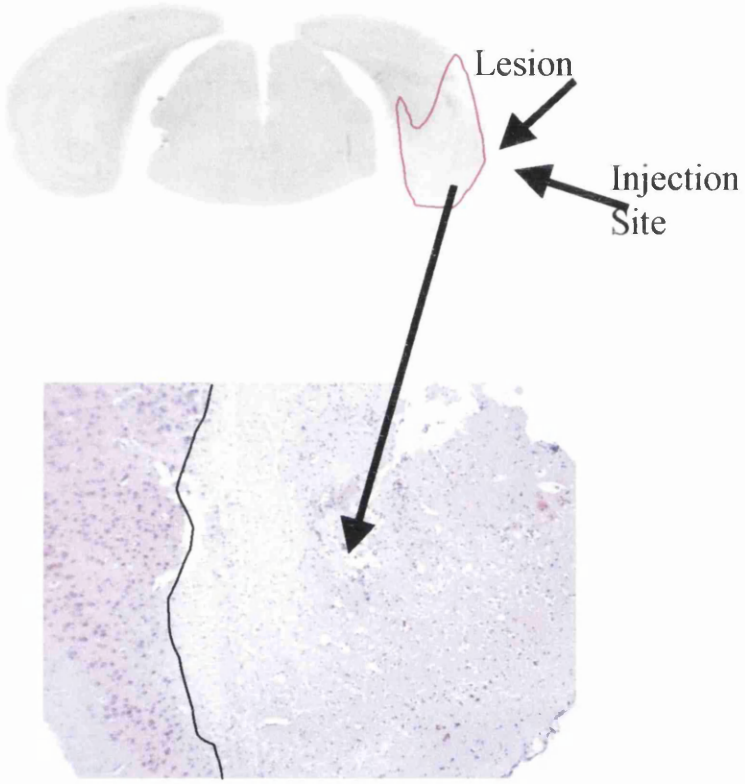

Figure 3.1 **Entorhinal cortex lesion**

Illustrative example of the entorhinal cortex lesion as shown in haematoxylin and eosin histologically stained sections. The lesion was induced by intracortical injection of ibotenic acid at specific stereotactic co-ordinates. This produces excitotoxic cell death and a change in pallor within the cortex. This pattern of staining is typical of that produced throughout the studies regardless of genotype.

More sections were taken rostral to the injection site and histologically stained to ensure the lesion did not directly involve the hippocampus. If no visible lesion was apparent, the animal was excluded from the study although this was extremely rare.

3.4.2 Temporal Profile of Degeneration and Reinnervation

3.4.2.1 Alterations in synaptophysin immunoreactivity

Synaptophysin immunoreactivity displayed a time-dependent loss and increases in synapse density within the hippocampus following injury. Synaptophysin immunoreactivity in unlesioned animals displayed a regular dense pattern of staining throughout all regions of the hippocampus. The molecular layers take on a trilaminar pattern with the inner staining most intensely. After ECL, synaptic alterations were most apparent within the MML and OML with very few alterations within the IML. Synaptophysin immunoreactivity in the MML decreased gradually and at day 7 the ipsilateral MML showed a significant decrease in staining when compared to the contralateral hippocampus ($p<0.0001$). Maximal synaptic loss was achieved by day 28 post-ECL ($p<0.0001$) where levels were approximately 40% of control levels (Figure 3.2 and 3.4). At day 90 synaptophysin immunoreactivity in the ipsilateral MML had returned towards baseline levels and was not significantly different to the contralateral hippocampus. The optical density was approximately 80% of control levels at this time. Synaptic decline within the OML was not observed until day 28, when the ipsilateral hippocampus displayed a slight decrease compared to the contralateral side ($p<0.05$). At 90 days post-ECL the ipsilateral hippocampus staining had increased and was not significantly different to that in the contralateral hippocampus. Analysis of variance on the contralateral hippocampal density measurements revealed no statistically significant variance and therefore all significant changes observed in the paired *t*-tests were attributed to alterations in the ipsilateral hippocampus.

Western blotting data revealed that synaptophysin levels were similar in the ipsilateral and contralateral hippocampus. At day 7 synaptophysin levels had decreased by 25% in the ipsilateral hippocampus ($p<0.01$) (Figure 3.5). By day 28 synaptophysin immunoreactivity had increased within the ipsilateral hippocampus and was approximately 25% greater than baseline control values. These data did not accurately reflect alterations within the small discrete regions of the molecular layers. These data highlights the inability Western blotting to analyse small localised alterations of proteins.

3.4.2.2 Alterations in growth associated protein-43 (GAP-43) immunoreactivity

GAP-43 immunoreactivity displayed a time-dependent loss and gain of synapses within the hippocampus. In unlesioned control animals, GAP-43 labelled the hippocampus intensely compared to other brain regions. The IML was most intensely stained, with the outer two thirds stained equally. The most significant alterations occurred within the outer two thirds of the molecular layer. Within the MML fibre density progressively decreased and maximal fibre loss was achieved at day 7 post-ECL, where GAP-43 levels were found to be approximately 25% of control levels and 40% of contralateral levels ($p<0.01$) (Figure 3.3 and 3.4). At day 90 post-ECL, GAP-43 immunoreactivity increased towards baseline levels and there was no significant difference between the ipsilateral and contralateral hippocampus. GAP-43 levels at this time were approximately 70% of control values. The OML exhibited a similar pattern of alterations to the MML but were delayed in comparison. At day 90 post-ECL ipsilateral hippocampal GAP-43 staining had increased and was not significantly different to that in the contralateral hippocampus. The IML did not exhibit any loss of fibre density, but at day 90 post-ECL fibre density increased and was significantly greater than that of the contralateral hippocampus ($p<0.05$). Analysis of variance on the contralateral hippocampal density measurements revealed no statistically significant variance and therefore all significant changes observed in the paired *t*-tests were attributed to alterations in the ipsilateral hippocampus.

Western blotting data revealed GAP-43 levels were similar in the ipsilateral and contralateral hippocampus. At day 7, GAP-43 levels had decreased by 40% in the ipsilateral hippocampus compared to the contralateral hippocampus ($p<0.01$) (Figure 3.5). At day 28, GAP-43 immunoreactivity had increased within the ipsilateral hippocampus and was approximately 25% greater than baseline control values. These data did not accurately reflect alterations within the small discrete regions of the molecular layers and are more a representation of GAP-43 behaviour within the entire hippocampus.

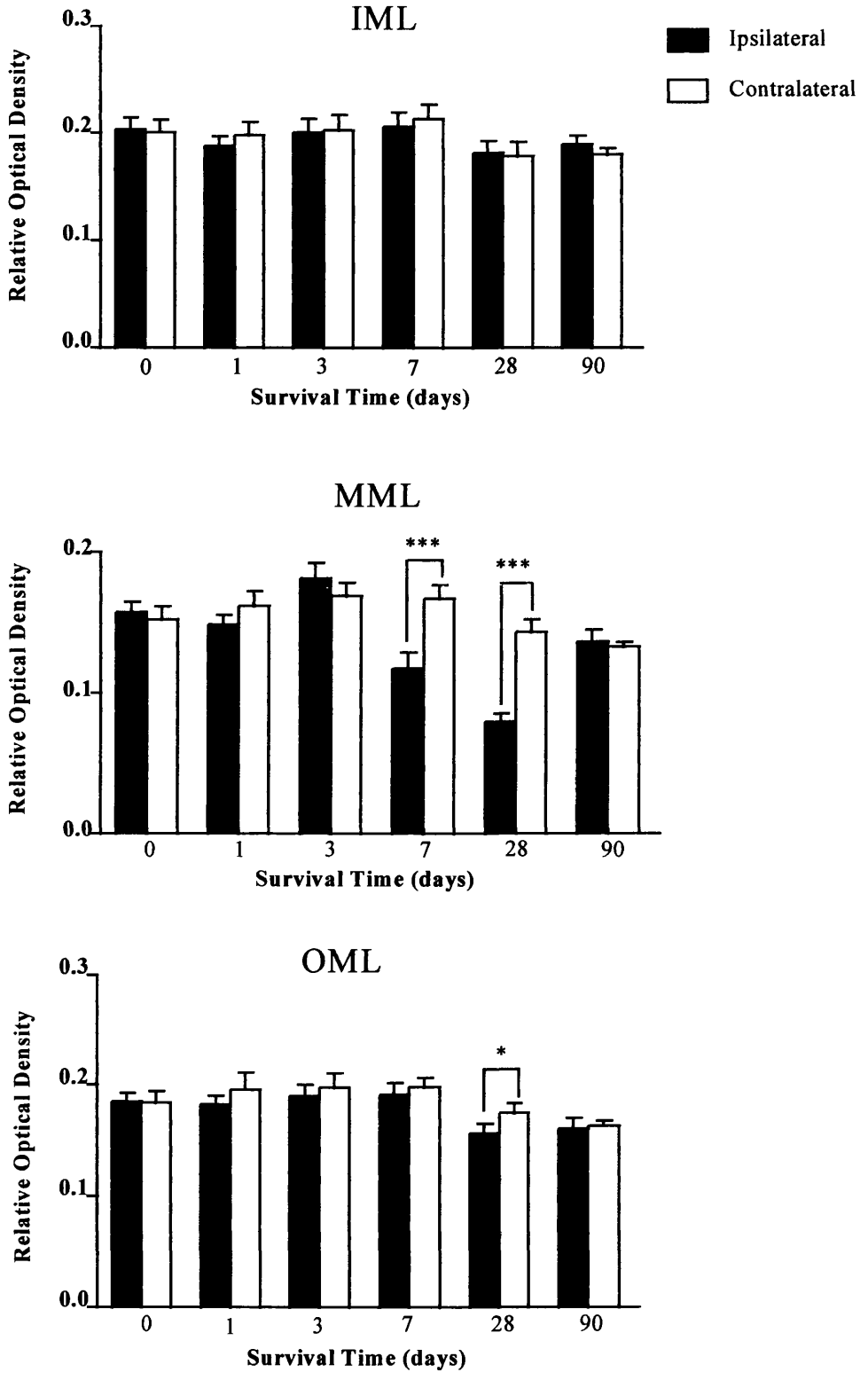

Figure 3.2 Quantification of synaptophysin immunoreactivity within the inner, middle and outer molecular layers (IML, MML, OML) of the hippocampal dentate gyrus at 0, 1, 3, 7, 28 and 90 days post-lesion measured as relative optical density values. The ipsilateral and contralateral optical density measurements were compared using a Student's paired *t*-test. *****p<0.0001 and *p<0.05**

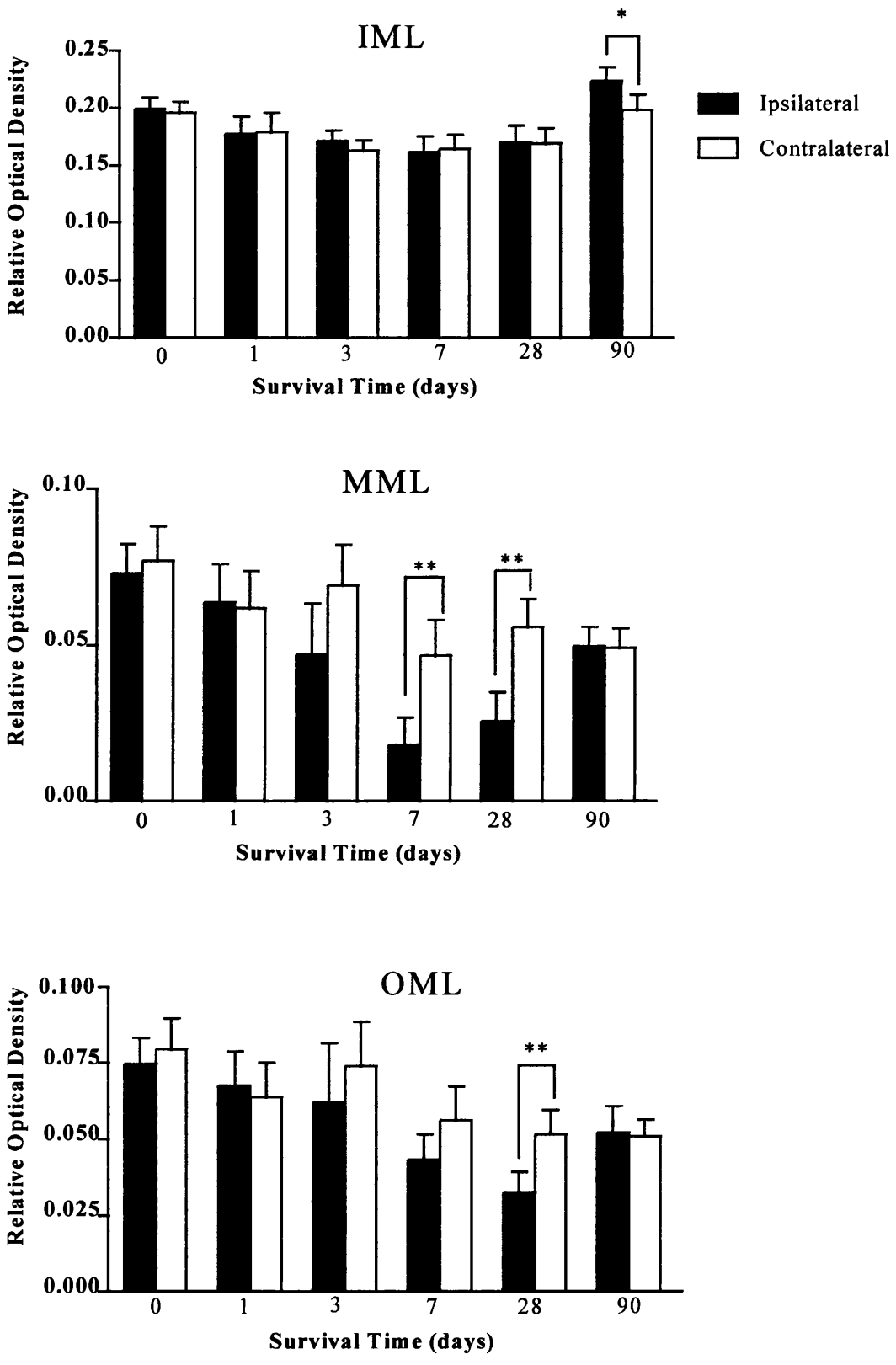

Figure 3.3 Quantification of GAP-43 immunoreactivity within the inner, middle and outer molecular layers (IML, MML, OML) of the hippocampal dentate gyrus at 0, 1, 3, 7, 28 and 90 days post-lesion measured as relative optical density values. The ipsilateral and contralateral optical density measurements were compared using a Student's paired *t*-test. ****p<0.01 and *p<0.05**

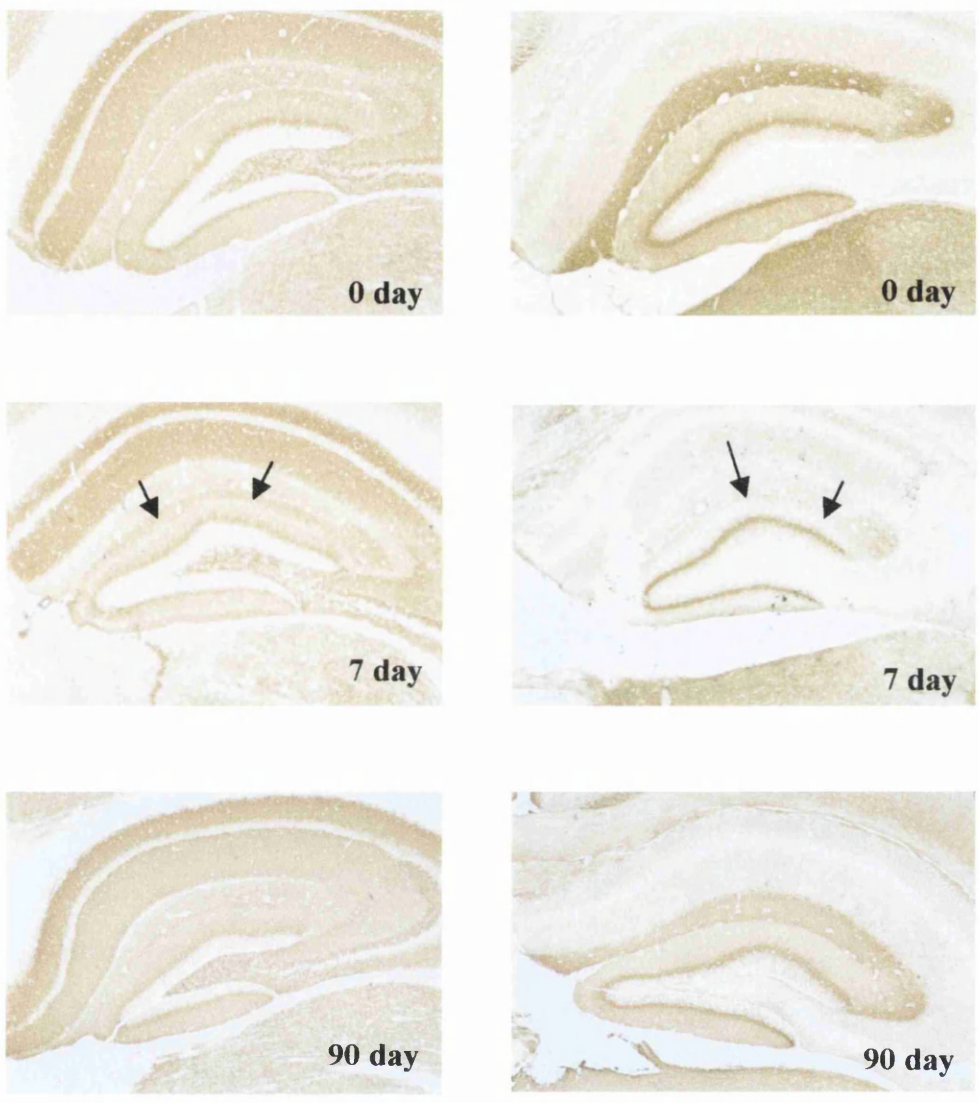

Figure 3.4 **Degeneration and regeneration post-ECL**

Illustrative examples of ipsilateral synaptophysin and GAP-43 immunoreactivity at 0, 7 and 90 days post-ECL within the hippocampal dentate gyrus. Contralateral immunoreactivity (not shown) remained relatively unchanged post-ECL and is similar to that shown in the 0 day control illustrations. The arrows indicate the regions affected by the lesion. x50 magnification

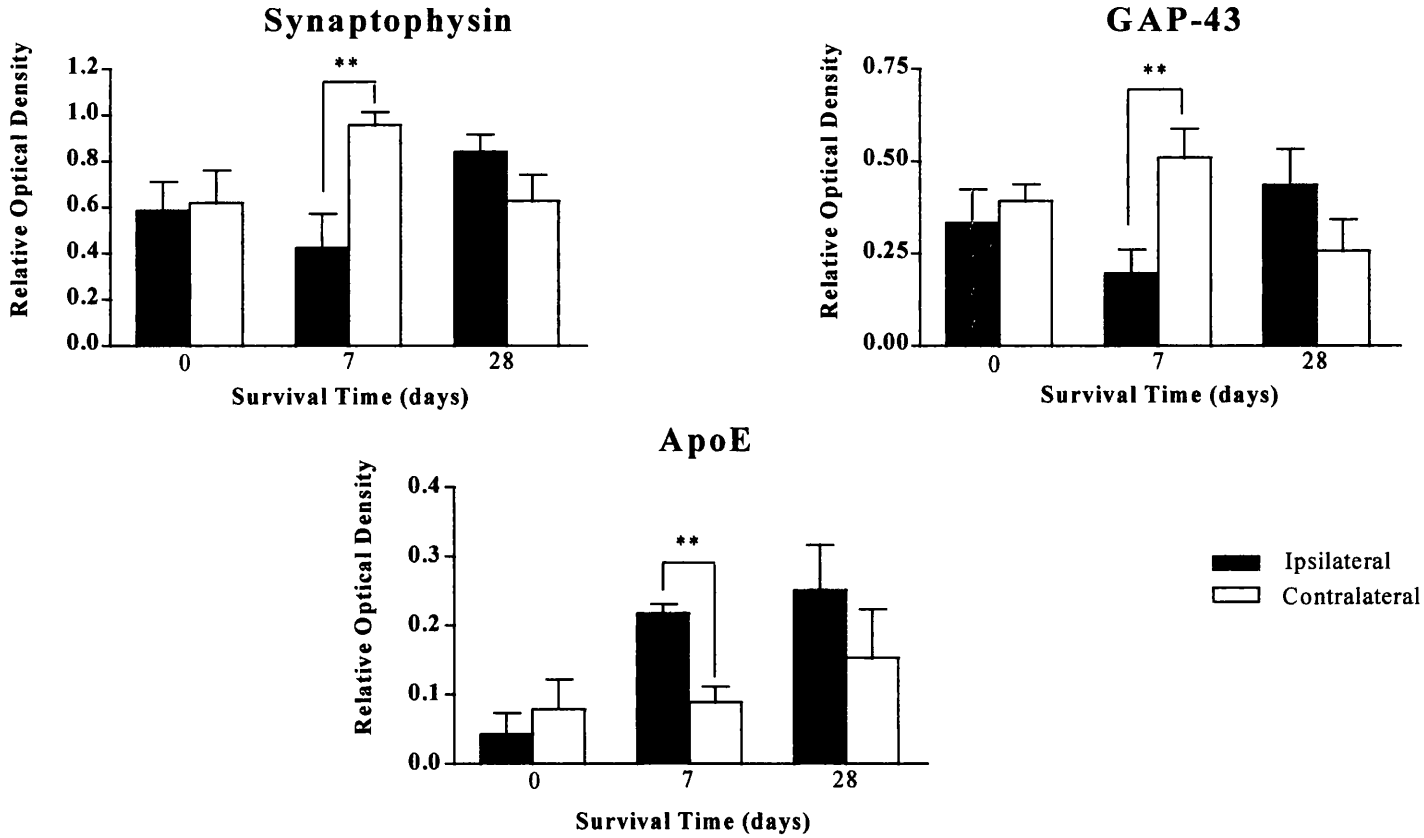

Figure 3.5 Quantification of Western blots of tissue from C57BL/6J wild-type animals at days 0, 7 and 28 days post-lesion immunolabelled with synaptophysin, GAP-43 and apoE and assessed as relative optical density values. Ipsilateral and contralateral hippocampal immunoreactivity was compared using a Student's paired *t*-test. **$p<0.01$

3.4.2.3 IML width alterations post-ECL

The IML width was measured at days 0 and 90 post-ECL in GAP-43 immunostained sections to determine if sprouting from the commissural-associational fibres had occurred. In 0 day control animals the width of the IML was similar in the ipsilateral and contralateral hippocampus (55μm). At day 90 post-ECL the width of the ipsilateral IML had expanded by approximately 30% compared to the contralateral IML (90μm) ($p<0.0001$) (Figure 3.6).

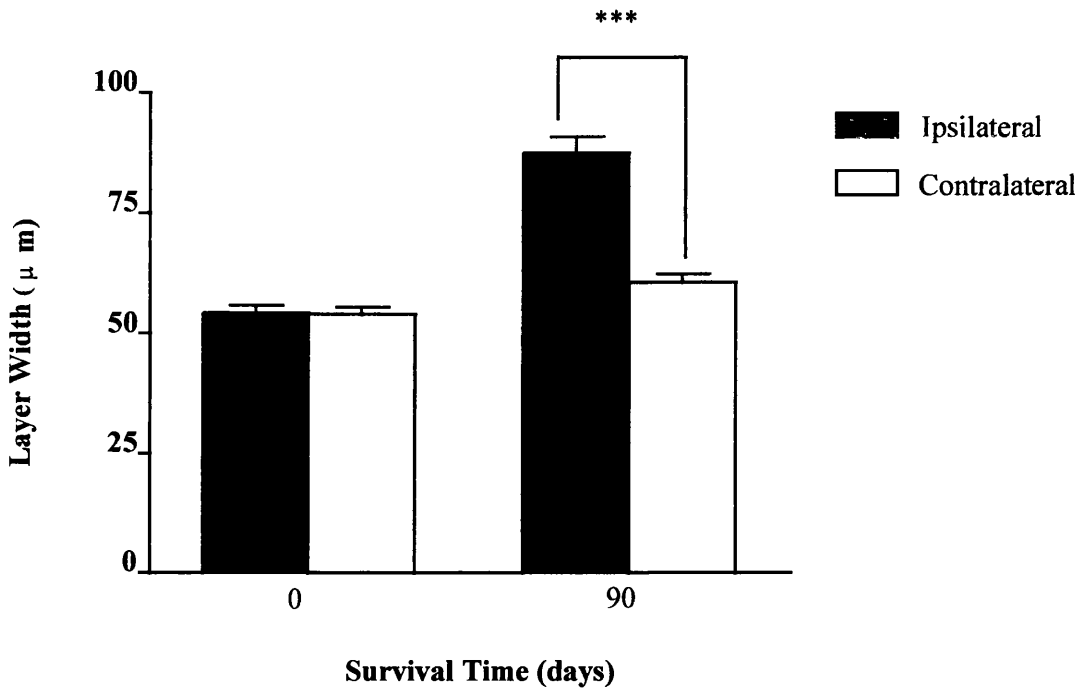

Figure 3.6 Quantification of the width of the inner molecular layer (IML) of the dentate gyrus as assessed in GAP-43 immunostained section. Expansion of this layer gives an indication of the sprouting index from the commissural-associational fibre pathway. The ipsilateral and contralateral IML width was compared using a Student's paired *t*-test. *****p<0.0001**

3.4.3 Apolipoprotein Response to Injury

3.4.3.1 Apolipoprotein E

Cellular immunoreactivity

In unlesioned control animals only faint neuropil staining was present and was similar within both the ipsilateral and contralateral hippocampus. No neuronal cell body staining was present at any time. At day 7 post-ECL, intense cellular apoE immunoreactivity was noted which was exclusively confined to cells that had the morphological appearance of glia (Figure 3.9). At day 28 post-ECL, very little cellular apoE immunoreactivity was evident. No cellular immunostaining was present by day 90 post-ECL. The contralateral hippocampus exhibited no increase in glial immunoreactivity. Labelling with GFAP (astrocytes) and mrf-1 (microglia), indicated a marked astrocytic and microglial proliferation response within the injured hippocampus. Double labelling of adjacent sections at day 7 post-ECL with GFAP and apoE confirmed that apoE was localised to some GFAP-positive astrocytes. Double labelling with apoE and mrf-1 indicated localisation of apoE in microglia (Figure 3.10).

Neuropil immunoreactivity

Alterations in neuropil apoE immunoreactivity were measured within the molecular layers as relative optical density values. By day 1 post-ECL, apoE immunoreactivity increased within the MML and OML of the ipsilateral hippocampus by approximately 20% ($p<0.05$ and $p<0.01$ respectively) compared to the contralateral hippocampus (Figure 3.7 and 3.9). Levels remained relatively elevated within these layers compared to control values, however the contralateral hippocampal apoE levels increased also so there was no statistically significant difference between the ipsilateral and contralateral hippocampus. At day 28, apoE immunoreactivity had declined to below baseline levels in all layers. At day 90 post-ECL, only within the OML neuropil, apoE had increased to the highest levels observed at any time-point. At that time apoE immunoreactivity had increased to approximately 40% above baseline levels. This was significantly different to the immunoreactivity in the contralateral hippocampus ($p<0.0001$). ApoE increased within the IML at day 7 post-ECL to approximately

20% above baseline levels and then declined to below baseline levels by day 28. ANOVA revealed variance in both hemispheres. Contralateral apoE may be elevated slightly because a small percentage of entorhinal fibres project contralaterally.

Western blotting data revealed apoE levels were similar in the ipsilateral and contralateral hippocampus. At day 7 GAP-43 levels had increased 4 fold in the ipsilateral hippocampus and was significantly greater than that of the contralateral hippocampus ($p<0.01$) (Figure 3.5). At day 28 apoE levels still remained elevated. These data did not accurately reflect alterations within the small discrete regions of the molecular layers and are more a representation of apoE behaviour within the entire hippocampus. This data also highlights how inefficient Western blotting performs in the analysis of small localised alterations.

3.4.3.2 Apolipoprotein J

Cellular immunoreactivity

In unlesioned control animals, neuropil immunoreactivity was faint and did not significantly differ from that observed in the contralateral hippocampus. Light apoJ neuronal immunoreactivity was evident, but was similar in the ipsilateral and contralateral hippocampus. At day 7 post-ECL, the MML and OML were densely populated with apoJ-immunopositive cells with the morphological appearance of glia (Figure 3.9). At day 28 post-ECL, these cells remained intensely immunolabelled, however by day 90 no glial cell immunoreactivity was evident. Double labelling of sections from 7 day survival subjects with apoJ and GFAP confirmed apoJ was localised predominantly to GFAP-positive astrocytes. There were no additional cells, which displayed apoJ immunoreactivity and double labelling of sections with apoJ and mrf-1 indicated that very few microglia were apoJ immunopositive (Figure 3.10).

Neuropil immunoreactivity

Neuropil alterations were also evident for apoJ. Immunostaining within the MML and OML increased by approximately 20% at day 3 post-ECL, in the ipsilateral hippocampus compared to the contralateral hippocampus ($p<0.05$) (Figure 3.8 and 3.9). Immunoreactivity declined thereafter, towards or below baseline levels at day 90 post-ECL except within the OML, in which at day 90, apoJ immunoreactivity was

dramatically increased to 40% above control levels within the ipsilateral hippocampus and this was significantly greater than that of the contralateral hippocampus ($p<0.0001$). ApoJ immunoreactivity did not significantly alter except that at day 90 post-ECL, intensity declined and was approximately 50% of control levels. Analysis of variance revealed no significant variance in the hippocampal immunoreactivity.

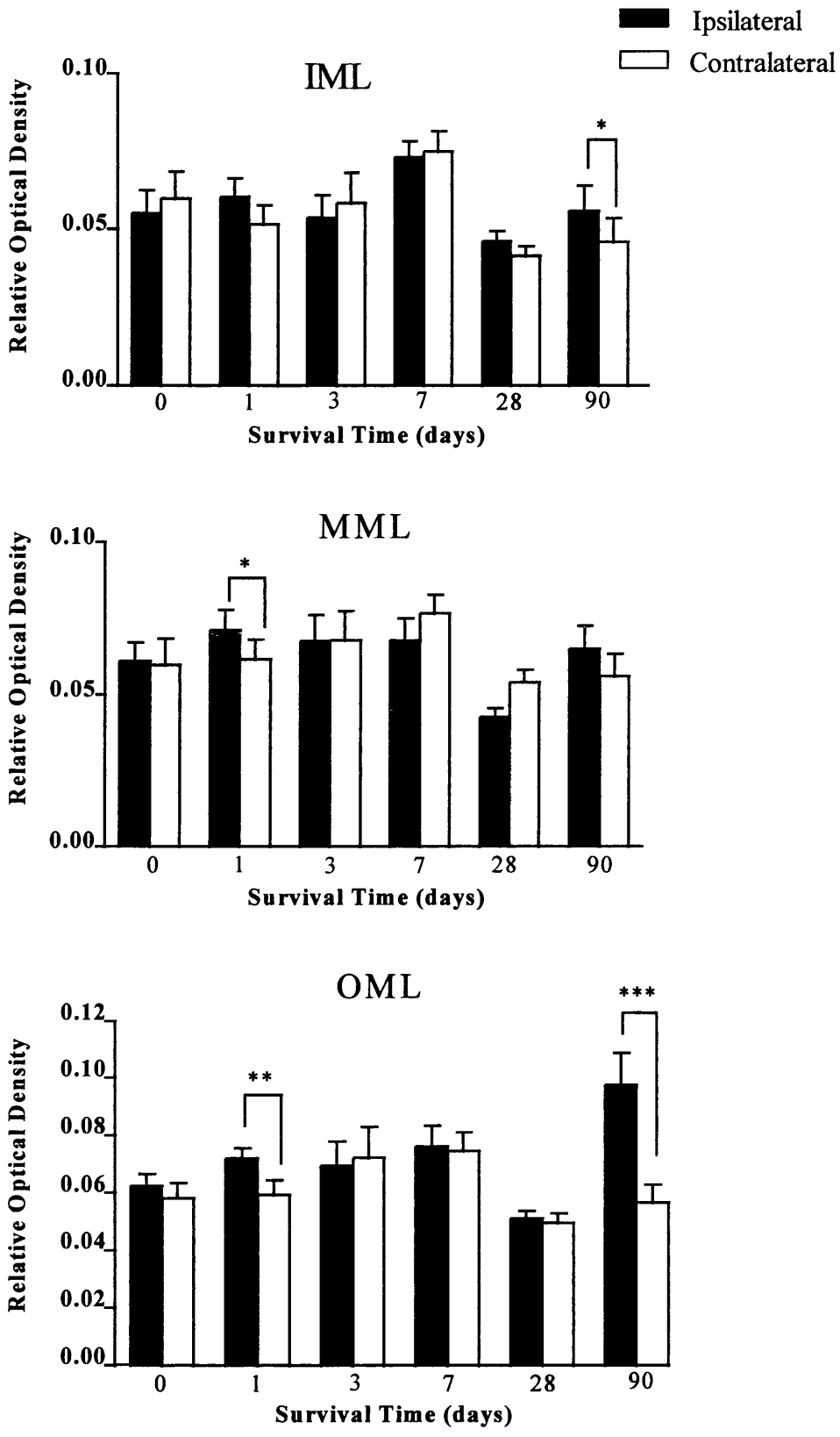

Figure 3.7 Quantification of neuropil apoE immunoreactivity in the inner, middle and outer (IML, MML, OML) molecular layers of the hippocampal dentate gyrus at 0, 1, 3, 7, 28 and 90 days post-lesion measured as relative optical density values. ApoE immunoreactivity in the ipsilateral and contralateral hippocampus was compared using a Student's paired t-test. *****p<0.0001, **p<0.01 and *p<0.05**

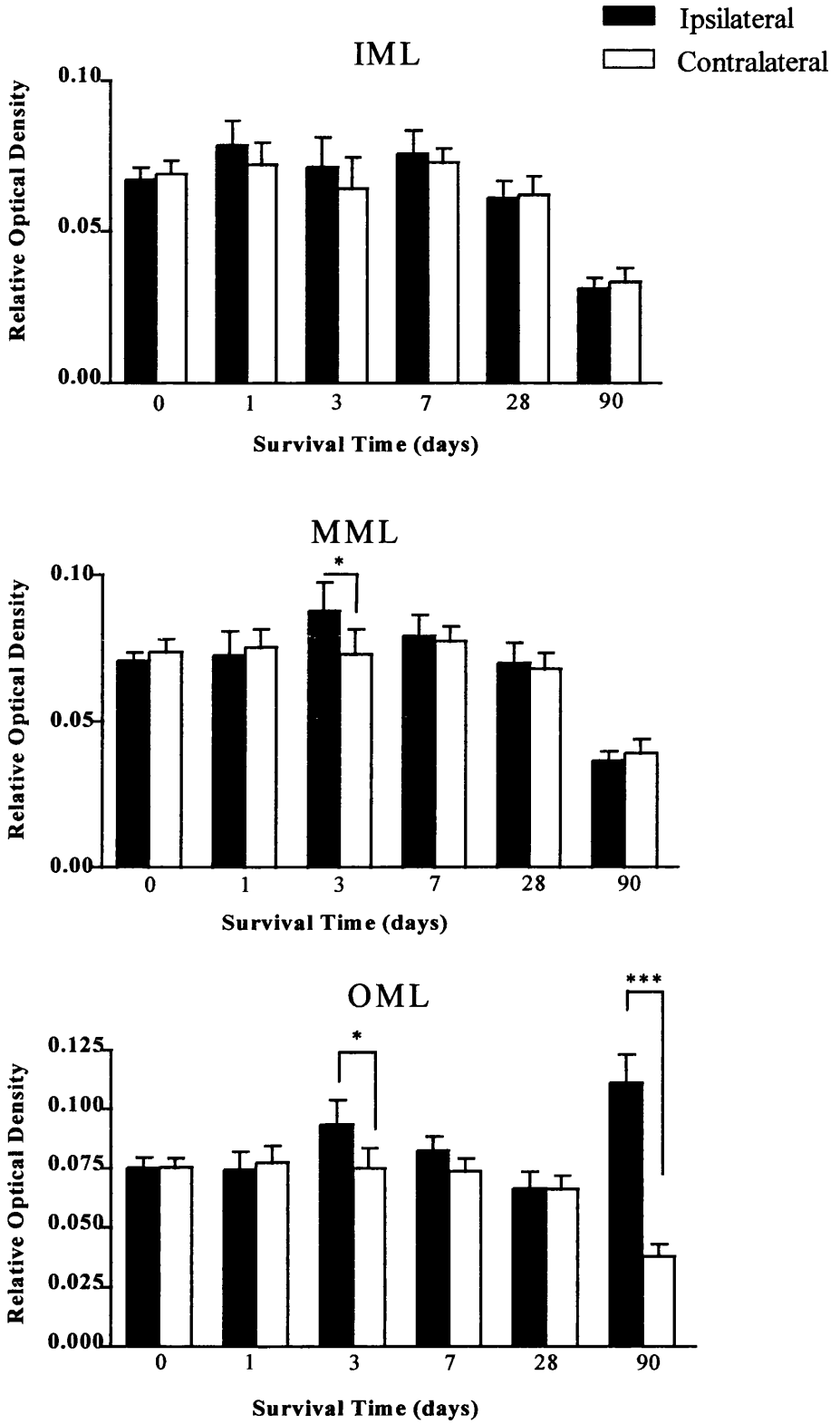

Figure 3.8 Quantification of neuropil apoJ immunoreactivity in the inner, middle and outer (IML, MML, OML) molecular layers of the hippocampal dentate gyrus at 0, 1, 3, 7, 28 and 90 days post-lesion measured as relative optical density values. ApoJ immunoreactivity in the ipsilateral and contralateral hippocampus was compared using a Student's paired *t*-test. *****p<0.0001 and *p<0.05**

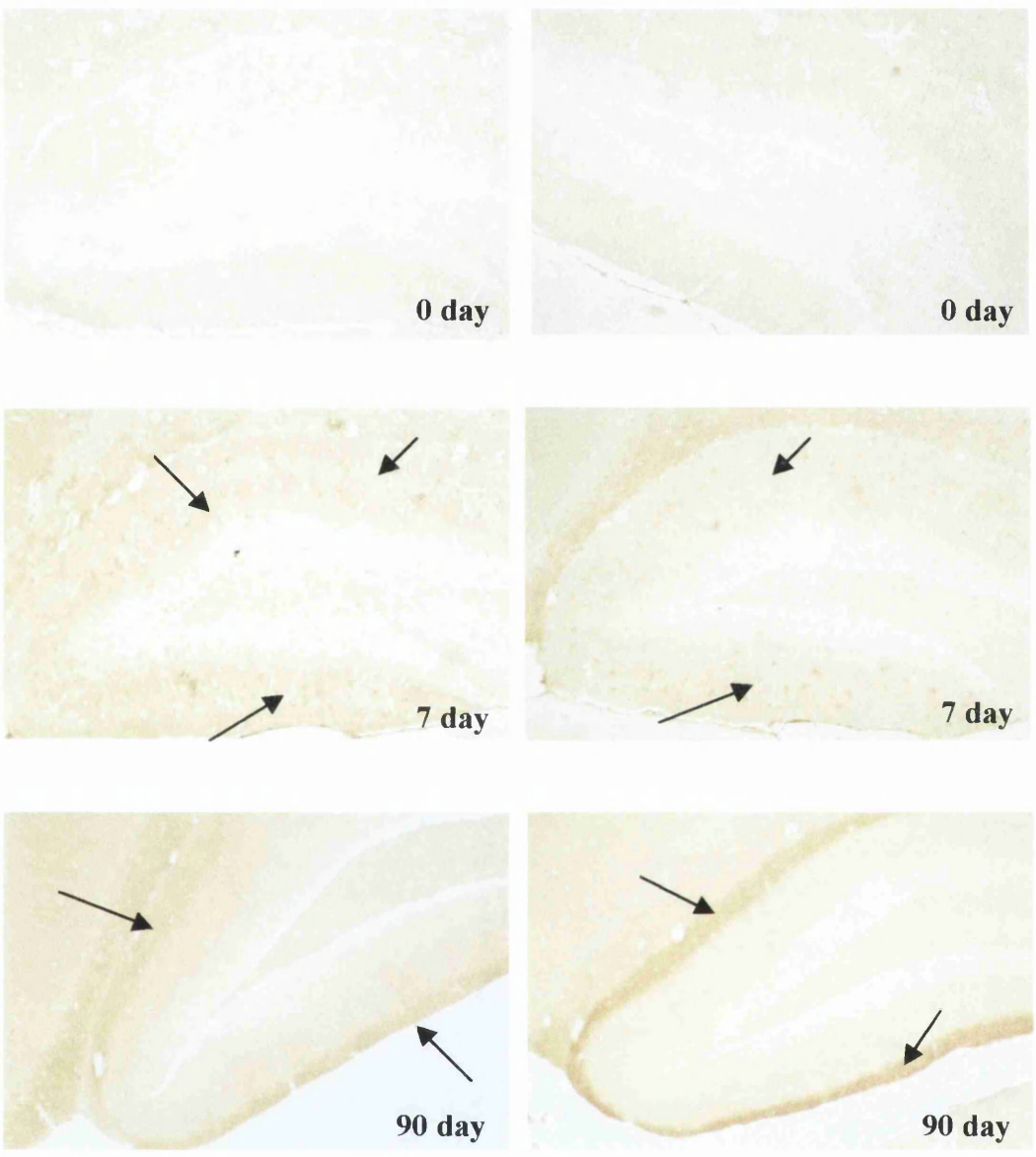

Figure 3.9 **Increased apolipoprotein E and apolipoprotein J post-ECL**

Illustrative examples of apoE and apoJ immunoreactivity in the ipsilateral hippocampus at day 0, 7 and 90 post-ECL. Increased glial and neuropil immunoreactivity is evident at day 7 post-ECL. In contrast, at day 90 post-ECL only intense neuropil immunoreactivity is evident. x100 magnification

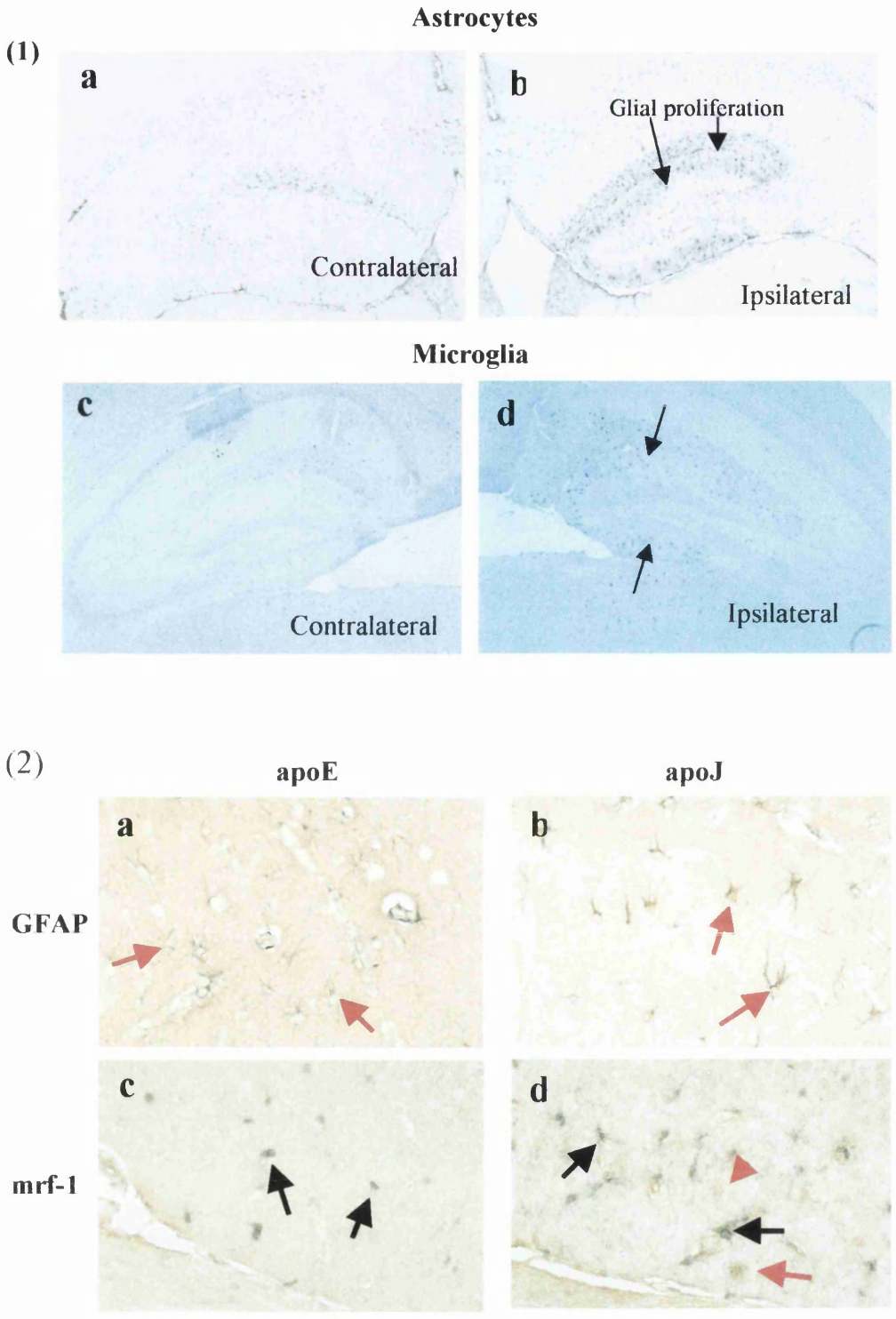

Figure 3.10 **Cellular localisation of apoE and apoJ**

(1) Illustrative examples of astrocyte (GFAP) and microglial (mrf-1) proliferation post-ECL in the contralateral (a,c) and ipsilateral (b,d) respectively. x25 magnification (microglia black arrows and astrocytes red arrows)

3.4.4 Cytoskeletal Alterations Post-Lesion

3.4.4.1 Alterations in MAP-2 immunoreactivity

In unlesioned control animals, MAP-2 characteristically labelled the soma of neurons and the associated dendritic networks most intensely. This resulted in the molecular layers of the dentate gyrus being heavily labelled but of a similar intensity across all molecular layers. Over days 1 and 3 post-ECL, MAP-2 immunoreactivity increased in a stepwise fashion in increments of 10% within all layers. This was also observed contralaterally. At days 7 and 28 post-ECL, MAP-2 immunoreactivity decreased within the ipsilateral MML and was significantly different to the contralateral immunoreactivity ($p<0.0001$). At day 90 post-ECL, MAP-2 immunoreactivity increased greatly within both the ipsilateral and contralateral hippocampus where immunoreactivity was approximately 20% greater than baseline levels. Similarly to the MML, MAP-2 immunoreactivity increased within the OML at day 90 post-ECL, but was not significantly different to the contralateral side (Figure 3.11 and 3.12). Analysis of variance on the contralateral hippocampal optical density values revealed statistically significant variance in these readings, suggesting both the ipsilateral and contralateral hemisphere contribute to the statistically significant difference found.

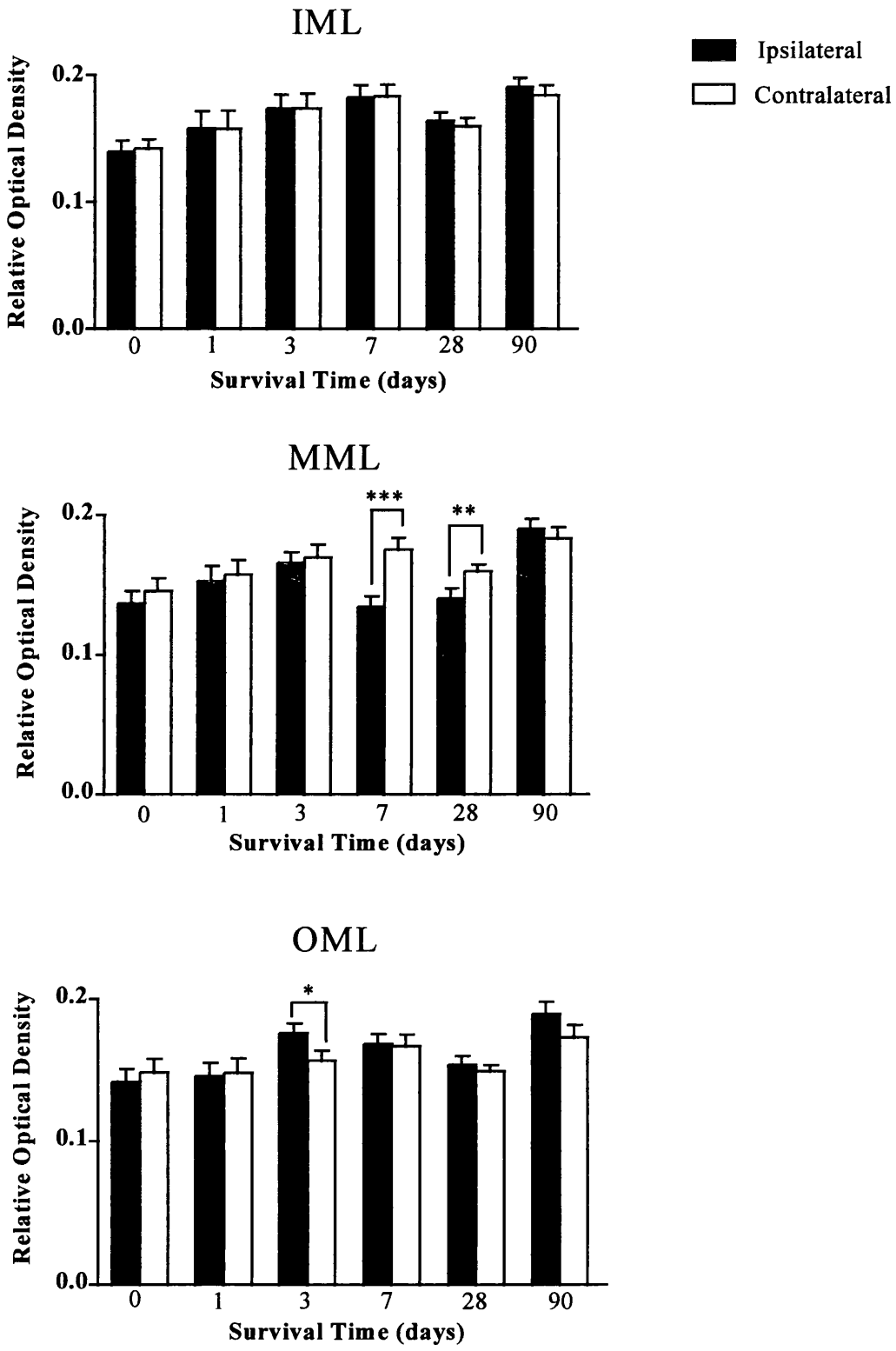

Figure 3.11 Quantification of MAP-2 immunoreactivity within the inner, middle and outer molecular layers (IML, MML, OML) of the hippocampal dentate gyrus at 0, 1, 3, 7, 28 and 90 days post-lesion measured as relative optical density values. The ipsilateral and contralateral optical density measurements were compared using a Student's paired *t*-test. *****p<0.0001, **p<0.01 and *p<0.05**

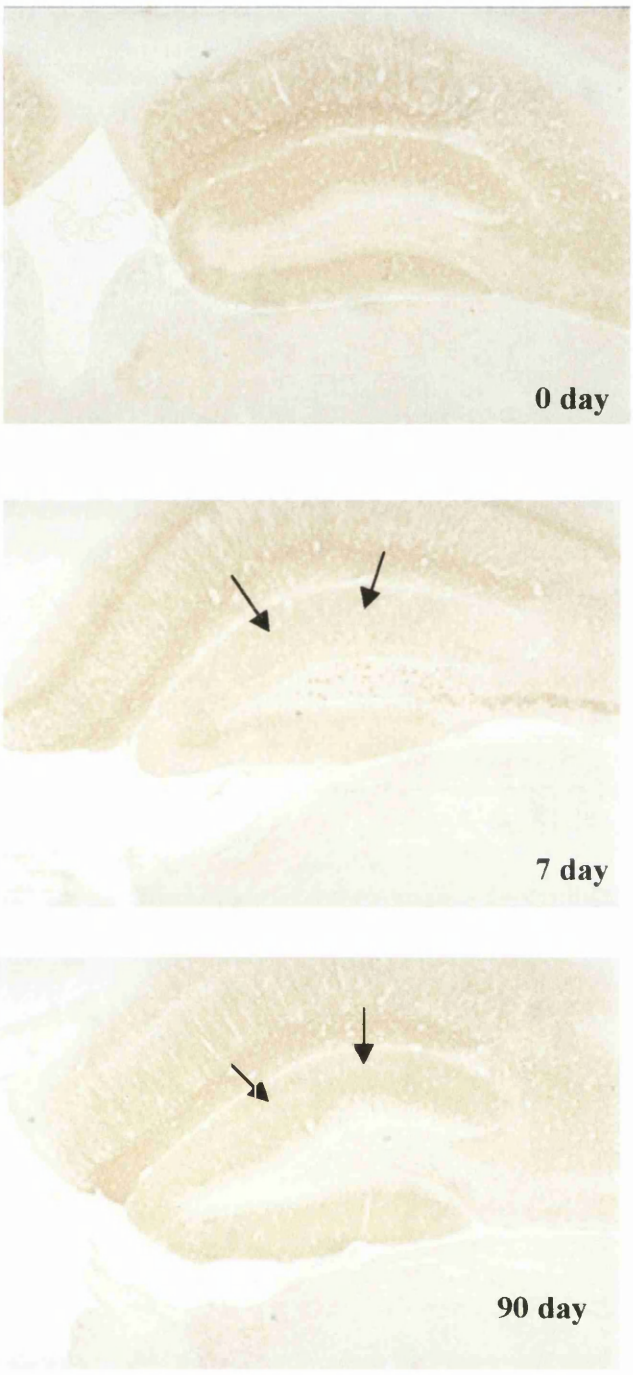

Figure 3.12 **MAP-2 immunoreactivity post-ECL**

Illustrative examples of MAP-2 immunoreactivity in the ipsilateral hippocampus at day 0, 7 and 90 post-ECL. MAP-2 immunoreactivity decreases at day 7 post-ECL and is increased at day 90 post-ECL. Contralateral MAP-2 immunoreactivity did not significantly alter post-ECL. The arrows indicate the region of the hippocampus affected post-ECL. Ocassionally increased staining was seen in pyramidal layers with injury and this has been noted in other models of injury x50 magnification

3.4.5 Clearance of Degeneration Products Post-Lesion

This method of labelling degeneration products specifically highlighted the time course of deposition and clearance of lipid and cholesterol (lipid laden lysosomes) materials from terminals. The stain appeared as a rich brown background with the degenerating processes labelled with an intense black deposit. In 0 day control animals and at day 1 post-ECL there were no silver deposits indicating there were no degeneration products. In contrast, at day 3 post-ECL, an intense black punctate deposit was present throughout all regions of the molecular layer in the ipsilateral hippocampus (n=8/8) (Figure 3.13). Deposition was also evident in the ipsilateral stratum lacunosum moleculare. At day 7 post-ECL only a thin band of degeneration material staining remained, localised specifically within the MML of the ipsilateral hippocampus (n=7/8). This band was still present at day 28 however at day 90 post-ECL, no silver labelled degeneration products were present.

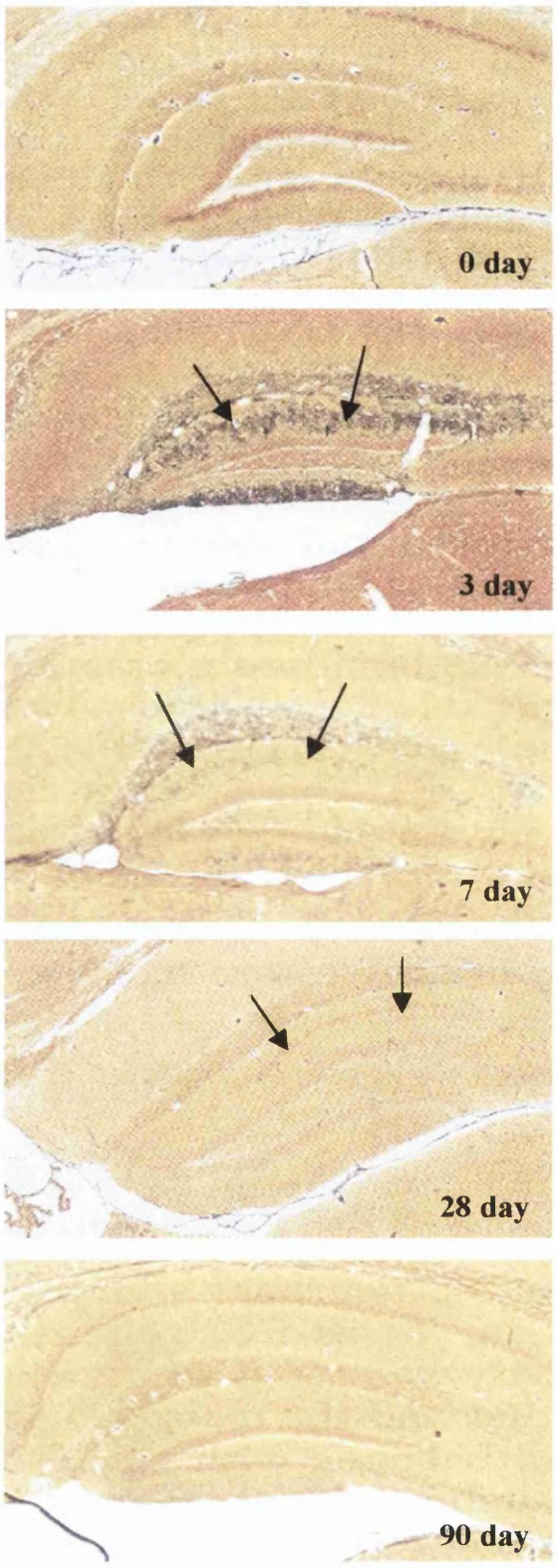

Figure 3.13 **Degeneration product deposition and clearance**

Fink-Heimer silver staining of lipid laden degeneration products at day 0, 3, 7, 28 and 90 post-ECL. The contralateral hippocampus displayed no degeneration products.

3.4.6 LRP Receptor Expression Post-Lesion

Cellular immunoreactivity

In 0 day control mice no astrocytic LRP immunoreactivity was evident. At day 7 post-ECL the MML and OML were densely populated by LRP immunoreactive astrocytes (Figure 3.15). At day 28 post-ECL, the number of immunoreactive astrocytes declined until, at day 90, no glial immunoreactivity was evident. Neuronal immunoreactivity did not significantly alter with the injury.

Neuropil immunoreactivity

In unlesioned control animals, LRP immunoreactivity was evident on neuronal cell bodies and in the neuropil but was similar in the ipsilateral and contralateral hippocampus. LRP neuropil immunoreactivity did not alter within the molecular layers of the dentate gyrus post-ECL (Figure 3.14). Analysis of variance on the contralateral hippocampal optical density values revealed no statistically significant variance in optical density values.

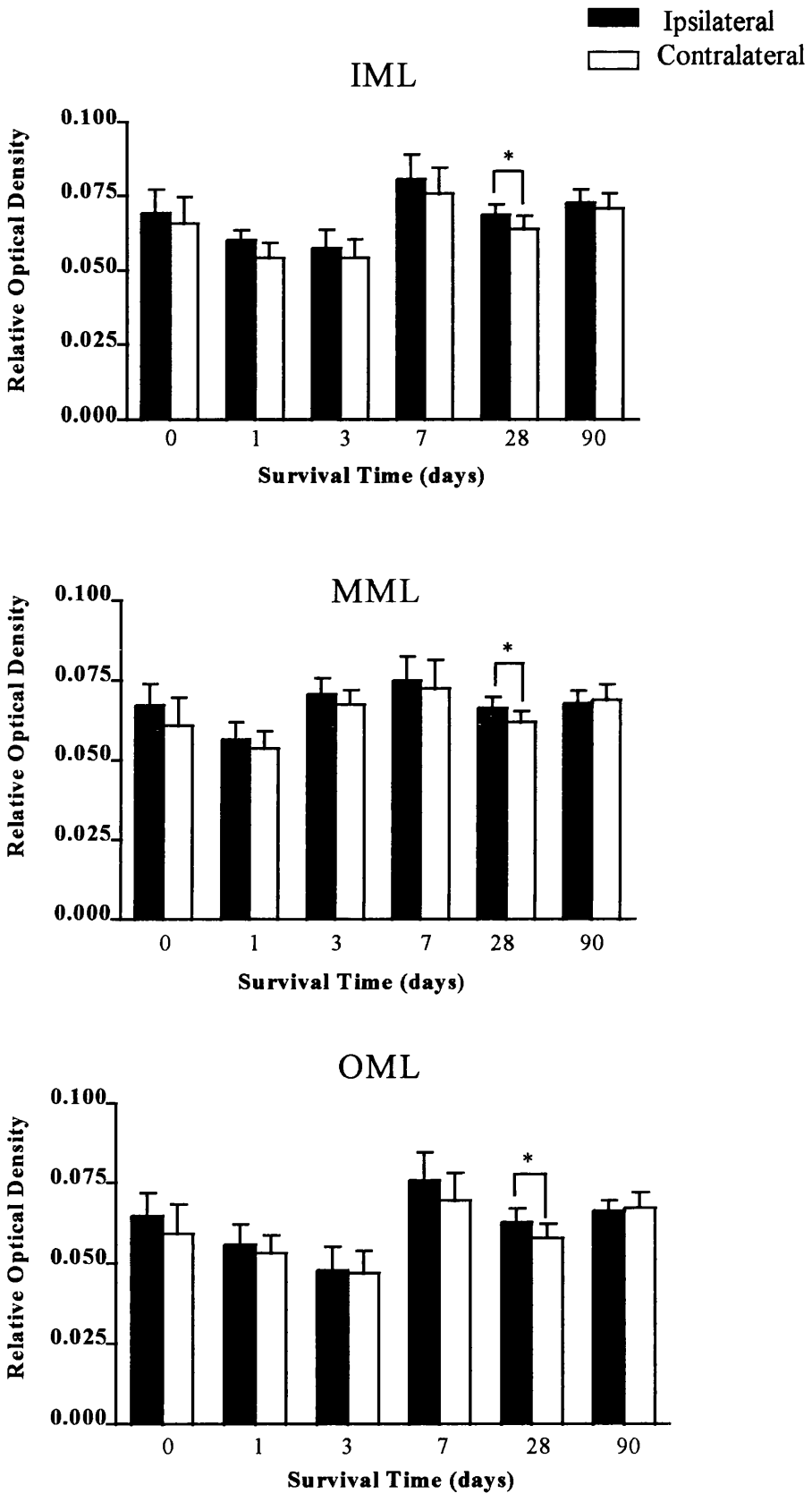

Figure 3.14 Quantification of LRP receptor immunoreactivity in the inner, middle and outer molecular layers (IML, MML, OML) of the hippocampal dentate gyrus at 0, 1, 3, 7, 28 and 90 days post-lesion measured as relative optical density values. LRP immunoreactivity was compared in the ipsilateral and contralateral hippocampus using a Student's paired *t*-test. ***p<0.05**

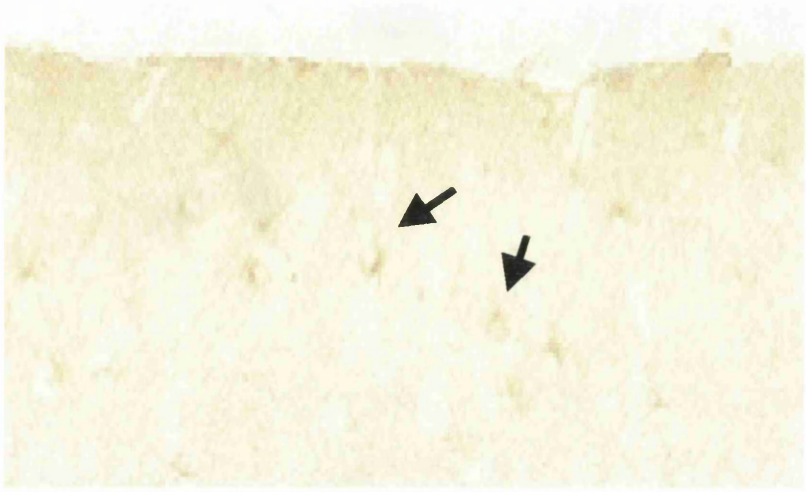

Figure 3.15 **Increased astrocytic LRP receptor immunoreactivity at day 7 post-ECL**

Illustrative example of LRP immunoreactivity in the ipsilateral hippocampal molecular layer at day 7 post-ECL. No astrocytic staining is evident at day 0 or 90 post-ECL. x200 magnification

3.5 Discussion

This study demonstrated that upregulation of apoE and apoJ occurs in the hippocampus after ECL and this parallels the immediate response and long-term recovery to injury. The data supports the hypothesis that both apolipoproteins E and J may be involved in the clearance and redistribution of lipid and cholesterol material from the site of injury, for reutilization in the reconstruction of neuronal cell elements, such as membrane in the regeneration process (Holtzman and Fagan, 1998). This function may be crucial in long-term plasticity alterations following brain injury.

3.5.1 Experimental deafferentation: an animal model for studying CNS plasticity

Mechanical lesioning of the entorhinal cortex has been employed in a number of studies to illustrate the role of apolipoproteins in relation to plasticity within the adult CNS after injury (Masliah *et al,* 1991; Poirier *et al,* 1991; Anderson *et al*, 1998). In the present study, chemical lesioning of the mouse entorhinal cortex results in degeneration of the perforant pathway to the hippocampus that causes time-dependent structural alterations within specific layers of the hippocampus. The C57BL/6J mouse strain is the background strain of the transgenic mice to be employed in the proceeding studies and therefore, it was essential to characterise plasticity in these mice in response to injury. Synaptic decline, as assessed using synaptophysin immunoreactivity, became apparent 7 days post-ECL and maximal loss was achieved at day 28 post-ECL where immunoreactivity was approximately 40% of that of the unlesioned side and control mice. However, at day 90 post-ECL, synaptophysin immunoreactivity had increased within the ipsilateral hippocampus and was similar to that observed in the contralateral hippocampus, indicating compensatory reactive synaptogenesis had occurred. Other groups have reported increases in synaptophysin levels reaching 80% recovery within the ML by day 30 (Masliah *et al*, 1991; Poirier *et al*, 1990, 1991). Synaptic loss is accompanied by fibre and terminal degeneration within the same region as determined using GAP-43 immunohistochemistry (Lin *et al*, 1999) (MAP-2 data also reflects fibre loss via cytoskeletal breakdown). GAP-43 immunoreactivity decreased within the MML and OML and fibre density loss was maximal at day 7 post-ECL. At day 28 post-ECL

immunoreactivity had begun to increase, suggesting terminal proliferation and collateral sprouting and at day 90 post-ECL, immunoreactivity had increased to 70% of control levels. These findings contrast with other groups, who witnessed partial recovery as early as day 7 post-ECL and full recovery to pre-lesion levels at day 28 (Anderson *et al*, 1998). The differences in neuropathology may reflect the inherent differences in the method applied to induce the lesion. Chemical lesioning of the EC ablates afferent input into the hippocampus via extensive cellular death rostrocaudally, whereas mechanical methods render only partial severance of the pathway (Cho and Jaffard, 1995). This allows compensation by the entorhinal cortex itself, which occurs over a shorter time course consequently in these less severe models, compensatory plasticity alterations may occur earlier post-ECL. In addition, there are innate differences in the behaviour of each layer within the molecular layers. The most striking differences were found, in our hands, to occur within the MML, a finding that agrees with the results of Anderson *et al* using the electrolytic lesion model in mice. Others analyze the MML and OML as a single entity. In the present study, the results accentuate the innate divide in behaviour in the two layers and a need for separate analysis. Several intra and extrahippocampal fibre systems are capable of reinnervating the denervated granule cells and this study has shown this from the commissural-associational fibre system by expansion of the IML. Other fibre systems, such as cholinergic fibres from the septum and crossed temperodentate fibres, may also participate in this response and have been identified in rat models (Steward and Vinsant, 1983; Fagan and Gage, 1994; Deller *et al*, 1996; Deller and Frotshcer, 1997).

There is information, albeit limited, to suggest that analogous sprouting processes may occur in the human brain. Grady *et al* (1989) reported evidence of reinnervation in the hippocampus of two patients who had died following an intracerebral haemorrhage which had caused uncal herniation with subsequent damage to the entorhinal cortex. The study mentioned only presented two cases, however our group is presently assessing hippocampal sprouting in a larger cohort of patients who have experienced a similar injury. Aberrant sprouting witnessed in AD postmortem brains also suggests that the human CNS is capable of reinnervation (Masliah *et al*, 1991; Arendt *et al*, 1998; Danik and Poirier, 1998).

3.5.2 Apolipoprotein E is upregulated in the neuropil and glia following injury

Upregulation of apoE in the brain in experimental animal models of injury has been well documented (Horsburgh *etal*, 1996; Poirier *etal*, 1991) as in human brain injury (Horsburgh et al, 1999). In the present study apoE was markedly increased within the neuropil when synaptic loss was first detected and later apoE was increased and localised to glial cells. Most surprisingly, a dramatic increase in apoE occurred by day 90 post-ECL specifically within the OML neuropil. In rodent brain apoE is localised exclusively to glia (Boyles *et al*, 1985). ApoE protein and mRNA increases have been identified in astrocytes associated with GFAP mRNA following ECL (Poirier *et al*, 1990; Zarow *et al*, 1998). Glial staining within the present study peaked at day 7 post-ECL within the molecular layers of the dentate gyrus in the present study. It is possible this cellular staining has resulted from the reuptake of apoE from the local environment (Poirier *et al*, 1993; Ji *et al*, 1998), or indeed it could represent a secondary upregulation for functioning in the progressive plasticity changes which occur over a period of months following injury (Masliah *et al*, 1991; Danik and Poirier, 1998; Holtzman *et al*, 1998). This is substantiated by the occurrence of elevated apoE levels within the OML even by day 90 post-ECL. Levels were higher than at any other survival point post-ECL. This supports a role for its involvement in long-term repair.

Although no increase in neuronal cell body staining was evident in this study, it is possible apoE is endocytosed into neurons, but via receptor interactions on terminals and dendrites (Mahley *et al*, 1988). Neuronal cell bodies, dendrites, and proximal axons express the endogenous apoE receptor; LRP (Rebeck *et al*, 1993). Several groups have shown dendrosomatic localisation of the receptor and suggest it is likely to be expressed in regions of high synaptic density (Page *et al*, 1998; Stockinger *et al*, 1998), where uptake would be required for the reconstruction of cellular elements in membrane maintenance and repair following injury. Since it is not required by the cell body in this type of injury it may be trafficked to the region of most need. It has been shown in this study that the LRP receptor displays a dense neuropil localisation in conjunction with expression on astrocytes and neurons.

In this study, the majority of apoE-positive cells were not GFAP-positive but appeared to be localised to microglia. *In situ* hybridisation studies have also indicated localisation of apoE to microglia (Stone *et al*, 1997). We have used the antibody mrf-1, which is a well characterised antibody raised against a microglial gene (Tanaka *et al*, 1998) (this antibody is the only microglial marker for paraffin tissue at present). The main aim of this study was to determine if apolipoproteins played a role in long-term repair processes following injury when sprouting and synaptogenesis are occurring.

3.5.3 Apolipoprotein J is upregulated in the neuropil and glia following injury

Under normal physiological conditions apoJ is expressed at low levels within neurons, glia and the neuropil (Rebeck *et al*, 1993) and indeed faint neuronal staining was evident in control tissue. Neuronal cell body immunoreactivity did not alter with the injury. Upregulated expression of apoJ occurs when the CNS is stressed (Michel *et al*, 1997). Lampert-Etchells *et al* (1991), who first determined increases in apoJ following ECL, employed the protien as a marker of neurodegeneration. In the present study, apoJ immunoreactivity increasd within the neuropil and also within glial cells of dentate molecular layer, a finding in agreement with others (Johnson *et al*, 1996). This suggests that, like apoE, apoJ is present within the extracellular space around terminals with subsequent increases in reactive glia (Danik *et al*, 1995) either via uptake or *de novo* synthesis. All apoJ-positive cells were astrocytes (GFAP-positive) in contrast to apoE. At day 28 post-ECL, apoJ cellular immunoreactivity remained intense, a time when apoE immunoreactivity had declined to below baseline levels. Similarly, apoJ immunoreactivity significantly increased within the OML at day 90 post-ECL ($p<0.0001$). It is thought that apoJ functions predominantly in lipid transport, but also that it performs similar functions in maintenance and repair to apoE and thus warranted its investigation in this thesis (Jordan-Starck *et al*, 1992). This is especially important in the later chapters when *APOE* knockout mice will be investigated (Bertrand *et al*, 1995). ApoJ uptake is mediated mainly via the gp330 receptor (Beffert *et al*, 1998; Page *et al*, 1998; Niemeier *et al*, 1999), however the presence and functionality of this receptor in the brain has not been fully elucidated (De Silva *et al*, 1990).

3.5.4 Alterations in apoE and apoJ parallel clearance of cellular debris from the environment

Both apolipoproteins E and J are involved in the transportation and redistribution of lipids and cholesterol. Poirier (1993) suggested apoE was mobilised to clear cellular breakdown products from the site of injury. In the present study was illustrated a time-course for the deposition of degeneration products using silver staining. Deposition was maximal at day 3 post-ECL. Clearance of material coincided with the increased expression of both apoE and apoJ, thus at day 7 post-ECL only a thin band of degeneration material remained within the MML. At day 90 post-ECL, no degeneration products were evident within the dentate molecular layers. This temporal profile of alterations in apolipoproteins in redistribution suggests that both apoE and apoJ may be involved in the ongoing, long-term plasticity changes post-ECL (Holtzman and Fagan, 1998). In this study we have also identified a range of markers, which accurately reflect degeneration and reinnervation in this mouse model. Using wild-type mice we have studied endogenous mouse apoE and apoJ function in the clearance of cellular debris.

Chapter IV

Analysis of *APOE* Genotype Influence on CNS Plasticity in Transgenic Mice Expressing Human *APOE* ε3 and ε4 Alleles (Under a Human Promoter Sequence) Following Entorhinal Cortex Lesion

4.1 Introduction

Animal models are an essential tool for the study of human disease and injury (Roses *et al*, 1997). However, alone they do not allow the study of genetic components of human disease and injury. Rat models of global ischaemia were initially used for determining the role of apoE in acute brain injury, where it was determined that apoE was upregulated primarily in astrocytes and then translocated to neurons following 72 hours of survival (Horsburgh *et al*, 1996). However, rodents do not have the *APOE* allelic heterogeneity which humans express. Transgenic animals were produced which had the endogenous mouse *APOE* gene deleted but human *APOE* gene sequences inserted which encode the ε2, ε3 or ε4 human alleles.

The transgenics that will be discussed in this chapter, have human ε3 and ε4 inserts that are driven by the human promoter sequence (Xu *et al*, 1996). This gives these mice an apoE expression pattern similar to that observed in human brain tissue, in that apoE is expressed in astrocytes, microglia and oligodendrocytes (Boyles *et al*, 1985). The influence of *APOE* genotype has been investigated using animal models of acute brain injury, where it has been found that the E4 isoform confers a poor outcome and accentuated brain damage (Sheng *et al*, 1998; Horsburgh *et al*, 1999; Sabo *et al*, 2000). However it is now evident that apoE may modulate the progression of chronic brain injury possibly through a process affecting CNS plasticity and that this process may be influenced by *APOE* genotype. The next step was to use the entorhinal cortex lesion model to study *APOE* genotype influence on long-term plasticity post-ECL.

4.2 Aims

To test the hypothesis that the possession of an *APOE*ε4 genotype is associated with an impaired long-term reparative response post-ECL.

4.3 Materials and Methods

4.3.1 *APOE* transgenic mice on a human promoter

*APOE*ε3 and ε4 heterozygous mice were generated as previously described (Xu *etal*, 1996). The mice were transported to Glasgow according to Home Office Regulations, acclimatised and maintained in an animal unit at the University of Glasgow. The genotype of the transgenic mice was confirmed using PCR analysis.

4.3.2 Entorhinal cortex lesion

The entorhinal cortex was lesioned in male transgenic mice (12 weeks old) which were allowed to survive for periods of 7, 28 or 90 days (n=11/time-point). 0 day control animals received ibotenic acid injection but were terminated immediately after the procedure. Sections from the entorhinal cortex were histologically stained using haematoxylin and eosin to confirm lesion placement. Immunohistochemistry for synaptophysin, GAP-43, apoE, apoJ, LRP and MAP-2 was performed on hippocampal sections (see chapter II). IML width was measured in GAP-43 immunostained sections. Separate tissue was dissected out from naïve animals for Western blotting to check expression levels of apoE between the two genotypes.

4.3.3 Quantification of immunohistochemistry and statistical analysis

Relative optical density values were collected from the inner, middle and outer molecular layers from both the ipsilateral and contralateral hippocampus using an MCID image analysis system connected to a microscope. For each antibody, six optical density readings were collected from the expanse of each layer using a $1cm^2$ sampling box and an average taken. Readings were taken from a reference area to ensure consistency of staining. Two way ANOVA was carried out on the contralateral hippocampal readings to allow changes in immunostaining to be attributed to the ipsilateral hemisphere. Percentage difference between the ipsilateral and contralateral hippocampus was compared in *APOE*ε3 and ε4 mice using a Student's one-tailed unpaired *t*-test. Bonferroni correction for multiple comparisons was applied where appropriate. All data is represented graphically using the mean +/- S.E.M.

4.3.4 Silver staining

Fink Heimer silver staining was carried out to assess terminal degeneration products and to determine a time-course for clearance (see Chapter II). Deposition of silver labelled degeneration products within the ipsilateral hippocampus was semi-quantified using a scoring method (0= no staining, 1= minimal, 2= moderate and 3= extensive). Differences between *APOE*ε3 and *APOE*ε4 mice were compared using a Mann Whitney U statistical test for non-parametric data.

4.4 Results

4.4.1 *APOE* levels

The brains of 12 week old *APOE*ε3 and ε4 mice were harvested, the hippocampus dissected and frozen in liquid nitrogen. Tissue homogenates were produced and 10μg of protein separated by SDS-PAGE gel electrophoresis. Immunoblotting for apoE was then carried out as previously described (see Chapter II). Protein bands were assessed as relative optical density values using an image analyser (MCID). The average optical density value for the apoE protein bands was 0.6405 in *APOE*ε3 mice and 0.7762 in *APOE*ε4 mice. The protein levels in *APOE*ε4 mice being approximately 19% greater than that of *APOE*ε3 mice (Figure 4.1). This is similar to the difference observed in baseline optical density values obtained from immunostained sections.

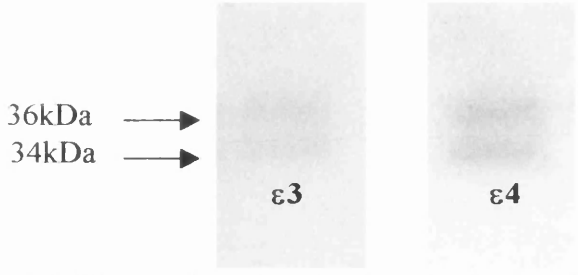

Figure 4.1 Western blotting showing the levels of apoE in the ε3 and ε4 transgenic lines. The apoE band appears as a doublet because in the CNS it exists in the 34 kDa form and a differently sialyated form at 36kDa.

4.4.2 Statistical design

Taking the percentage difference between the ipsilateral and contralateral hippocampal optical densities allowed for correction of differences which may be due to the variance in baseline levels of apoE between *APOE*ε3 and *APOE*ε4 animals. A one-tailed *t*-test was employed, as the hypothesis was that *APOE*ε4 mice would display a long-term impaired recovery to injury.

4.4.3 Lesion Assessment

Lesion placement was assessed histologically and appeared as an area of pallor in which cells were pyknotic in appearance. The lesions were restricted to the entorhinal cortex with no involvement of adjacent structures. Control animals displayed no excitotoxic damage to the entorhinal region, only the site of the needle placement was visible. No observable difference was evident between the lesion volumes of *APOE*ε3 and ε4 mice.

4.4.4 Temporal Profile of Degeneration and Regeneration Post-Lesion

4.4.4.1 Alterations in synaptophysin immunoreactivity

Synaptic alterations during degenerative and reinnervative events within the hippocampal dentate gyrus were assessed using synaptophysin immunohistochemistry. Percentage difference between the ipsilateral and contralateral hippocampus was compared for *APOE*ε3 and ε4 mice. Synaptophysin immunoreactivity in 0 day control animals displayed a regular dense pattern of staining throughout the dentate gyrus and did not differ between the *APOE*ε3 and ε4 mice. Synaptic alterations occurred within the outer two thirds of the molecular layer with little or no change within the IML. Synaptic density declined progressively and maximal synaptic loss was evident at day 28 post-ECL within the MML and OML (Figure 4.2 and 4.3). Ipsilateral hippocampal synaptophysin levels were approximately 60% of contralateral at this time-point. Synaptic loss was similar within the MML of both *APOE*ε3 and ε4 mice but was significantly greater within the OML of *APOE*ε3 mice compared to ε4 mice ($p<0.05$). At day 90 post-ECL, synaptophysin immunoreactivity had returned almost to pre-lesion levels in *APOE*ε3 mice. In contrast, in *APOE*ε4 mice, synaptophysin immunostaining levels remained well below pre-lesion levels and this was significantly different to the *APOE*ε3 mice ($p<0.05$). No significant difference in synaptic density was observed between the *APOE*ε3 and ε4 mice within the OML, although a similar trend was observed. Two way ANOVA on the contralateral hippocampal optical density values revealed no statistically significant difference.

4.4.4.2 Alterations in growth-associated protein immunoreactivity

In 0 day control animals, GAP-43 immunoreactivity exhibited a regular punctate stain within the outer two thirds of the molecular layer and denser labelling within the IML, however baseline GAP-43 immunoreactivity was significantly greater in *APOE*ε3 mice compared to *APOE*ε4 mice ($p<0.05$). The percentage differences between the ipsilateral and contralateral hippocampal optical density readings were taken to correct for this. Within the MML, GAP-43 immunoreactivity declined and maximal degeneration was observed at day 7 post-ECL where levels were approximately 40% below control levels (Figure 4.4 and 4.5). At day 90 post-ECL, the reduction in GAP-43 immunoreactivity had increased towards pre-lesion levels in *APOE*ε3 mice. In contrast, fibre density remained below pre-lesion levels in *APOE*ε4 mice, and this was significantly different to that of *APOE*ε3 mice ($p<0.05$). A similar progressive reduction in GAP-43 immunoreactivity occurred within the OML and at day 28 post-ECL, reduction in fibre density was maximal at approximately 40% of contralateral levels. At day 90 post-ECL, GAP-43 immunoreactivity in the OML of *APOE*ε3 mice had returned to, or was greater than, pre-lesion levels and this was significantly different to that observed in the OML of *APOE*ε4 mice. Two way ANOVA revealed no statistically significant variance in the contralateral readings from each genotype.

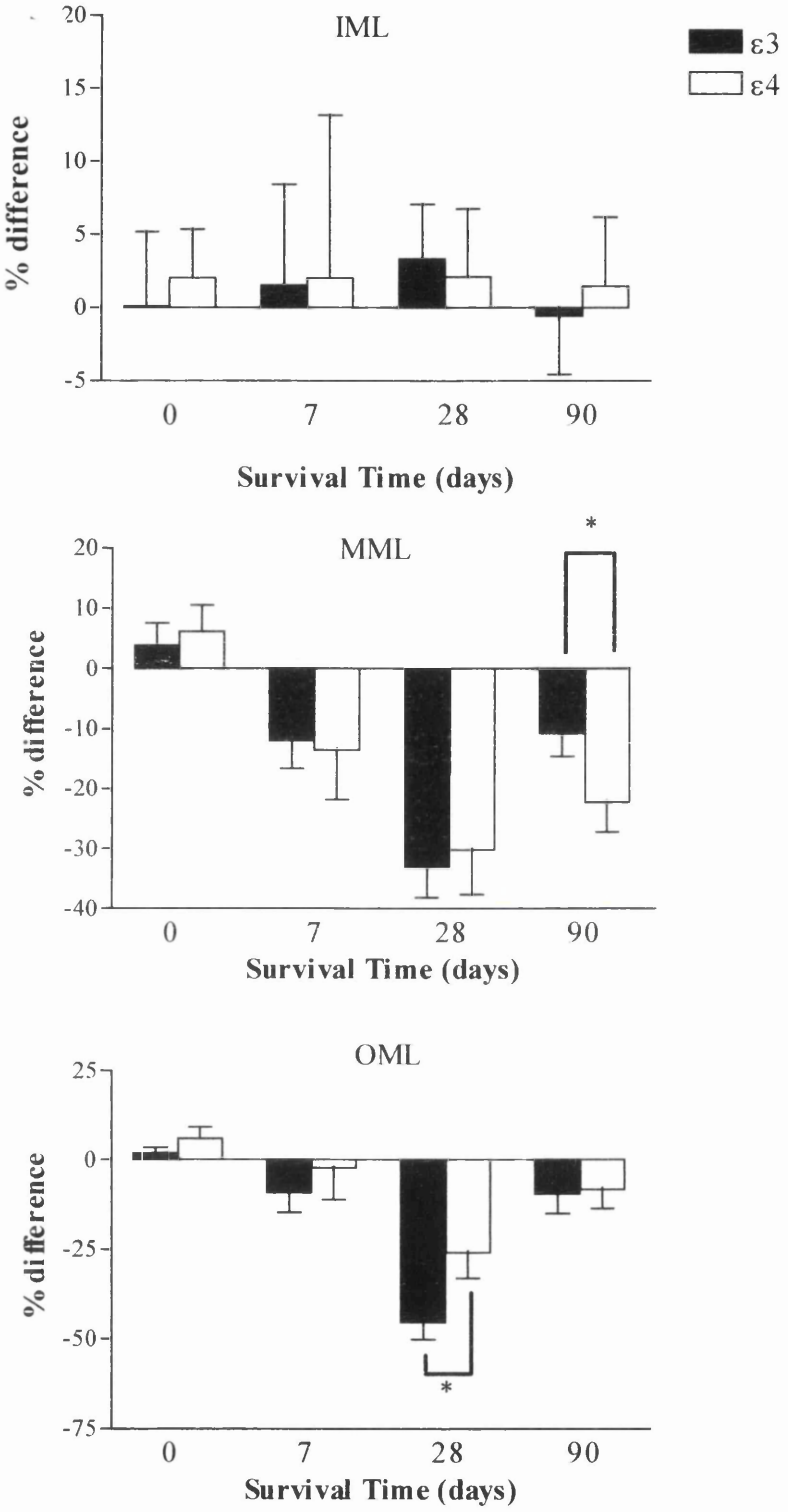

Figure 4.2 Quantification of synaptophysin immunoreactivity within the inner, middle and outer molecular layers (IML, MML, OML) of the hippocampal dentate gyrus at 0, 7, 28 and 90 days post-lesion measured as relative optical density values. Percentage difference between the ipsilateral and contralateral hippocampus immunoreactivity was compared in *APOE*ε3 and *APOE*ε4 mice using a Student's unpaired *t*-test. ***p<0.05**

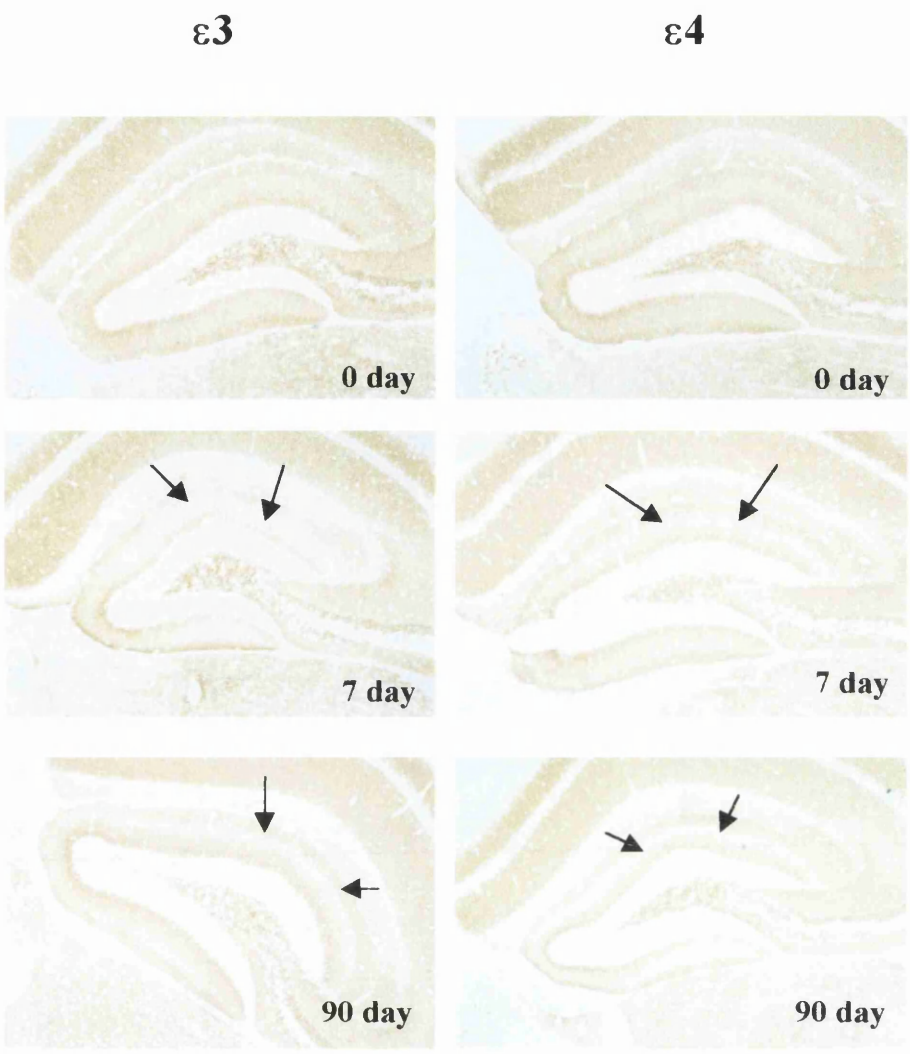

Figure 4.3 **Impaired synaptic recovery in *APOE*ε4 mice post-ECL**

Illustrative examples of synaptophysin immunoreactivity in transgenic mice expressing human *APOE*ε3 and ε4 alleles at day 0, 7 and 90 post-ECL. The contralateral hippocampus displays no significant synaptic alterations. The arrows delineate the region of the hippocampal dentate gyrus which experiences synaptic change post-ECL. x50 magnification

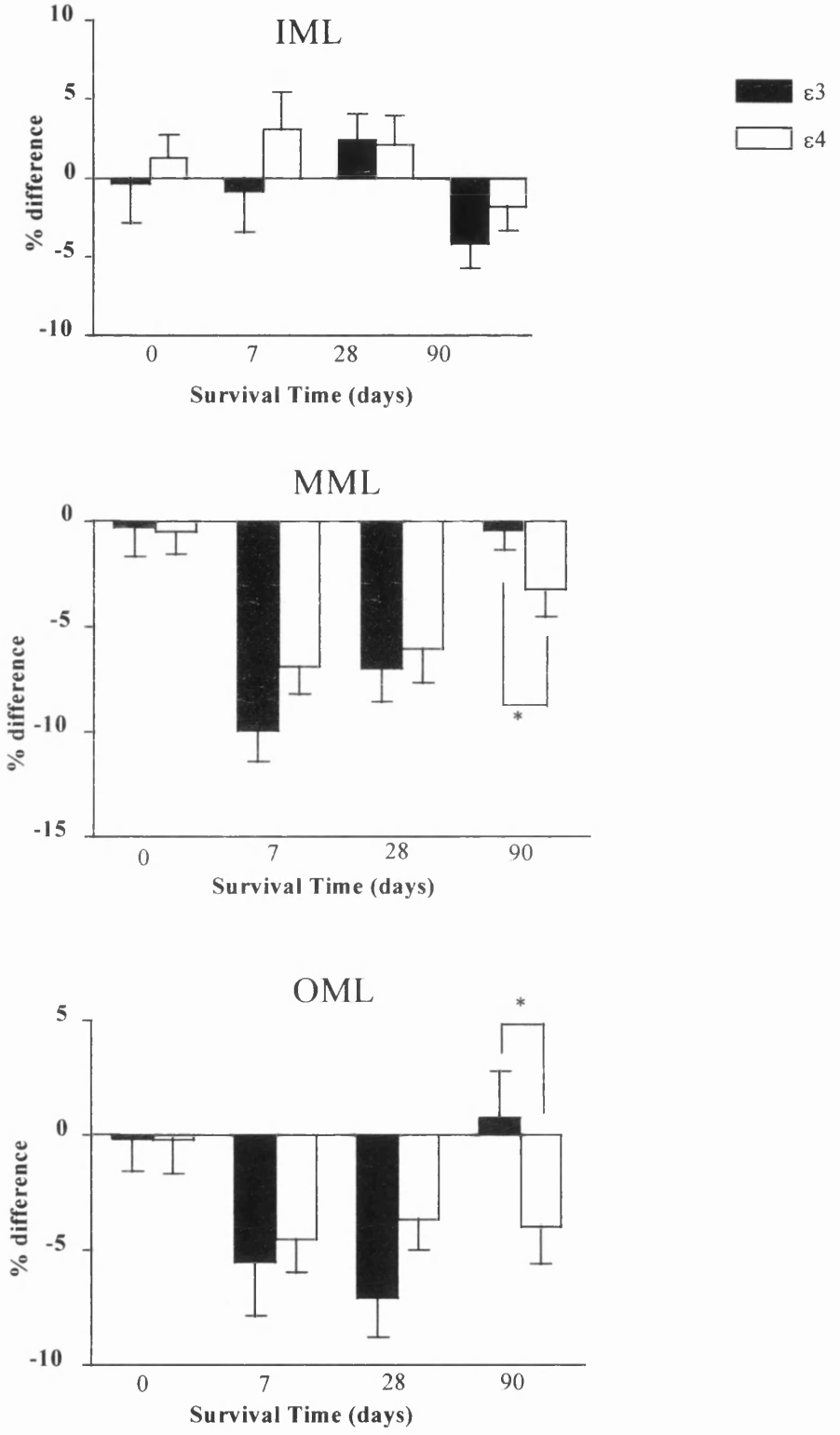

Figure 4.4 Quantification of GAP-43 immunoreactivity within the inner, middle and outer molecular layers (IML, MML, OML) of the hippocampal dentate gyrus at 0, 7, 28 and 90 days post-lesion measured as relative optical density values. Percentage difference between the ipsilateral and contralateral hippocampus immunoreactivity was compared in *APOE*ε3 and *APOE*ε4 mice compared using a Student's unpaired *t*-test. ***p<0.05**

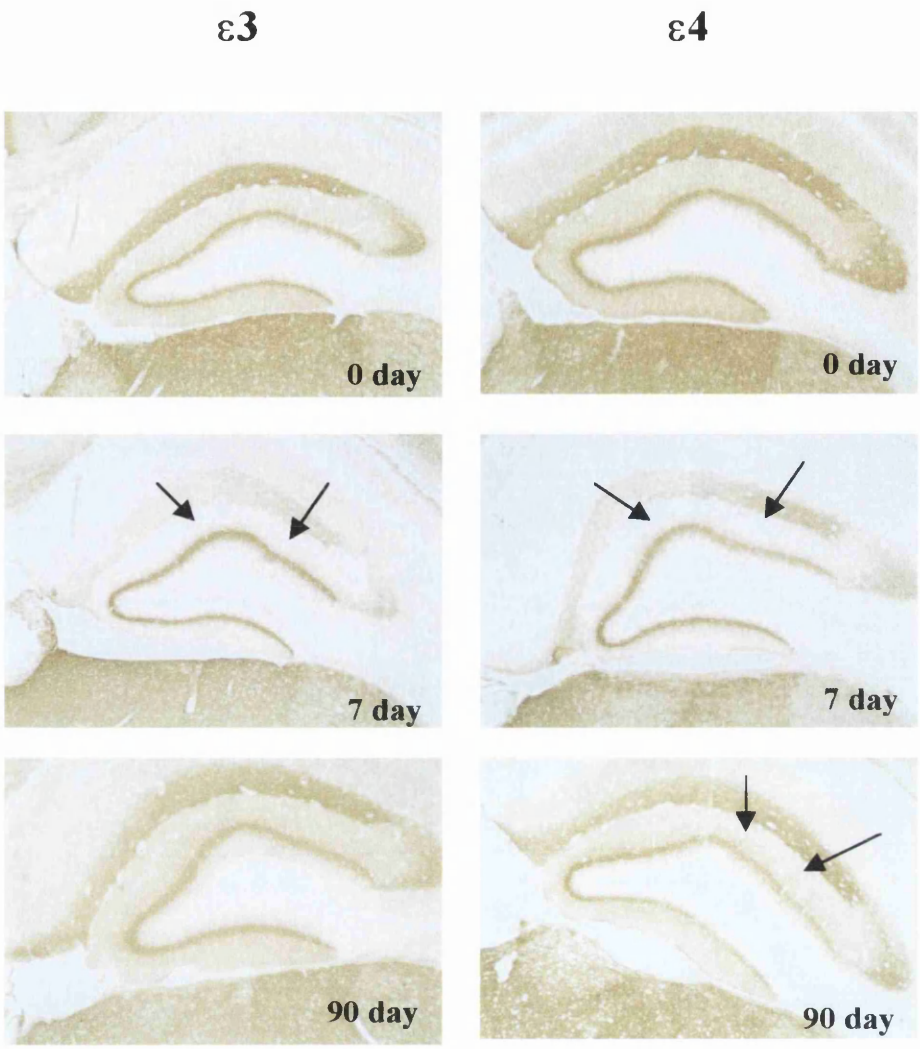

Figure 4.5 **Impaired sprouting response in *APOE*ε4 transgenic mice post-ECL**

Illustrative examples of GAP-43 immunoreactivity in transgenic mice expressing human *APOE*ε3 and ε4 alleles at day 0, 7 and 90 post-ECL. The contralateral hippocampus displays no significant fibre density alterations. The arrows delineate the region of the hippocampal dentate gyrus that experiences fibre density changes ppost-ECL. x50 magnification

4.4.4.3 IML width alterations post-lesion

The width of the IML in GAP-43 immunostained sections was measured in each animal to reflect the degree of sprouting from the commissural-associational fibres. In 0 day control animals, the width of the IML did not significantly differ between *APOE*ε3 and ε4 mice. At day 90 post-ECL, statistical analysis revealed the ipsilateral IML width increased significantly compared to that observed in the contralateral IML and this was noted for both genotypes ($p<0.0001$) (Figure 4.6). Comparison of the ipsilateral IML width of the *APOE*ε3 and ε4 mice revealed the width was significantly greater in *APOE*ε3 mice compared to that for *APOE*ε4 mice ($p<0.0001$). The width in *APOE*ε3 animals expanded by approximately 45% (to 100μm) whereas it increased by only 20% (to 75μm) in ε4 mice.

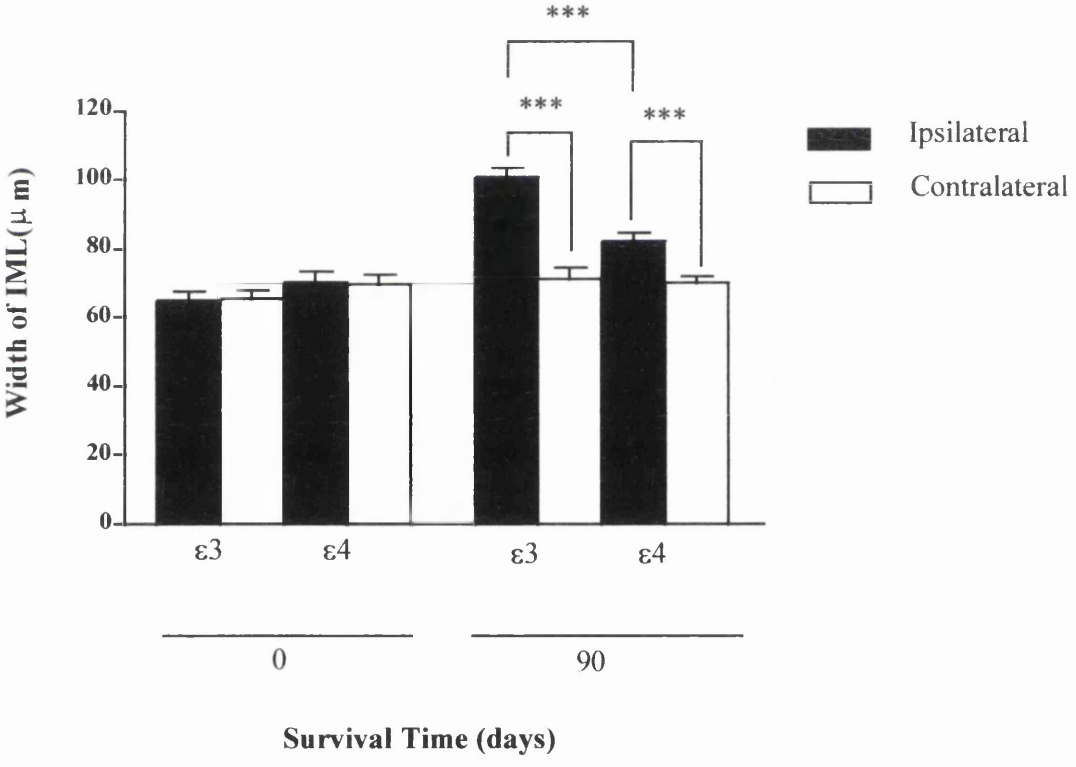

Figure 4.6 Quantification of the width of the inner molecular layer (IML) of the dentate gyrus as assessed in GAP-43 immunostained section. Expansion of this layer gives an indication of the sprouting index from the commissural-associational fibre pathway. The ipsilateral and contralateral hippocampus was compared using a Student's paired *t*-test. Sprouting in *APOE*ε3 and *APOE*ε4 mice was compared using a Student's unpaired *t*-test. *****p<0.0001**

4.4.5 Apolipoprotein Response to Injury: *APOE* Genotype Differences

4.4.5.1 Apolipoprotein E

(a) ApoE levels in APOE transgenic mice

ApoE levels in these mice *APOE*ε3 and ε4 transgenic lines were not exactly matched. In control animals, assessment of immunohistochemistry indicated significantly greater levels of apoE in the *APOE*ε4 line compared to the ε3 line (ROD- ε3: 0.1265 vs ε4: 0.1562: * $p<0.05$). Data has been published illustrating apoE levels in these lines (Xu *et al*, 1996, Horsburgh *et al*, 2000). The increased apoE levels in ε4 mice was found to be correlated with the increased GAP-43 immunoreactivity in control animals (MML: $p<0.01$ and OML: $p<0.05$) but no correlation existed between apoE and synaptophysin levels (Figure 4.7).

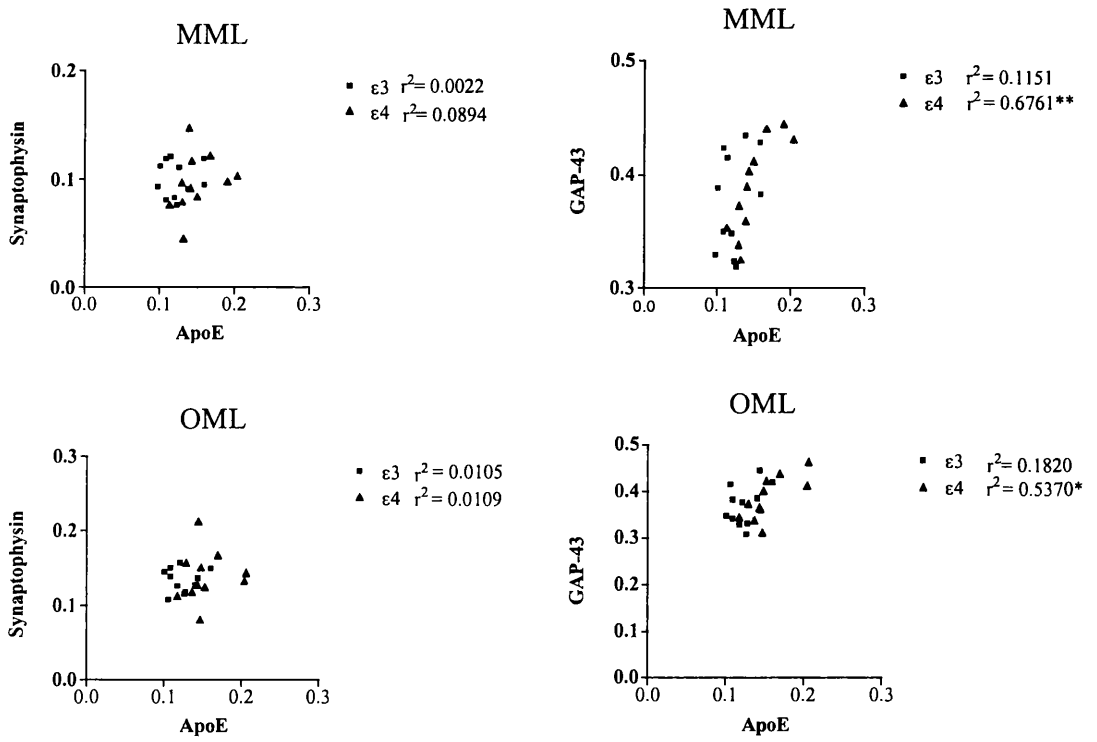

Figure 4.7 Graphical representation of data correlating GAP-43 and synaptophysin immunoreactivity to apoE immunoreactivity in *APOE*ε3 and *APOE*ε4, 0 day control animals. ApoE immunoreactivity was correlated with GAP-43 immunoreactivity in *APOE*ε4 mice but not in *APOE*ε3 mice. Synaptophysin and apoE immunoreactivity were not correlated in either *APOE*ε3 or *APOE*ε4 mice. R-squared values and p values are represented on the graphs. **$p<0.01$ and *$p<0.05$

(b) Alterations in cellular immunoreactivity

Intense apoE immuno-positive glial cells were evident within the molecular layers of the dentate gyrus by day 7 post-ECL and was similar in both *APOE*ε3 and ε4 mice (Figure 4.9). No glial staining was evident in the contralateral hippocampus. Faint neuronal staining was present in all animals but did not alter with the injury.

(c) Alterations in neuropil immunoreactivity

The percentage difference between the ipsilateral and contralateral hippocampus was taken to determine any difference between the *APOE*ε3 and ε4 mice. In 0 day control animals immunostaining was faint and was similar in pattern in both the ipsilateral and contralateral hippocampus. Ipsilateral neuropil apoE immunoreactivity increased within the IML and MML at day 7 post-ECL similarly in both *APOE*ε3 and ε4 mice (increases of 50% and 25% respectively) (Figure 4.8 and 4.9). ApoE immunoreactivity then declined towards pre-lesion levels at day 90 post-ECL. OML apoE immunoreactivity followed a similar pattern where apoE immunostaining increased and was maximal at day 7 post-ECL although levels were significantly greater in *APOE*ε4 mice ($p<0.05$) (increase of 35% approximately). ApoE immunoreactivity declined thereafter towards pre-lesion levels at day 90 post-ECL. Two way ANOVA revealed no statistically significant variance in contralateral ROD values for each genotype.

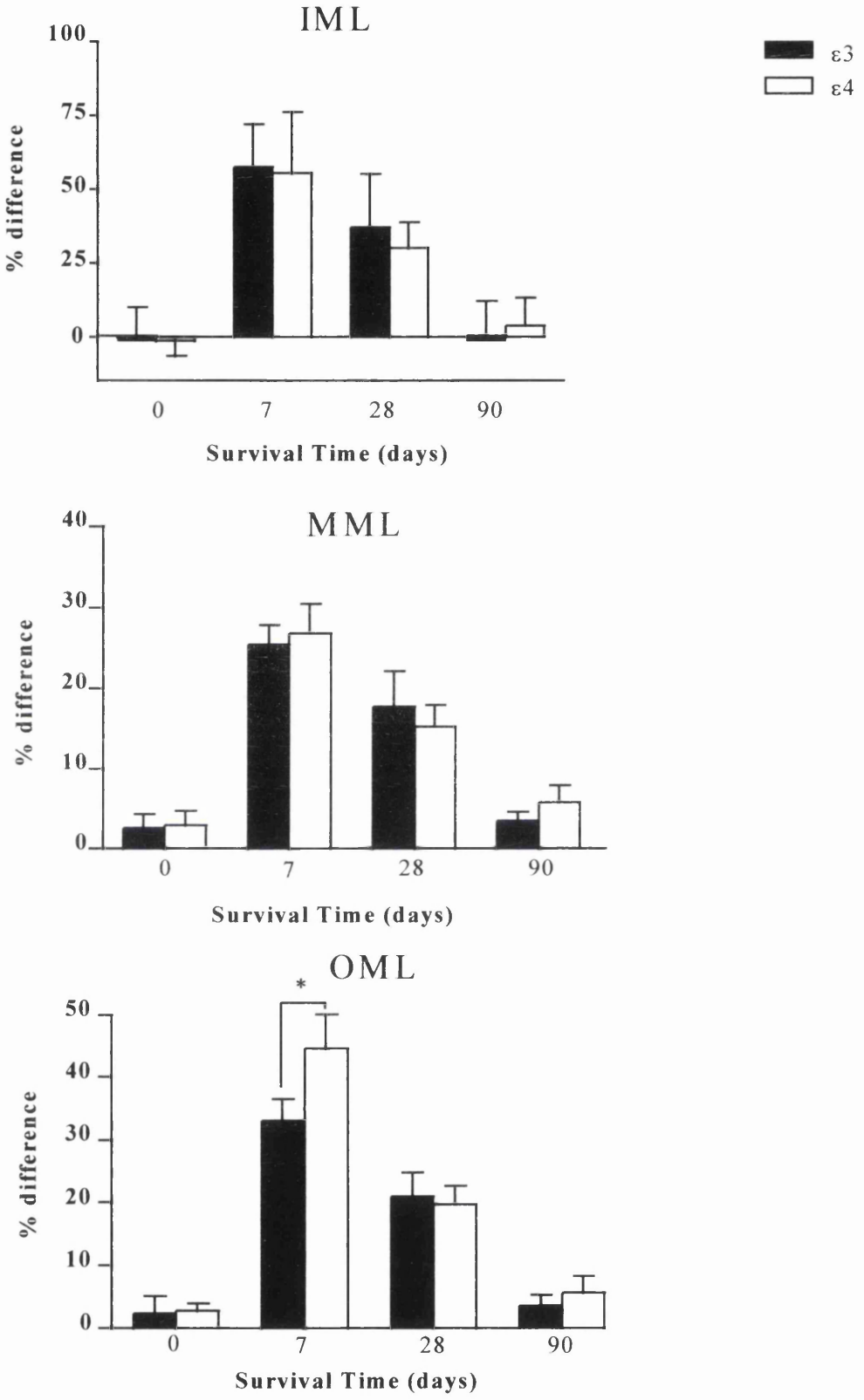

Figure 4.8 Quantification of apoE neuropil immunoreactivity within the inner, middle and outer molecular layers (IML, MML, OML) of the hippocampal dentate gyrus at 0, 7, 28 and 90 days post-lesion measured as relative optical density values. Percentage difference between the ipsilateral and contralateral hippocampus immunoreactivity was compared in *APOE*ε3 and *APOE*ε4 mice using a Student's unpaired *t*-test. ***p<0.05**

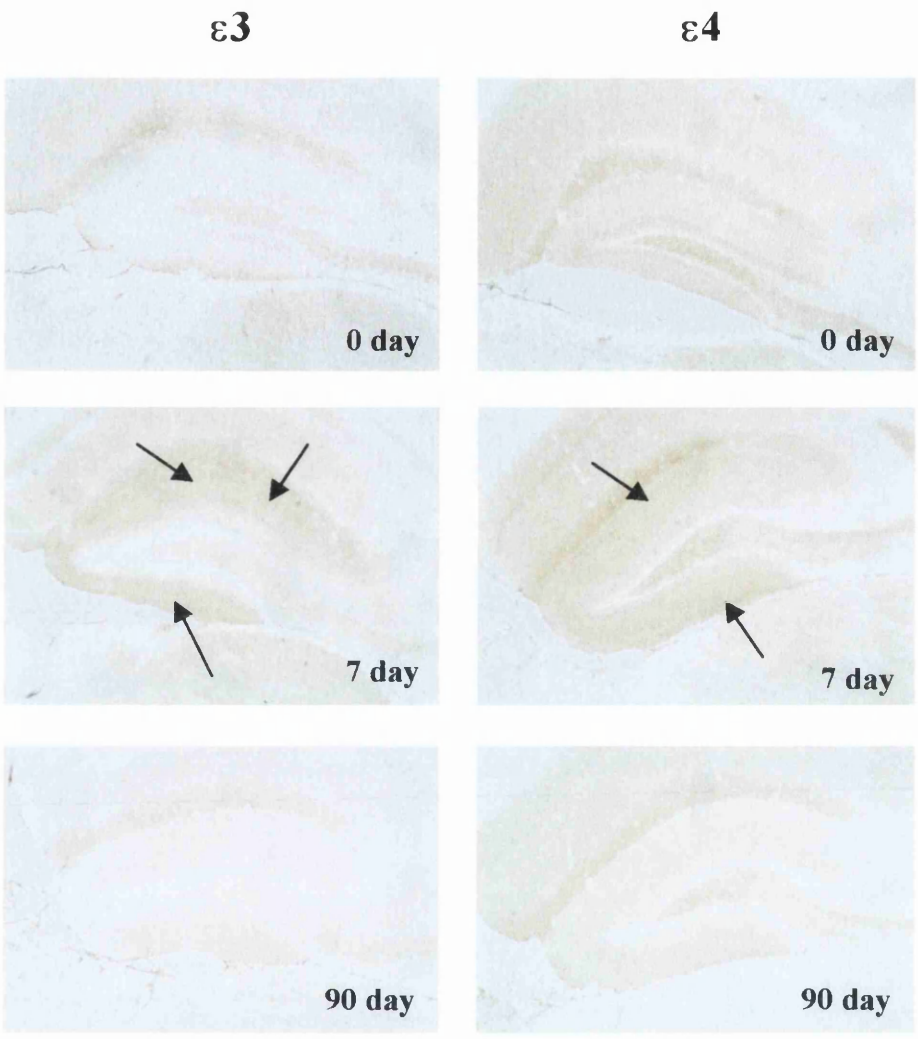

Figure 4.9 ApoE is increased at day 7 within the dentate molecular layers post-ECL

Illustrative examples of apoE immunoreactivity in transgenic mice expressing *APOE*ε3 and ε4 at day 0, 7 and 90 post-ECL. ApoE was increased within the neuropil and within some astrocytes. The contralateral hippocampus displayed no change in apoE immunoreactivity. The arrows highlight the region where apoE is upregulated. x50 magnification

4.4.5 Apolipoprotein J

(a) Cellular immunoreactivity

At day 7 post-ECL, apoJ immunoreactive glial cells were evident within the molecular layers of the dentate gyrus, but the extent was similar in *APOE*ε3 and ε4 mice (Figure 4.11).

Neuropil immunoreactivity

In 0 day control animals apoJ immunoreactivity was punctate and stained the molecular layers in a pattern similar to that observed for apoE. Pre-lesion apoJ optical density measurements were similar in *APOE*ε3 and *APOE*ε4 mice. Percentage difference between the ipsilateral and contralateral hippocampus was taken. ApoJ immunoreactivity increased within the molecular layers and was maximal at day 7 and 28 post-ECL, but was not statistically different between *APOE*ε3 and ε4 mice (Figure 4.10 and 4.11). ApoJ immunoreactivity then declined towards pre-lesion levels at day 90 post-ECL and was not statistically different in *APOE*ε3 and ε4 mice. Two way ANOVA on the contralateral hippocampal readings revealed no statistically significant variance.

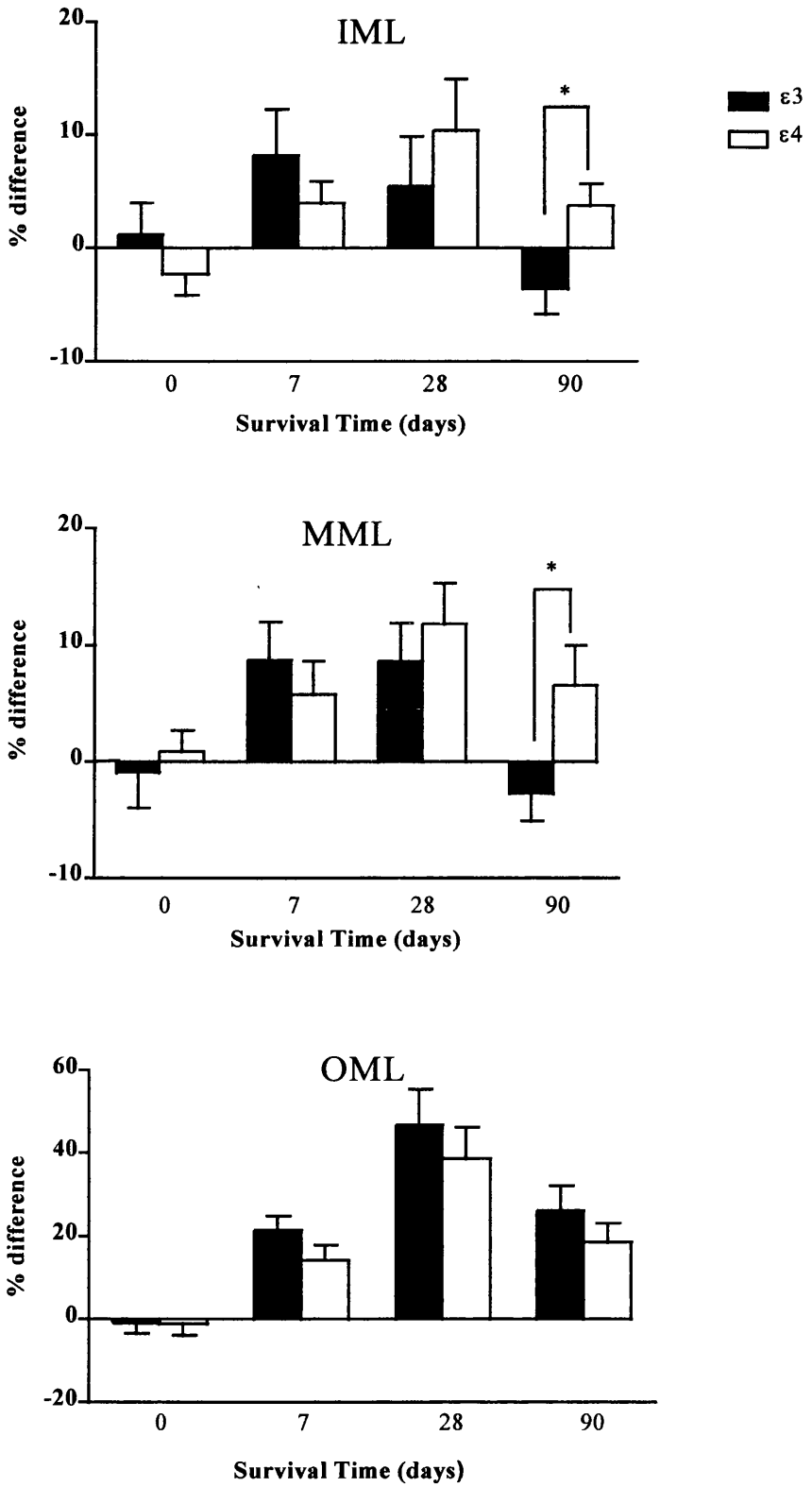

Figure 4.10 Quantification of apoJ neuropil immunoreactivity in the inner, middle and outer molecular layers (IML, MML, OML) of the hippocampal dentate gyrus at 0, 7, 28 and 90 days post-lesion measured as relative optical density values. Percentage difference between the ipsilateral and contralateral hippocampus immunoreactivity was compared in *APOE*ε3 and *APOE*ε4 mice using a Student's unpaired *t*-test. ***p<0.05**

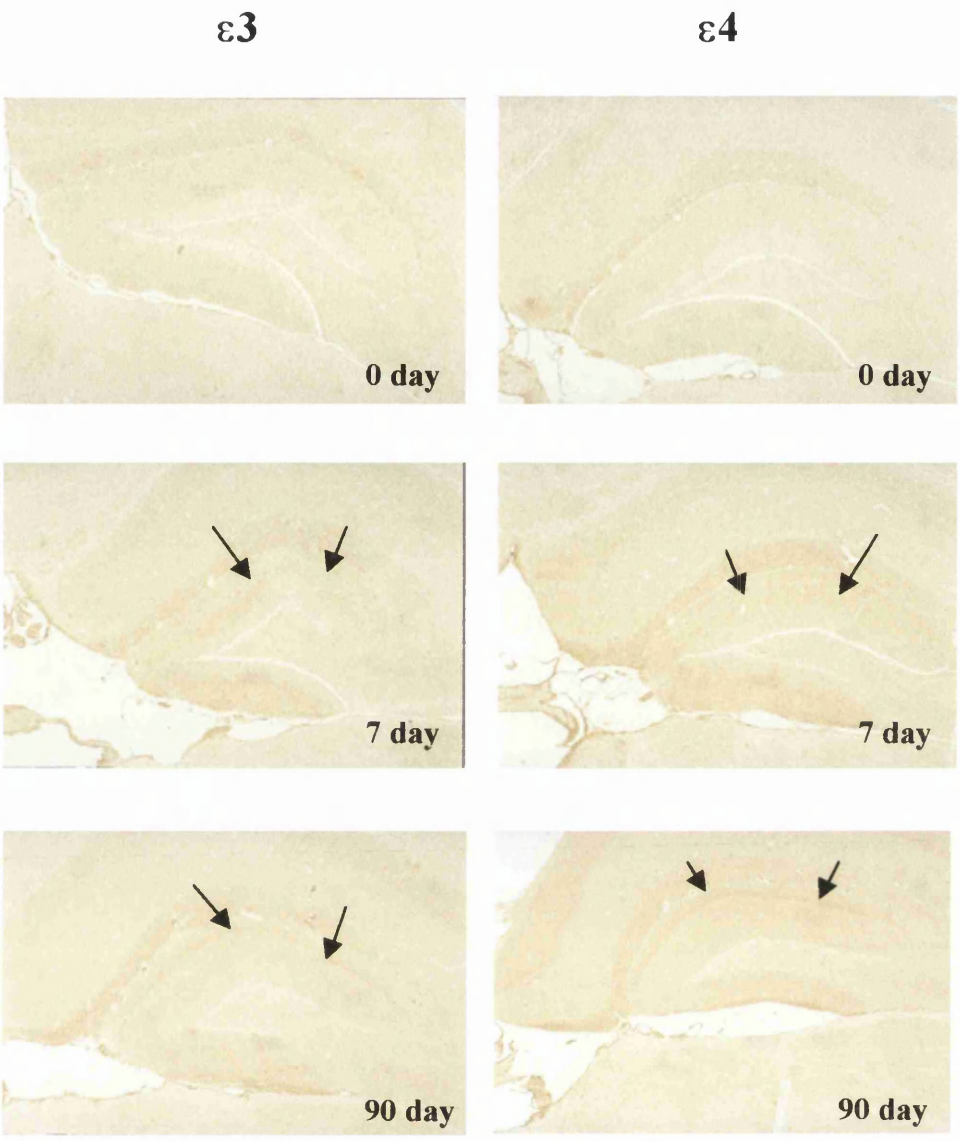

Figure 4.11 **ApoJ immunoreactivity is increased in astrocytes and the neuropil and is similar in both *APOE*ε3 and ε4 mice**

Illustrative examples of apoJ immunoreactivity in the ipsilateral hippocampus at day 0, 7 and 90 post-ECL in *APOE*ε3 and ε4 mice. ApoJ immunoreactivity is increased in astrocytes and the neuropil by day 7 post-ECL. At day 90 post-ECL apoJ immunoreactivity has declined within astrocytes however it remains elevated within the neuropil of the OML. There is no significant difference in apoJ immunoreactivity between ε3 and ε4 mice. x50 magnification

4.4.6 Cytoskeletal Alterations Post-Lesion

4.4.6.1 Alterations in MAP-2 immunoreactivity

One mechanism by which apoE isoforms may affect their differences in plasticity is by differential interaction with cytoskeletal components. It was hypothesised that there would be differences in the degree of MAP-2 immunoreactivity post-ECL. In 0 day control animals, MAP-2 characteristically labels the soma of neurons and the associated dendritic networks most intensely. Baseline MAP-2 immunohistochemistry was not significantly different between *APOE*ε3 and ε4 mice. Little or no alteration in MAP-2 was observed in the IML until day 90 post-ECL where the density of MAP-2 immunohistochemistry was increased within the ipsilateral hippocampus of *APOE*ε3 mice compared to ε4, however this was not a significant difference. Within the MML and OML, MAP-2 immunoreactivity declined slightly until day 28, however this was similar in both *APOE*ε3 and ε4 mice. MAP-2 staining then increased towards pre-lesion levels by day 90 post-ECL (Figure 4.12). At this time-point MAP-2 immunoreactivity was greater than contralateral levels in *APOE*ε3 mice however, in contrast, MAP-2 immunoreactivity remained below baseline levels in *APOE*ε4 mice ($p<0.05$). A similar pattern was observed within the OML, but at day 7 *APOE*ε3 mice displayed greater loss of MAP-2 immunohistochemistry compared to ε4 mice. At day 90 post-ECL MAP-2 levels had increased in *APOE*ε3 mice to above baseline levels and was significantly greater than that in *APOE*ε4 mice ($p<0.05$). Two way ANOVA revealed there was no statistically significant variance in the contralateral hippocampal immunostaining.

4.4.6.2 Alterations in microtubule organisation

These sections were also analysed using high power light microscopy to assess dendritic structure following the insult. It was found that in 0 day control animals, dendritic structure was uniform and similar in both *APOE*ε3 and ε4 mice. Fine fibrils run in parallel through the molecular layers in an well-organised fashion. At day 90 post-ECL, the dendritic networks in *APOE*ε3 mice recovered and were similar to that observed in 0 day control animals. In contrast, the dendritic networks in the molecular layers of *APOE*ε4 mice are very disarrayed. The MAP-2 labelled fibrils are fragmented and the fine fibrils normally observed are ill defined (Figure 4.14).

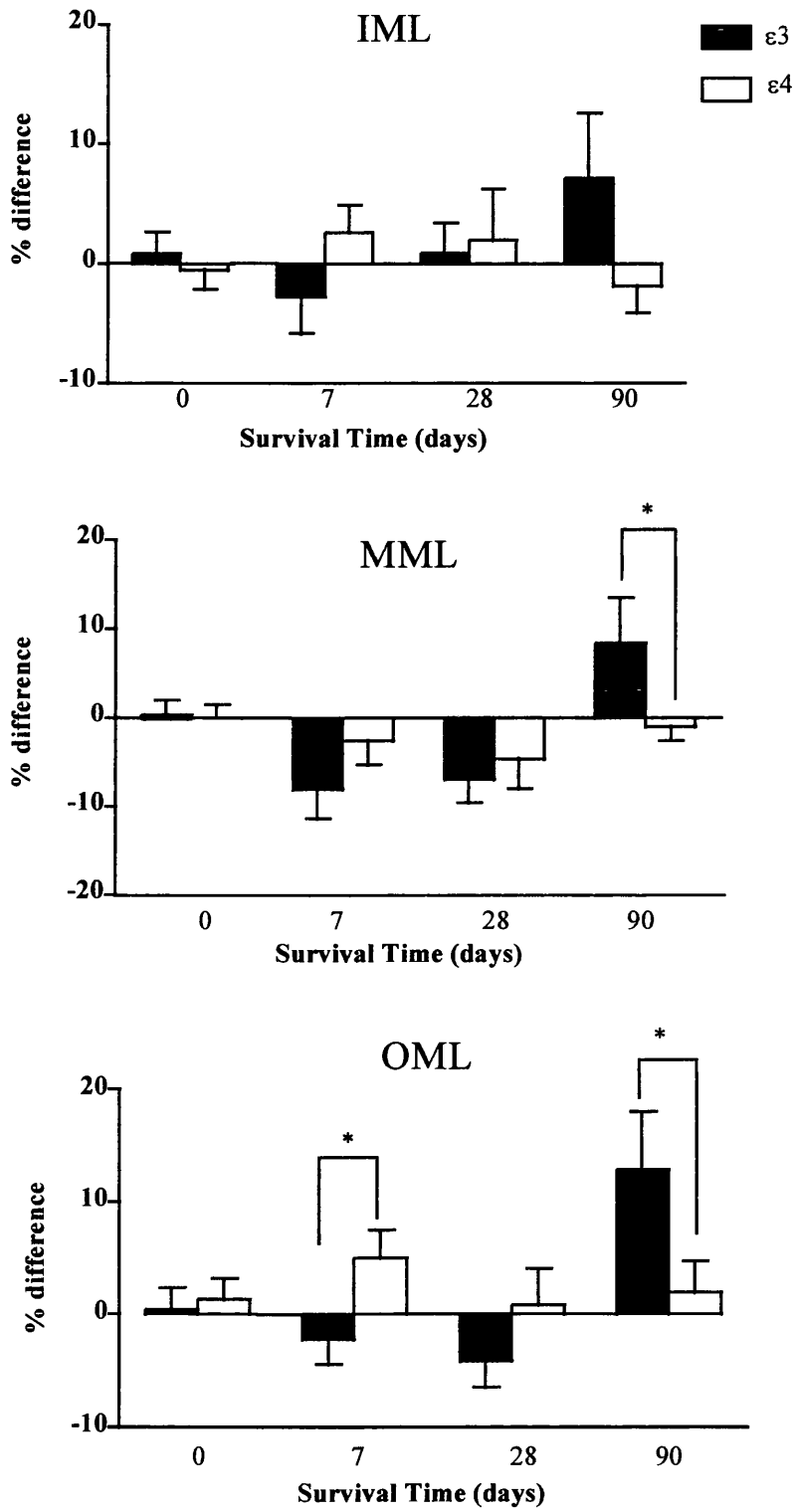

Figure 4.12 Quantification of MAP-2 immunoreactivity within the inner, middle and outer molecular layers (IML, MML, OML) of the hippocampal dentate gyrus at 0, 7, 28 and 90 days post-lesion measured as relative optical density values. Percentage difference between the ipsilateral and contralateral hippocampus immunoreactivity was compared in *APOE*ε3 and *APOE*ε4 mice using a Student's unpaired *t*-test. ***p<0.05**

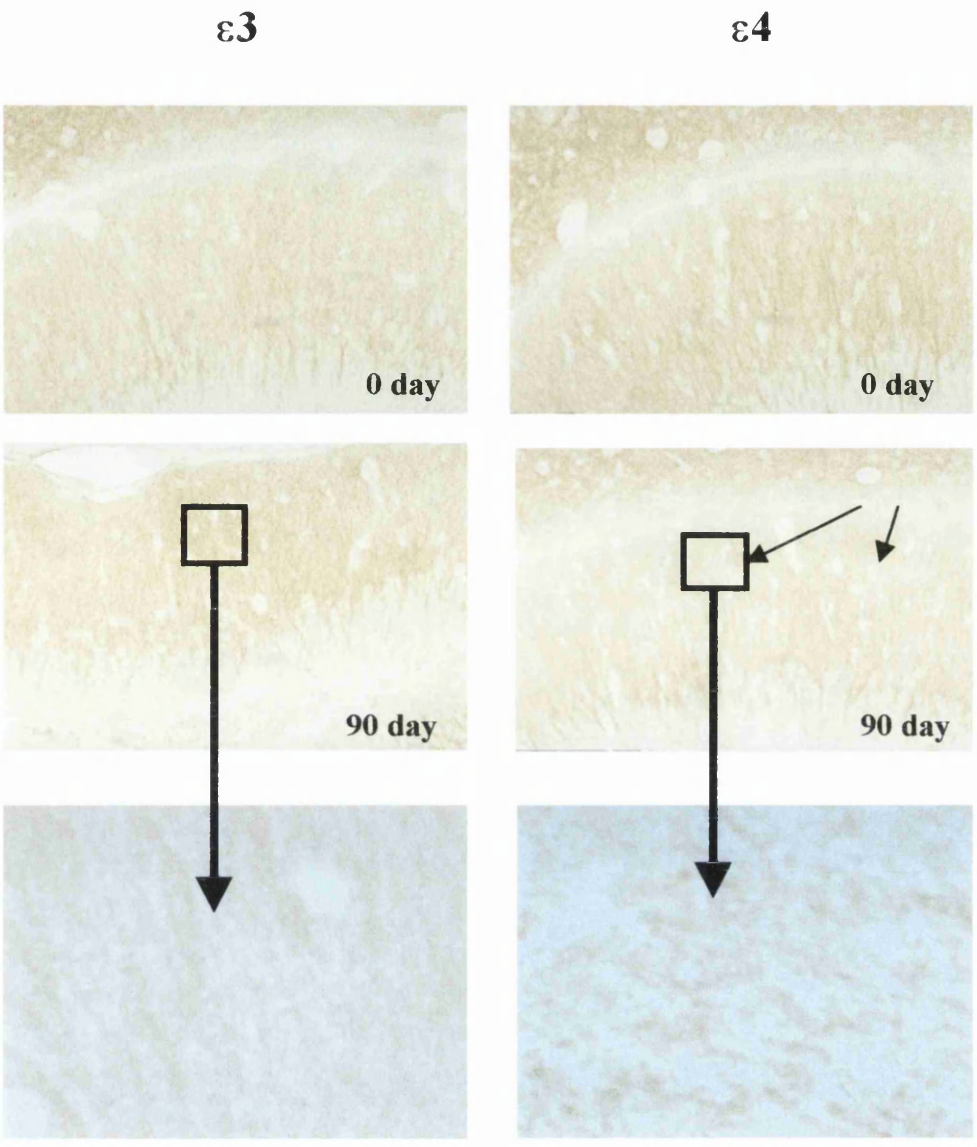

Figure 4.13 **Dendritic disorganisation in ε4 mice at day 90 post-ECL**

Illustrative examples of MAP-2 immunoreactivity in the ipsilateral hippocampus at day 0 and 90 post-ECL in *APOE*ε3 and ε4 mice. By day 90 post-ECL the dendritic networks in e3 mice are well-organised and fine fibrils can be seen passing through the molecular layers. In contrast, in ε4 mice, the dendritic networks are very disorganised, as highlighted by the arrows. x200 magnification (Inset x400 magnification)

4.4.7 Clearance of Degeneration Products Post-Lesion

It was hypothesised that differences in plasticity between *APOE*ε3 and ε4 mice may be dependent on the ability of the different isoforms to clear neuronal degeneration products. Sections from each subject were scored microscopically for degeneration product deposition. No degeneration products were present in 0 day control animals. No degeneration products were evident within the contralateral hippocampus, except for a thin band within the stratum lacunosum moleculare and thus only ipsilateral scores are represented graphically. From the studies in Chapter III it was shown that maximal degeneration product staining was achieved at day 3 post-ECL. For this reason two 3 day survival animals for each genotype were included in the study. Maximal accumulation of degeneration products was achieved by day 3 post-ECL. By day 7 post-ECL, degeneration products were cleared to leave only a thin band of material within the MML (Figure 4.14 and 4.15). This state persisted until day 28 post-ECL and thereafter degeneration products were cleared, until by day 90 post-ECL only minimal or no degeneration products were present within the dentate gyrus. No statistically significant difference in clearance was determined between *APOE*ε3 and ε4 mice at any time.

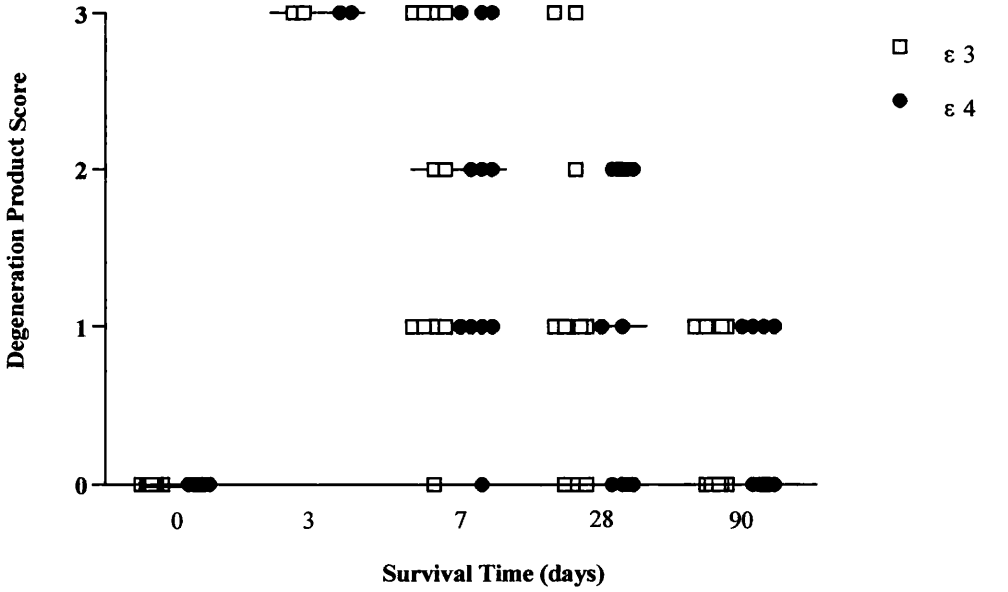

Fig 4.14 Quantification of Fink Heimer silver staining used to label degeneration products from axon terminals. Staining was scored on a scale of 0-3. 0- no degeneration products, 1-minimal, 2-moderate and 3-maximal. Scores from *APOE*ε3 and ε4 mice were compared using Mann-Whitney U test. No significant difference in clearance of degeneration products was detected. Bar indicates the median in each group +/- standard deviation.

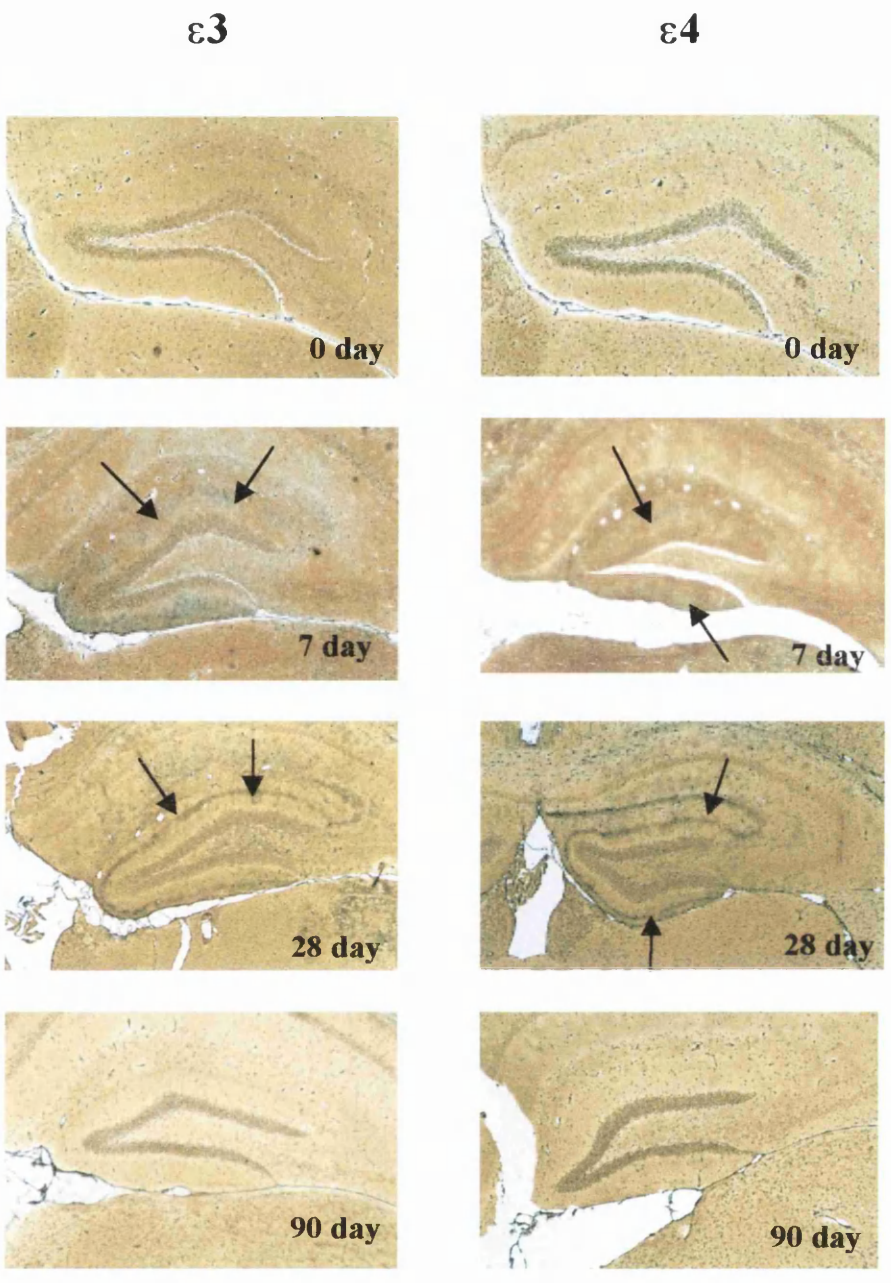

Figure 4.15 Equal rate of clearance of degeneration products in *APOE*ε3 and ε4 mice post-ECL

Illustrative examples of Fink-Heimer silver staining of degeneration products in human *APOE*ε3 and ε4 mice at day 0, 7, 28 and 90 post-ECL. The contralateral hippocampus displayed no degeneration products at any time. The arrows mark regions where degeneration products are present. x50 magnification

4.4.8 LRP Receptor Expression Post-Lesion

Cellular immunoreactivity

In 0 day control animals only minimal astrocytic LRP immunoreactivity was observed. At day 7 post-ECL (Figure 4.17), LRP immunoreactivity increased on reactive astrocytes within the dentate molecular layers, but was not present at day 28 post-ECL and astrocytic immunoreactivity was similar in both *APOE*ε3 and ε4 mice.

Neuropil immunoreactivity

In 0 day control animals LRP receptor immunoreactivity was evident on neuronal cell bodies and in the neuropil but was similar in *APOE*ε3 and ε4 animals. In general, there were no significant alterations in neuropil LRP immunoreactivity and certainly no statistical difference in staining between *APOE*ε3 and ε4 mice (Figure 4.16). Two way ANOVA revealed no significant variance in the contralateral hippocampal readings.

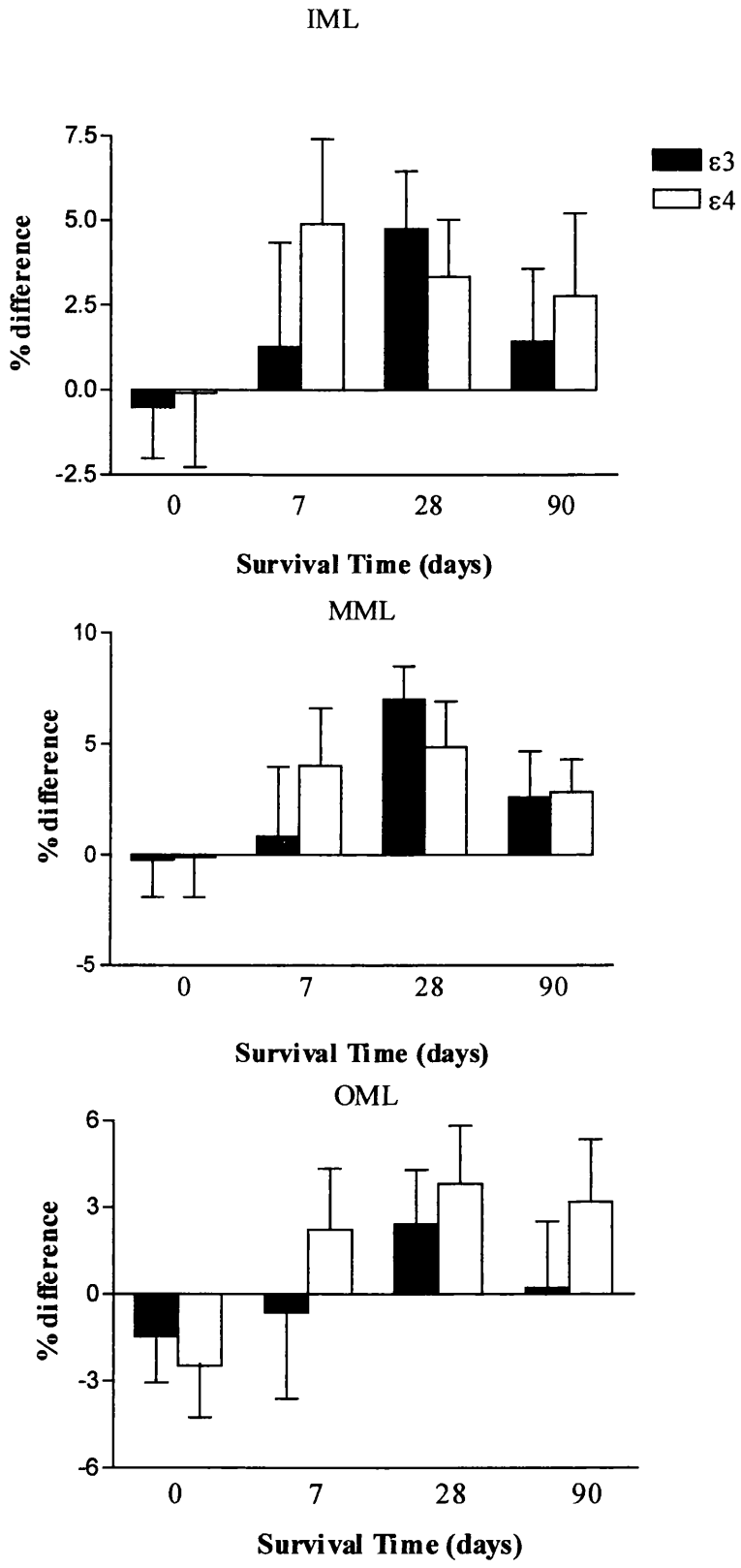

Figure 4.16 Quantification of LRP receptor neuropil immunoreactivity in the inner, middle and outer molecular layers (IML, MML, OML) of the hippocampal dentate gyrus at 0, 7, 28 and 90 days post-lesion measured as relative optical density values. LRP immunoreactivity in *APOE*ε3 and ε4 mice was compared using a Student's unpaired *t*-test.

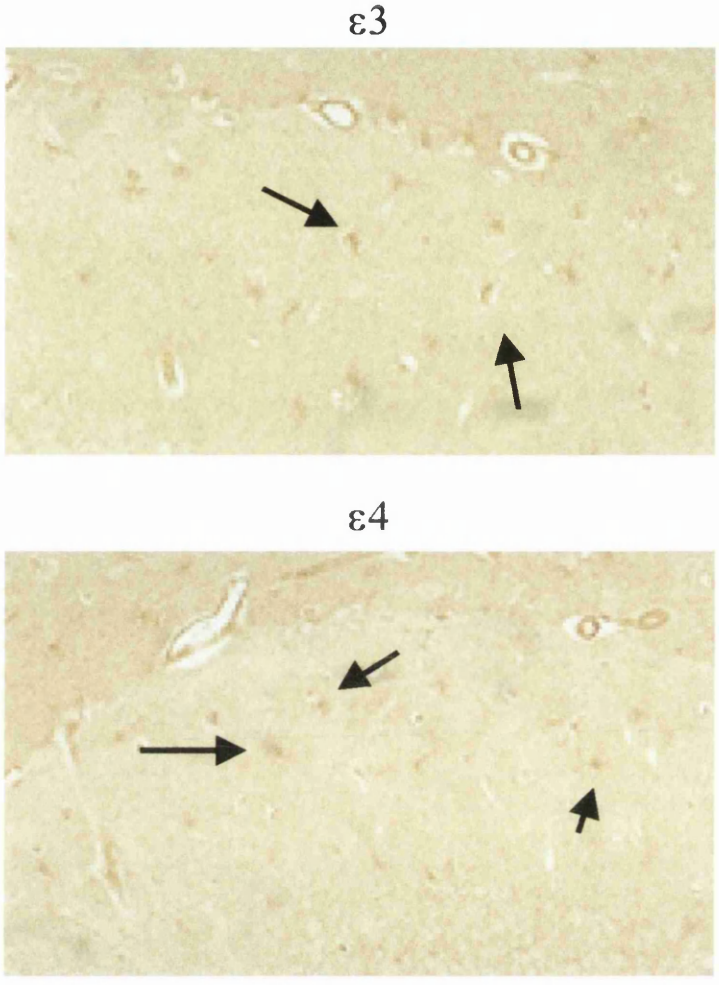

Figure 4.17 Increased LRP receptor immunoreactivity in astrocytes by day 7 post-ECL but similar in *APOE*ε3 and ε4 mice

Illustrative examples of LRP immunoreactivity at day 7 post-ECL in *APOE*ε3 and ε4 mice. 0 day LRP immunoreactivity is similar in ε3 and ε4 mice. By day 7 post-ECL, LRP immunoreactivity is increased in reactive astrocytes within the molecular layers but is similar in ε3 and ε4 mice (x200). At day 7 and 90 no astrocytic LRP immunoreactivity was evident.

4.5 Discussion

The ε4 allele of the *APOE* gene is associated with sporadic and late-onset AD (Corder *et al*, 1993; Saunders *et al*, 1993; Hyman *et al*, 1996; Roses *et al*, 1996; Roses *et al*, 1997) and a poor recovery after head injury in humans (Jang *et al*, 1996; Teasdale *et al*, 1997; Horsburgh *et al*, 2000). The present study indicates that long-term neuronal repair mechanisms are impaired in transgenic mice possessing human *APOE*ε4 alleles compared to *APOE*ε3 after denervative injury (Xu *et al*, 1996, 1998, 1999).

4.5.1 *APOE* genotype influence in the acute response to brain injury

In this study we hypothesised that *APOE*ε4 mice would have a poorer reparative capacity than *APOE*ε3 mice after ECL. This was primarily based on previous studies of these mice that highlighted an adverse influence of the ε4 allele to acute brain injury types. One of these studies which was carried out by our group, showed that *APOE*ε4 mice incurred a greater level of neuronal cell injury following a period of global ischaemia (Horsburgh *et al*, 2000). However contrary to this, the data indicated that in the acute phase after ECL, the *APOE*ε3 mice had a greater degenerative response than *APOE*ε4 mice, the ε3 mice experiencing greater fibre and synapse loss in the acute phase of the injury (28 days). One potential explanation for this is that the levels of apoE present may be crucial in the acute stage after injury. The *APOE*ε4 mice in this transgenic line express approximately 20% more apoE than the ε3 line and therefore this may cause an inherent difference in the initial response to injury. This is reflected in studies using *APOE* deficient mice, which show a markedly poorer response to an episode of global ischaemia compared to wild-type littermate controls (Horsburgh *et al*, 1999). However, increasing the levels of apoE by intraventricular infusion, greatly ameliorates this response in apoE deficient mice (Horsburgh *et al*, 2000). It has also been suggested that low levels of apoE, found in *APOE*ε4 individuals (Bertrand *et al*, 1995), underlie their susceptibility for the development of AD and potentially to the effects of trauma. Another possibility is that it could be a detrimental effect of the ε3 isoform in the acute response to ECL. However, there is no data to indicate that apoE E3 has a detrimental effect on neuronal integrity. Despite this initial poor response, *APOE*ε3 mice were able to compensate and

promote sprouting, unlike the *APOE*ε4 mice which demonstrated a poorer ability to recover post-ECL.

4.5.2 *APOE* genotype and its influence in the long-term response to brain injury

Most recently it has been determined by our group that, following a head trauma, individuals with an ε4 genotype have a significantly impaired recovery. This results in a greater number of these individuals being severely disabled or scoring lower on cognitive assessments compared to ε3 individuals on a 6 month outcome analysis. These findings were particularly important considering the individuals in question were under the age of 15 years and therefore, ruled out any of the amyloid depositon theories to isoform differences which had previously reigned (Teasdale *et al*, 2000). Inefficient plastic remodelling in AD patients possessing ε4 alleles of the *APOE* gene (Arendt *et al*, 1997) has also been shown. We found that plastic neuronal remodelling was impaired in *APOE*ε4 mice. In this study we analysed sprouting from the commissural-associational neurons by measuring the width of the IML as previously described (Anderson *et al*, 1998). At day 90 post-ECL, the IML of *APOE*ε3 mice had expanded by almost 45% compared to only 20% in ε4 mice. This is consistent with the poor recovery of the MML and OML shown in ε4 mice.

The present study substantiates other studies, which have indicated a role for apoE in the response of the brain to trauma (Poirier *et al*, 1993; Posse de Chaves *et al*, 1997). ApoE is produced and secreted by astrocytes, microglia (Boyles *et al*, 1985; Stone *et al*, 1997) and neurons (Han *et al*, 1994; Roses *et al*, 1997; Xu *et al*, 1998, 1999), and it functions primarily in the transport of lipids and cholesterol to cells requiring the material for remodelling (Holden, 1998; Holtzman and Fagan, 1998; Pitas *et al*, 1998). Lipid is essential for the long-term remodelling events after injury. This includes reconstruction of cellular elements (i.e. membrane) (Poirier *et al*, 1993; Poirier *et al*, 1995), if neurite outgrowth and dendritic field reorganisation is to occur. Further support for the involvement of apoE in long-term plasticity comes from studies employing *APOE*-deficient mice, in which entorhinal cortex lesioning is associated with severe neurodegenerative changes and compromised compensatory sprouting (Masliah *et al*, 1995; Anderson *et al*, 1998).

4.5.3 Alterations in apoE expression in transgenic mice post-ECL

In this study, apoE increased within the neuropil post-ECL equally for both *APOE*ε3 and ε4 mice and at day 90 post-ECL, apoE immunoreactivity had returned to baseline levels. Glial apoE within the dentate gyrus was also evident after the injury (Poirier *et al*, 1991; Boyles *et al*, 1995). This pattern of apoE expression has been identified within human AD brains (Kida *et al*, 1995; Harr *et al*, 1996; Hesse *et al*, 1999) and also in previous animal studies (Masliah *et al*, 1996; Terrisse *et al*, 1999). The transient increase in apoE immunoreactivity corresponded with the time period during which sprouting and synaptogenesis began to occur.

It has been suggested that the effects of *APOE* genotype on plasticity may be mediated by differences in the levels of apoE in the brain, rather than differences in the isoform of the protein. Support for this idea has come from the suggestion that brain levels are lower among AD patients possessing the *APOE*ε4 allele (Bertrand *et al*, 1995). This seems unlikely to explain the findings of this study, because baseline apoE levels were initially greater in *APOE*ε4 mice compared to ε3 yet they recovered poorly from the insult. Therefore the data would seem to suggest an isoform effect rather than a level effect in the chronic response to injury. This isoform hypothesis is supported in a study by Buttini *et al* (2000), which shows that *APOE*ε4 homozygotes recover poorly from excitotoxic injury compared to *APOE*ε3/ε4 heterozygotes. In the present study, the greater baseline levels of apoE in ε4 mice was found to correlate with increased GAP-43 immunoreactivity in control mice. This raises the possibility that fibre density in humans may be influenced by *APOE* genotype and this would suggest greater fibre density under normal physiological conditions however this does not have any implications for its behaviour in injury. In the present study, neither *APOE* genotype nor apoE levels had an influence on baseline synaptic density. Genotype influences on baseline fibre density have not been identified in humans as of yet.

4.5.4 Alterations in apoJ expression in transgenic mice post-ECL

It is hypothesised that apoJ may perform a similar function in lipid transportation and neuronal repair as apoE (Poirier *et al*, 1995). Recent studies in humans have shown

that apoJ is increased in senile plaques in the brains of AD sufferers (Kida *et al*, 1995), and that apoJ levels in the brain are associated with *APOE* genotype (Bertrand *et al*, 1995). The authors stipulated that apoE protein levels decreased with increasing number of inherited ε4 alleles, but apoJ protein levels increased. This suggests that apoJ increased perhaps as a function of apoE levels in the brain and not purely because of genotype. This is consistent with the finding that in this study, *APOE*ε3 mice displayed higher levels of apoJ immunoreactivity compared to that in ε4 mice but they also expressed lower levels of apoE. ApoJ increased similarly for both genotypes by day 7 and 28 post-ECL. However, at day 90 post-ECL apoJ immunoreactivity was significantly decreased in *APOE*ε3 mice compared to ε4. This would seem plausible, considering the ε4 mice are in an uphill struggle to repair.

4.5.5 ApoE isoform influence on factors which may modulate CNS plasticity

4.5.5.1 Lipid clearance post-ECL

The clearance of debris from the site of an injury is essential if the lipid materials are to be recycled for incorporation into cellular elements such as membrane. In apoE knockout mice, lipid clearance is deficient mainly due to the absence of apoE (Fagan *et al*, 1998) and thus these mice display deficient regenerative capabilities. Isoform-effects on this mechanism have not been addressed. However, in this study *APOE*ε3 and ε4 mice exhibited similar rates of clearance of degeneration products and by day 90 post-ECL, all debris had been cleared from the dentate gyrus in both lines. Therefore, this suggests both isoforms efficiently clear lipid and another mechanism may underlie the adverse effects of the apoE E4 protein (Jolivalt *et al*, 2000).

4.5.5.2 Actions on the LRP receptor

The neurotrophic effects of apoE have been directly demonstrated *in vitro*. Addition of lipidated apoE to a population of cultured neuronal cells enhances neurite outgrowth (Fagan *et al*, 1998, Pitas *et al*, 1998). The outgrowth promoting effects of apoE have been determined to be isoform specific such that neurite outgrowth in cultured cells was stimulated by apoE E3, but attenuated by apoE E4 (Nathan *et al*, 1994; Bellosta *et al*, 1995; DeMattos *et al*, 1998). This has been shown to be modulated via apoE interaction with the LRP receptor, an effect that may be

attenuated by administration of an LRP blocker. In this study there were no major alterations in LRP receptor neuropil immunoreactivity after the injury and staining was similar in *APOE*ε3 and ε4 mice. However, astrocytic LRP expression was increased at day 7 post-ECL but the levels were similar in *APOE*ε4 and ε3 mice. This type of analysis does not allow the functioning and binding of apoE to be determined however other groups have endeavoured to analyse this and will be discussed in chapter IX. Recent data has suggested that interaction of apoE with the LRP receptor modulates intracellular signalling pathways which may, in turn modulate intracellular proteins i.e. those affecting cytoskeletal structural alterations (Herz, 2001). These mechanisms will be elaborated upon in the final discussion.

4.5.5.3 Actions on the cytoskeleton

It is thought that the action of apoE on the neuronal cytoskeleton may play a large role in the plasticity response. In this study it was found that MAP-2 protein was reduced following the injury but increased towards baseline levels in *APOE*ε3 mice. In contrast, MAP-2 protein remained severely reduced in *APOE*ε4 mice. More importantly, it was found that dendritic structure was severely disrupted in *APOE*ε4 mice compared to *APOE*ε3 mice. ApoE plays a major role in maintaining the integrity of the microtubular system (Roses *et al*, 1996; Scott *et al*, 1998) and this relationship may be isoform-dependent (Sun *et al*, 1998). This adverse influence of apoE E4 on neurite outgrowth has been attributed to its function in microtubule depolymerisation and destabilization (Nathan *et al*, 1995; Pitas *et al*, 1998), an effect not favourable during neuronal remodelling and outgrowth. Although reorganisation of the cytoskeleton is important in the remodelling process the E4 isoform appears to cause significant depolymerisation without polymerisation and may not protect the microtubule from phosphorylative enzymes.

In summary, this data shows that long-term neuronal remodelling is impaired in *APOE*ε4 transgenic mice (on a human promoter) after injury and supports a role for apoE isoform influence on plasticity.

Chapter V
Analysis of *APOE* Genotype Influence on CNS Plasticity in *APOE* Knockout and Transgenic Mice Expressing Human *APOE ε3* and ε4 Alleles (GFAP Promoter) Following Entorhinal Cortex Lesion

5.1 Introduction

In the previous study it was demonstrated that *APOE*ε4 mice display poor neuronal repair capabilities following injury. The transgenic mice discussed in the previous chapter had the entire human *APOE* gene inserted, including promoter sequence, into their genome that resulted in expression of apoE similar to that found in human brain, that is they expressed apoE in neurons and glia. However, the contribution of endogenous neuronal apoE to plasticity was unclear. A different line of transgenics became available which possess an exogenous GFAP promoter sequence downstream of the gene, which drives astrocytic apoE expression (Sun *et al*, 1998). The investigation of these transgenic mice allows other questions to be addressed in terms of apoE expression and function after injury. This study was undertaken to determine if the *APOE*ε4 allele exerted its adverse effects on plasticity when it is expressed endogenously in astrocytes only. The hypothesis was that possession of the *APOE*ε4 genotype in these transgenic mice would result in impaired repair processes after injury.

5.2 Aims

To analyse *APOE* genotype on CNS plasticity in a line of *APOE* knockout mice and transgenic mice expressing human *APOE*ε3 and ε4 under an exogenous GFAP promoter sequence following entorhinal cortex lesion.

5.3 Materials and Methods

5.3.1 *APOE* transgenic mice on a GFAP promoter

*APOE*ε3 and ε4 heterozygous transgenic mice were generated as previously described (Holtzman *et al*, 1998). The coding sequences of the human *APOE* gene were inserted into the genome of B6/CBA mice. Mice were obtained from Dr Holtzman and transported to the UK according to Home Office Regulations and bred in an animal unit at the University of Glasgow. Knockout littermates are also produced in the breeding of these animals. The genotypes of all animals bred were checked using PCR analysis (see Chapter II).

5.3.2 Entorhinal cortex lesion

The entorhinal cortex was lesioned in male knockout, transgenic *APOE*ε3 and ε4 mice. The mice were then allowed to survive for periods of 90 days (KO/n=12, ε3/n=8, ε4/n=7). 0 day control animals underwent an identical procedure but were terminated immediately after the procedure (KO/n=11, ε3/n=8, ε4/n=8). Tissue was also harvested from naïve mice and homogenised for separation by gel electrophoresis. Sections from the entorhinal cortex were histologically stained using haematoxylin and eosin to confirm correct lesion placement. Immunohistochemistry for synaptophysin, GAP-43, apoE, apoJ, LRP and MAP-2 was performed on hippocampal sections. The IML width, in GAP-43 immunostained sections, was measured and analysed as outlined in chapter II.

5.3.3 Quantification of immunohistochemistry and statistical analysis

Relative optical density values were collected from the inner, middle and outer molecular layers of both the ipsilateral and contralateral hippocampus using an MCID image analysis system connected to a microscope. Six optical density readings were collected from the expanse of each layer using a $1cm^2$ sampling box and an average taken. The percentage difference between the ipsilateral and contralateral hippocampus was taken for comparison between the genotypes. The groups were compared using ANOVAR and the genotypes compared using a post-hoc Student's

unpaired *t*-test with Bonferroni correction for multiple comparisons. All data is represented graphically using the mean +/- S.E.M.

5.3.4 Silver Staining

Fink Heimer silver staining was carried out to assess terminal degeneration products and to determine a time-course for clearance (see chapter II). Deposition of silver labelled degeneration products within the ipsilateral hippocampus was semi-quantified using a scoring method (0= no staining, 1= minimal, 2= moderate and 3= extensive). Scores were tested for variance using a Kruskal Wallis test and the genotypes compared using a Mann Whitney U statistical test for non-parametric data.

5.4 Results

5.4.1 *APOE* levels

The brains of 12 week old *APOE*ε3 and ε4 mice were harvested, the hippocampus dissected and rapidly frozen in liquid nitrogen. Tissue homogenates were produced and 10μg of protein separated by SDS-PAGE gel electrophoresis. Immunoblotting for apoE was performed as previously described (chapter II). Protein bands were assessed as relative optical density values using an image analyser (MCID). ApoE levels were found to be comparable in the ε3 and ε4 mice (Figure 5.1).

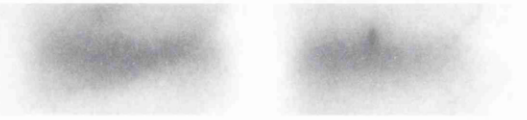

ε3 ε4

Figure 5.1 Western blotting bands showing apoE levels in *APOE*ε3 and ε4 transgenic mice. Levels are comparable in ε3 and ε4 mice.

5.4.2 Lesion assessment

Lesion placement was assessed histologically and appeared as an area of pallor in which cells were pyknotic in appearance. The lesions were restricted to the entorhinal cortex, with no involvement of the adjacent structures. Control animals displayed no excitotoxic damage to the entorhinal region, only the site of the needle placement was visible. No observable difference was evident between the lesion volumes of knockout, *APOE*ε3 or ε4 mice.

5.4.3 Temporal Profile of Degeneration and Regeneration Post-Lesion

5.4.3.1 Alterations in synaptophysin immunoreactivity

Synaptic alterations during degenerative and reinnervative events within the hippocampal dentate gyrus were assessed using synaptophysin immunohistochemistry. Percentage difference between the ipsilateral and contralateral hippocampus was compared in knockout, *APOE*ε3 and *APOE*ε4 mice. Synaptophysin immunoreactivity in 0 day control mice displayed a regular dense pattern of staining throughout the

dentate gyrus and did not differ significantly between the genotypes. At day 90 post-ECL, ipsilateral synaptophysin immunoreactivity was significantly reduced in all layers (20-30%). There was no statistically significant difference between *APOE* knockout, ε3 and ε4 mice (Figure 5.2 and 5.4).

5.4.3.2 Alterations in growth-associated protein immunoreactivity

In 0 day control mice, GAP-43 immunoreactivity exhibited a regular dense, punctate, stain within the outer two thirds of the molecular layer and denser labelling within the IML and there was no statistically significant difference in GAP-43 levels between the genotypes. At day 90 post-ECL, GAP-43 immunoreactivity was not significantly altered in the ipsilateral hemisphere in *APOE* knockout and ε3 mice in the IML, but ε4 mice displayed a deficit. In the MML and OML, *APOE* knockout, ε3 and ε4 mice displayed a deficit in GAP-43 immunoreactivity in the ipsilateral hemisphere compared to the contralateral at 90 days. This deficit was most marked in the ε4 mice ($p<0.05$) (Figure 5.3 and 5.5).

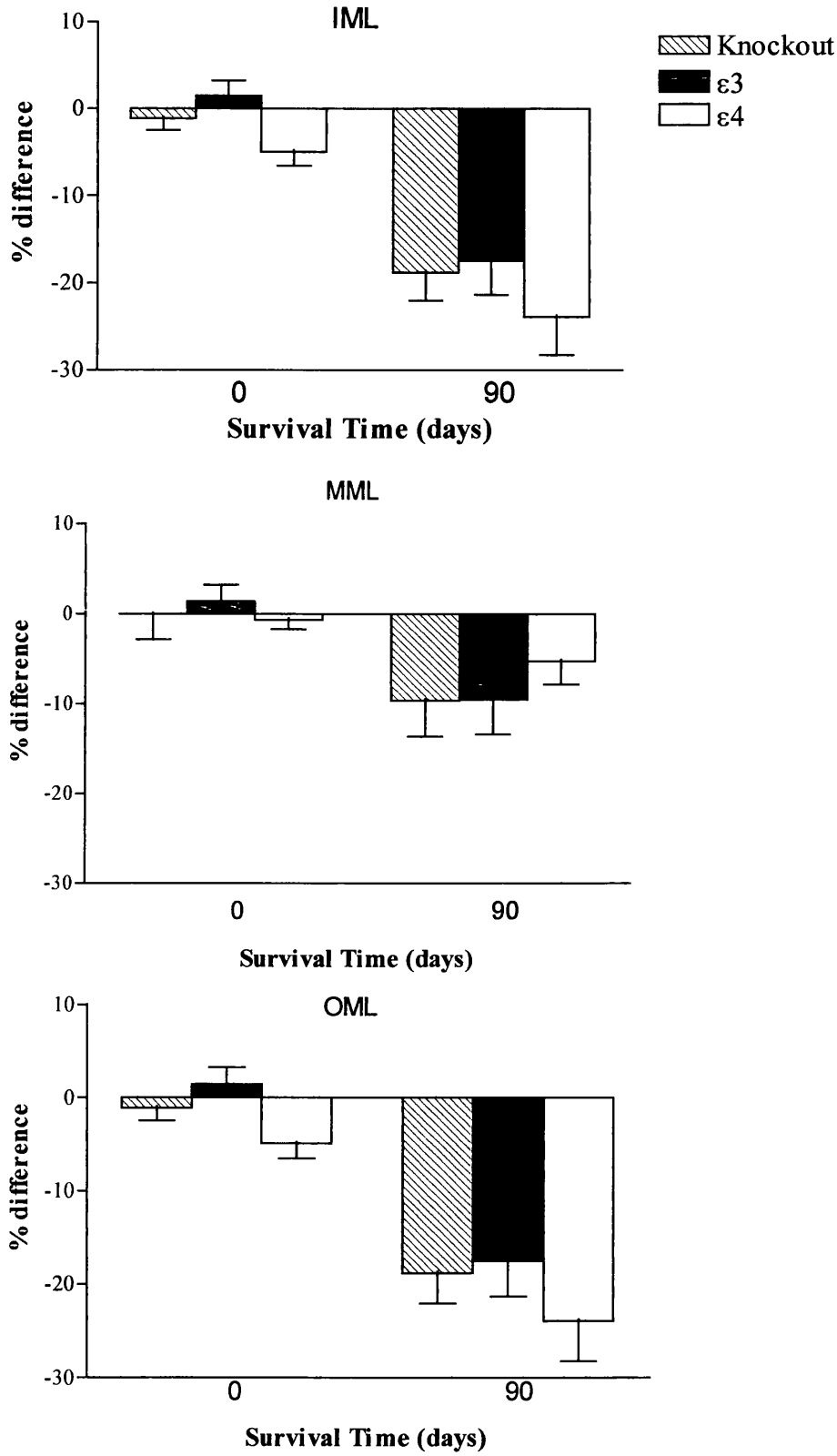

Figure 5.2 Quantification of synaptophysin immunoreactivity in the inner, middle and outer molecular layers (IML, MML and OML) of the hippocampal dentate gyrus measured as relative optical density values at 0 and 90 days post-lesion. Percentage difference between the ipsilateral and contralateral hippocampus immunoreactivity was compared in *APOE* knockout, ε3 and ε4 transgenic mice using a Student's unpaired *t*-test with Bonferroni correction for multiple comparisons.

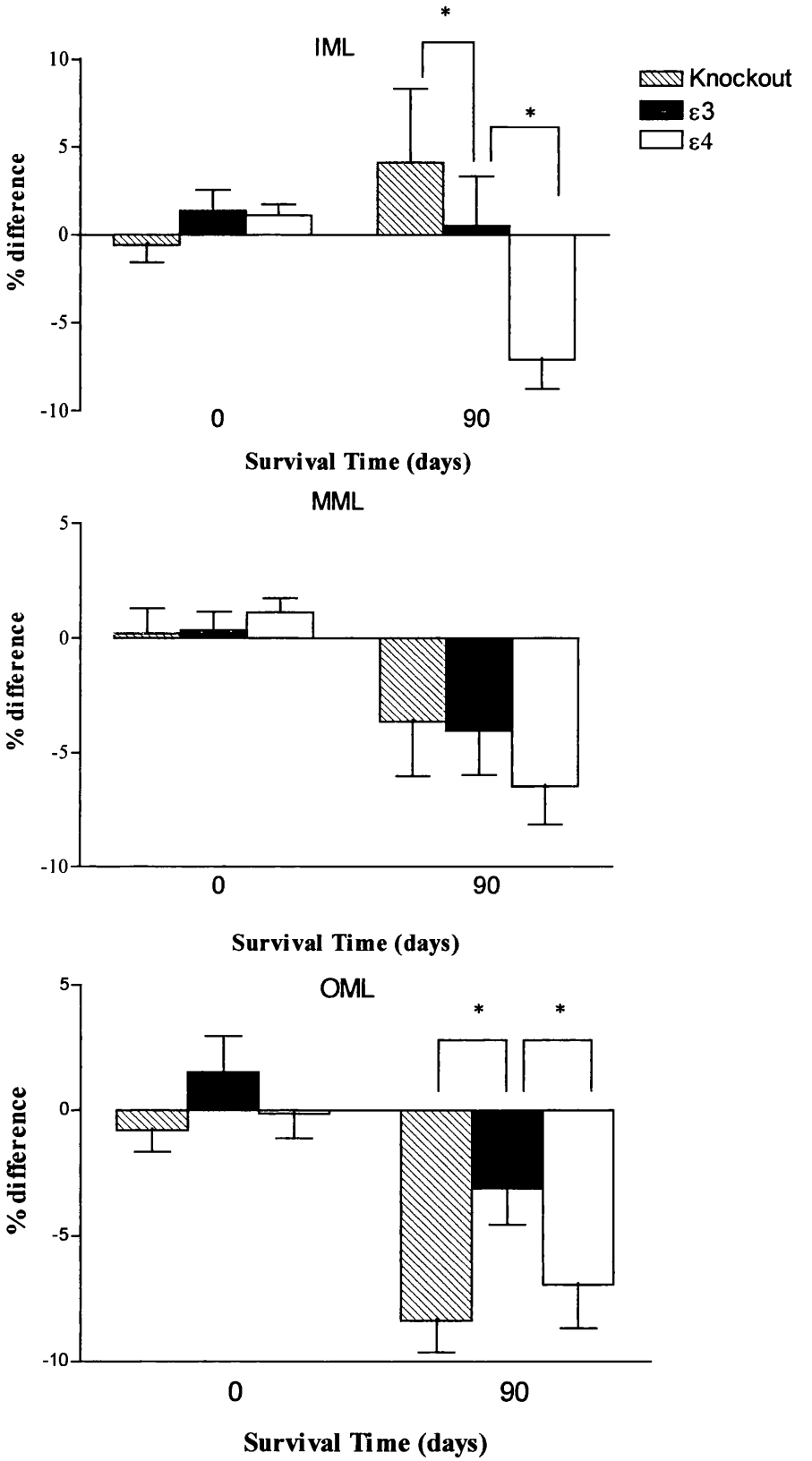

Figure 5.3 Quantification of GAP-43 immunoreactivity in the inner, middle and outer molecular layers (IML, MML and OML) of the hippocampal dentate gyrus, measured as relative optical density values at 0 and 90 days post-lesion. Percentage difference between the ipsilateral and contralateral hippocampus immunoreactivity was compared in *APOE* knockout, ε3 and ε4 transgenic mice using a Student's unpaired *t*-test with Bonferroni correction for multiple comparisons. ***p<0.05**

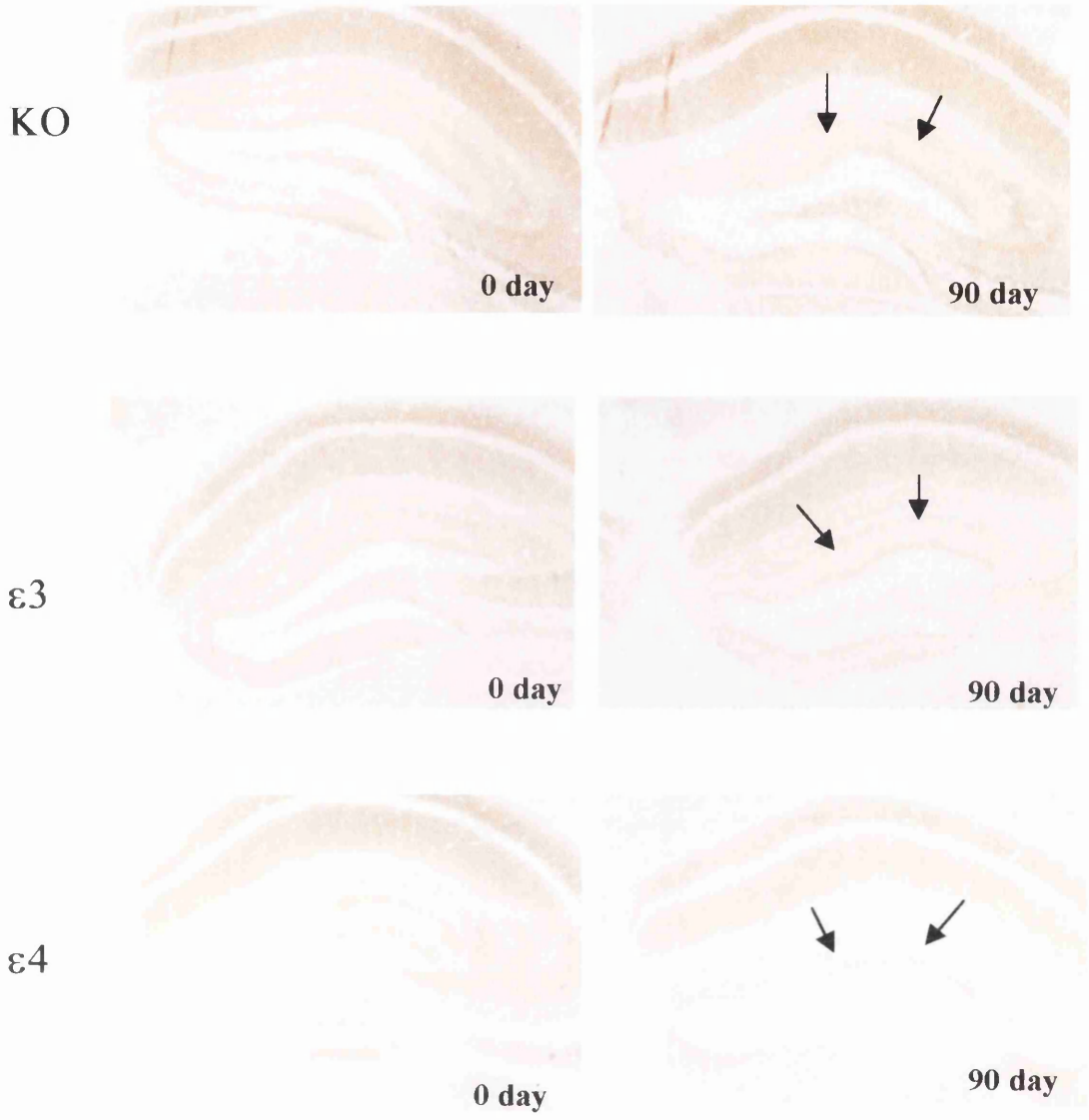

Figure 5.4 **Synaptophysin immunoreactivity in *APOE* knockout (KO), ε3 and ε4 mice post-ECL**

Illustrative examples of synaptophysin immunoreactivity in the ipsilateral hippocampus at day 0 and 90 post-ECL in *APOE* knockout, ε3 and ε4 transgenic mice. Contralateral synaptophysin immunoreactivity does not alter post-ECL. x50 magnification

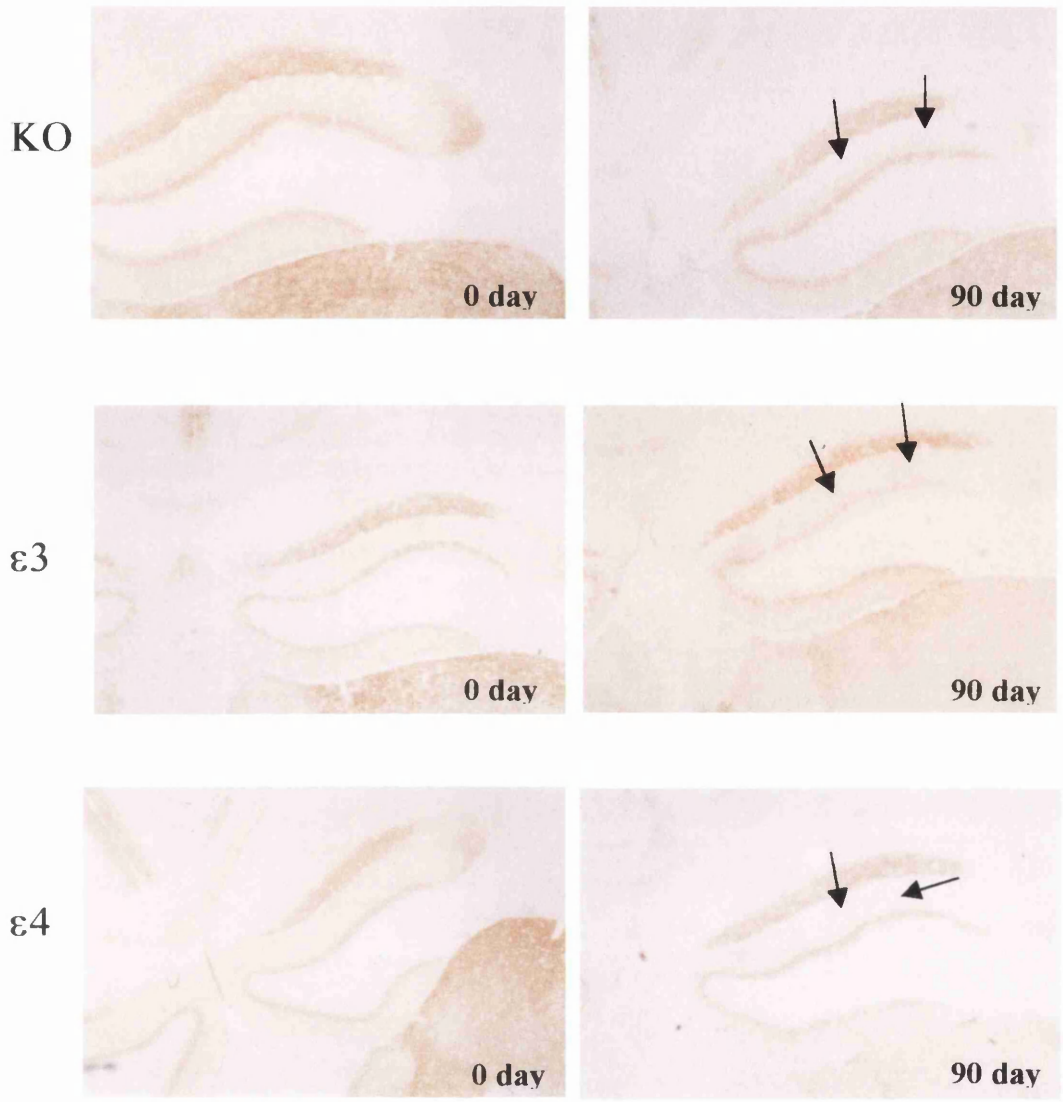

Figure 5.5 **Impaired sprouting in *APOE*ε4 mice at day 90 post-ECL**

Illustrative examples of GAP-43 immunoreactivity in the ipsilateral hippocampus at day 0 and 90 post-ECL in *APOE* knockout, ε3 and ε4 mice. GAP-43 immunoreactivity in the contralateral hippocampus did not alter post-ECL. The arrows delineate the region of the hippocampus affected by the lesion. x50 magnification

5.4.3.3 IML width alterations post-lesion

The width of the IML in GAP-43 immunostained sections was measured in each animal to give an indication of the degree of sprouting from the commissural-associational fibres. In 0 day control animals there was no statistically significant difference in IML width between the genotypes. At day 90 post-ECL, IML width increased in mice of all genotypes, but more so in *APOE*ε3 mice (30%) and knockout mice (25%) compared to *APOE*ε4 mice (20%). Comparison of the IML widths at day 90 revealed IML width was significantly greater in *APOE*ε3 mice compared to *APOE*ε4 but was not significantly different to that of knockout mice ($p<0.05$) (Figure 5.6).

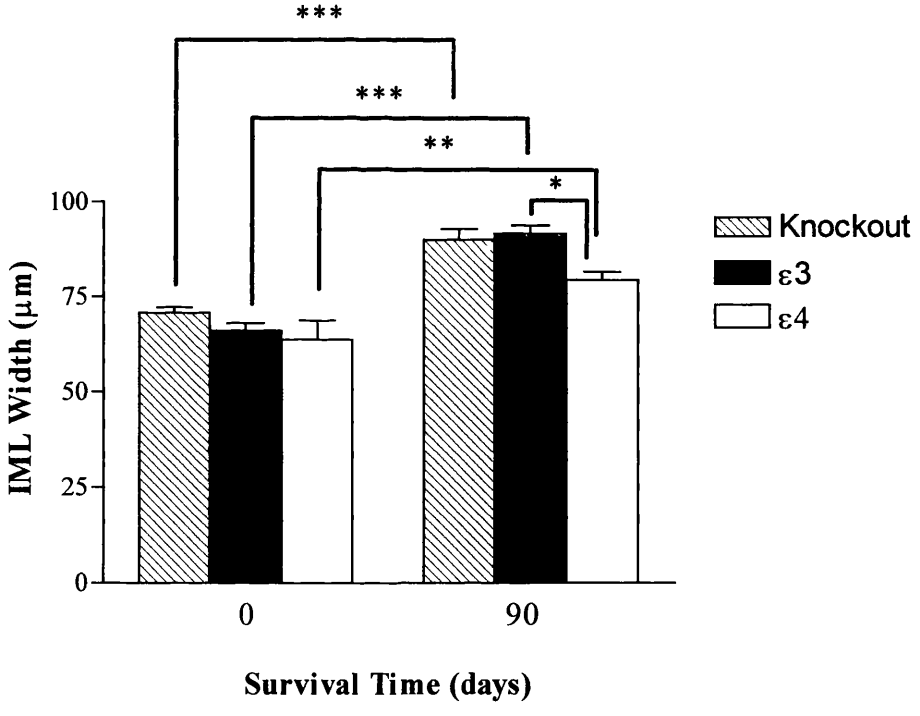

Figure 5.6 Quantification of hippocampal IML width in GAP-43 immunostained sections from *APOE* knockout and *APOE*ε3 and ε4 transgenic mice at 0 and 90 days post-lesion. The width was compared between the genotypes using a Student's unpaired *t*-test with Bonferroni correction for multiple comparisons. *****p<0.0001, **p<0.01 and *p<0.05**

5.4.4 Apolipoprotein Response to Injury

5.4.4.1 Apolipoprotein E

(a) Alterations in cellular immunoreactivity

No apoE immunoreactivity was evident in *APOE* knockout mice. 0 day control *APOE* transgenics displayed astrocytic immunostaining throughout the entire brain. At day 90 post-ECL astrocytic apoE was increased slightly but was similar in *APOE*ε3 and ε4 mice.

(b) Neuropil immunoreactivity

The percentage difference between the ipsilateral and contralateral hippocampal apoE immunoreactivity was taken. *APOE* knockout mice displayed no immunoreactivity. In 0 day control *APOE*ε3 and ε4 mice apoE immunoreactivity was faint and similar in both *APOE*ε3 and ε4 mice. At day 90 post-ECL, apoE immunoreactivity was increased within the MML and OML of both *APOE*ε3 and ε4 mice. At this time ε4 mice displayed slightly greater apoE immunoreactivity compared to ε3 mice, however this was not statistically significant (Figure 5.7 and 5.8).

5.4.4.2 Apolipoprotein J

(a) Cellular immunoreactivity

In 0 day control mice, neuronal apoJ immunoreactivity was present within mice of all genotypes. No astrocytic immunostaining was present. By day 90 post-ECL minimal astrocytic immunoreactivity was evident.

(b) Neuropil immunoreactivity

In 0 day control animals, apoJ neuropil immunoreactivity was punctate and stained the molecular layers in a dense pattern of staining which was similar across all genotypes. Percentage difference between the ipsilateral and contralateral hippocampus was taken. At day 90 post-ECL, apoJ immunoreactivity was no different in the IML and MML compared to 0 day control mice. In contrast, apoJ immunoreactivity was intense within the OML but did not differ significantly between genotypes (Figure 5.9).

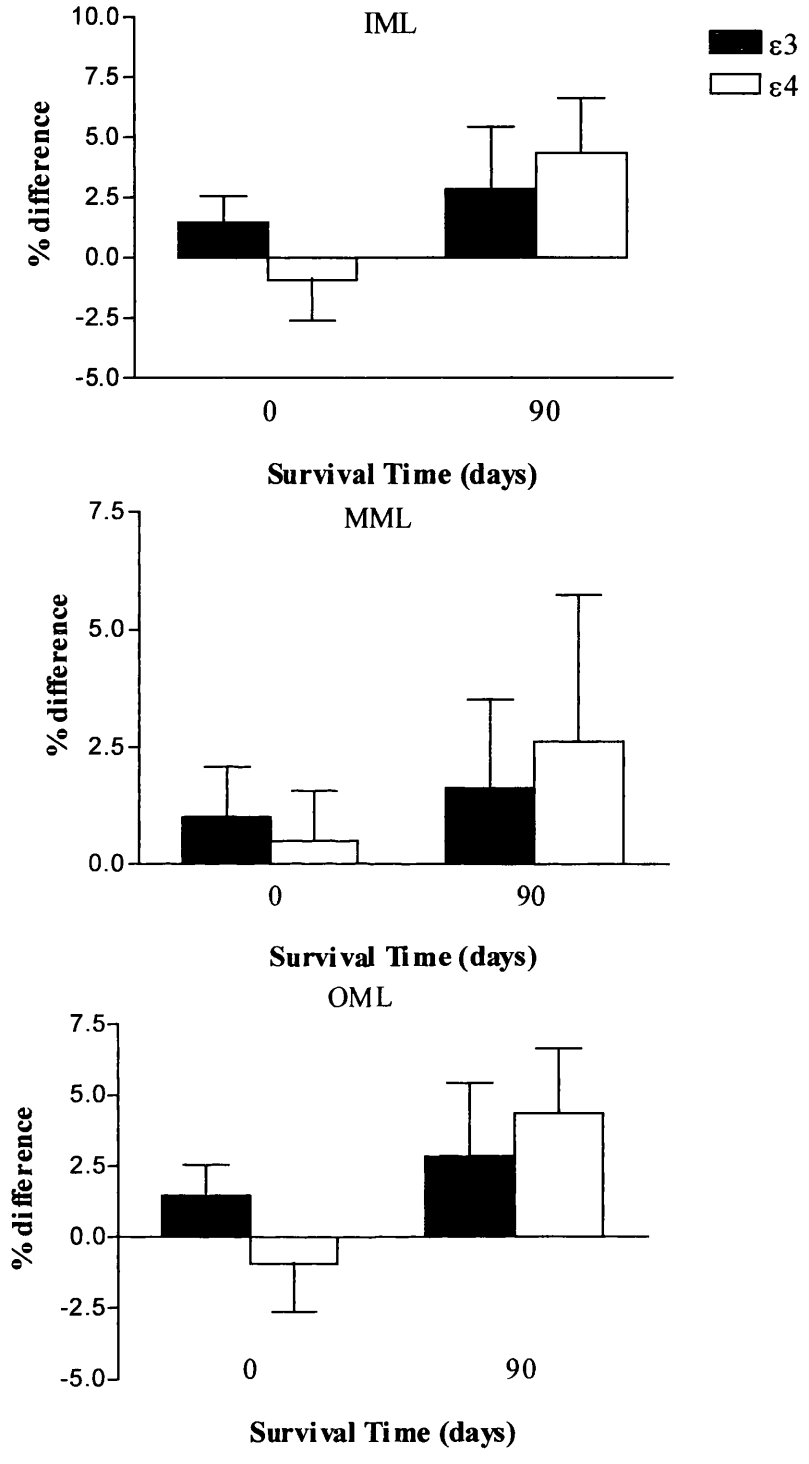

Figure 5.7 Quantification of apoE neuropil immunoreactivity in the inner, middle and outer molecular layers (IML, MML and OML) of the hippocampal dentate gyrus measured as relative optical density values at 0 and 90 days post-lesion. Percentage difference between the ipsilateral and contralateral hippocampus immunoreactivity was compared in ε3 and ε4 transgenic mice using a Student's unpaired *t*-test with Bonferroni correction for multiple comparisons.

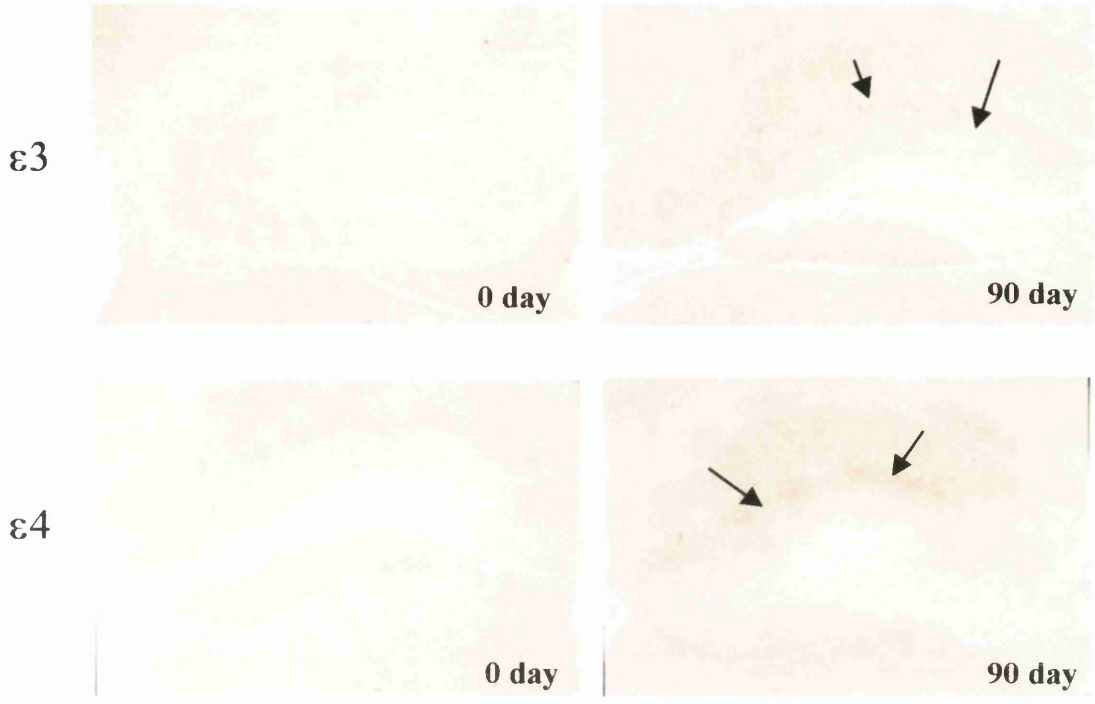

Figure 5.8 **ApoE is elevated at day 90 post-ECL**

Illustrative examples of apoE immunoreactivity in the ipsilateral hippocampus at day 0 and 90 post-ECL in ε3 and ε4 transgenic mice. Knockout mice do not display any apoE immunoreactivity at any time. In 0 day control mice, apoE immunoreactivity is light within the neuropil and immunoreactive astrocytes are evident throughout the entire brain. ApoE immunoreactivity is increased in ε3 and ε4 mice at day 90 post-ECL but is sightly more elevated in ε4 mice. x 50 magnification

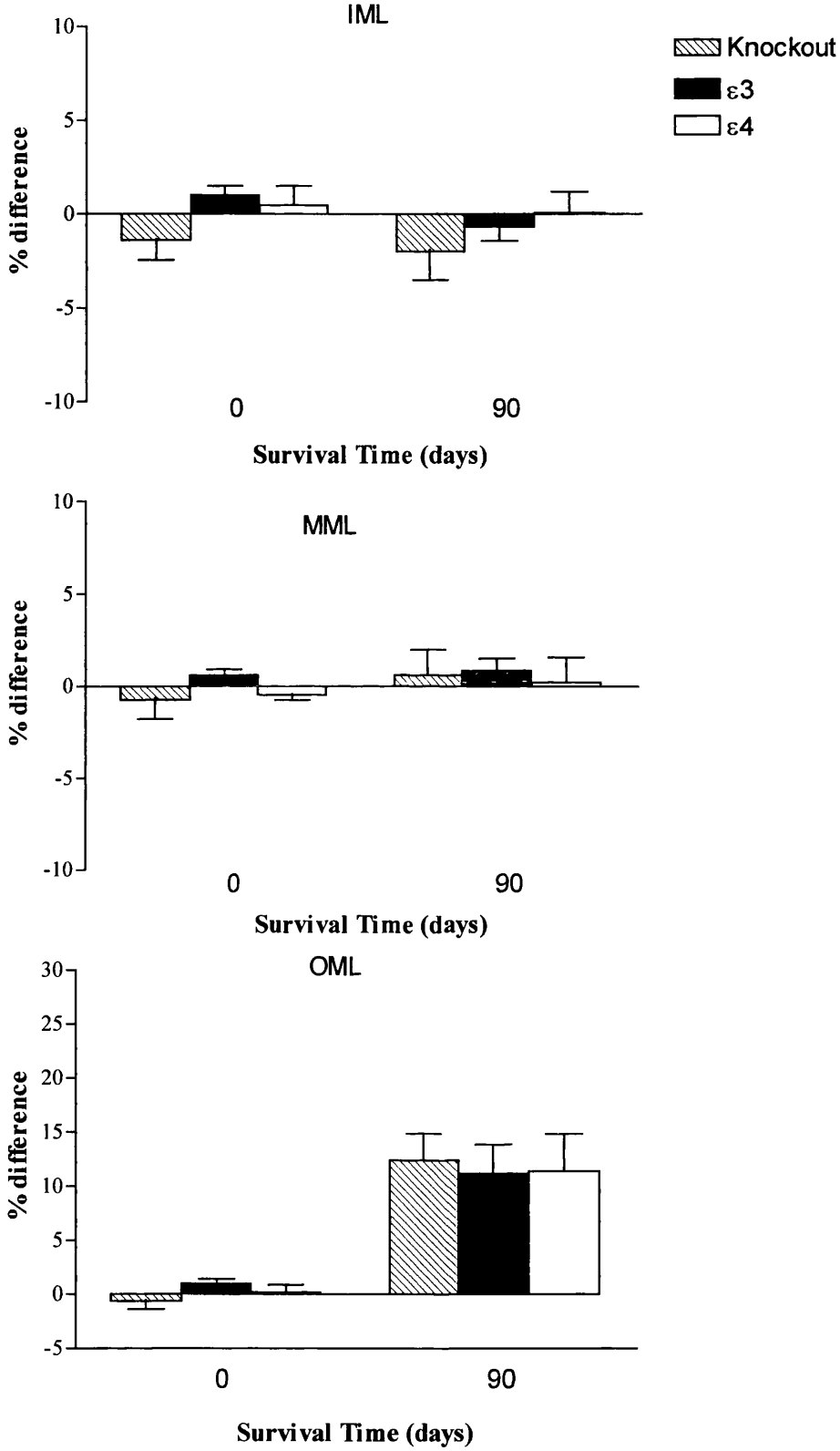

Figure 5.9 Quantification of apoJ neuropil immunoreactivity in the inner, middle and outer molecular layers (IML, MML and OML) of the hippocampal dentate gyrus measured as relative optical density values at 0 and 90 days post-lesion. Percentage difference between the ipsilateral and contralateral hippocampus immunoreactivity was compared in *APOE* knockout, ε3 and ε4 transgenic mice using a Student's unpaired *t*-test with Bonferroni correction for multiple comparisons.

5.4.5 Cytoskeletal Alterations Post-Lesion

5.4.5.1 Alterations in MAP-2 immunoreactivity

In 0 day control mice MAP-2 immunoreactivity displayed a regular pattern of staining, with dendritic processes being visible throughout the entire molecular layer. At day 90 post-ECL MAP-2 immunoreactivity was reduced in all layers compared to 0 day, however this deficit was similar in *APOE*ε3, ε4 and knockout mice (Figure 5.10).

5.4.5.2 Alterations in microtubule organisation

Sections were analysed using high power light microscopy to assess dendritic structure following the insult. In 0 day control animals of all genotypes, microtubule organisation was well-organised and fine fibrils were evident running through the entire molecular layer. At day 90 post-ECL, although there was a clear reduction in MAP-2 immunoreactivity, dendritic structure did not differ significantly between *APOE* knockout, ε3 and ε4 mice (Figure 5.11).

5.4.6 Clearance of Degeneration Products

Silver stained sections from each subject were scored microscopically for the presence of degeneration product deposition. No silver labelled degeneration products were present at day 0 or day 90 post-ECL in any *APOE* knockout, ε3 or ε4 mice (Figure 5.12). Silver labelled degeneration products were present within a 3 day control mouse brain used as a positive control.

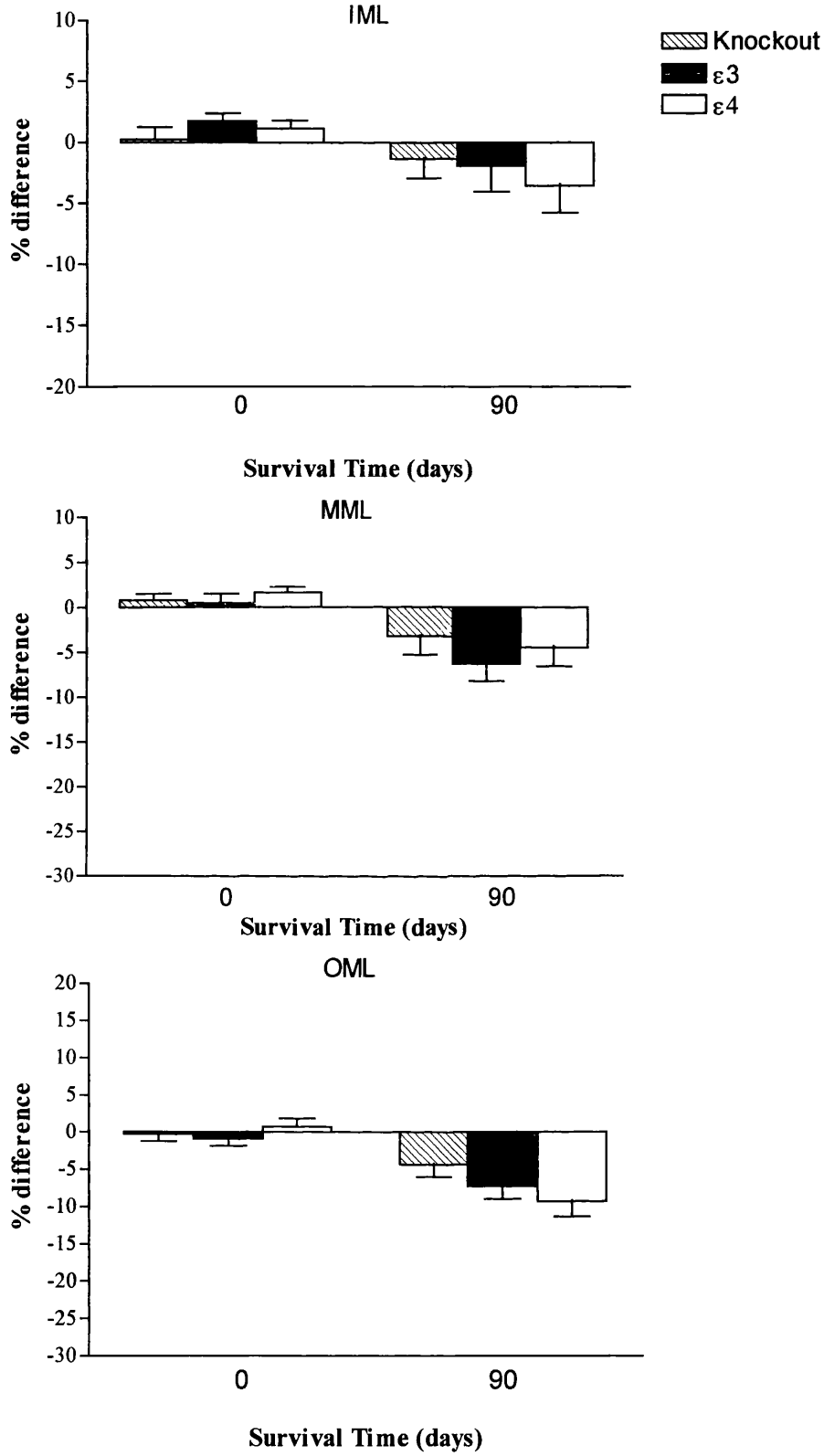

Figure 5.10 Quantification of MAP-2 immunoreactivity in the inner, middle and outer molecular layers (IML, MML and OML) of the hippocampal dentate gyrus measured as relative optical density values at 0 and 90 days post-lesion. Percentage difference between the ipsilateral and contralateral hippocampus immunoreactivity was compared in *APOE* knockout, ε3 and ε4 transgenic mice using a Student's unpaired *t*-test with Bonferroni correction for multiple comparisons.

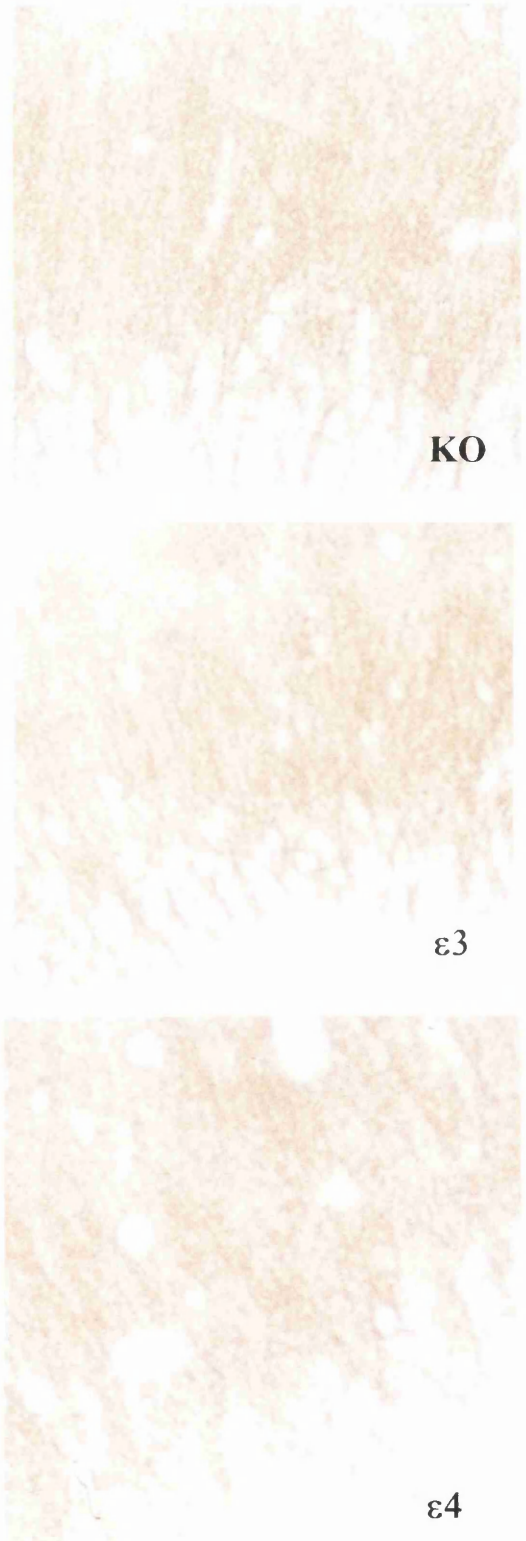

Figure 5.11 **High power MAP-2 immunoreactivity**

There is no difference in MAP-2 immunoreactivity between *APOE* knockout, ε3 and ε4 transgenic mice at day 90 post-ECL. x400 magnification

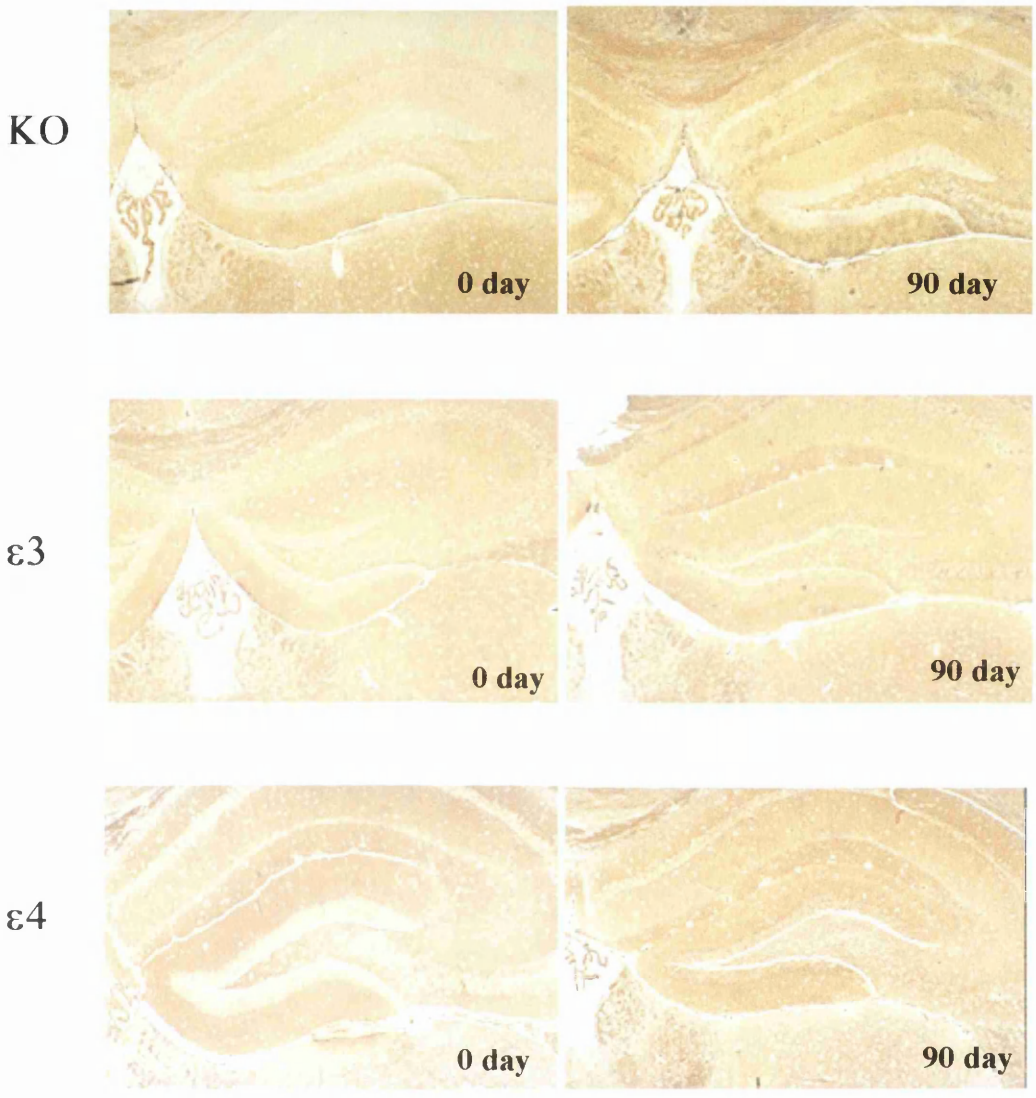

Figure 5.12 **Silver labelled degeneration products**

Illustrative examples of degeneration products silver staining in the ipsilateral hippocampus at day 0 and 90 post-ECL in *APOE* knockout (KO), ε3 and ε4 transgenic mice. No injury related degeneration products were present at any time in either *APOE* knockout, ε3 or ε4 mice.

5.4.7 LRP Receptor Expression Post-Lesion

(a) Cellular immunoreactivity

In 0 day control mice, LRP immunoreactivity was evident on neurons with minimal astrocytic immunoreactivity and this pattern was similar in *APOE* knockout, ε3 and ε4 mice. No astrocytic immunoreactivity was present by day 90 post-ECL. Neuronal cell body LRP immunreactivity did not alter with the injury.

(b) Neuropil immunoreactivity

In 0 day control mice, LRP immunoreactivity optical density values were found to be comparable in *APOE* knockout, ε3 and ε4 mice. At day 90 post-ECL, LRP immunoreactivity was slightly elevated within all layers but was statistically similar between *APOE* knockout, ε3 and ε4 mice (Figure 5.13).

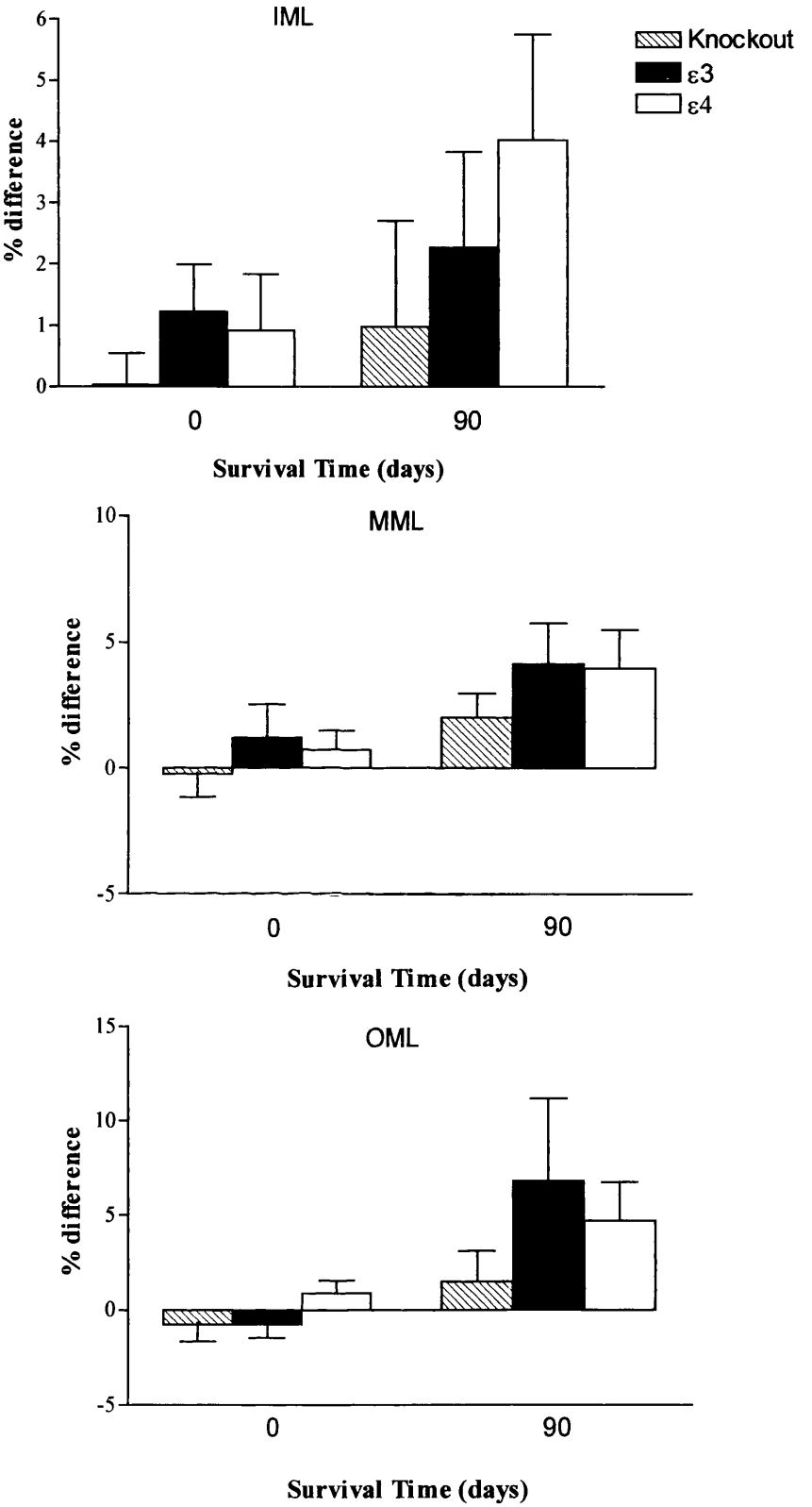

Figure 5.13 Quantification of LRP neuropil immunoreactivity in the inner, middle and outer molecular layers (IML, MML and OML) of the hippocampal dentate gyrus measured as relative optical density values at 0 and 90 days post-lesion. Percentage difference between the ipsilateral and contralateral hippocampus immunoreactivity was compared in *APOE* knockout, ε3 and ε4 transgenic mice using a Student's unpaired *t*-test with Bonferroni correction for multiple comparisons.

5.5 Discussion

ApoE is involved in the long-term plasticity changes that occur in the weeks to months following brain injury. In the previous chapters, a role for apoE in neuronal cell maintenance was established. Using a line of transgenic mice, with both neuronal and glial cell apoE expression, it was shown that the human *APOE*ε4 allele was associated with impaired neuronal cell plasticity following injury (White *et al*, 2001). In this study we have employed the same animal model but have assessed recovery from chronic brain injury in *APOE* knockout and transgenic mice possessing human *APOE*ε3 and ε4 alleles under an astrocytic promoter. This dictates that apoE expression is strictly astrocytic in nature. The present study suggests that there may be an impairment of long-term neuronal repair mechanisms in transgenic mice possessing the human *APOE*ε4 genotype compared to *APOE*ε3 transgenic mice. However, the extent of this impairment is more pronounced than that observed in the transgenic mice expressing apoE protein neuronally.

5.5.1 *APOE* genotype and the acute response to brain injury

It is becoming increasingly clear that the localisation of apoE within the brain may be crucial to the way in which it influences recovery. In contrast to the mice employed in the previous study, this line of transgenic mice express apoE astrocytically and this could have vital implications for recovery from brain injury. If apoE is not expressed neuronally can it modulate neuronal plasticity? The acute response to injury was not the focus of this study. Following the injury, apoE was increased within the neuropil and also within glia in the dentate molecular layer. A study by Horsburgh *et al* (2001) found that following a period of global ischaemia, there was no statistically significant difference in the extent of ischaemic cell death between *APOE*ε3 and ε4 mice. In this study, a marked increase in apoE levels was determined after ischaemia. There is little data on acute brain injury in these transgenic mice, other than the study mentioned, however the results from that would suggest that at least in the acute phase, *APOE* genotype does not influence outcome. Traditionally it has been thought, that to function in neuronal repair mechanisms, apoE would be required to enter the neuronal cell, or at the very least interact with its receptors on the neuron cell surface. Although no neuronal cell body staining was evident at any time, it would seem

unlikely that the dramatic increase in neuropil staining observed in the dentate molecular layers would be due solely to the presence of apoE in astrocyte processes. It would seem possible that at least some of the protein was present within neuronal cell processes, or in the extracellular space, ready for utilisation in membrane biosynthesis. This issue would need to be resolved using electron microscopy.

5.5.2 *APOE* genotype and the chronic response to brain injury

The present study is the first to use this transgenic mouse line in the study of chronic brain injury. We have found that *APOE*ε4 mice recover poorly from the injury compared to *APOE*ε3 and *APOE* knockout mice. At 90 days post-ECL, *APOE*ε4 mice display significant deficits in GAP-43 immunoreactivity compared to *APOE* knockout and ε3 mice. No genotype effect on synaptic density was evident. As previously described the width of the IML serves as an efficient indicator of the sprouting response from the commissural-associational neurons. The IML width increased by approximately 25-30% in *APOE*ε3 and knockout mice but only increased by 15-20% in *APOE*ε4 mice. ApoE immunoreactivity was elevated at 90 days post-ECL within all layers but to a greater extent in *APOE*ε4 mice compared to ε3. This increase in apoE at 90 days post-ECL is a similar finding to that observed in the C57BL/6J mice (see chapter III). In contrast, the transgenic mice expressing apoE in neurons do not experience this late increase post-ECL. Wild-type mice express apoE in glial cells but not neurons similar to the mice in this chapter and therefore the late expression of apoE post-injury could be dependent on the initial localisation of expression. It must also be noted that although the mice in this study display a certain ability to repair, even at 90 days there remains a significant deficit in fibre and synapse density (20-30%) compared with 0 day control levels in each genotype. This is in contrast to the previous neuronally expressing mice where all mice displayed a complete recovery by day 90 post-ECL. This could indicate the importance of the presence of neuronal apoE in brain injury.

5.5.3 Uptake of the apoE/lipid complex by the LRP receptor

The entrance of apoE into neuronal cells is primarily mediated by the LRP receptor. This receptor is expressed on neuronal cell bodies and also on neurite processes, especially in regions of high synaptic density (Herz *et al*, 1990, Rebeck *et al*, 1993, Bu *et al*, 1994). The most common hypothesis, based on its basic function, is that, in response to stress, apoE is released by astrocytes into the extracellular space to scavenge lipid material from degenerating neurons (Poirier *et al*, 1993). ApoE may only bind efficiently to its receptor when lipid bound. Once taken up, the lipid is cleaved from the particle (for membrane integration) and apoE may be recycled to the cell surface or interact with cytoskeletal proteins (Roses *et al*, 1996). This process is particularly important in the model described in this chapter, since it is the only means by which apoE could possibly enter the cell. It would therefore take longer for apoE to reach the neuron than if synthesised endogenously. This also has implications for the pathway by which the apoE travels. In a study by DeMattos *et al* (1999) it was shown that apoE fails to escape the endocytic/lysosomal pathway intracellularly as previously thought and suggests that direct expression of apoE in the cytosol is toxic. The authors suggest that the signalling events at the cell surface are the crucial factors in the function of apoE in plasticity. This is corroborated by studies released recently by Herz *et al*, (2001) which have shown the activation of extensive signalling pathways on binding of apoE to the LRP receptor. These pathways are detailed in chapter IX.

5.5.4 Brain injury in *APOE* knockout mice

Several studies have shown the poor outcome of *APOE* knockout mice after acute brain injury. This has been demonstrated following closed head injury (Chen *et al*, 1997; Genis *et al*, 2000), focal cerebral ischaemia (Laskowitz *et al*, 1997) and global ischaemia (Horsburgh *et al*, 1999; Sheng *et al*, 1999) when compared to wild-type C57BL/6J mice. Studies of chronic brain injury have also been carried out using *APOE* knockout mice. Anderson *et al* (1998) used the entorhinal cortex lesion model to assess plasticity in *APOE* knockout mice and wild-type C57BL/6J mice. The authors found that following 140 days of survival post-injury, both *APOE* knockout and wild-type groups showed immunohistochemical evidence of reactive synaptogenesis although the *APOE* knockout group initially displayed greater synaptic

loss. In the present study we also found that *APOE* knockout mice displayed a significant degree of plasticity which was more substantial in some layers than that observed in *APOE*ε4. The finding that *APOE* knockout mice are capable of plasticity suggests that another protein may compensate for the absence of apoE. Could this be the function of apoJ in the brain?

5.5.5 Alterations in apoJ expression in transgenic mice post-ECL

It is hypothesised that apoJ may perform a similar function in lipid transportation and neuronal repair, to apoE (Poirier *et al*, 1995). In conditions where apoE is absent or reduced, apoJ is thought to compensate (Anderson *et al*, 1998). Bertrand *et al* (1995) showed that apoE levels in human brain were reduced with the increasing ε4 allele number and apoJ levels were found to increase. In the present study we have found that apoJ is slightly greater in 0 day control, *APOE* knockout mice, although not significantly so when compared to *APOE*ε3 and ε4 mice. By day 90 post-ECL, apoJ immunoreactivity was comparable in the IML and MML to control levels but was elevated within the OML. Again no significant difference in immunoreactivity could be detected between the genotypes. The fact that *APOE* knockout mice display slightly greater baseline apoJ levels may suggest that it is elevated to compensate for the lack of apoE. However, apoJ levels are comparable between the genotypes post-ECL may suggest that levels expressed post-injury are not dependent on the presence or absence of apoE.

5.5.6 ApoE isoform influence on factors that may influence CNS plasticity

5.5.6.1 Clearance of degeneration products

There are several factors that may account for the isoform differences observed in this study. Initially it was important to determine if E3 and E4 both cleared degeneration material from the site of the injury efficiently. In the present study it was found that at day 90 post-ECL, there was no evidence of lesion induced degeneration products in *APOE*ε3 or ε4 mice. Most surprisingly, it was also found that degeneration products were efficiently cleared in *APOE* knockout mice. The only study which found impaired degeneration product clearance is that by Fagan *et al* (1998) who found that knockout mice displayed impaired clearance of degeneration products but only when

aged. The clearance of degeneration material post-injury has not previously been analysed in these mice before the carrying out of this study.

5.5.6.2 LRP receptor expression

The outgrowth promoting effects of apoE from this line of transgenic mice have been shown *in vitro*. It was noted that hippocampal neurons grown on a monolayer of astrocytes, derived from these astrocyte-expressing mice, produced long neurites when the astrocytes were derived from *APOE*ε3 expressing mice. Outgrowth was inhibited when hippocampal neurons were grown on *APOE*ε4 expressing astrocytes (Holtzman *et al*, 1995; Sun *et al*, 1998). In addition it was found that by blocking the LRP receptor, the outgrowth promoting effects of apoE E3 could be attenuated (Holtzman *et al*, 1995). *APOE* knockout mice express the LRP receptor throughout the brain even in the absence of apoE expression (Ishibashi *et al*, 1994). However, the LRP receptor has a host of ligands and functions in a number of other processes. No significant difference in LRP expression between the genotypes was noted at any time in this study, however, this does not reflect functional variations of the isoforms at the receptor. Although LRP was increased on reactive astrocytes, generally endocytic receptors are shown not to increase expression significantly under stress but increase turnover, therefore it is not surprising that increased neuropil expression was not witnessed.

5.5.6.3 Cytoskeletal structure

In the neuronally expressing transgenic mice it was found that dendritic structure, as labelled with the MAP-2 antibody, was disrupted and disorganised in *APOE*ε4 mice post-ECL compared to ε3 mice. This was not the case in this study. No genotype effect on MAP-2 immunoreactivity density was observed. Additionally, there was no observable difference in dendritic structure in *APOE* knockout, ε3 or ε4 mice post-ECL. This could reflect the role of intraneuronal apoE interaction with the cytoskeleton. If E3 and E4 behave differently when they enter the neuron i.e. E3 escapes the endosomal pathway but E4 does not, this could mean that E3 is able to interact with microtubules to promote polymerisation and extension. In neuronally expressing mice the apoE is readily available intraneuronally for immediate

interactions with the cytoskeleton, without the added complication of cell entry primarily. This could reflect why the neuronally expressing mice repair so efficiently and the astrocytically expressing mice do not.

Chapter VI

APOE Genotype Influence in the CNS of Aged *APOE* Knockout, ε3 and ε4 Transgenic Mice (GFAP Promoter).

6.1 Introduction

At birth the normal human brain is composed of 10^{12} cells, approximately 20,000 cells for every $1mm^3$ of brain mass (Principles of Behavioural Neuroscience, 1995). This population of cells is composed predominately of neurons and glial cells of various types. Glial cells of the brain are capable of dividing however, neurons are unique, in that, unlike cells of other major organs, they are not capable of division. New neuronal cells cannot be manufactured in the CNS, a process call neurogenesis. Thus, we are born with a full complement of brain cells. In the process of ageing, brain cells are lost and this combined with the associated loss of synaptic contacts can have a devastating effect on function, an exaggerated example of this being Alzheimer's disease (AD). The brain is capable of compensating for this to a certain extent through a process of synaptic plasticity. Existing fibres produce outgrowth in an attempt to form new contacts. Isoform specific effects on brain ageing have not been clearly elucidated and in this chapter the *APOE* genotype influence on the ageing process, will be assessed in *APOE* knockout, ε3 and ε4 transgenic mice. The hypothesis of this study is that *APOE*ε4 mice will display impaired hippocampal plasticity with increasing age.

6.2 Aims

This study will assess *APOE* genotype influence on CNS plasticity with ageing in *APOE* knockout, human *APOE*ε3 and ε4 transgenic mice (GFAP promoter).

6.3 Materials and Methods

6.3.1 APOE transgenic mice on a GFAP promoter

*APOE*ε3 and ε4 heterozygous transgenic mice were generated as previously described (Sun *et al*, 1998). Homozygous knockout littermates are also produced in the breeding of these animals. The *APOE* genotypes of all animals bred were checked using PCR analysis (see Chapter II).

6.3.2 Tissue

APOE knockout, ε3 and ε4 transgenic mice were bred and maintained in an animal house until the age of either 3 months (knockout: n=5, ε3: n=5, ε4: n=5) or 1 year (knockout: n=12, ε3: n=6, ε4: n=7). The mice were halothane anaesthetised and perfused transcardially with heparinised saline followed by buffered 4% paraformaldehyde. The brains were processed and paraffin embedded and 6μm coronal sections were cut on a microtome. Immunohistochemistry for GAP-43, synaptophysin, apoE, apoJ and MAP-2 was performed on tissue sections from each subject. IML width was measured in GAP-43 immunostained sections and analysed as outlined in chapter II.

6.3.3 Quantification of immunohistochemistry and statistical analysis

Relative optical values for immunostaining were collected from the inner, middle and outer molecular layers of the dentate gyrus from both the ipsilateral and contralateral hippocampus of each subject using an MCID image analysis system. Six optical density readings were taken from each layer using a $1cm^2$ sampling box and averaged to give a representative reading from the layer. The measurements from the ipsilateral and contralateral hippocampus were averaged for each subject. ANOVAR was carried out on the measurements taken from each antibody of both the 3 month and 1 year old mice. The genotypes were then compared using a post-hoc Student's unpaired *t*-test with Bonferroni correction for multiple comparisons. Histograms are presented as the mean +/- S.E.M.

6.4 Results

6.4.1 Temporal Profile of Degeneration

6.4.1.1 *APOE* genotype and synaptic loss in ageing

Synaptophysin immunoreactivity displayed a regular, dense, trilaminar pattern of staining with the IML most intensely stained. In 3 month old mice, there was no statistically significant difference in synaptophysin immunoreactivity. Genotype differences in synaptophysin immunoreactivity were compared between *APOE* knockout, ε3 and ε4 mice. In 1 year old mice, synaptophysin immunoreactivity was not significantly altered compared to those at 3 months of age. There was a trend for greater synaptophysin immunoreactivity in 1 year old, *APOE*ε3 transgenic mice compared to the other genotypes although this did not achieve statistical significance (Figure 6.1).

6.4.1.2 *APOE* genotype and fibre degeneration in ageing

GAP-43 immunoreactivity displayed a regular punctate staining with the IML being most densely immunoreactive. In 3 month old mice, a statistically significant difference in GAP-43 immunostaining was observed within the IML where GAP-43 immunoreactivity was found to be significantly reduced in *APOE*ε4 mice compared to *APOE* knockout and ε3 mice ($p<0.05$). GAP-43 immunoreactivity decreased within all layers of *APOE* knockout and *APOE*ε3 mice at 1 year compared to 3 months. However, the levels of GAP-43 immunoreactivity were not different in *APOE*ε4 mice at 1 year compared to 3 months. There was no statistical difference in the levels of GAP-43 between *APOE* knockout, ε3 and ε4 mice at 1 year (Figure 6.2).

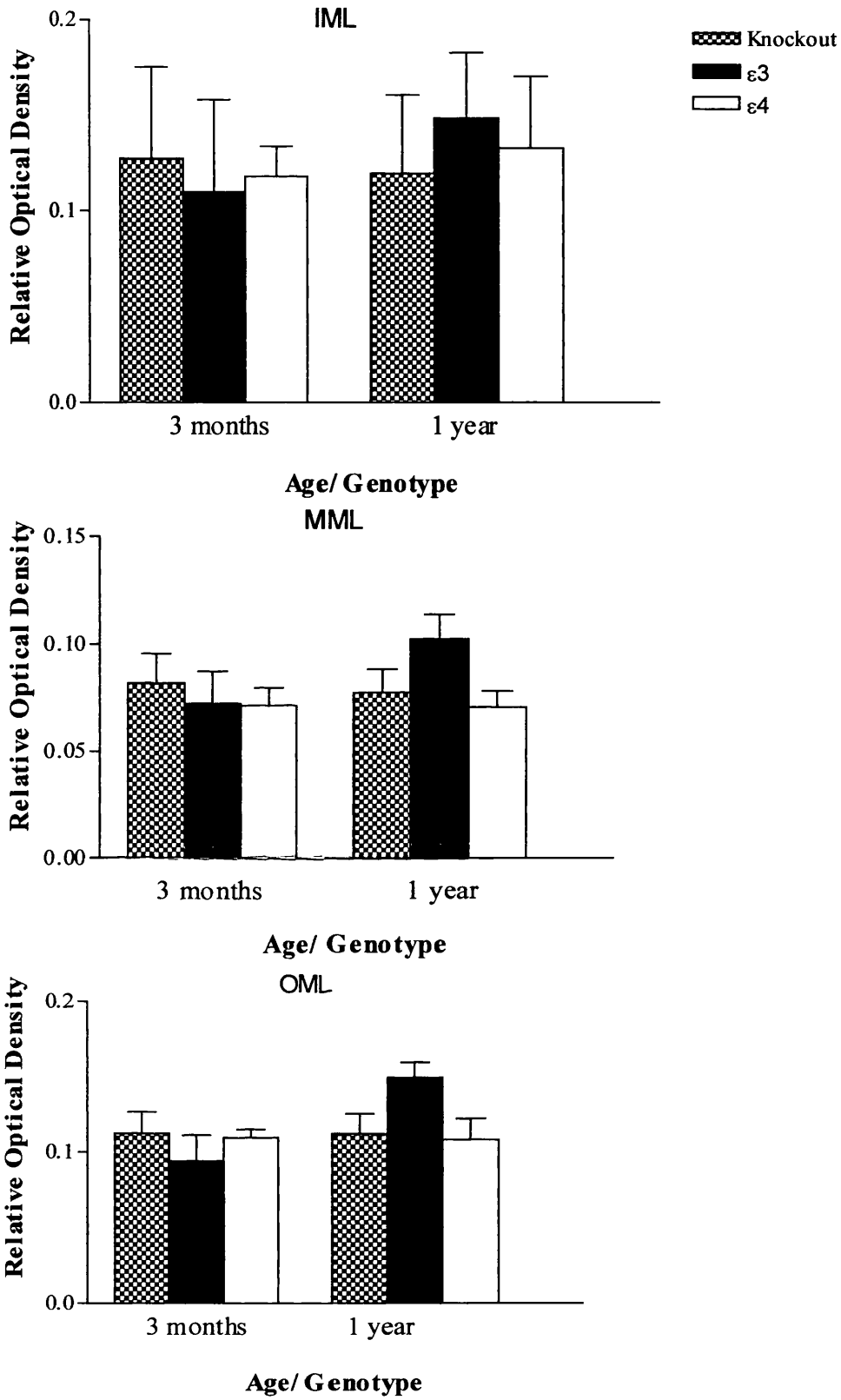

Figure 6.1 Quantification of synaptophysin immunoreactivity within the inner, middle and outer molecular layers (IML, MML and OML) of the hippocampal dentate gyrus of 3 month adult mice and 1 year old aged *APOE* knockout, ε3 and ε4 transgenic measured as relative optical density values. ANOVAR was carried out on the groups and the genotypes compared using a Student's unpaired *t*-test with Bonferroni correction for multiple comparisons.

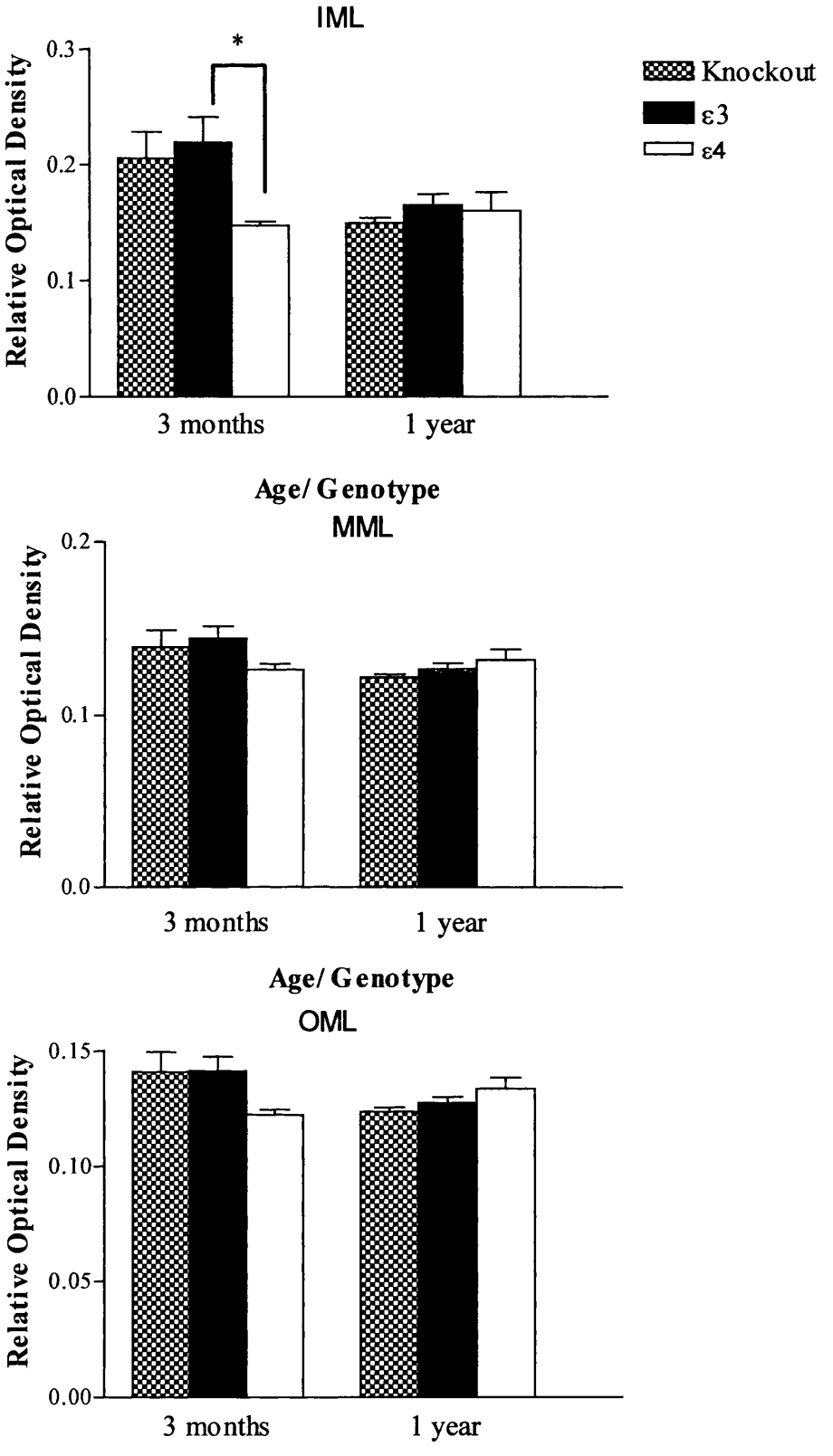

Figure 6.2 Quantification of GAP-43 immunoreactivity within the inner, middle and outer molecular layers (IML, MML and OML) of the hippocampal dentate gyrus of 3 month old adult mice and 1 year aged *APOE* knockout, ε3 and ε4 transgenic mice measured as relative optical density values. ANOVAR was carried out on the groups and the genotypes compared using a Student's unpaired *t*-test with Bonferroni correction for multiple comparisons. ***p<0.05**

6.4.1.3 IML width alterations in ageing

IML width acts as an indication of the degree of sprouting from the commissural associational neurons. This fibre system has been shown to sprout in conditions of chronic injury (see chapter IV and V). Statistically significant variance in the baseline optical density readings of GAP-43 immunostained sections was detected in 3 month old mice. This suggested that there may be baseline differences in sprouting between the genotypes which may be detected by measurement of IML width.

The IML at 3months of age was similar in *APOE* knockout and ε3 mice. However, IML width was significantly narrower in *APOE*ε4 mice compared to *APOE* knockout and ε3 mice ($p<0.05$). At 1 year, IML width is still significantly narrower in *APOE*ε4 mice compared to *APOE* knockout ($p<0.05$) and ε3 mice ($p<0.01$). This is because IML width increases in ε3 mice between 3 months and 1 year of age but does not increase in *APOE*ε4 mice (Figure 6.3).

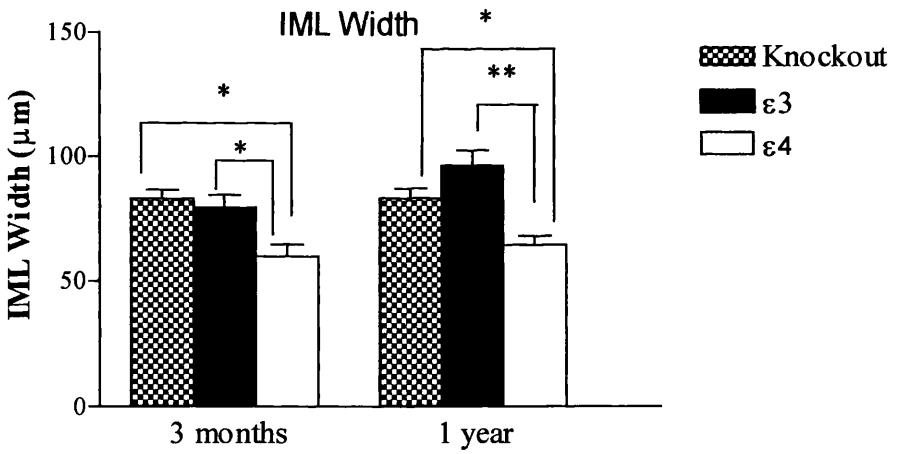

Figure 6.3 Quantification of hippocampal IML width in GAP-43 immunostained sections from 3 month old adult and 1 year old aged *APOE* knockout, ε3 and ε4 transgenic mice. ANOVAR was carried out on the groups and the genotypes compared using a Student's unpaired *t*-test with Bonferroni correction for multiple comparisons. **$p<0.01$ and *$p<0.05$

6.4.2 Apolipoprotein Response to Ageing

6.4.2.1 Apolipoprotein E

(a) Astrocytic immunoreactivity

Apolipoprotein E immunoreactivity was pale within the neuropil. Astrocytic staining was present throughout the hippocampus and throughout the whole brain. This staining was similar in both ε3 and ε4 mice. The degree of astrocytic staining did not alter with age. *APOE* knockout mice displayed no apoE immunoreactivity.

(b) Neuropil immunoreactivity

Optical density readings were collected from the neuropil of *APOE*ε3 and ε4 mice at 3 months and 1 year of age. ANOVAR revealed no statistically significant variance in apoE neuropil immunostaining in the 3 month old *APOE*ε3 and ε4 mice. ApoE immunoreactivity was similar in 1 year old *APOE*ε3 mice compared to levels at 3 months of age (Figure 6.4 and 6.5). ApoE immunoreactivity was significantly greater in *APOE*ε4 mice compared to ε3 mice at 1 year old ($p<0.05$).

6.4.2.2 Apolipoprotein J

ApoJ immunoreactivity was present within the neuropil and also lightly stained neurons. The degree of staining was similar in *APOE* knockout, *APOE*ε3 and ε4 transgenic mice. ANOVAR revealed no statistically significant variance in apoJ staining intensity in 3 month old mice in any layer. ApoJ immunoreactivity did not alter significantly between 3 months and 1 year of age in *APOE*ε3 mice (Figure 6.6). There was trend for greater apoJ immunoreactivity in *APOE* knockout and ε4 mice compared to *APOE*ε3 mice within all layers.

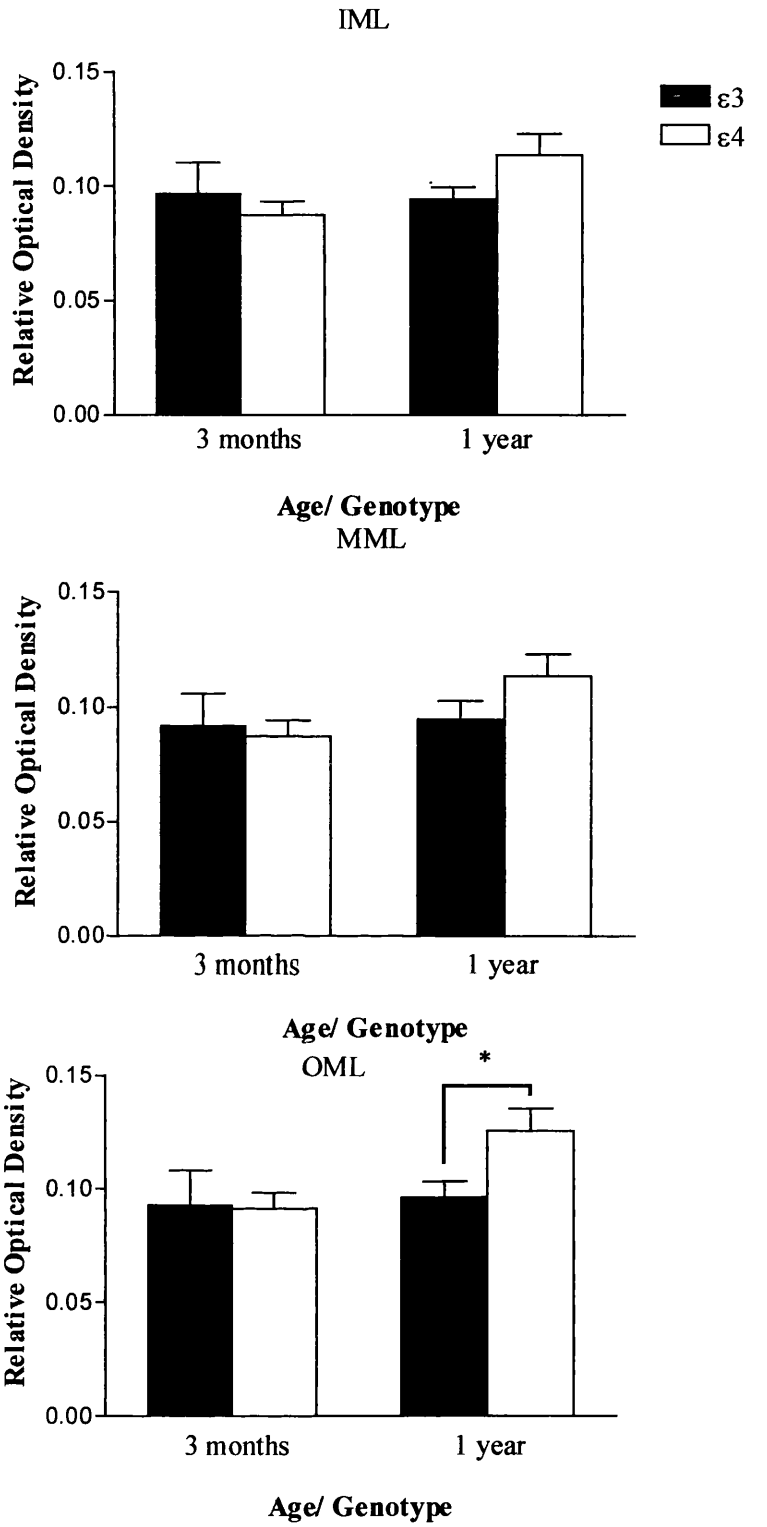

Figure 6.4 Quantification of apoE immunoreactivity within the inner, middle and outer molecular layers (IML, MML and OML) of the hippocampal dentate gyrus of 3 month old adult and 1 year old aged *APOE*ε3 and ε4 transgenic mice measured as relative optical density values. ANOVAR was carried out on each group and the genotypes compared using a Student's unpaired *t*-test with Bonferroni correction for multiple comparisons. ***p<0.05**

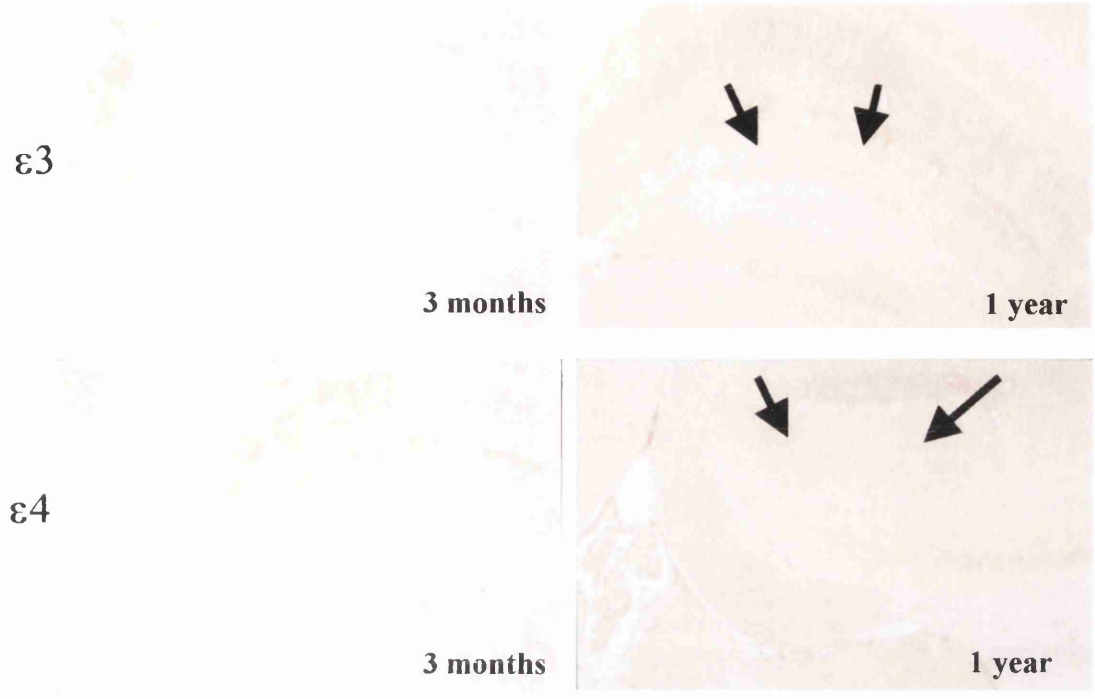

Figure 6.5 **Increased apoE immunoreactivity at 1 year of age**

Illustrative examples of apoE immunoreactivity in *APOE*ε3 and ε4 transgenic mice at age 3 months and 1 year. Neuropil apoE immunoreactivity is increased at 1 year of age throughout most regions of the brain including the hippocampus. x50 magnification

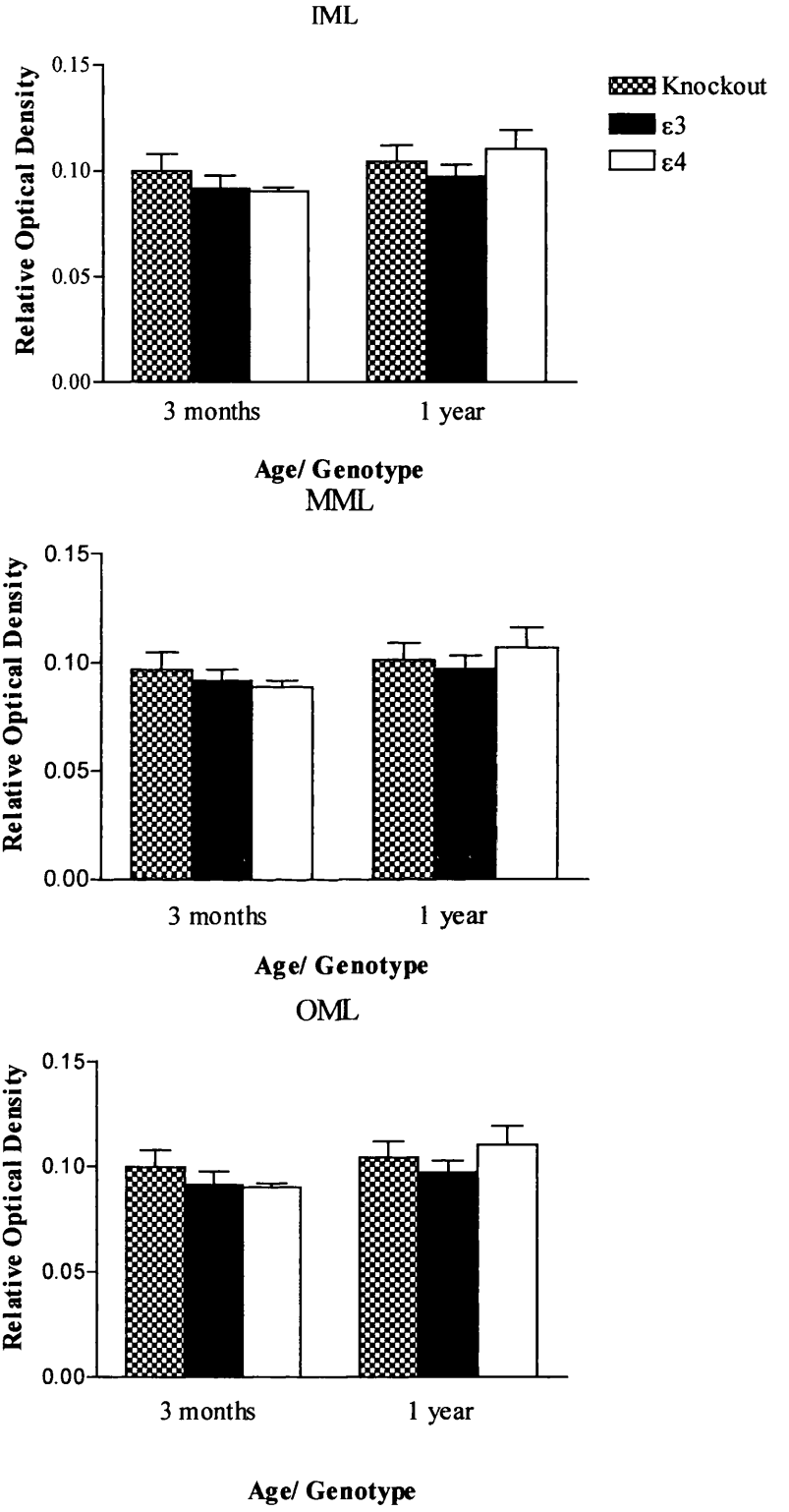

Figure 6.6 Quantification of apoJ immunoreactivity within the inner, middle and outer molecular layers (IML, MML and OML) of the hippocampal dentate gyrus of 3 month old adult and 1 year old aged *APOE* knockout, ε3 and ε4 transgenic mice measured as relative optical density values. ANOVAR was carried out on the groups and the genotypes compared using a Student's unpaired *t*-test with Bonferroni correction for multiple comparisons.

6.4.3 Cytoskeletal Alterations in Ageing

6.4.3.1 Alterations in MAP-2 immunoreactivity

MAP-2 characteristically labelled the soma of neurons and associated dendritic networks most intensely. At 3 months of age, *APOE*ε3 mice and *APOE* knockout mice displayed a trend for slightly greater MAP-2 immunostaining compared to *APOE*ε4 mice but this did not reach statistical significance (Figure 6.7). At 1 year of age MAP-2 immunostaining was reduced in *APOE* knockout and ε3 transgenic mice compared to 3 month old animals. MAP-2 immunoreactivity remained similar in *APOE*ε4 mice between the age of 3 months and year. There was no significant difference in MAP-2 immunoreactivity between *APOE* knockout, ε3 and ε4 mice at this timepoint although ε3 mice did show a trend for slightly greater MAP-2 immunoreactivity compared to ε4 mice. No difference in dendritic structure was evident at 3 months or 1 year of age in *APOE* knockout, ε3 or ε4 mice (Figure 6.8).

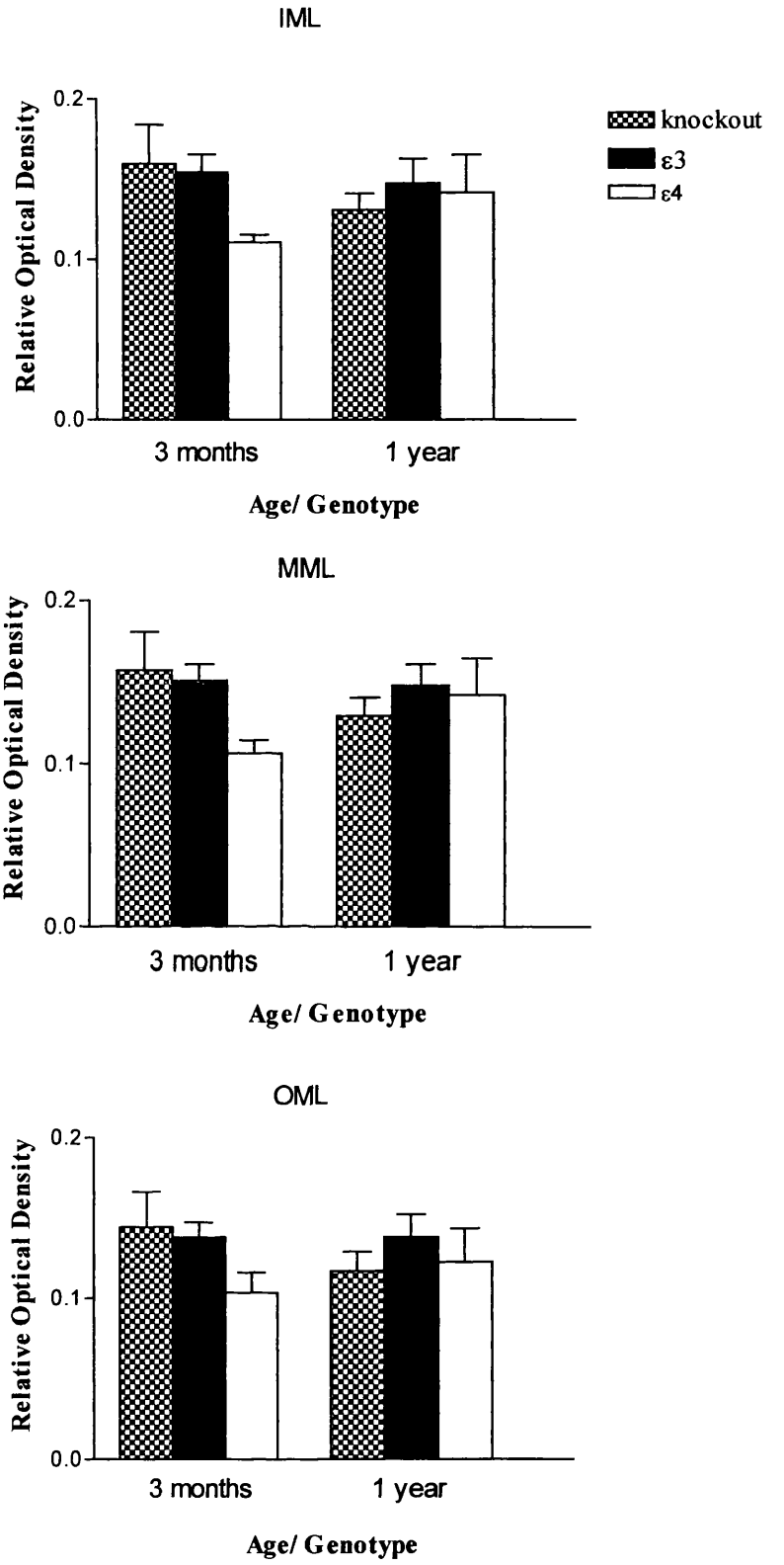

Figure 6.7 Quantification of MAP-2 immunoreactivity within the inner, middle and outer (IML, MML and OML) of the hippocampal dentate gyrus of 3 month old adult and 1 year old aged *APOE* knockout, ε3 and ε4 mice measured as relative optical density values. ANOVAR was carried out on the groups and the genotypes compared using a Student's unpaired *t*-test with Bonferroni correction for multiple comparisons.

Figure 6.8 MAP-2 immunoreactivity in the dentate molecular layer of aged *APOE* knockout, ε3 and ε4 transgenic mice. Dendritic structure is similar in all mice although less dendritic processes are visible in some knockout mice. x400 magnification

6.5 Discussion

6.5.1 Ageing and the human brain

In the last hundred years, with the improvement of medical care around the world, humans are living longer with the number of individuals who are octogenarians or above increasing sharply. Care of the elderly is an economical burden around the world and in association with this, much investment has been made in the investigation of age related diseases such as AD and factors involved in the ageing process. Ageing is a form of chronic brain injury. The characteristic loss of cells and synapses in the aged brain is well defined and ultimately leads to memory impairment, dementia and cognitive deficits. One of the regions of the brain most vulnerable to cell loss is the entorhinal cortex. The death of cells in this region triggers a cascade of degenerative events within the hippocampus. *APOE* genotype may affect the process of brain ageing as it does the progression of AD and outcome after head injury. The results of this study indicated that *APOE* genotype does not influence hippocampal plasticity in response to ageing.

6.5.2 APOE genotype influence on effects of ageing in *APOE* knockout, ε3 and ε4 mice

In the present study, using markers for synaptic, fibre and dendritic alterations, there was no evidence that *APOE* genotype influenced alterations in these markers at 1 year of age compared to 3 months. There was also no indication that deficiency of apoE produced synaptic, fibre and dendritic alterations at 1 year compared to 3 months. However, there was some subtle evidence, using width of IML as a measure of sprouting, that the ε4 allele was associated with reduced sprouting in both 3 month and 1 year old *APOE*ε4 mice compared to knockout and ε3 mice. There was also some evidence in 3 month old mice that the ε4 allele was associated with reduced GAP-43 immunoreactivity indicative of reduced fibre density compared to *APOE* knockout and ε3 mice. This may suggest that there are underlying structural differences although no gross dendritic abnormalities were immediately apparent using MAP-2 immunoreactivity.

Several studies have investigated the effects of ageing in *APOE* knockout mice. Masliah *et al* (1995) found that *APOE* knockout mice displayed an age-dependent 15-40% loss of synaptophysin and MAP-2 immunoreactivity in the neocortex and hippocampus at 20 months of age (changes could result from extreme ageing) compared to wild-type C57BL/6J controls. The authors highlighted that dendritic changes were evident as early as 4 months of age, suggestive of a role for apoE in the modulation of cytoskeletal structure. In association with this, *APOE* knockout mice also displayed an age-dependent decline in cognitive capabilities (Masliah *et al*, 1997; Veinbergs *et al*, 1999). The studies by Masliah *et al* conflict with the findings of other groups. Studies of other *APOE* knockout mice have indicated that there is no evidence of exaggerated synaptic degeneration with age (Anderson *et al*, 1998; Cambon *et al*, 2000). Similarly, the present study indicated there was no evidence of synaptic, fibre or dendritic alterations. Although controversial, studies by Masliah *et al* have shown that the ageing effects in knockout mice may be ameliorated by administration of apoE protein. Intraventricular infusion of recombinant apoE E3 and E4 has been found to improve performance in learning tasks and this was correlated with the restoration of neuronal integrity in *APOE* knockout mice.

Ageing studies in transgenic mice expressing apoE neuronally have shown that neuronal integrity is not dramatically altered in *APOE*ε3 and knockout mice with age but *APOE*ε4 mice display a significant age-dependent loss in synapses and MAP-2-positive dendrites (Buttini *et al*, 1999, 2000). The effect of *APOE* genotype on ageing was assessed in another study which compared axonal structure in astrocytically and neuronally-expressing transgenic mice. Prominent axonopathy was found in mice expressing *APOE*ε4 neuronally however astrocytically expressing *APOE*ε4 mice remained relatively normal throughout life (Tesseur *et al*, 2000). These results parallel the findings of the present study, which also found no genotype difference in pathology between astrocyte expressing ε3 and ε4 mice. The contrast in the findings of the present study (also Tesseur *et al*) and the study by Buttinis group could reflect a detrimental effect of endogenous neuronal apoE expression in ageing. Behavioural phenotyping studies in the line of transgenic mice employed in the present study has revealed that *APOE*ε4 mice express profound working memory impairments with age,

even in the absence of Alzheimer's-like pathology (Hartman *et al*, 2001). The authors also highlight that there was no significant difference in the level of synaptic, neuronal or glial markers between the genotypes, also a similar finding to that of the present study. Ultrastructural studies of aged transgenic mice have shown that in *APOE*ε4 mice, the synapse per neuron is greatly reduced compared to *APOE*ε2 and knockout mice (Cambon *et al*, 2000). This is also associated with an increase in synapse zone area in *APOE*ε4 mice. These findings could explain the unaltered synaptophysin immunoreactivity with age, in *APOE*ε4 mice, in our study.

The neuropathological changes that occur with age are very subtle and are certainly not of the magnitude observed in the lesioning studies. The techniques employed in this study may not be appropriate to detect these very small changes and techniques such as electrophysiology may be more sensitive for detecting loss of cell connections. The end survival point may also be a crucial factor. In the present study, the oldest mice were all approximately 1 year old and are classed as aged in mouse lifespan terms. In other studies, some investigators have allowed survival terms of up to 20 months and this may allow manifestation of more exaggerated neuropathological abnormalities. Perhaps extending survival time in future studies may allow visualisation of more exaggerated changes with age. In previous chapters, it has been shown that the *APOE*ε4 allele is detrimental to the plasticity response following injury. Therefore, *APOE* genotype effects may only manifest themselves when the system is stressed in some way leading to greater changes in pathology. It will be interesting in the future to study plasticity in aged transgenic mice.

6.5.3 Evidence for an *APOE* genotype influence on ageing in the human brain

ApoE performs an important role in the maintenance of neuronal integrity under normal physiological conditions. Aside from the multitude of investigations highlighting that the *APOE*ε4 allele is associated with AD in humans, it is now apparent that *APOE* genotype may modulate the brains response to the normal ageing process. Studies in middle-aged humans have shown that individuals with an *APOE*ε4 genotype perform poorly in memory and learning tasks compared to individuals not possessing an ε4 genotype suggesting some vital synaptic connections may already be

lost (Flory *et al*, 2000). In a study of non-demented individuals, hippocampal atrophy was found to be significantly greater in individuals carrying an ε4 allele compared with control groups (Crook *et al*, 1986; Bigler *et al*, 2000). In addition, the hippocampal and entorhinal cortex volume of ε4 AD patients is significantly reduced compared to control groups (Lehtovirta *et al*, 1995). A cohort of 563 elderly patients without AD were analysed over a period of 7 years for cognitive and visuospatial skills. The *APOE*ε4 allele was found to be associated with a more rapid decline in memory with time compared with control individuals (Mayeux *et al*, 2001). With the use of transgenic animal models the role of apoE in ageing can now be more fully addressed in mice expressing human *APOE* alleles.

Chapter VII

An *In Vitro* Organotypic Hippocampal Slice Model to Study *APOE* Genotype Influence on Synaptic Plasticity and Analysis of Herpes Simplex Virus as a Vector for *APOE* Delivery

7.1 Introduction

Organotypic hippocampal slices possess a network of connections and cells, which allow the tissue to function in a more physiologically similar manner, to that of the whole animal. The tissue, which is most commonly used for organotypic culture is derived from neonatal animals and therefore will display a certain degree of natural plasticity due to ongoing developmental changes (Bolz *et al*, 1990).

The hippocampus is dissected from the surrounding cortical tissue before culturing and this results in removal of the perforant pathway to the dentate gyrus of the hippocampus (Heimrich and Frotscher, 1990). This is somewhat analogous to the hippocampal denervation by entorhinal cortex lesion discussed in previous chapters. The *in vitro* slice method results in a period of degeneration and reinnervation at longer culture periods. The process of sprouting within the hippocampus has been identified in previous studies and is a well-characterised response to removal of cortical inputs (Frotscher and Gahwiler, 1988; Stoppini *et al*, 1993, 1997). In the study discussed within this chapter the plasticity response of hippocampal slices is assessed in wild type mice and *APOE* knockout, ε3 and ε4 transgenic mice. This method was established to allow more dynamic alterations to be studied. *In vivo*, regenerative alterations do not occur until about 90 days post-lesion whereas *in vitro* this occurs much earlier. This study tested the hypothesis that the plasticity response in *APOE*ε4 slices would be impaired. The Herpes Simplex virus as a vector for gene delivery of *APOE* is also assessed.

7.2 Aims

(1) To validate an organotypic hippocampal slice culturing model and use this model to characterise plasticity in hippocampal slices derived from C57BL/6 mice, *APOE* knockout, ε3 and ε4 transgenic mice.

(2) To determine Herpes Simplex virus (HSV) expression in slices after exogenous administration.

7.3 Materials and Methods

7.3.1 Mice

7.3.1.1 C57BL/6

Breeding pairs of male and female mice were obtained from Harlan Olac and bred in an animal unit at the University of Glasgow. Only male pups were employed in the study and were used at approximately 7 days old.

7.3.1.2 Human *APOE* transgenic mice on a GFAP promoter

APOE transgenic mice were generated as previously described in chapter II.

7.3.2 Organotypic Hippocampal Slice Culture

7.3.2.1 Tissue harvest and culturing periods

Slices were derived from male neonatal mouse pups and cultured as explained in detail in Chapter II. Tail tips were collected from the transgenic mice for PCR analysis to determine *APOE* genotype. Slices were cultured as previously described (see Chapter II). Cultures were maintained for a period of 7 or 18 DIV (days *in vitro*) (n=5/6 C57BL/6J and n=8 transgenic per time-point). Following the desired culture period the medium was removed and the slices submersion fixed in 4% paraformaldehyde for 2 hours. The fixative was then removed, phosphate buffer added and the tissue stored at 4^0C. Immunohistochemistry for apoE, synaptophysin, GAP-43, apoJ and MAP-2 was carried out as outlined in chapter II.

7.3.2.2 Quantification of immunohistochemistry and statistical analysis

Relative optical density values (ROD) for immunostaining were measured using an image analyser connected to a microscope. Optical density readings were collected from the dentate molecular layers and from the CA1 pyramidal layer to ensure consistency of immunostaining. Ten optical density readings were collected across the expanse of the molecular layers. Five from the IML/MML and five from the MML/OML using a $1cm^2$ sampling box and an average of the ten readings taken. In C57BL/6J mice optical density readings were compared in the 7 day and 18 day slices using a Student's unpaired *t*-test. In the tissue derived from the transgenic mouse lines, ANOVAR was carried out on the optical density readings and the genotypes

compared using a Student's unpaired *t*-test with Bonferroni correction for multiple comparisons. Readings were also collected from a region not directly affected by the culturing process as a reference area to ensure consistency of staining between slices.

7.3.3 Herpes Simplex Virus as a Vector for Gene Therapy

7.3.3.1 Addition of Herpes Simplex virus 1716 to hippocampal slice preparations

The virus employed in this study was produced by Prof Moira Brown and this work was carried out in collaboration with her laboratory. Briefly, the gene endocing ICP34.5 protein in HSV was deleted producing ICP34.5 null mutant virus that is avirulent. The virus contains a green fluorescent protein (GFP) reporter gene and therefore when replicated in cells fluorescence green allowing detection. Hippocampal slices were prepared from C57BL/6J wildtype mice and *APOE*ε3 transgenic mice as previously described and transported to the Neurovirology Unit at the Southern General Hospital. All virus handling was carried out within a category 2 culture hood. Following virus use all instruments were submerged in detergent and the culture hood exposed to U.V. radiation for at least half an hour to exterminate any stray virus particles. 10^6 and 10^5 virus particles were diluted in culture medium and added directly onto the slices as a single dose of 10µl of the mixture pipetted directly onto the surface of the slices. The slices were then returned to an incubator and maintained for a period of 3, 7, 12 or 18 DIV with changing of the medium every 3 DIV. Control cases received no infection by HSV1716 virus. GFP labelled wild type virus was also employed.

7.3.3.2 Fluorescence microscopy

Following the appropriate survival period the slices were submersion fixed in 4% paraformaldehye for 2 hours. The slices were mounted onto glass slides and coverslipped, sumberged in hardening medium or the slices were removed unfixed, attached to the membrane and visualised without the addition of a coverslip.

7.4 Results

7.4.1 Setting up the model and technical considerations

Initially mouse hippocampal slices were cultured using the method learned using rat tissue including the culture medium which consisted of 70.5% basal medium, 24% normal horse serum, 4% glucose, 0.5% glutamax and 1% streptomycin/penicillin (a method employed by Dr B Morris, University of Glasgow). However, the slices would only survive for short periods of time. The method therefore had to be adapted for long-term survival of the slices. Advice given to us by Dr Bruce Teter (UCLA) about culture medium consistency allowed adaptation of the system for long-term survival. Using this culture medium, slices could be maintained for over 20 days. The slices were taken at 300μm to maximise the number of slices that could be obtained from each brain, but also so that they remained structurally robust.

Immunohistochemistry was optimised for the antibodies used employing standard procedures. Analysis of immunohistochemistry was slightly different to that previously employed. Due to the thickness of the slices the trilaminar pattern was not as obvious as in the microtome sections. Therefore measurements were taken from approximate combined regions IML/MML and MML/OML and averaged to give a representative measurement of the entire molecular layer. Readings were also taken from the pyramidal layer, which remains relatively unaffected by dissection of the hippocampus to ensure consistency of staining between slices.

7.4.2 Slice viability

Cell viability of the slice was assessed by analysis of neuronal morphology in MAP-2 immunostained slices. Neuronal morphology within the pyramidal layer and dendritic network structure is assessed. Healthy cells have a normal round morphology and are strongly MAP-2 immunoreactive (Figure 7.1).

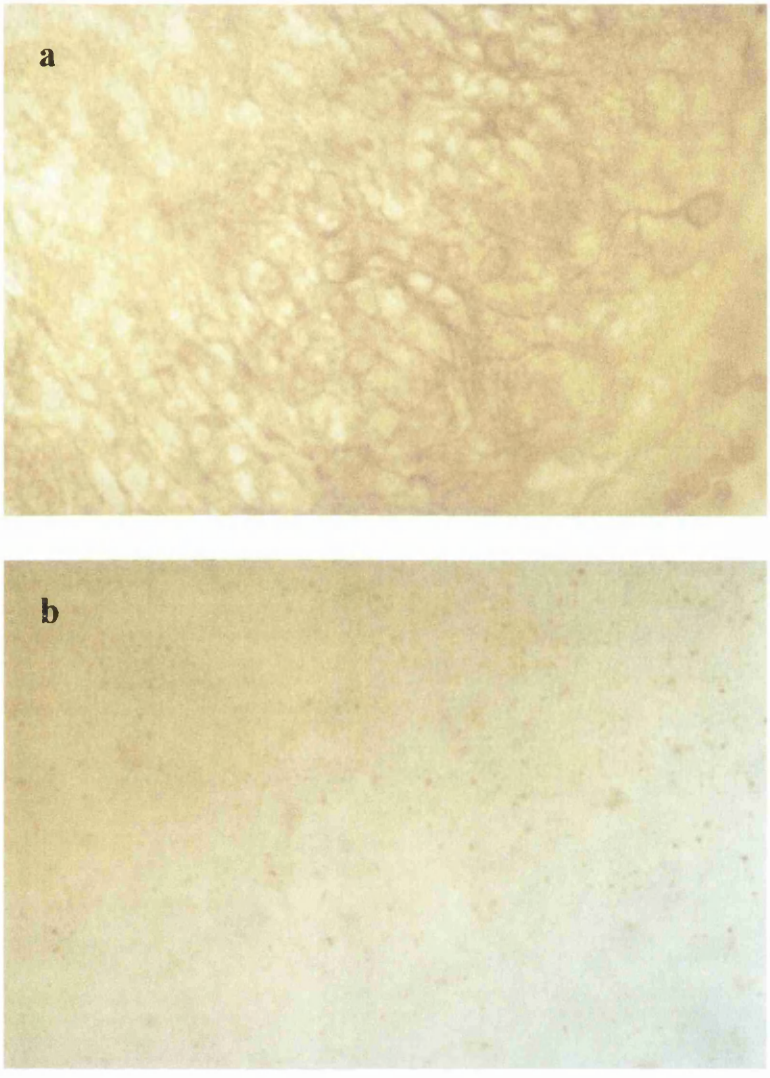

Figure 7.1 **MAP-2 immunoreactivity in hippocampal slice cultures**

Illustrative examples of MAP-2 immunoreactivity post-ECL in hippocampal slices cultured for 18 days. Healthy slices display clear defined neuronal cell bodies with dendritic processes evident (a). Although the slices are very thick, the CA1 pyramidal layer can always be seen clearly in healthy slices. When slices are non-viable, neuronal cell bodies are no longer evident in the pyramidal layer and often stain very poorly with MAP-2. The illustration (b) shows the grainy appearance of MAP-2 staining in a dead slice.

7.4.3 Analysis of Plasticity in Hippocampal Slices Derived from C57BL/6J Mice

7.4.3.1 Alterations in synaptophysin immunoreactivity

Synaptophysin immunoreactivity within the molecular layers of the dentate gyrus of cultured slices is regular, punctate and similar to that observed in the paraffin embedded sections from *in vivo* studies. The granular layer and pyramidal cell layers are stained only lightly. Optical density readings were collected from the molecular layers of the dentate gyrus of slices cultured for 7 or 18 days. At day 7 *in vitro* synaptic loss occurs in the dentate molecular layers degenerate due to removal of the cortical input. At day 18 *in vitro*, synaptophysin immunoreactivity increased within the molecular layers and was significantly different to that of the 7 day slices when compared using a Student's unpaired *t*-test ($p<0.05$) (Figure 7.2 and 7.3).

7.4.3.2 Alterations in GAP-43 immunoreactivity

GAP-43 immunoreactivity within the molecular layers of the dentate gyrus in cultured slices is regular, with the inner molecular layer being slightly more darkly stained compared to the middle and outer layers. Optical density readings were collected from the molecular layers of the dentate gyrus of slices cultured for 7 or 18 days. At day 7 in culture, fibre loss occurs within the dentate gyrus due to removal of the cortical input. At day 18 *in vitro*, GAP-43 immunoreactivity increased within the molecular layers and was significantly different to that of the 7 day slices when compared using a Student's unpaired *t*-test ($p<0.05$) (Figure 7.2 and 7.4).

7.4.4 Apolipoprotein Alterations in C57BL/6J Derived Hippocampal Slices

Neuropil apolipoprotein E immunoreactivity within the hippocampus was present as a uniform punctate stain with no evidence of neuronal staining. In 7 day slices, apoE immunoreactivity within the neuropil was darker within the molecular layers of the dentate gyrus than in any other region. Some astrocytic apoE immunoreactivity was also evident at this time-point. At day 18 *in vitro*, apoE immunoreactivity was reduced within the molecular layers and this was significantly different to immunoreactivity in the 7 day slices when compared using a Student's unpaired *t*-test

($p<0.01$). Only minimal astrocytic immunoreactivity was evident at this timepoint (Figure 7.2 and 7.5).

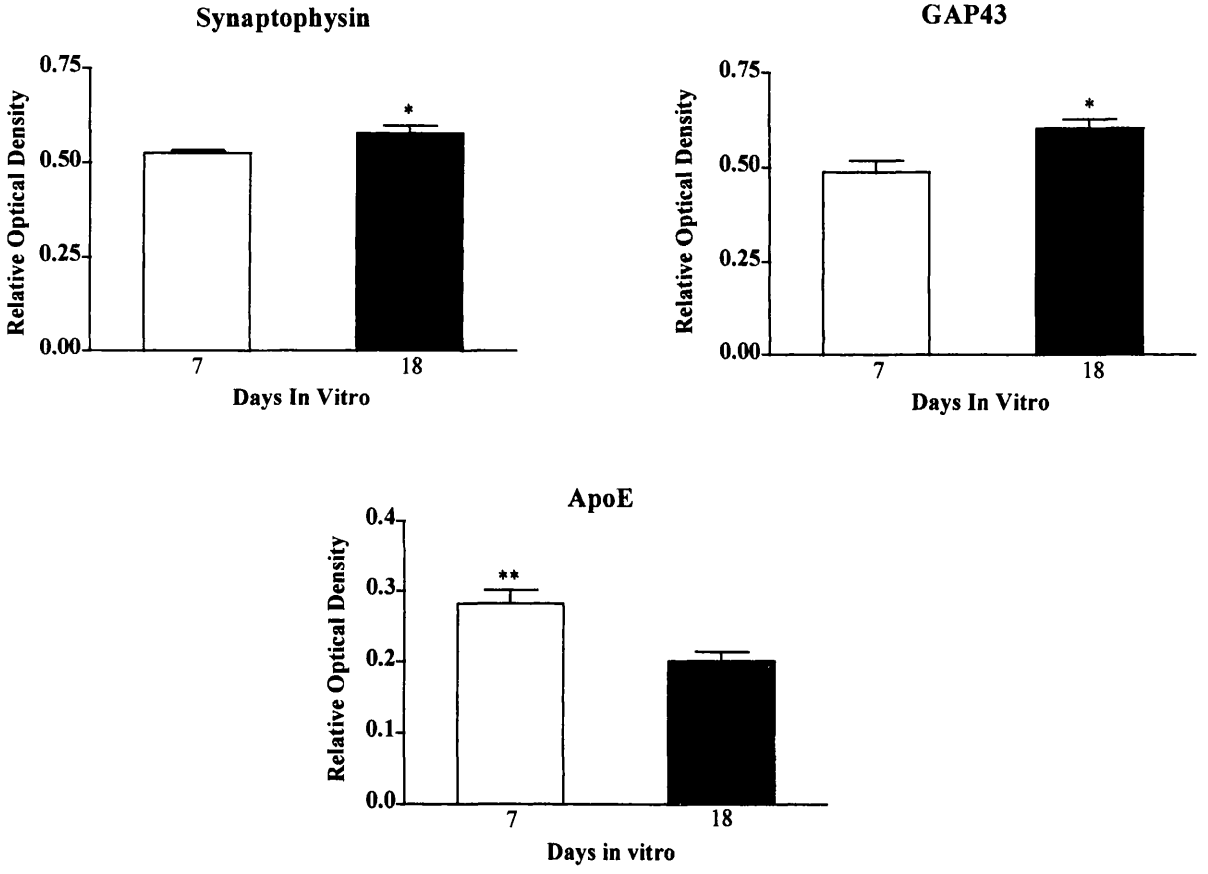

Fig 7.2 Quantification of synaptophysin, GAP-43 and apoE immunoreactivity from the dentate molecular layers of hippocampal slices derived from C57 wild type mice cultured for 7 or 18 days. Immunoreactivity was assessed as relative optical density values. The optical density values from the 7 and 18 day slices were then compared using a Student's unpaired *t*-test. **$p<0.01$ and *$p< 0.05$

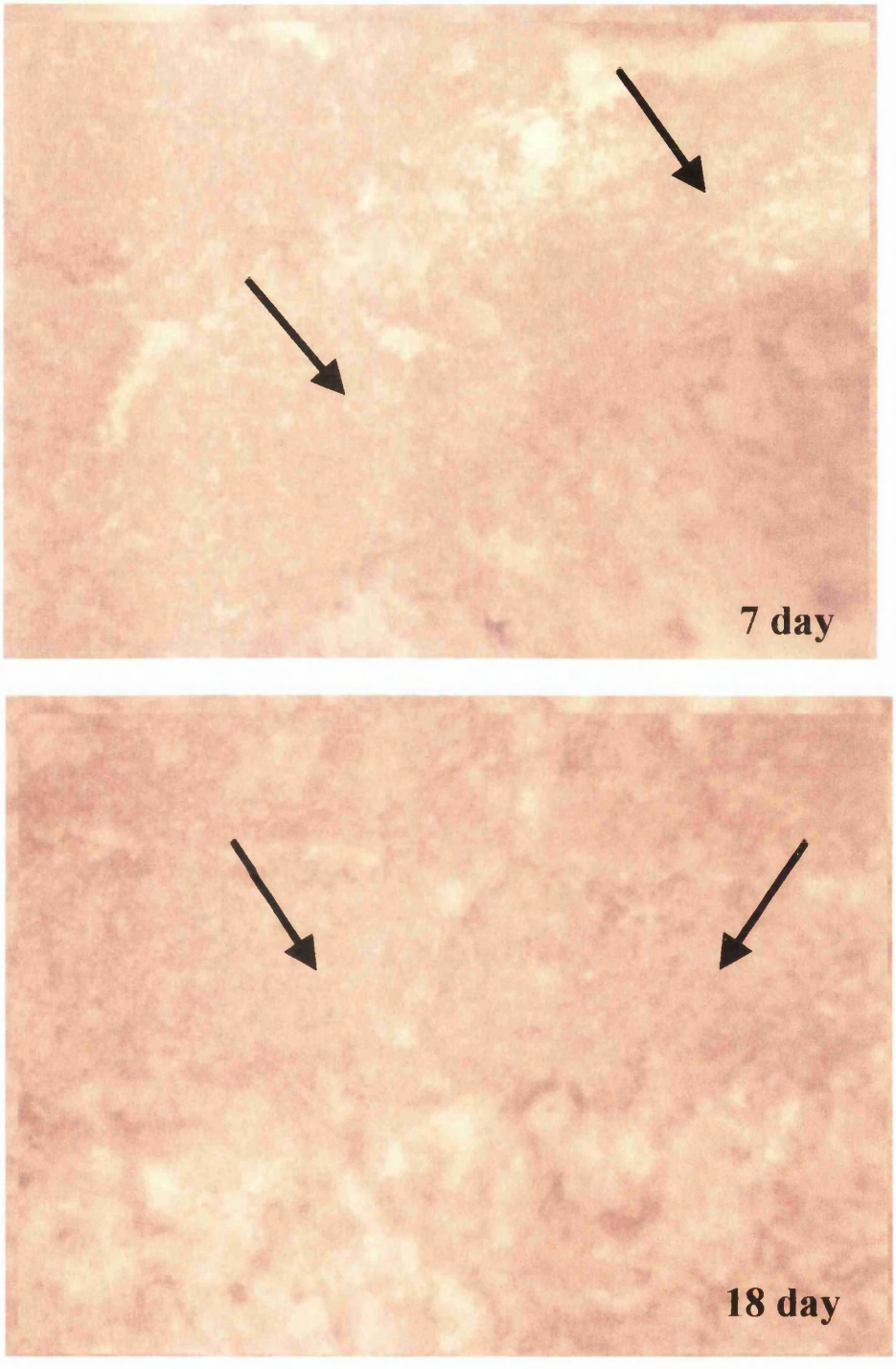

Figure 7.3 **Increased synaptophysin immunoreactivity by day 18 *in vitro***
Illustrative examples of synaptophysin immunoreactivity in the dentate molecular layers of the hippocampus of hippocampal slices derived from C57BL/6 mice cultured for 7 and 18 days *in vitro*. The arrows highlight the molecular layers. x 400 magnification. As can be seen from the illustrations the stratum lacunosum moleculare (slm) also alters post-culture.

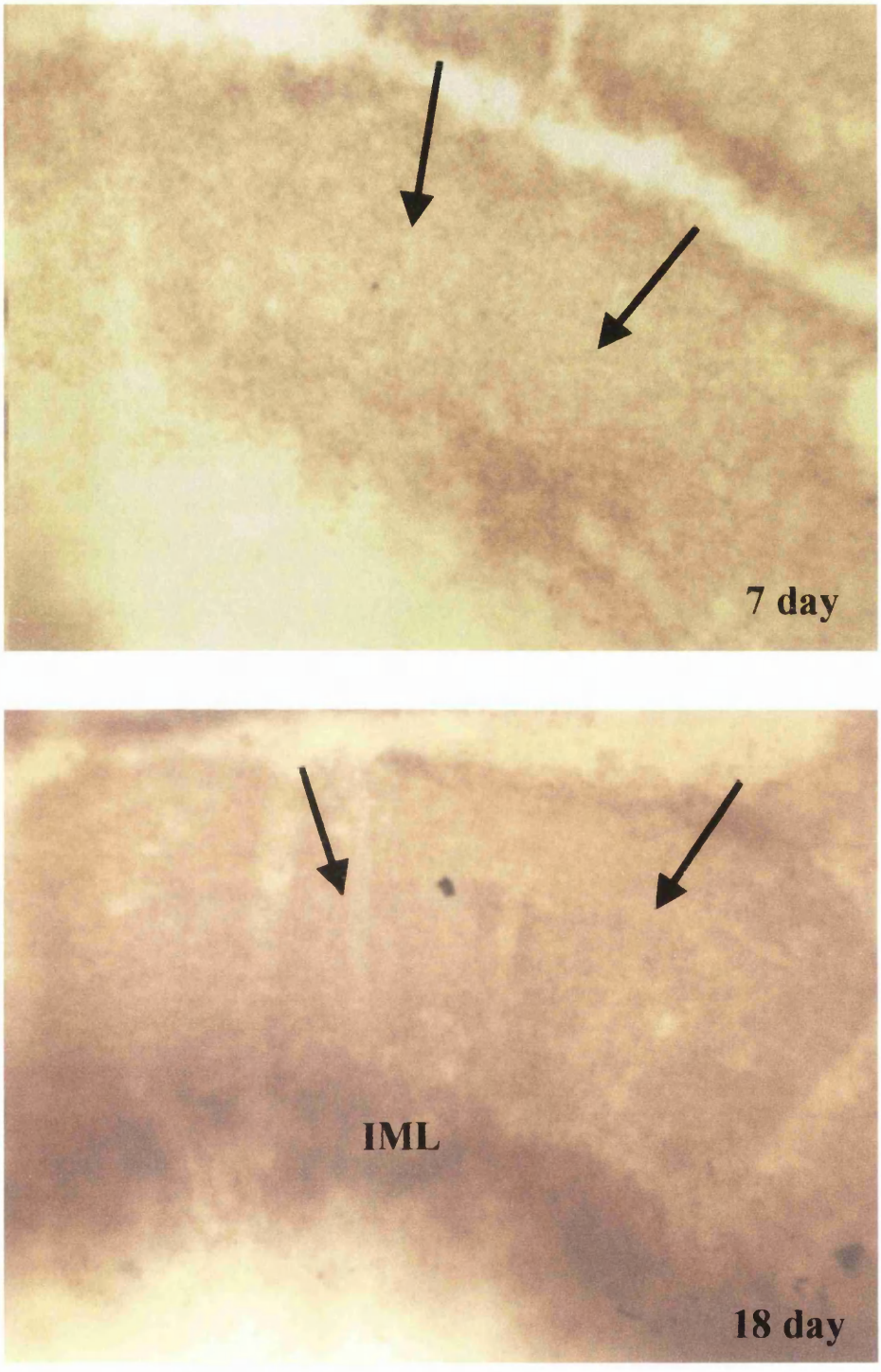

Figure 7.4 **Increased GAP-43 immunoreactivity by day 18 *in vitro***

Illustrative examples of GAP-43 immunoreactivity in the dentate molecular layers of the hippocampus in hippocampal slices derived from C57BL/6 mice cultured for 7 and 18 days *in vitro*. The arrows highlight the molecular layers. x 400 magnification. As can be seen from the illustrations, the stratum lacunosum moleculare (slm) also alters post-culture and immunoreactivity is increased there also by day 18 *in vitro*.

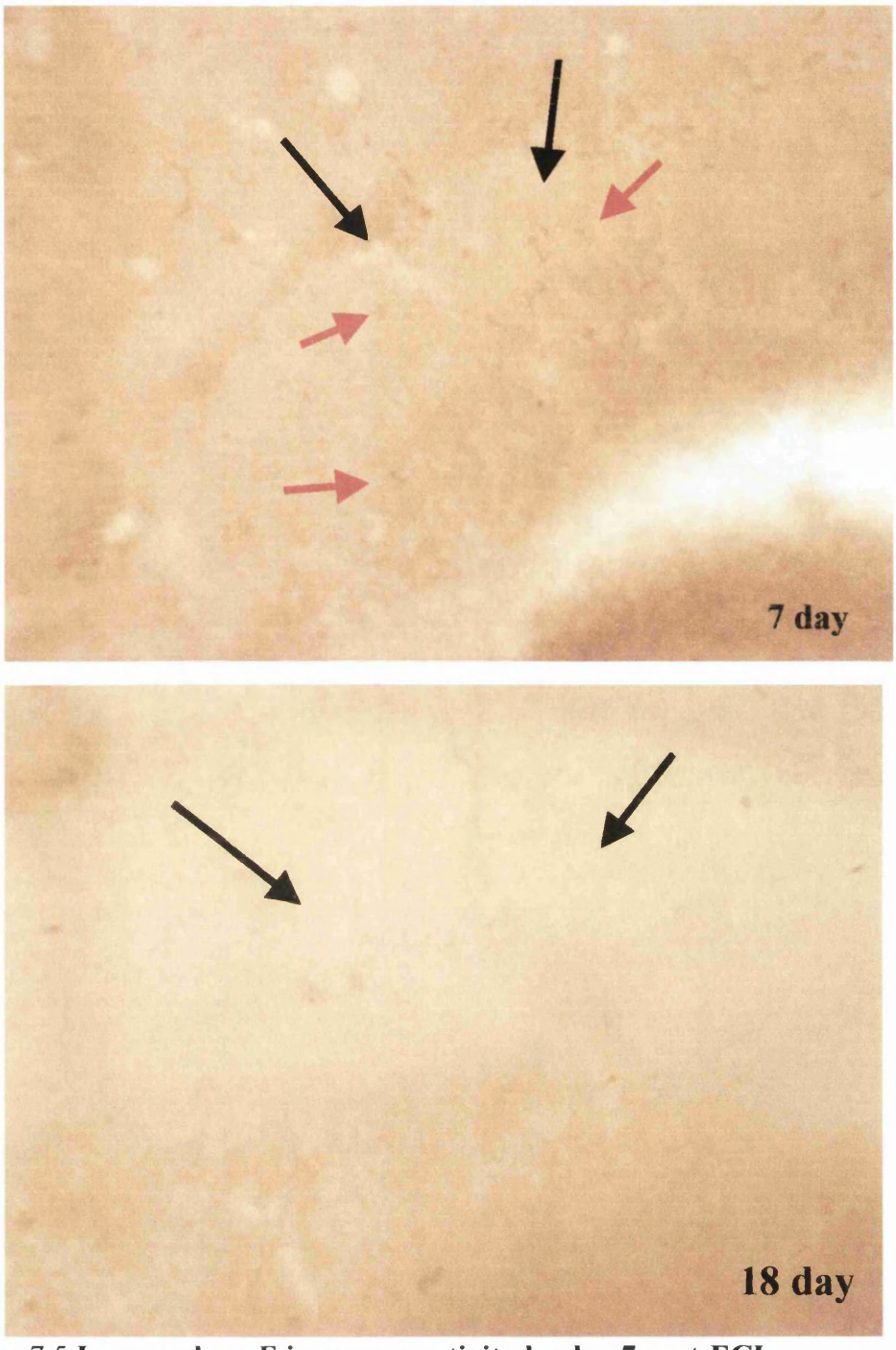

Figure 7.5 **Increased apoE immunoreactivity by day 7 post-ECL**

Illustrative example of apoE immunoreactivity in the hippocampal molecular layers in hippocampal slices derived from C57BL/6 mice and cultured for 7 or 18 days. ApoE immunoreactivity is increased within the neuropil and within astrocytes by day 7 *in vitro*. By day 18 apoE immunoreactivity has declined. The arrows highlight the molecular layers. x 400 magnification. The red arrows indicate astrocytic immunoreactivity.

7.4.5 Analysis of Plasticity in Hippocampal Slices Derived from *APOE* Knockout, ε3 and ε4 Transgenic Mice

7.4.5.1 Alterations in synaptophysin immunoreactivity

Synaptophysin immunoreactivity in slices derived from transgenic mice displayed a similar pattern as previously outlined for C57BL/6J mice and was similar in pattern between *APOE* knockout, ε3 and ε4 slices. In 7 day slices, synaptophysin immunoreactivity was compared in knockout, *APOE*ε3 and ε4 derived hippocampal slices. Synaptophysin immunoreactivity was significantly greater in ε4 slices compared to ε3 and knockout slices ($p<0.01$). Synaptophysin immunoreactivity in ε3 slices was not significantly different to that in knockout slices. By day 18 *in vitro*, synaptophysin immunoreactivity increased within the dentate molecular layers of ε3 derived slices and *APOE* knockout slices however in contrast immunoreactivity in ε4 slices was not significantly different between 7 DIV and 18 DIV. Synaptophysin immunoreactivity was significantly greater in *APOE*ε3 mice at 18 DIV compared to *APOE*ε4 slices ($p<0.05$) and *APOE* knockout slices ($p<0.01$) (Figure 7.6 and 7.8).

7.4.5.2 Alterations in GAP-43 immunoreactivity

GAP-43 immunoreactivity in *APOE* transgenic derived slices displayed a similar pattern of staining as observed in slices derived from C57BL/6J mice and was grossly similar in pattern between *APOE* knockout, ε3 and ε4 slices. GAP-43 immunoreactivity was compared in day 7 slices and it was found that there was no statistically significant difference in intensity of immunostaining between *APOE* knockout, ε3 and ε4 slices. By day 18 *in vitro*, GAP-43 immunoreactivity was increased within the molecular layers of the dentate gyrus in all genotypes. However, GAP-43 immunoreactivity is greatly increased in *APOE*ε3 slices and was significantly greater compared to *APOE* knockout ($p<0.01$) and *APOE*ε4 slices ($p<0.01$) at this time-point (Figure 7.7 and 7.9).

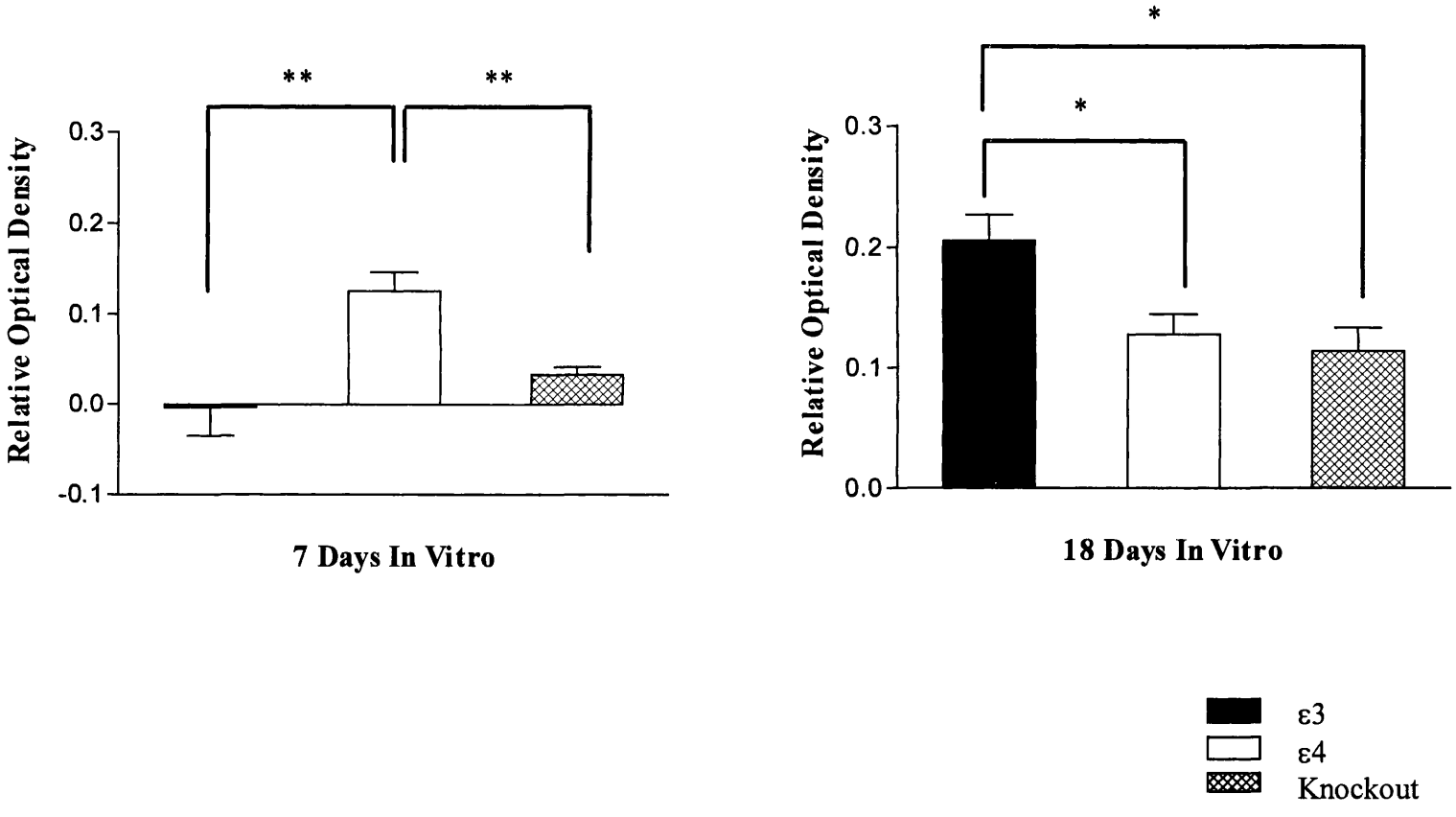

Figure 7.6 Quantification of synaptophysin immunoreactivity in the dentate molecular layer of hippocampal slices derived from *APOE*ε3, *APOE*ε4 and KO transgenic mice, cultured for 7 or 18 days. Immunoreactivity was assessed as relative optical density values and compared between groups using a Student's unpaired *t*-test and Bonferroni corrected for multiple comparisons. ****p<0.01 and *p<0.05**

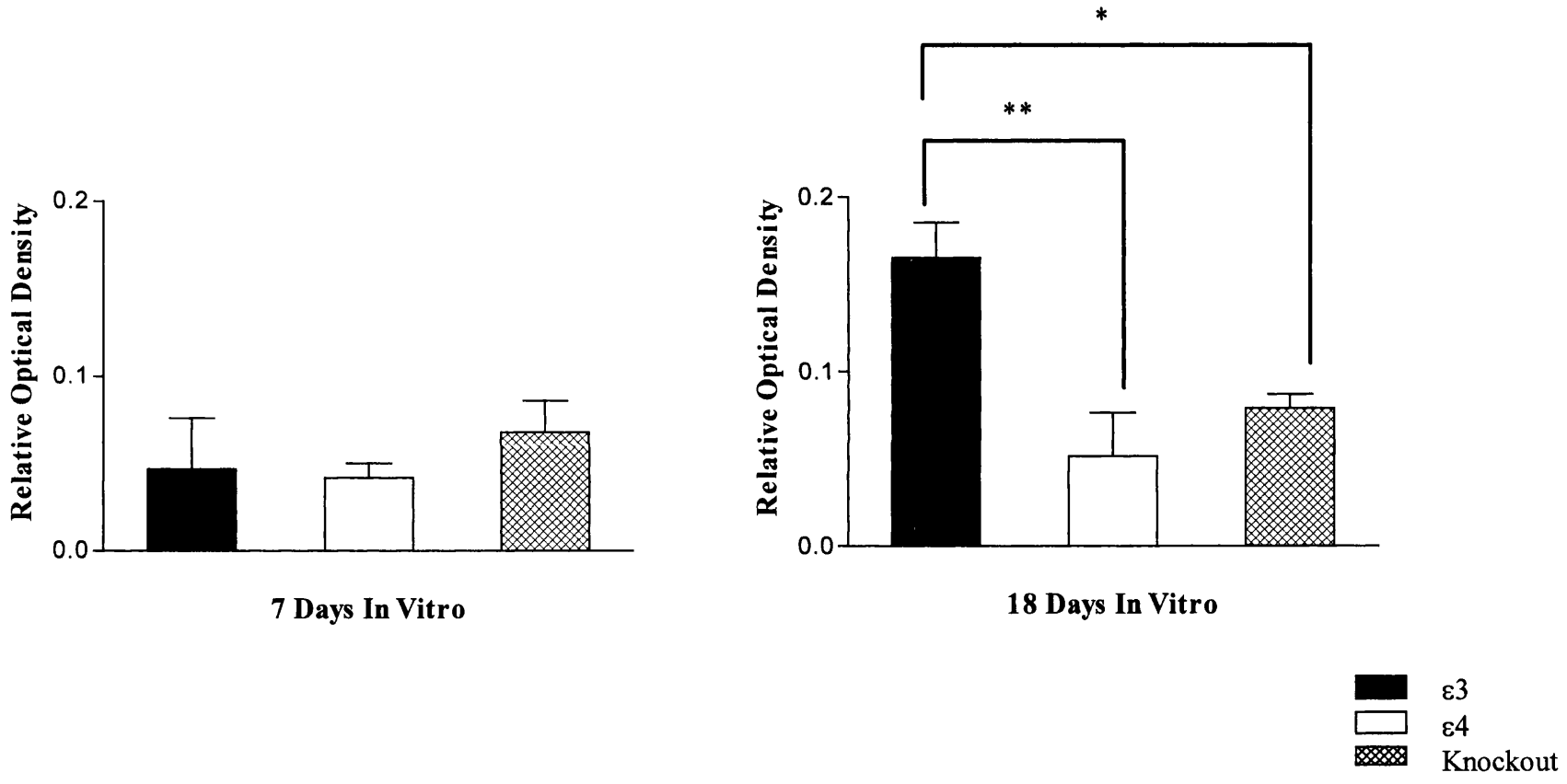

Figure 7.7 Quantification of GAP-43 immunoreactivity in the dentate molecular layer of hippocampal slices derived from *APOE*ε3, *APOE*ε4 and KO transgenic mice, cultured for 7 or 18 days. Immunoreactivity was assessed as relative optical density values and compared between groups using a Student's unpaired *t*-test and Bonferroni corrected for multiple comparisons. ****p<0.01 and *p<0.05**

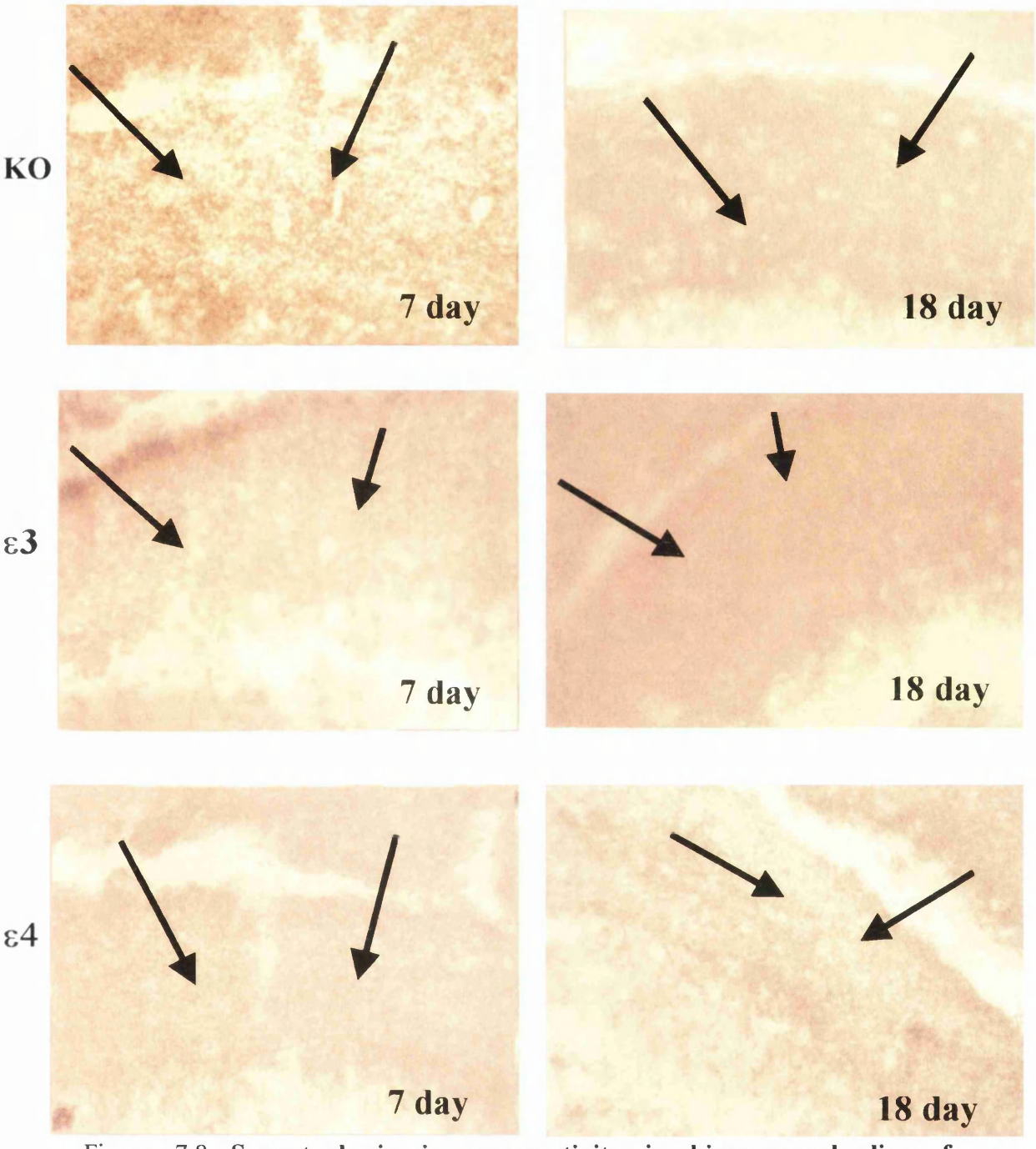

Figure 7.8 **Synaptophysin immunoreactivity in hippocampal slices from transgenic mice**

Illustrative examples of synaptophysin immunoreactivity in the molecular layers of hippocampal slices, derived from *APOE* knockout (KO), ε3 and ε4 transgenic mice. The arrows highlight the molecular layer region. x 400 magnification

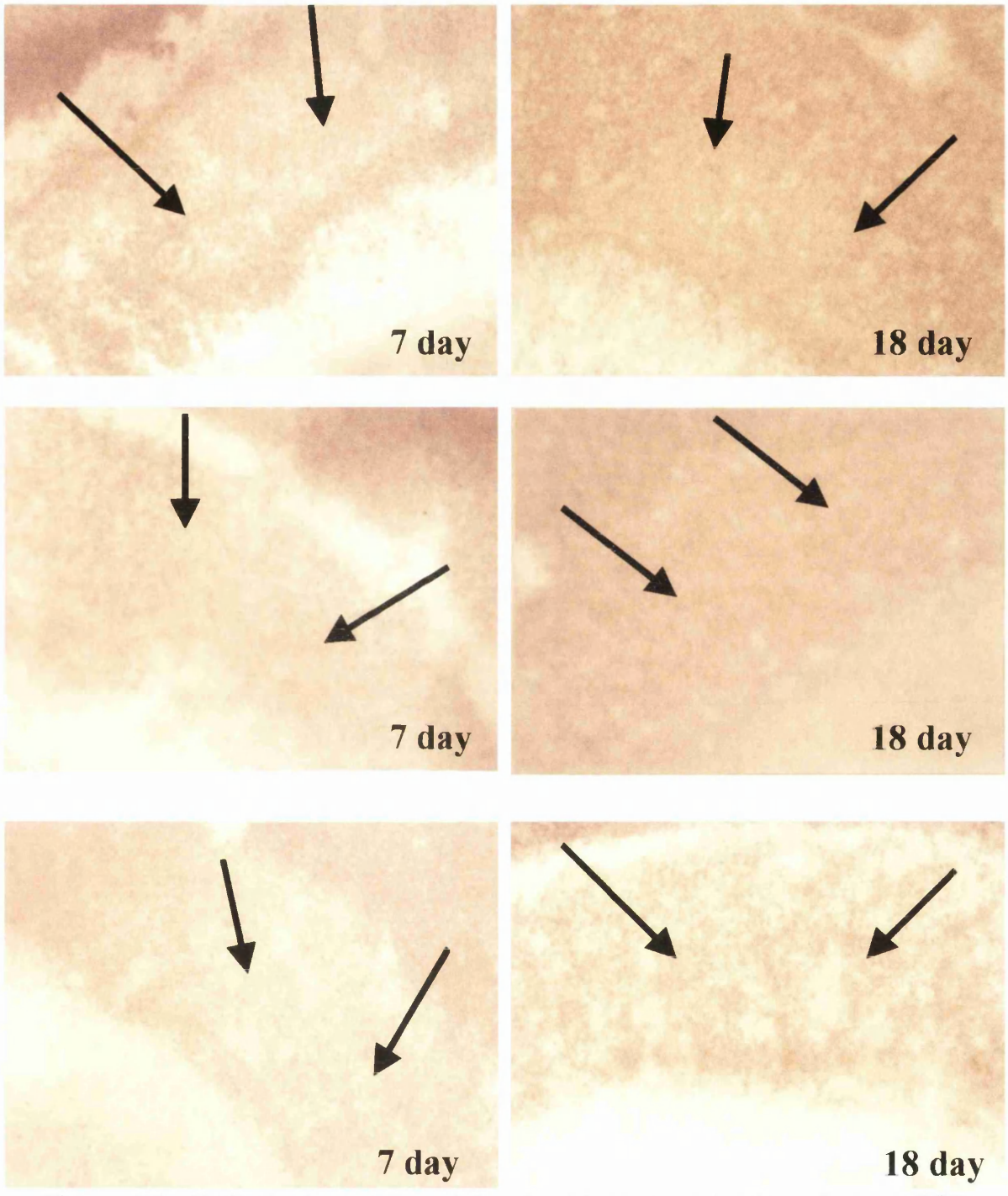

Figure 7.9 **GAP-43 immunoreactivity in hippocampal slices from *APOE* transgenic mice** Illustrative examples of GAP-43 immunoreactivity in the molecular layers of hippocampal slices derived from *APOE* knockout (KO), ε3 and ε4 transgenic mice. The arrows highlight the molecular layer region. The stratum lacunosum moleculare GAP-43 immunoreactivity also increases by day 18 *in vitro*. x 400 magnification

7.4.6 Apolipoprotein Alterations in *APOE* Transgenic Derived Hippocampal Slices

7.4.6.1 Apolipoprotein E

Baseline apoE levels in this line of transgenic mice have been assessed and *APOE*ε3 and ε4 mice display comparatively similar levels of apoE (see Chapter V). *APOE* knockout slices do not display any apoE immunoreactivity at any time. Neuropil apoE immunoreactivity was measured using relative optical density measurements and compared between *APOE*ε3 and ε4 slices using a Student's unpaired *t*-test. In 7 day slices, apoE immunoreactivity was significantly greater in *APOE*ε3 slices compared to ε4 slices ($p<0.0001$). The entire hippocampus displayed dense astrocytic apoE immunoreactivity and was particularly dense in the dentate molecular layers, but was similar in both *APOE*ε3 and ε4 slices. In day 18 slices, apoE neuropil apoE immunoreactivity declined in both *APOE*ε3 and ε4 slices and was similar in each genotype. Astrocytic apoE immunoreactivity also declined within the molecular layers at this timepoint (Figure 7.10 and 7.12).

7.4.6.2 Apolipoprotein J

ApoJ immunoreactivity was present within the neuropil and labelled some neurons lightly. In day 7 slices, apoJ immunoreactivity was also evident within the dentate molecular layers. At this time-point there was no statistically significant difference in apoJ immunoreactivity between the three genotypes. In 18 day cultures, apoJ immunoreactivity declined in all slices but was not significantly different between the three genotypes (Figure 7.11). No astrocytic apoJ immunoreactivity was evident at this time. (ApoJ immunoreactivity not illustrated)

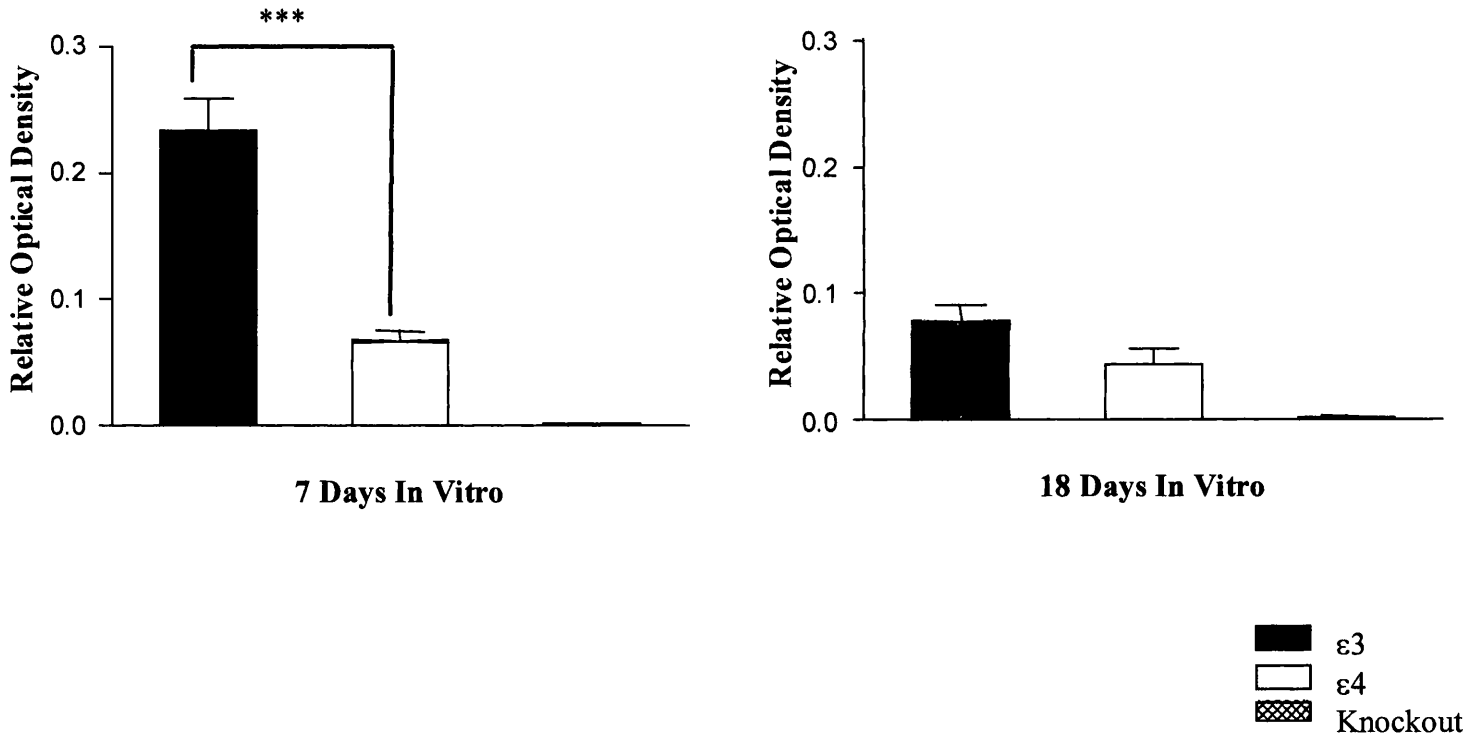

Figure 7.10 Quantification of apoE immunoreactivity in the dentate molecular layer of hippocampal slices derived from *APOE*ε3, *APOE*ε4 and KO transgenic mice, cultured for 7 or 18 days. Immunoreactivity was assessed as relative optical density values and compared between groups using a Student's unpaired *t*-test and Bonferroni corrected for multiple comparisons. ***$p<0.0001$ with Bonferroni correction for multiple comparisons.

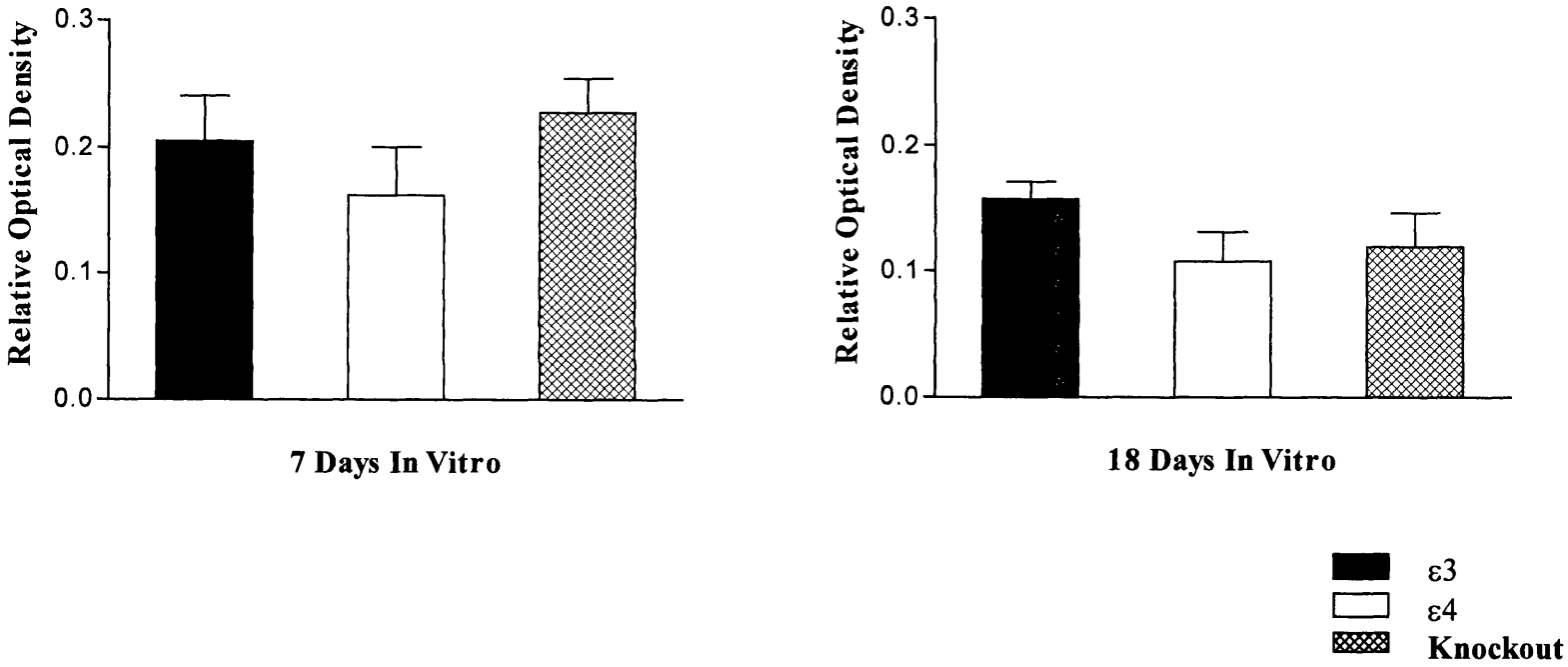

Figure 7.11 Quantification of apoJ immunoreactivity in the dentate molecular layer of hippocampal slices derived from *APOE*ε3, *APOE*ε4 and KO transgenic mice, cultured for 7 or 18 days. Immunoreactivity was assessed as relative optical density values and compared between groups using a Student's unpaired *t*-test and Bonferroni corrected for multiple comparisons. No difference in apoJ immunoreactivity was noted between groups at any time-point.

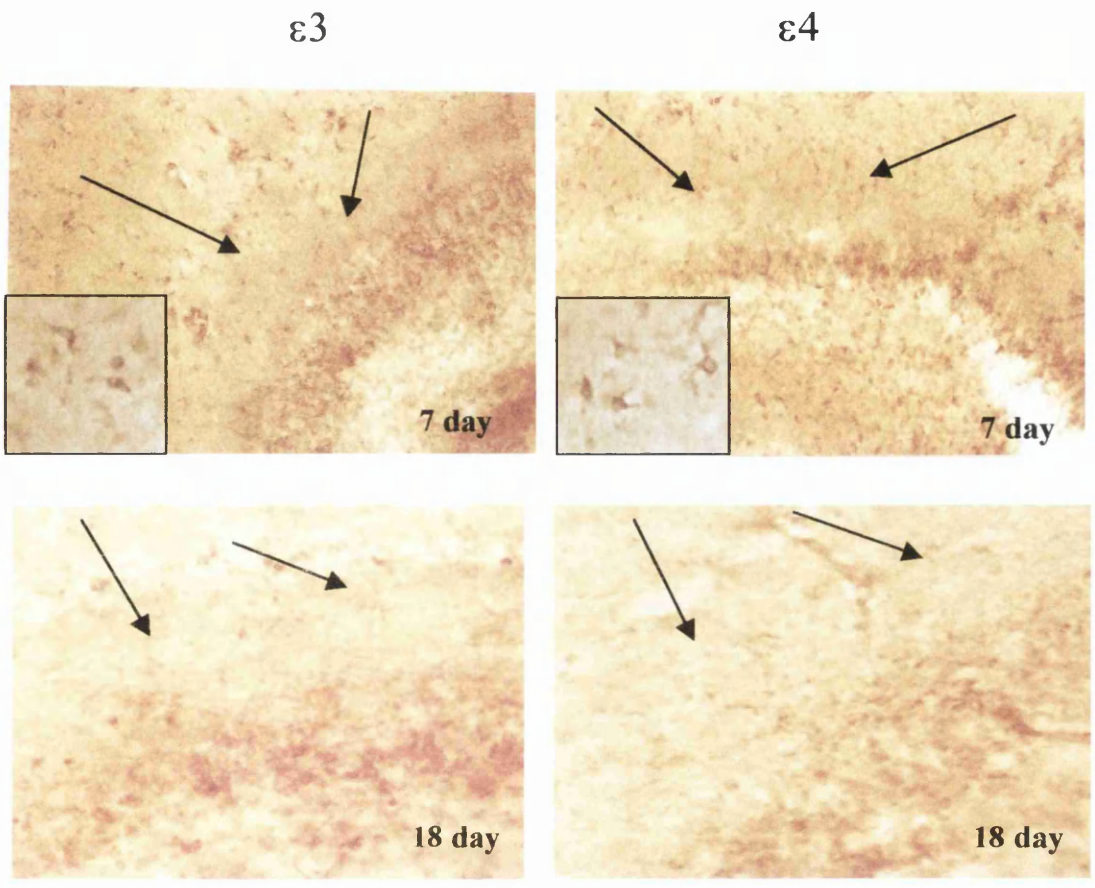

Figure 7.12 **ApoE immunoreactivity is increased by day 7 *in vitro* in ε3 and ε4 mice.**

Illustrative examples of apoE immunoreactivity in the molecular layers of hippocampal slices from *APOE*ε3 and ε4 transgenic mice cultured for 7 or 18 days. ApoE is increased in the neuropil and also within astrocytes within the molecular layers (see inlay) by day 7 *in vitro*. *APOE* knockout slices do not display any apoE immunoreactivity. X200 magnification

7.4.7 Uptake and Replication of Herpes Simplex Virus 1716 in Hippocampal Slices

7.4.7.1 Expression of HSV 1716 in C57BL/6J derived hippocampal slices

Slices were allowed to survive for periods of 3, 7, 12 and 18 DIV. Following this they were fixed and mounted for viewing by fluorescence microscopy. Control slices displayed no GFP expression at any timepoint. GFP expression was present in all slices at every timepoint studied. The expression was localised to the dentate gyrus and was cellular in nature (Figure 7.13). Some staining was also evident within the granule cell layer. The occasional GFP expressing cell could be visualised within the CA1 pyramidal cell layer. Expression was least intense in 3 day slices and was increased in day 7, 12 and 18 slices however expression levels were similar at these time-points.

7.4.7.2 Expression of HSV 1716 in *APOE*ε3 transgenic mice derived hippocampal slices

Slices were allowed to survive for periods of 3, 7, 12 and 18 DIV. *APOE*ε3 transgenic mice were chosen for these preliminary expression studies to eliminate any unforseen adverse effects which may be associated with being ε4 i.e. viral uptake. Control slices displayed no GFP expression at any timepoint. Slices from transgenic mice displayed similar expression to that observed in C57BL/6J wildtype mice. The expression was localised to the dentate gyrus and was cellular in nature (Figure 7.14). Dense expression was present within the molecular layers of the dentate gyrus although some staining was also evident within the granule cell layer. The occasional GFP expressing cell could be visualised within the CA1 pyramidal cell layer. At day 7, 12 and 18 slices expression levels were similar in all slices. Astrocytic proliferation occurs post-culture and this would suggest that the virus expression is located there (Appendix A3.3).

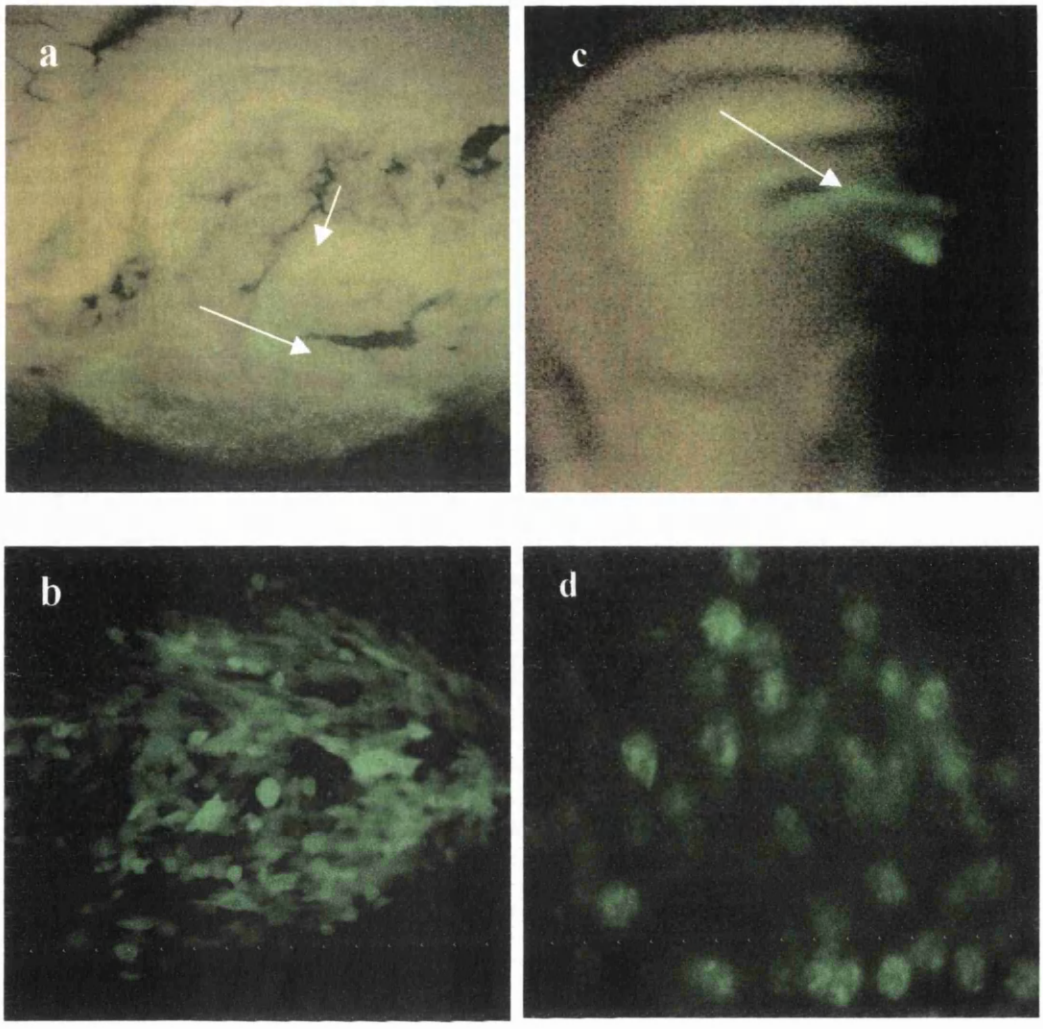

Figure 7.13 **Expression of HSV 1716 GFP in hippocampal slice cultures from a C57BL/6J mouse**

Illustrative example of HSV 1716 expression in the molecular layers of the dentate gyrus after 7 days (a, b) and 18 day (c, d) *in vitro*. (a, c) x50 (b, d) x400 magnification

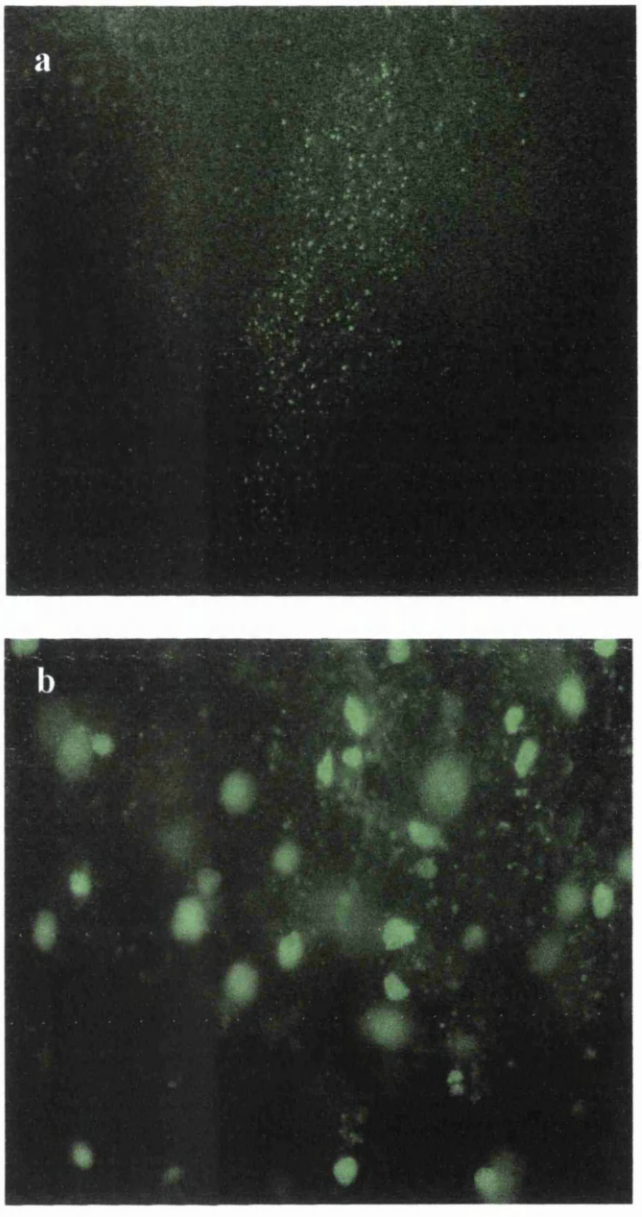

Figure 7.14 **Expression of HSV 1716 in hippocampal slices from an *APOE*ε3 transgenic mouse**

Illustrative example of HSV 1716 expression in a hippocampal slice cultured for 18 days *in vitro*. Expression is still intense within the hippocampal dentate molecular layers at this timepoint. (a) x100 magnification and (b) x 400 magnification

7.5 Discussion

In this study, a model of organotypic hippocampal slice culture was developed in the laboratory at the Wellcome Surgical Institute. This model was developed because it allows simple manipulation of environmental conditions. Exogenous compounds and treatments may be applied with relative simplicity compared to trials in *vivo*. In this study, the model was validated in C57BL/6J slices and at 18 days sprouting was detected. This model was then used to examine *APOE* genotype differences in sprouting and it was determined that neuronal repair was impaired in hippocampal slices derived from *APOE*ε4 mice. Lastly, the model was used to examine the utility of HSV as a delivery vector for apoE. Expression of HSV was found up to 18 days *in vitro*.

7.5.1 Plasticity in hippocampal slices derived from C57BL/6J mice

As previously mentioned, the process of culturing slices causes a cascade of events within the hippocampus, which mimic the events that occur after entorhinal cortex lesion. This entails a period of degeneration and with longer survival periods, subsequent reinnervation (Stoppini *et al*, 1991; Gahwilwer *et al*, 1997). It was necessary to determine if we could detect these events in slices derived from C57BL/6J wild-type mice using the markers previously employed in the *in vivo* studies. Using the time periods suggested to us by Dr Teter it was determined that by day 18 *in vitro* slices displayed sprouting and reactive synaptogenesis. This study is in accordance with what other investigators have determined in slices derived from rodents (Frotscher and Gahwiler, 1988; Stoppini *et al*, 1993, 1997). Additional to this, it was also found that apoE was increased within the neuropil by day 7 *in vitro,* where levels were approximately 30 % greater than at 18 days *in vitro* (Teter *et al*, 1999). This model was chosen on the basis that it provided a more physiologically relevant system to study apoE, rather than the commonly chosen single cell preparations. Tissue culturing of this kind allows the ease of manipulation that single cell cultures afford. However, cells within organotypic cultures exist within an environment of networked cells that more closely mimic the environment in the whole animal.

7.5.2 *APOE* genotype influence on plasticity in slices derived from transgenic mice

The data from the *in vivo* studies in this thesis indicate that *APOE* genotype influences plasticity mechanisms. Several *in vitro* studies, using single cell culture, have shown a role for apoE in neurite outgrowth and have highlighted also the impaired capacity of apoE E4 in producing this neurite outgrowth. Using more advanced culture techniques such as hippocampal slice culture it is possible to assess *APOE* genotype influence on plasticity in a more physiologically relevant system. Hippocampal slices derived from human *APOE*ε4 transgenics with the human promoter sequences, have been shown to display impaired sprouting capabilities (Teter *et al*, 1999). In that study by Teter *et al* it was determined that slices from *APOE* knockout mice did not exhibit any Timm's-stained sprouting in the dorsal hippocampus. The ability of the *APOE*ε3 and ε4 allele to rescue sprouting was analysed and it was found that expression of the ε3 allele fully restored dorsal hippocampal sprouting. The ε4 allele also increased sprouting but to only 58% of that caused by *APOE*ε3. The medium from *APOE*ε3 transgenic mice was collected and administered to slices derived from *APOE* knockout mice. Sprouting was increased by 20% in these knockout slices highlighting the plasticity promoting effects. In the present study, evidence of sprouting and reactive synaptogenesis was found in *APOE* knockout, ε3 and ε4 slices. Plasticity was impaired in *APOE*ε4 slices where synaptophysin and GAP-43 immunoreactivity was significantly lower at day 18 *in vitro* compared to that in *APOE* knockout and *APOE*ε3 derived slices. *APOE*ε3 mice displayed the greatest capacity for plasticity. However, interestingly in 7 day cultured slices, apoE increased within the neuropil but to a greater extent in *APOE*ε3 slices than in *APOEε4* slices. At day 18 *in vitro,* apoE levels were not significantly different between the genotypes. This greater increase in ε3 slices may indicate why there is such a degree of plasticity within the *APOE*ε3 slices. The slices derived from *APOE* knockout mice also display repair processes at day 18 *in vitro*, a finding paralleled in the *in vivo* study (see Chapter V). The plasticity observed in *APOE* knockout mice may be due to some other contributory factor, such as apoJ. At day 7 *in vitro,* apoJ immunoreactivity is increased within the neuropil in all slices and to a greater extent in *APOE* knockout slices although not significantly so. At day 18, apoJ immunoreactivity had decreased

and was similar in *APOE* knockout, ε3 and ε4 slices. The present study indicated the utility of organotypic hippocampal slice culture as a system to study the role of apoE and *APOE* genotype differences in neuronal repair.

7.5.3 Adenoviral vector therapy in the treatment of atherosclerosis

The studies presented in this thesis build on clinical work to strongly indicate the *APOE*ε4 allele is associated with a poor recovery after injury via a poor reparative capacity. It would therefore be beneficial to be able to increase the levels of 'good' forms of apoE (E2, E3) in an attempt to ameliorate effects of the *APOE* ε4 allele. There is evidence to suggest that increasing exogenous levels of apoE may improve outcome after brain injury or improve the effects of ageing (Masliah *et al*, 1997, Horsburgh *et al*, 1999). However these studies are limited because of acute short-term administration and problems with the crossing of the blood-brain barrier (Laskowitz *et al*, 2000). Obviously intraventricular infusion of apoE is not a valid option in therapy for humans. This has lead to the search for more effective techniques of treatment such as gene therapy. This is not a new advance in the field of apoE research. For a number of years several groups have been investigating the merits of using adenoviral vector delivery of apoE to *APOE* knockouts to reduce atherosclerosis (Kashyap *et al*, 1995; Stevenson *et al*, 1995; Cioffi *et al*, 1999, Hasty *et al*, 1999; Desurmont *et al*, 2000). The outcome of these animal studies proved that using adenoviral vectors to deliver apoE, the atherosclerotic plaque formations, which occurred in the arterial walls of *APOE* knockout mice, could be completely regressed. This therapy also reversed the hypercholesterolaemic phenotype evident in these mice. However, a finding that has hampered the development of any adenoviral treatment into human therapies is that adenovirus actually causes massive complications in the brain. Investigators in the States, researching adenovirus mediated therapy in humans, found that there was a high mortality rate. They did not report these findings and unfortunately several other patients died in the process. All adenovirus therapies have now been withdrawn from clinical trials. In this study our aim was to carry out a pilot study assessing viral vector expression in hippocampal slices, but using a Herpes Simplex Virus.

7.5.4 Herpes Simplex virus as a vector for gene delivery

The herpes simplex virus (HSV) exists naturally within the human body and exists in many forms. The most common form being that which travels in the trigeminal nerve and causes the common cold sore. Under normal conditions the virus may invade and replicate within any cell in body. The virus employed in this study was engineered in the laboratories of Prof Moira Brown, University of Glasgow. The herpes simplex virus (HSV) protein ICP34.5 is a specific determinant of virulence. When this protein is removed (null mutant), the virus is avirulent and may only replicate in replication competent cells (Dolan *et al*, 1972). In this capacity the virus has already been developed into a therapy for the treatment of malignant melanoma. The virus was first tested, *in vitro,* for its ability to replicate in cells derived from human glioblastomas cells (Brown *et al*, 1994) and then in a rodent model of intracranial murine melanoma. Stereotaxic injection of the HSV 1716 mutant resulted in complete tumour regression and a significantly increased survival time of each animal (McLean *et al*, 1991; Randazzo *et al*, 1995). Histopathological analysis of the brains of mice administered the virus display mild meningoencephalitis at early timepoints, which is associated with virus antigen expression. At day 28 post-injection, no virus antigen could be detected and therefore proved to be self-limiting in terms of expression. No other adverse neuropathological alterations were noted (McKie *et al*, 1998, Howard *et al*, 1998). The success of this work allowed the virus to be approved for Phase 1 toxicity trials and a group of patients, with recurrent glioblastoma, have already received direct intratumoural injection of the ICP34.5 null mutant 1716 in patients (Rampling *et al*, 1998). The patients treated thus far have not shown any adverse side effects even though they are immunosuppressed. Although these were merely toxicity tests, it is worth mentioning that these patients showed tumour regression and prolonged survival (unpublished data). Although lacking the ICP34.5 gene, the HSV 1716 may establish cell latency *in vivo* (Robertson *et al*, 1992) and may therefore act as an efficient delivery system for genes into the CNS. It is with this in mind that we embarked on the pilot studies of HSV treatment in hippocampal slices. The aim is to develop a gene based apoE therapy where perhaps an individuals' *APOE* genotype may be manipulated by administration of a beneficial *APOE* genotype mediated by HSV delivery. Therapies such as this would not only be beneficial following head

injury and in AD but also a host of other human diseases, with which the *APOE*ε4 genotype is adversely associated. We found that the HSV 1716 mutant was taken up and expressed by hippocampal slices following direct application to its surface. Expression was evident by day 3 post-culture and persisted until the longest culture period of 18 days. As yet it is unclear what cell types were expressing the virus however, much of the GFP expression was confined to the hippocampal dentate gyrus. It is likely that the majority of the expression is astrocytic, because astrocyte proliferation occurs within the molecular layers post-culture. However, cells of the dentate granule layer also appeared to express GFP. Whether these are neurons is unclear, however, this virus strain can establish cell latency *in vivo* as previously stated. It may also be possible that these cells are neuronal progenitors as neurogenesis has been witnessed in the hippocampus. This study is by no means a complete work as the virus is now being tested for expression and toxicity after intracerebral injection *in vivo*. *APOE* gene sequences and promoter sequences must also be attached to the virus, a process that will obviously take a considerable length of time. Nevertheless, we are one step closer in the engineering of an efficient gene-based therapy.

Chapter VIII

APOE Genotype Influence on Apolipoprotein E Interaction with Microtubules

8.1 Introduction

Eukaryotic cells have an internal structural support system called the cytoskeleton which not only functions in cell structure maintenance but also intracellular transport and neurite outgrowth (Alvarez *et al*, 2000). The cytoskeleton is composed of three classes of filaments: microfilaments, intermediate filaments and microtubules (Barr and Keirnan, 1993). Microtubules will be the main focus of this chapter. Microtubules are hollow cylindrical structures composed of two 55 kDa subunit proteins, α and β tubulin and are approximately 25nm in diameter (Figure 8.1).

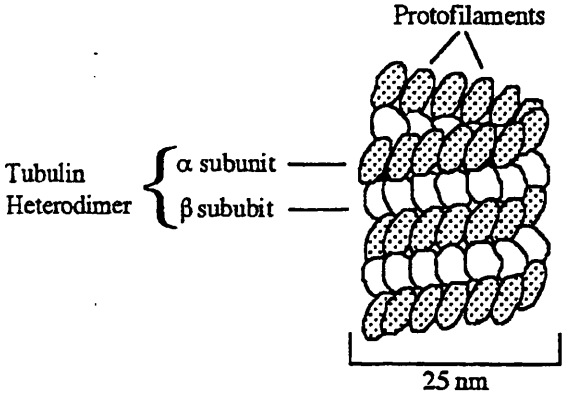

Figure 8.1 Diagram illustrating microtubule structure.

It was suggested, at the outset of this thesis, that apoE binding to microtubules defended the structure from phosphorylative enzymes and the process also aided in neuronal sprouting after injury (Roses *et al*, 1995). However, studies in this thesis and other studies have shown that neuronal plasticity is severely impaired in humans and mice carrying *APOE*ε4 alleles. In Chapter IV of this thesis it was shown that dendritic structure (by MAP-2 immunostaining) is severely disrupted in *APOE*ε4 mice after injury. This chapter tested the hypothesis that different apoE isoforms interact differently with microtubules and this may underlie the observed difference in plasticity after injury.

8.2 Aims Microtubular binding of apoE E3 and E4 protein was analysed and apoE isoform specific differences were determined.

8.3 Materials and Methods

8.3.1 Immunohistochemistry on paraffin sections

The microtubules to be used in this study are composed of pure tubulin. Thus tubulin immunohistochemistry was carried out on the tissue sections obtained from transgenic mice (both human and GFAP promoter) to determine firstly, whether there were *APOE* genotype differences in alterations in tubulin after entorhinal cortex lesion. Sections from 0 day control and 90 day survival mice were used. Relative optical density values of immunohistochemistry were collected using an MCID analysis system. Six readings were collected from each molecular layer using a $1cm^2$ sampling box and the readings averaged. The percentage difference between the ipsilateral and contralateral hippocampal values was taken and the *APOE*ε3 and ε4 genotypes compared using a Student's unpaired *t*-test. The data is represented graphically as the mean +/- S.E.M.

8.3.2 Microtubule Associated Spin-Down Assay

8.3.2.1 Microtubule assembly

Tubulin protein was diluted in 2.5µl of microtubule cushion buffer and incubated at 35^0C for exactly 20 minutes. Simultaneously, 180µl of tubulin dilution buffer and 40µM of taxol were mixed together and incubated at 35^0C. 180µl of this solution was then added to the polymerised tubulin. The solution now contains a population of microtubules at a concentration of $1x10^{12}$ microtubules/ml and 5-10µm in length.

8.3.2.2 Microtubule binding activity

A preliminary experiment to determine if apolipoprotein E shows microtubule binding activity was carried out as outlined in Chapter II. Microtubule preparations were incubated with apoE E3 or E4 (derived from human plasma)(8 reactions/genotype/concentration) at a concentration of 5µg/ml or 20µg/ml and centrifuged at 48,000 rpm. The supernatant and pellet fractions were then separated by electrophoresis, transferred and immunoblotted for apoE (see chapter II). The membranes were stripped and reprobed with the tubulin antibody to check for the presence of microtubule protein in the pellet fraction. A molecular weight marker was run simultaneously.

8.3.2.3 Quantification of microtubular binding and statistical analysis

For analysis purposes it was initially determined, on gross examination of blots, whether apoE was present in the supernatant or pellet fraction. Any protein that is microtubule bound should be present within the pellet fraction. Any unbound protein remains within the supernatant fraction. Protein bands were analysed as relative optical density values using a $1cm^2$ sampling box. Optical density values from the pellet and supernatant fractions were then compared between apoE E3 and apoE E4 containing microtubule preparations using a Student's unpaired *t*-test. Data is represented graphically as the mean values +/- S.E.M

8.3.3 ApoE Binding in Fluorescent Microtubule Preparations

8.3.3.1 Microtubule assembly

It was determined from an initial study that the final labelling stoichiometry of the microtubules should be 0.33 labels per tubulin heterodimer. Microtubules were assembled as outlined in Chapter II. This solution contains a population of taxol stabilised microtubules at a concentration of $7x10^{10}$/ml. The microtubules can be visualised microscopically at this stage by diluting 1µl of the microtubule preparation in 10µl of taxol/microtubule buffer containing 20µl of antifade solution. This solution is then smeared onto a slide, coverslipped and visualised using fluorescence microscopy.

8.3.3.2 Addition of lipidated human apoE E3 and E4 to microtubule preparations

Microtubule populations were split so the apoE isoforms were being tested in a homogenous population of microtubules. The microtubules were incubated with apoE E3 and E4 bound to HDL, at a concentration of 5µg/ml or 20µg/ml for 20 mins at room temperature to allow binding to occur. An apoE polyclonal antibody (Chemicon) was added to the microtubule/HDL/apoE mixture at a concentration of 1:100 and incubated for 30 mins. Goat secondary antibody was then applied for 30 mins (1:100) and the signal amplified using fluorescein avidin D (30 mins). 1µl of this final mixture was dissolved in 10µl of taxol/microtubule and 10µl of antifade and

smeared onto a microscope slide. The microtubules appear red (rhodamine) and the apoE appears green (fluorescein).

8.3.3.3 Confocal imaging of fluorescent microtubules

Images were visualised using confocal microscopy and the binding of apoE described qualitatively. Z-stack projections were collected from representative microtubules for illustrative purposes.

8.4 Results

8.4.1 Cytoskeletal Alterations Post-Lesion

8.4.1.1 Alterations in β-tubulin following ECL in *APOE*ε3 and ε4 transgenic mice (human promoter)

β-tubulin immunostaining was punctate and intense throughout the entire molecular layer. In 0 day control mice β-tubulin immunoreactivity was similar in the ipsilateral and contralateral hippocampus and was similar in both *APOE*ε3 and ε4 mice. At day 90 post-ECL, tubulin immunoreactivity was greater in *APOE*ε3 mice compared to ε4 mice, where immunoreactivity was up to 10% below levels in 0 day controls. This did not reach statistical significance (Figure 8.2).

8.4.1.2 Alterations in β-tubulin following ECL in *APOE*ε3 and ε4 transgenic mice (GFAP promoter)

In 0 day control, mice tubulin immunoreactivity was punctate and densely stained the molecular layers of the dentate gyrus, but was similar in *APOE*ε3 and ε4 mice. At day 90 post-ECL, *APOE*ε3 mice displayed a trend for greater recovery of tubulin immunoreactivity at this time-point compared to *APOE*ε4 mice, however this did not reach statistical significance (Figure 8.3).

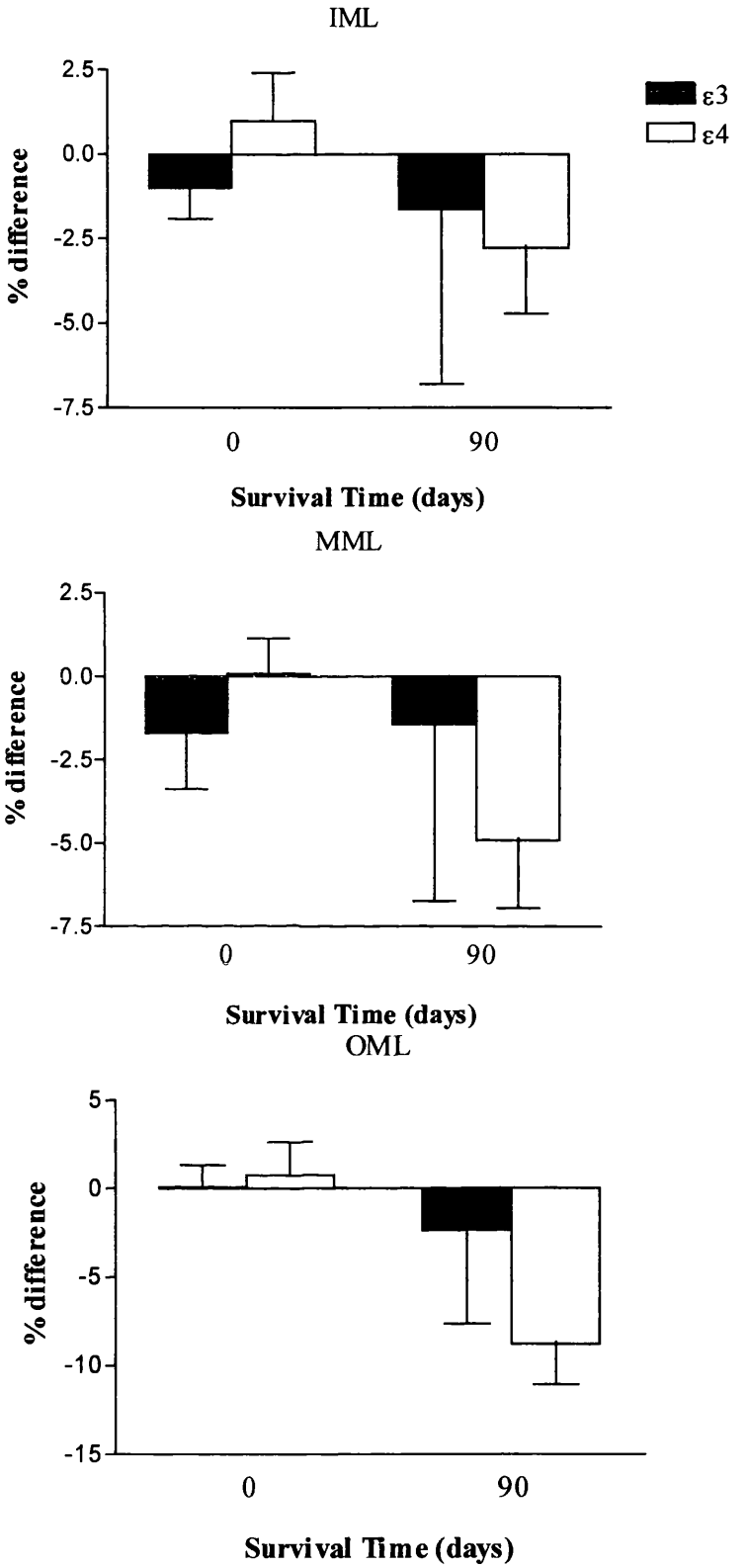

Figure 8.2 ***APOE* expressing mice driven by the human promoter**
Quantification of β-tubulin immunoreactivity in the inner, middle and outer molecular layers (IML, MML and OML) of the hippocampal dentate gyrus measured as relative optical density values at 0 and 90 days post-lesion. Percentage difference between the ipsilateral and contralateral hippocampus immunoreactivity was compared in ε3 and ε4 transgenic mice using a Student's unpaired *t*-test.

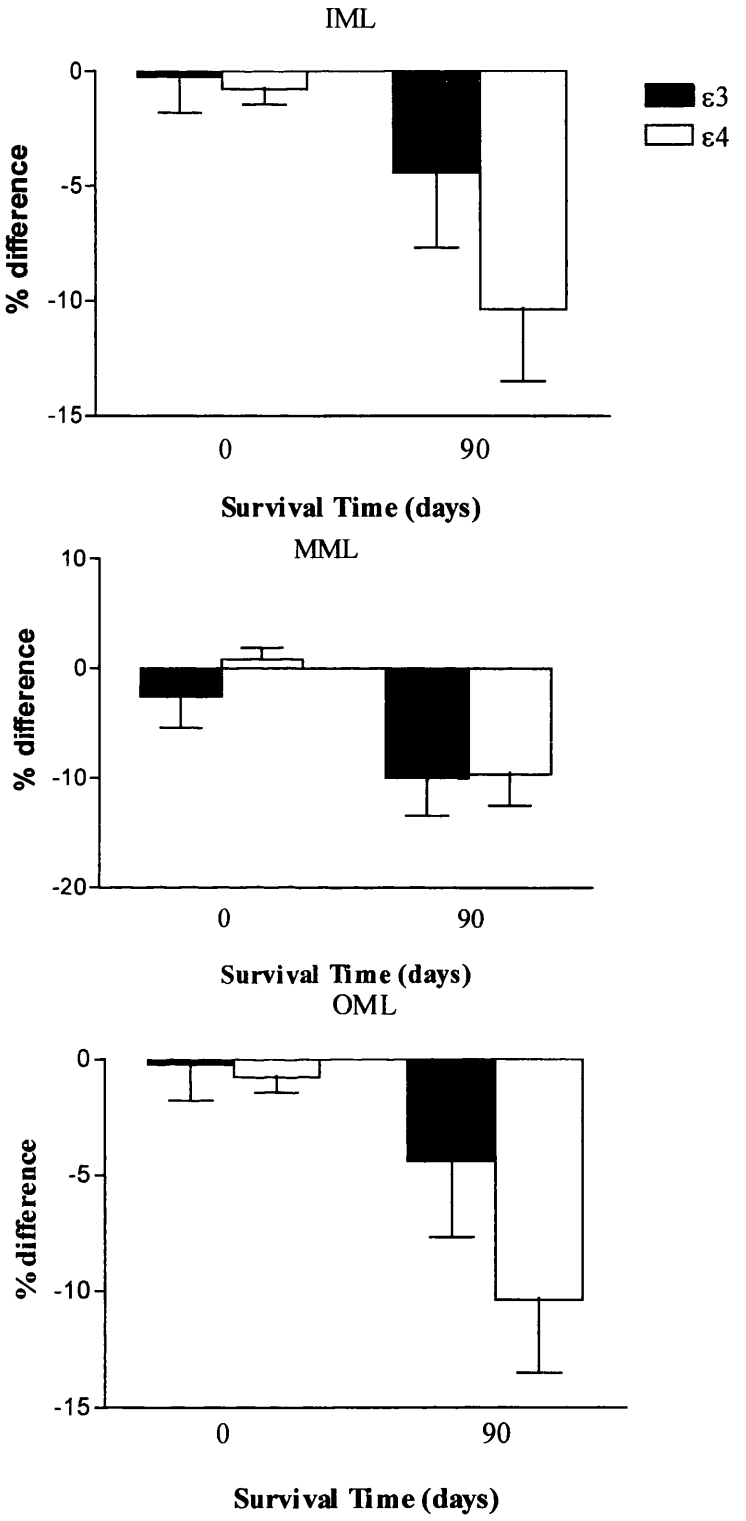

Figure 8.3 ***APOE*** **expressing mice driven by a GFAP promoter**
Quantification of β-tubulin immunoreactivity in the inner, middle and outer molecular layers (IML, MML and OML) of the hippocampal dentate gyrus measured as relative optical density values at 0 and 90 days post-lesion. Percentage difference between the ipsilateral and contralateral hippocampus immunoreactivity was compared in ε3 and ε4 transgenic mice using a Student's unpaired *t*-test.

8.4.2 ApoE Derived from Human Plasma

8.4.2.1 Enzyme linked-immunosorbent assay (ELISA) determination of apoE concentration

An ELISA was carried out on the human plasma samples to determine the concentration of apoE in each sample. The stock solutions were then diluted to a concentration of 5μg/ml and checked by ELISA to ensure that the apoE concentration was identical for each isoform. This was also checked by dot blotting (Figure 8.4). These concentrations were chosen because apoE is at a concentration of 5μg/ml within the CSF. ApoE is increased within the brain following injury and therefore a higher concentration (20μg/ml) of apoE was chosen to see if this altered the manner in which each isoform bound to the microtubules.

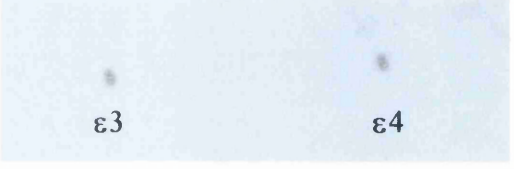

Figure 8.4 Dot blot showing similar apoE levels in a defined quantity of HDL isolated from human plasma.

8.4.3 *APOE* Genotype Influence on Microtubule Binding (microtubule spin-down assay)

8.4.3.1 Microtubule binding of apoE isoforms at a concentration of 5μg/ml

Any protein that is microtubule bound segregates into the pellet fraction and any unbound protein remains within the supernatant fraction. Tubulin protein was identical in E3 and E4 reactions and was only present within the pellet fraction (Appendix A3.4). No tubulin protein was present within the supernatant fraction. At 5μg/ml, significantly greater amounts of apoE E4 were present within the pellet fraction compared to apoE E3 ($p<0.0001$). In the supernatant fraction however, apoE E3 was found to significantly greater compared to apoE E4 ($p<0.01$). Combining protein band levels showed there was no statistically significant difference in protein levels between apoE E3 and E4 reactions (Figure 8.5) (also see appendix A3.5).

8.4.3.2 Microtubule binding of apoE isoforms at a concentration of 20μg/ml

At an apoE concentration of 20μg/ml, significantly greater amounts of apoE E4 were present within the pellet fraction compared to apoE E3 ($p<0.05$). In the supernatant fraction however, apoE3 was found to be significantly greater compared to apoE E4 ($p<0.05$). Combining protein band levels showed there was no statistically significant difference in protein levels between apoE E3 and E4 reactions (Figure 8.6) (also see appendix A3.5).

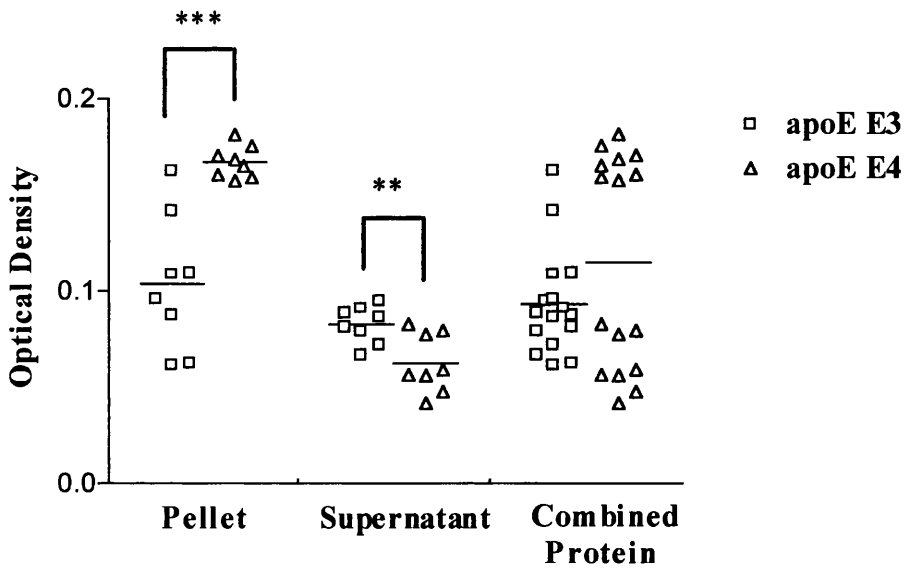

Figure 8.5 Semi-quantification of western blotting bands showing microtubule binding of apoE E3 and E4 at a concentration of 5μg/ml. *****p<0.0001 and **p<0.01**

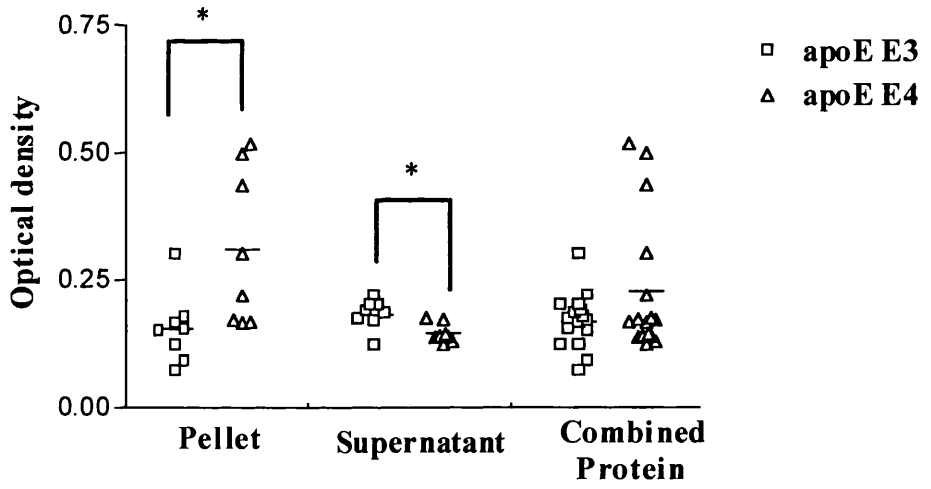

Figure 8.6 Semi-quantification of western blotting bands showing microtubule binding of apoE E3 and E4 at a concentration of 20μg/ml. ***p<0.05**

8.4.4 Fluorescent microtubule assay

8.4.4.1 Characterisation of microtubule structure

Microtubules under normal conditions appear almost 'star-like' in shape where the tubulin, once polymerised, forms an organising centre with processes radiating from the centre point and are all approximately 5-7μm in diameter. Microtubule structure was then assessed following addition of apoE E3 and E4 protein. Microtubules exposed to apoE E3 protein were found to have a regular shape with an identifiable organising centre with many processes radiating from the centre. There was also a tendancy for microtubules exposed to apoE E3 to form aggregates where multiple microtubule structures formed clusters (Figure 8.7 and 8.8). Microtubules exposed to apoE E4 were very irregularly shaped. These microtubules tended to be long and 'spindle' shaped with fewer processes radiating from the organising centre. Microtubules treated with apoE E4 were also less often found in aggregates and on the occasion they did form clusters, these too were irregularly shaped.

8.4.4.2 Microtubule binding of apoE isoforms

The microtubules were examined initially to determine localisation of binding. There were no gross differences in the location to which each isoform bound. ApoE E3 and E4 were both found to bind along the full length of the microtubule processes (Figure 8.9). At both apoE concentrations, it appeared that there was significantly greater apoE immunoreactivity on microtubules incubated with apoE E4 compared to those incubated with apoE E3, although this was most apparent at the 20μg/ml concentration (Figure 8.7 and 8.8).

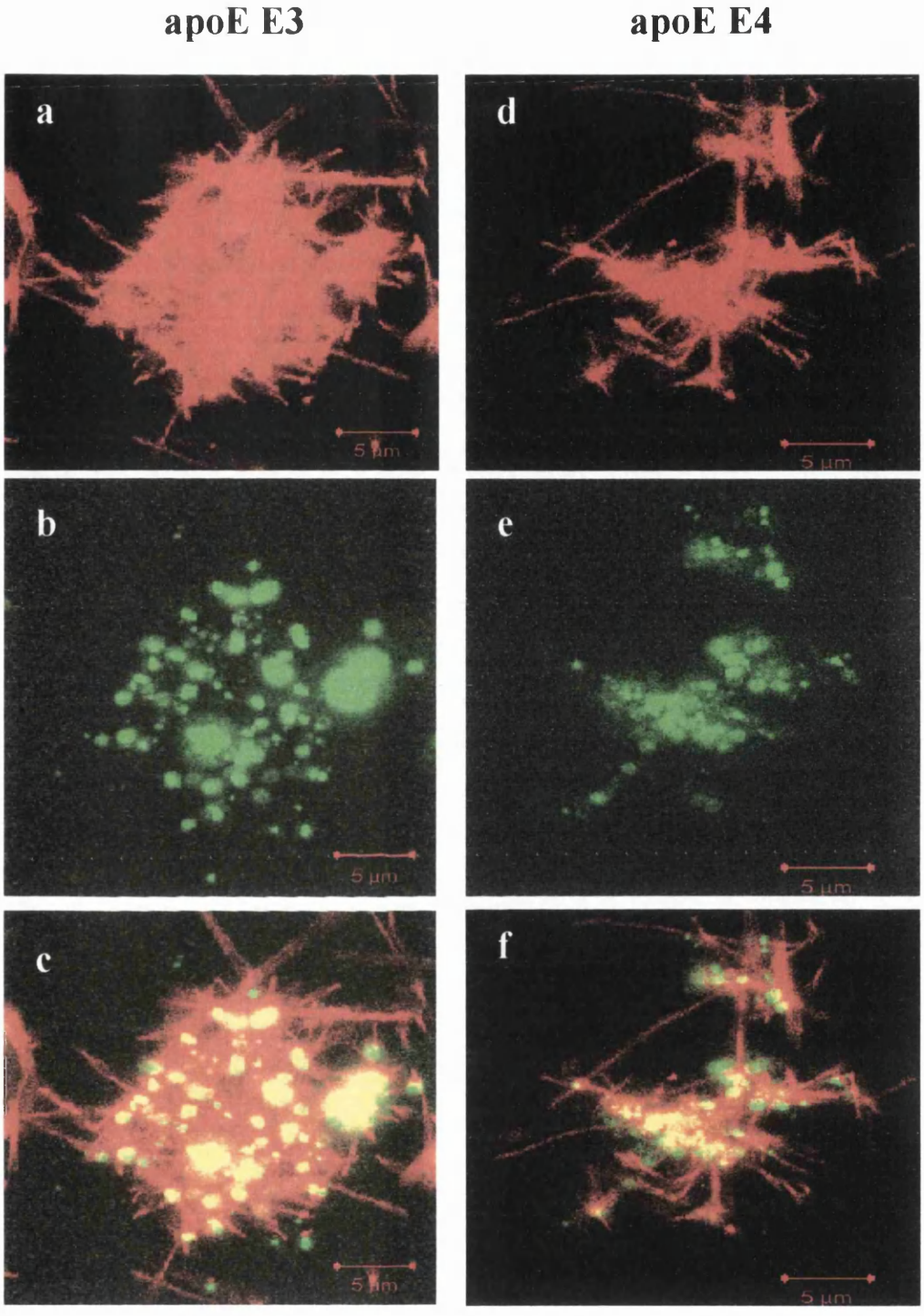

Figure 8.7 **Confocal images of microtubule bound apoE**

ApoE E3 and E4 binding to microtubules at an apoE concentration of 5µg/ml. The illustrations show (a, d) microtubules (red), (b, e) apoE protein (green) and (c, f) a combined image.

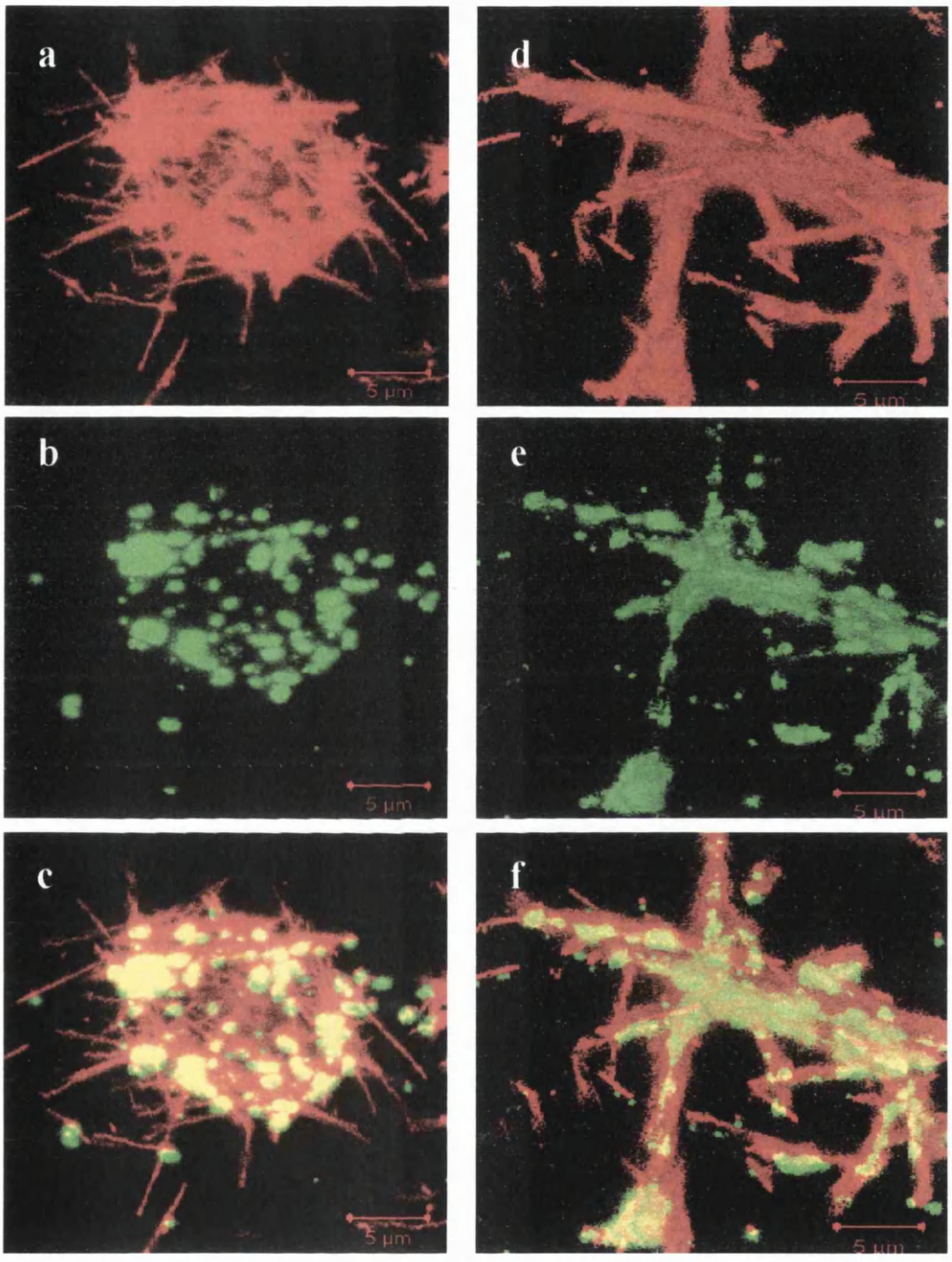

Figure 8.8 ApoE E3 and E4 binding to microtubules at an apoE concentration of 20µg/ml. The illustration show (a, d) microtubules (red), (b, e) apoE protein (green) and (c, f) a combined image.

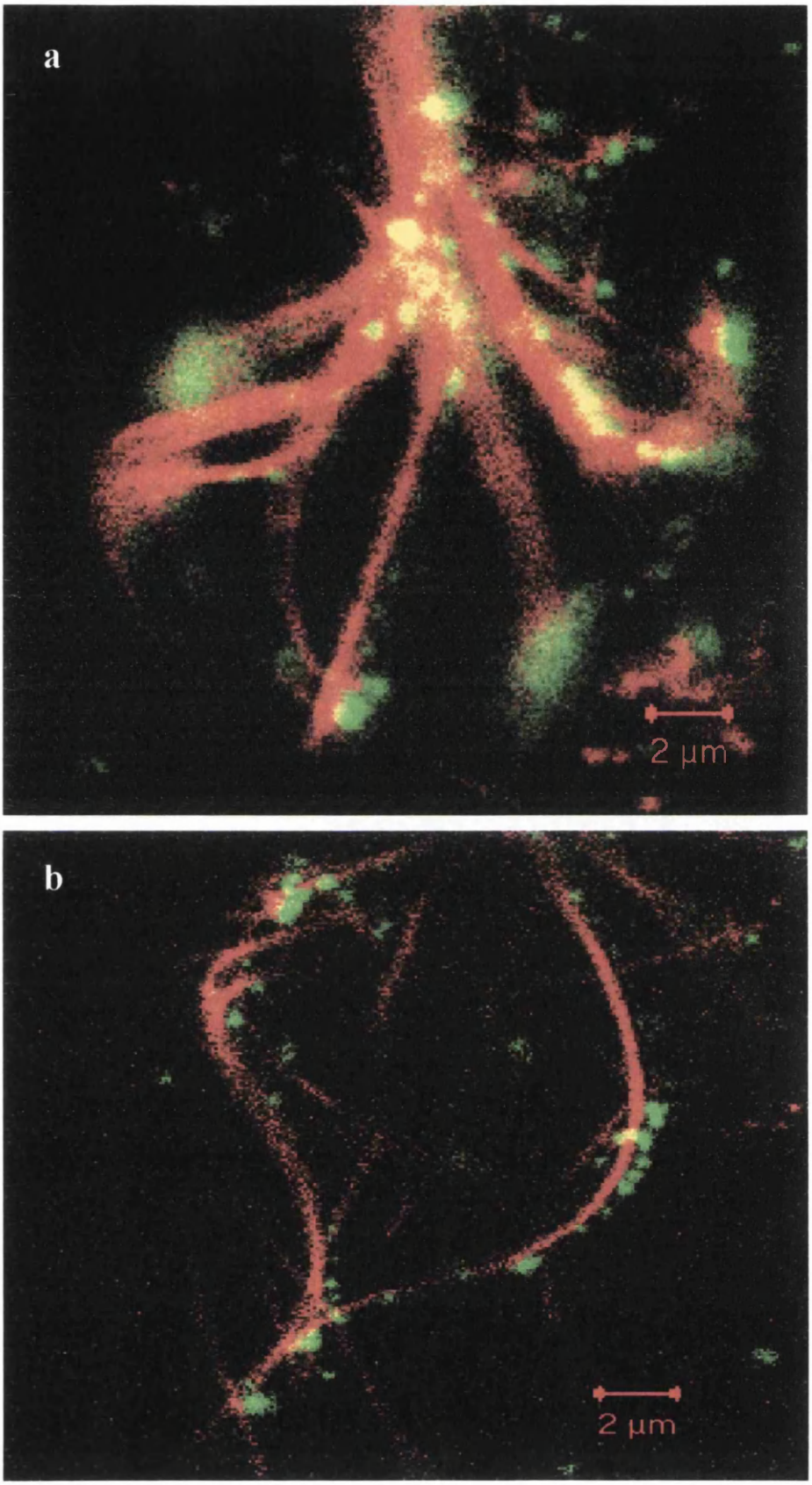

Figure 8.9 High power magnification of microtubule processes with (a) apoE E3 and (b) apoE E4 bound.

8.5 Discussion

Microtubules play a key role in a cell's ability to alter shape and how efficiently they perform this task may depend upon how several other proteins interact. In previous chapters of this thesis, it has been shown that neuronal repair mechanisms are impaired in transgenic mice expressing human *APOE*ε4 alleles. These studies parallel human studies which have shown impaired repair responses after head injury (Teasdale *et al*, 1997) and in AD (Arendt *et al*, 1999) in individuals possessing *APOE*ε4 alleles. One mechanism of how apoE may modulate plasticity is via differential interactions with the neuronal cytoskeleton. In this chapter, microtubule binding of apoE E3 and E4 isoforms was analysed. The present study is the first to study direct apoE interactions with the major microtubule protein, tubulin. It was found that not only did apoE E4 bind to microtubules to a greater extent than apoE E3, but that microtubules incubated with apoE E4 displayed an irregular structure. The data suggests that apoE E4 may have a detrimental effect on microtubule metabolism.

8.5.1 The role of the microtubule in plasticity

Microtubules are important in determining the shape of cells. Microtubules are present in the cytoplasm of cells and can also be found at the poles of mitotic spindles. Microtubules radiate from centrosomes. These centrosomes are the sites of initiation of microtubule growth and are called microtubule organising centres (MTOC). Microtubules have an intrinsic polarity where one end is called the plus end and the other, the minus end. Both ends are capable of assembly and disassembly but the plus end extends more rapidly. The minus end is nearest the MTOC. Microtubules extend under conditions where a cell requires them to polymerise for cell membrane extesnsion (Caroni *et al*, 1997; Alvarez *et al*, 2000) This process occurs most prominently in the growth cone of extending neurites, in an attempt to extend and support the new cell process. The microtubules in the present study are stabilised with taxol and this compound promotes polymerization of tubulin monomers into microtubules.

8.5.2 Abnormalities in dendritic process structure in *APOE*ε4 transgenic mice

ApoE is believed to play a role in modulation of the neuronal cytoskeleton. *APOE* genotype may influence the behaviour of the neuronal cytoskeleton. In Chapter IV, it was shown that there was impaired dendritic reorganisation post-ECL where at day 90, *APOE* ε4 mice (human promoter) displayed a deficit in MAP-2 immunoreactivity compared with *APOE* ε3 mice. In addition, there was also a marked difference in dendritic structure between *APOE* ε3 and ε4 mice. The dendritic networks in *APOE*ε4 mice were highly disorganised and irregular compared to ε3. This structural abnormality may arise as a result of differential interaction of each apoE isoform with certain cytoskeletal proteins. In the transgenic mice expressing human *APOE* alleles under the GFAP promoter (Chapter V), no such isoform effect on dendritic structure was detected. The findings could reflect the fact that apoE is only expressed in astrocytes in these mice. When expressed endogenously in neurons, apoE does not have to overcome the problems of escaping the endocytic pathway to interact with intracellular elements. At present, it is unclear whether apoE which enters a neuron via receptor mediated mechanisms is even capable of escaping endosomes. This could have vital implications as to how apoE interacts with the cytoskeleton, if at all. These isoform specific differences on the cytoskeleton may only arise when apoE is free to interact i.e. when present endogenously within the neurons. Tubulin staining in both transgenic lines suggests there is also a deficit in tubulin immunoreactivity at day 90 post-ECL in *APOE*ε4 mice, where an impairment in the reparative capacity is evident.

8.5.3 *In vitro* evidence for a role of apoE in microtubule metabolism

Using cell culture techniques, the outgrowth promoting effects of apoE have been demonstrated. Initially, it was shown that apoE promoted neurite extension in the presence of an exogenous lipid source (VLDL) in dorsal root ganglia (Handelmann *et al*, 1992). Further studies revealed that this outgrowth promoting effect was *APOE* genotype dependent. ApoE E3/ VLDL complex promoted neurite extension in dorsal root ganglia, whereas apoE E4 did not (Nathan *et al*, 1994). The type of lipoprotein bound to apoE may also be important in the promotion of plasticity. In the CNS, apoE is mainly associated with HDL and this is the most physiologically relevant to employ in studies of this sort. Neuro-2A cells incubated with apoE E3/HDL complex

display extensive outgrowth, but when incubated with apoE E4 outgrowth is attenuated (Bellosta *et al*, 1995). This effect is also evident when neuro-2A cells are grown on a monolayer of astrocytes secreting either apoE E3 or E4 (Fagan *et al*, 1996). These differential effects on outgrowth may be due to the way in which the cytoskeleton behaves in response to apoE E3 and E4.

Analysis of cytoskeletal structure in cells incubated with apoE E3 and E4 has shown that cells treated with apoE E4 display depolymerisation of microtubules (Nathan *et al*, 1995). Another study showed that apoE E3 and E4 accelerated microtubule assembly equally, however that study did not allow analysis of microtubule structure (Scott *et al*, 1996). In the present study, it was found that microtubules incubated with apoE E3 are regularly shaped, with many processes radiating from the organising centre. In contrast, microtubules incubated with apoE E4 are highly irregular. They appear extremely spindle-like in morphology with a reduced number of processes radiating from the organising centre. Those incubated with apoE E3 also tended to form networks and regularly existed as clusters. This was not true of those incubated with apoE E4 and when these did form networks they were highly irregular in shape. Although the apoE protein was added to the microtubules after the majority of assembly had taken place, they are bathed in taxol buffer, which means the microtubules continue to polymerise because there is always some monomeric tubulin available. Therefore when the apoE was added, it became involved in the assembly process. This allowed insights into apoE isoform effect on microtubule structure. In future experiments of this type, it would be interesting to have the apoE isoforms present from the beginning of the polymerisation process. In general, it would seem that the apoE E4 isoform has a detrimental effect on microtubule structure.

8.5.4 ApoE isoforms and binding to cytoskeletal proteins

One mechanism of how apoE may modulate microtubule structure, is by the manner in which it binds to microtubules and microtubule-associated proteins. The binding of apoE isoforms to microtubule-associated proteins has previously been investigated (Huang *et al*, 1996). ApoE E3 has been shown to bind with high-avidity to the microtubule-associated protein tau. ApoE E4 does not bind as avidly. The fact that apoE E3 binds efficiently means it can protect microtubule structure from

hyperphosphorylation. Hyperphosphorylation of tau results in the protein binding to itself, which causes the formation of neurofibrillary tangles. Higher avidity binding of apoE E3 has also been shown in association with the MAP-2c protein. In this chapter the binding of apoE to the major microtubule protein, tubulin was studied. Using non-denaturing polyacrylamide gel electrophoresis, it was found that at both apoE concentrations, apoE E4 protein was present predominantly within the pellet fraction (microtubule bound) whereas greater levels of apoE E3 were present within the supernatant fraction (unbound). This suggested that more apoE E4 was bound to microtubules than apoE E3. Images of microtubules with apoE bound, analysed by confocal microscopy revealed similar results, where it appeared that greater apoE immunoreactivity was present on the microtubules treated with apoE E4 than those treated with apoE E3. This type of study would further benefit from a time course study to analyse interaction and dissociation with time. In this study, apoE E4 protein was found to bind microtubules to a greater extent than apoE E3 protein. A previous study looking at binding of apoE isoforms to various cytoskeletal proteins found that there was no difference in the binding avidity of apoE E3 and apoE E4 at an apoE concentration of 5μg/ml (Fleming *et al*, 1996). This study did not examine apoE at higher concentrations and it also failed to combine the apoE with a lipoprotein source. In the present study the apoE was isolated from plasma but it was associated with the endogenous HDL lipoprotein. This makes this assay more physiologically relevant as apoE is always lipoprotein bound within the CNS. The presence of lipoprotein may have vital implications to the way in which an apolipoprotein interacts with cytoskeletal components.

8.5.5 Technical considerations and concluding remarks

This study was the first step to understand the interactions of apoE with microtubules. Ideally, this experiment would have benefited from using apoE/HDL isolated from CSF. However, at the time of these studies it was impossible to concentrate apoE-HDL from CSF. Furthermore a large volume of CSF would be required and this was not available. The use of apoE from plasma provided the best physiologically relevant information. This study also benefited from the fact that apoE is combined with the endogenous lipoprotein source. In the CNS, apoE is bound to HDL and although

slightly different between the CNS and plasma, it again was more physiologically relevant than using recombinant apoE and a false lipoprotein source.

The concentrations of apoE were chosen on the basis that apoE in the CNS exists at a concentration of approximately 5μg/ml. A higher concentration was also chosen on the basis that apoE is increased after injury and it was important to establish the effect of elevated apoE on microtubule interactions. In these studies it was found that greater levels of apoE E4 were bound to microtubules. This result was surprising in view of other studies that indicate apoE E3 binds with greater avidity to MAP and tau. The explanation as to why apoE E4 should bind tubulin to a greater extent is unclear. However, it may be that apoE E4 binds more strongly and once associated with microtubules is not easily dissociated whereas apoE E3 binds, transports and dissociates readily and would be available for further interaction. If for instance, the apoE E4 cannot become dissociated, it is not free for subsequent interactions. This has not yet been studied and further investigation may be required to confirm this. This study also highlighted that microtubule structure was highly irregular when incubated with apoE E4 and may explain the dendritic abnormalities observed in the *in vivo* studies.

Chapter IX General Discussion

	Is there a genotype effect?						
		Synaptic Density	**Fibre Density**	**ApoE Expression**	**ApoJ Expression**	**Cytoskeletal Changes**	**LRP Receptor expression**
Chapter IV	**Transgenic Mice (Human Promoter)**	Yes	Yes	No	Yes	Yes	No
Chapter V	**Transgenic Mice (GFAP Promoter)**	Yes n.s*	Yes	Yes n.s*	No	No	No
Chapter VI	**Ageing (GFAP Promoter)**	No	Yes n.s* (IML width)	Yes	No	No	No
Chapter VII	**Hippocampal Slice (GFAP promoter)**	Yes	Yes	Yes	No	-	-
Chapter VIII	**Microtubule Binding**	-	-	-	-	Yes	-

n.s* - not statistically significant
yes - there was a genotype influence on that component
no - there was no genotype influence on that component

Table 9 Table summarising the results of the entire thesis (minus chapter III characterisation), indicating which components were influenced by *APOE* genotype

9.1 Evidence for a role of apoE in regeneration

Studies in the PNS and in populations of neurons in culture have shown that apoE is involved in regeneration. ApoE is upregulated in transected peripheral nerves and this increase has been shown to coincide with regeneration (Ignatius *et al*, 1987). Similarly apoE promotes neurite outgrowth from Neuro-2A cells incubated with apoE (Pitas *et al*, 1998). A model of entorhinal cortex lesion and an *in vitro* organotypic hippocampal slice culture method was established in this thesis to assess apoE function in compensatory sprouting in the hippocampus post-injury. The brain maintains an incredible capacity to repair itself. This manifests itself as an ability to compensate for loss of function but also the ability to compensate at the cellular level. ApoE is believed to play an important role in this regeneration process by providing lipid and cholesterol material for the reconstruction of cellular elements. Data in this thesis supports this contention with the finding that apoE is upregulated following injury at periods which parallel regeneration and clearance of lipid material from the local environment post-ECL. The actions of apoE on other cellular elements may also contribute to its ability to stimulate sprouting mechanisms and these will be discussed later.

9.2 Overwhelming evidence for an adverse effect of the *APOE*ε4 allele on long-term neuronal plasticity: impaired clinical recovery

Numerous human studies have highlighted an adverse effect of the *APOE*ε4 allele on the brains response to disease and trauma, primarily mediated by its effects on brain plasticity. This includes impaired neuronal remodelling in ε4 individuals suffering from AD, attenuated recovery from stroke, cardiopulmonary bypass and intracerebral haemorrhage and adverse effects on the progression and severity of neurodegenerative disorders such as Multiple Sclerosis, Parkinsons disease and Motor Neuron disease. This is only to mention a few instances with which the *APOE*ε4 allele is adversely associated. The ε4 allele has also been shown to associated with a poor outcome following traumatic brain injury. The most compelling evidence supporting this hypothesis, was the recent finding by Teasdale *et al* (2000) showing a poorer long-term outcome following head injury in *APOE*ε4 individuals, compared to non-ε4 individuals. This is particularly significant considering the subjects were under the age of 15 years. This reinforces the fact that the adverse effect is not due primarily to age-related mechanisms

(i.e. increased amyloid deposition), but a mechanism mediating brain plasticity. In addition, animal studies have confirmed there is a genotype effect not only in acute brain injury but that there is also a pronounced effect on the brains long-term response to injury (Buttini *et al*, 2000; White *et al*, 2001). Studies in this thesis have shown for the first time that *APOE* genotype modulates the long-term recovery of the brain following injury and have provided strong evidence for an adverse effect of the *APOE*ε4 allele in brain plasticity. This thesis has also attempted to establish some of the mechanisms that underlie the genotype specific effects on brain plasticity after injury, some of which are discussed in the following sections.

9.3 Influence of the localisation of apoE within the brain on recovery after injury

9.3.1 Neuronal apoE expression versus glial apoE expression

Human neurons and glia express apoE endogenously. This thesis has shown that the compartmentalisation of apoE within the nervous system could have vital implications for how it modulates neuronal plasticity. The transgenics studied in Chapter IV, express apoE within neurons and glia, due to expression being regulated by the endogenous human promoter sequence. Transgenic mice such as these, are believed to have a pattern of apoE expression similar to that in the human brain. The transgenic mice employed in Chapter V express apoE within astrocytes only, because expression is regulated by a GFAP promoter sequence. In both studies, the *APOE*ε4 mice exhibited a poor recovery from the injury, when compared with *APOE*ε3 and knockout mice. However, comparing the degree of recovery within the two different transgenic lines it is evident that, in general, the line that expresses neuronal apoE display a greater capacity for regeneration, by day 90 post-ECL. Synaptophysin and GAP-43 immunoreactivity recovers close to, or above baseline levels in this line and although transgenics expressing glial apoE display some ability to recover from the injury, there remains a significant deficit in synaptophysin and GAP-43 levels at day 90 post-ECL. This difference between the different lines may indicate the importance of endogenous

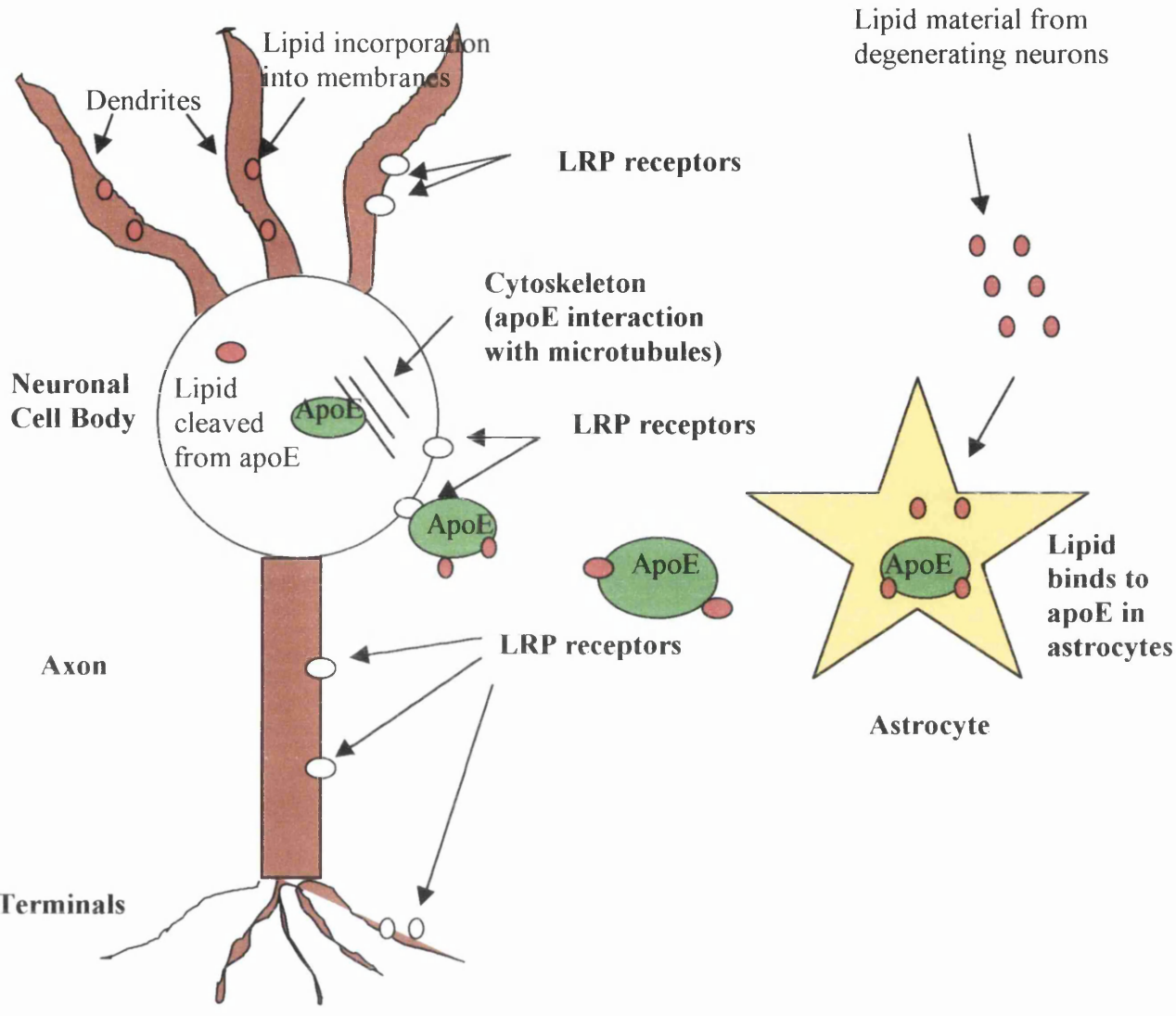

Figure 9.1 Diagram illustrating apoE trafficking. Neuronally expressing transgenics express apoE endogenously in neurons and therefore it is immediately available for the response to injury/ stress. These transgenic mice also express astrocytic apoE and this is readily available to scavenge lipid from the environment. In contrast, 'GFAP' mice only benefit from astrocytic expression. The processes of lipid clearance may remain intact but the lack of endogenous neuronal expression could have profound effects on the response to injury and the interaction with the cytoskeleton.

neuronal expression to repair in response to injury. It could also reflect a delayed response in the mice expressing astrocytic apoE. ApoE (and its lipid components) is transported from distant sites i.e. astrocytes to neuropil/neurons in response to injury and thus the effectiveness of apoE to promote neuronal repair is slower than in endogenously neuronal expressing transgenic mice (see Figure 9.1). The function of apoE may be seen as twofold. These are (1) scavenging of lipid from the environment and (2) intracellular effects. Astrocytic apoE has been shown to be involved in the lipid scavenging process. In this respect it is likely that the two types of transgenic mouse do not differ significantly as they both express apoE astrocytically and it is shown in this thesis that lipid degeneration products are cleared efficiently post-injury in both mouse lines.

In the human transgenics, neurons also endogenously express apoE and it is therefore readily available for emergency use intracellularly after injury (to interact with cellular elements), something which is not possible for the GFAP transgenics or indeed wild-type mice. In addition, neurons are capable of synthesising cholesterol and phospholipid and therefore all the tools required for membrane biosynthesis are immediately available without having to be transported from great distances away and then being endocytosed. There is also evidence to suggest that endocytosed apoE may not be capable of interacting with the cytoskeleton because it does not escape from the endocytic trafficking pathway (DeMattos *et al*, 2000). This could also have important implications for recovery in GFAP transgenic mice. In this study, it is also evident that localisation of expression of apoE, influences the pattern of apoE and apoJ expression post-ECL. In wild-type C57BL/6J and GFAP transgenic mice, there is increased expression at day 7 post-ECL, but also at day 90 there is increased expression within the OML. This late expression is absent from the response in the human transgenic mice. This could reflect a last 'ditch' attempt by the 'GFAP' expressors to compensate for the deficit in synapse and fibre density with a late surge of astrocytic apoE release. This is consistent with the demonstration that upregulation of apoE occurs in a region of the molecular layer, which has sustained the most severe damage.

The location of apoE in the brain appears also to be crucial in its response to the ageing process. In previous studies it has been shown that when expressed neuronally, apoE4 has an adverse effect on neurodegeneration in the ageing CNS (Buttini *et al*, 1999;

Tesseur *et al*, 1999) and when expressed astrocytically it is not detrimental. This is in agreement with the ageing study in this thesis, which did not observe any genotype effects on ageing in 'GFAP' transgenic mice. The response in the brain to injury and ageing appears to be almost the complete opposite in terms of outcome, where neuronal apoE expression may be more beneficial in recovery from brain injury, and astrocytic apoE more beneficial in ageing. This also highlights that how apoE functions in ageing and after injury may be two completely different mechanisms.

9.4 Mechanisms of Isoform Effect on Plasticity

There are several mechanisms by which apoE isoforms may differentially influence plasticity and these will be discussed in the following sections.

9.4.1 Isoform-specific differences in receptor interactions

Although no fundamental differences in LRP receptor expression between the genotypes could be detected in this thesis, this obviously does not account for functional differences in the way each isoform interacts with the receptor. In the brain, the LRP receptor is expressed on neurons and astrocytes, where it is located on cell bodies and also on processes (Stockinger *et al*, 1998). The presence of LRP on processes is especially important in the models employed in this thesis. This is because apoE is upregulated in regions where there are no neuronal cell bodies, only dendritic processes, where its lipid uptake mediating effects are most required for repair. Several studies have indicated that apoE E3 promotes neurite extension in cultured cells but apoE E4 does not, an effect that is mediated by the LRP receptor (Holtzman et al, 1995; Poirier *et al*, 1995; Bellosta *et al,* 1995; Pitas *et al*, 1997). The outgrowth promoting effects of apoE E3, may be abolished by blocking the receptor (Holtzman *et al*, 1995; Fagan *et al*, 1996). The single amino acid change in the protein, which results in the E4 isoform, is in the receptor-binding domain (Mahley *et al*, 1988; Rebeck *et al*, 1993). However, binding studies have revealed that E3 and E4 do not differ greatly in their affinity for the LRP receptor (Weisgraber *et al*, 1982), whereas E2 shows a reduced capacity for binding (Beffert *et al*, 1998). However, it is not the receptor itself that is responsible for a genotype effect but an associated protein. Heparin sulphate proteoglycan (HSPG) is closely associated with the receptor and functions in the initial capture of lipid from the environment (Mahley and Ji, 1999). Treatment of cells with heparinase abolishes uptake of apoE and attenuates the outgrowth promoting effects of apoE E3 (Bellosta *et al*, 1995; Ji *et al*, 1998). HSPG sequesters apoE-enriched lipoprotein particles before being endocytosed via the LRP receptor (Mahley *et al*, 1994). Incubation of Neuro-2A cells with apoE E3 and E4-VLDL resulted in a similar increase in the cholesterol content of the cells, suggesting a similar ability to internalise lipoprotein particles (Nathan *et al*, 1995). In contrast, cells were found to contain a greater accumulation of apoE E3 than

E4. The authors suggested that this may be due to an isoform difference in accumulation or retention but the effect is primarily mediated by the HSPG (Ji *et al*, 1998). This differential effect at the receptor surface may also have implications on how the apoE is trafficked throughout the rest of the cell.

9.4.2 Endocytosis and intracellular trafficking

The differential accumulation and retention of apoE3 and E4 in cells may be due to a variation in storage once inside the cell. One hypothesis is, that apoE3 is directed to an intracellular pool (Ji *et al*, 1998). It is also believed that once endocytosed, apoE4 is unable to escape the endosomal packaging and is rapidly trafficked through the cell without interacting with intracellular elements (i.e. membrane) and may even be rapidly resecreted (Rensen *et al*, 2000). Experiments by Lovestone *et a*l (1996), have shown that apoE3 is retained throughout cells and is present within the cytoplasm however, apoE4 was present within vesicles, presumably of the endocytic class. A study by Demattos *et al* (1999) showed that when apoE was bound to a nuclear localisation signal (NLS), apoE was able to enter the nucleus when it reached the cytosol. In contrast, when an exogenous apoE source (+NLS) was endocytosed into cells, it failed to escape the endocytic pathway. In addition, direct expression of apoE within the cytosol was found to be extremely toxic to the cell however this effect was possibly due to free apoE.

Proteins such as Rab-4, Rab-5A and rabaptin have recently been identified as proteins involved in endocytosis (Neve *et al*, 1998). Rab-4 is a marker of endosome recycling, whereas Rab-5A and rabaptin are proteins, which function in membrane fusion in the endocytosis process. Studies using Rab-5a in particular, have shown that apoE is endocytosed but that there may be an isoform difference in the way the isoforms are trafficked following this. After 1 hour of uptake, it was found that apoE3 no longer co-localised with vesicle-associated proteins, whereas apoE4 was found to be 87% co-localised. This was even apparent using a marker of late-endosomes (Cathepsin D) (DeKroon *et al*, 2001). It is also important to note that Cathepsin D also has secretase activity, which could have implications for amyloid deposition in AD. Endocytic pathway abnormalities have been found to be associated with sporadic AD. In one study, it was found that endocytic pathway abnormalities occur, before amyloid deposition is apparent, and the authors suggest that this is the earliest upstream event in the

pathogenesis of AD (Cataldo *et al*, 2001). Specifically, early endosomes have been found to be enlarged in the brains of AD patients (Cataldo *et al*, 1997). Further to this, studies in fetuses and children with Down's syndrome, have shown that these endosomal abnormalities are even evident at this early stage, long before any other pathological hallmarks of AD have been identified. The *APOE*ε4 allele was found to promote early enlargement of endosomes, when compared with individuals not possessing an *APOE*ε4 genotype. Endosomes appeared as normal when tissue from familial AD cases as a result presenilin mutations.

9.4.3 Evidence for an *APOE* genotype influence on cytoskeletal interactions

Once inside the cell, the lipid from the complex may be cleaved and reutilised in a number of ways. Little is known however, of what becomes of apoE. ApoE may remain within the endocytic system and pass straight through the cell. One hypothesis is that apoE is able to interact with cytoskeletal proteins inside the cell and it is via this mechanism that apoE functions in neuronal process extension. Microtubules have been shown to function in several important processes within neurons, including neurite extension and retraction (Mitchison *et al*, 1988). Analysis of the ability of apoE E3 and E4 to promote neurite extension was assessed in Neuro-2A cells and it was found that cells incubated with apoE E3, produced long neurites but those incubated with apoE E4 did not. The authors hypothesised that this may be due in part, to microtubule status within the cells. It was found that, in the apoE E4 treated cells, microtubules were poorly formed and there was a greater amount of monomeric tubulin as opposed to polymeric tubulin, compared with that of apoE E3 treated cells (Nathan *et al*, 1995). Further analysis revealed that apoE E3 bound to the cellular microtubules with a greater affinity than apoE E4. In similar studies, it has been shown that apoE E3 binds more readily to the microtubule associated proteins tau and MAP-2 (Strittmatter *et al*, 1994; Huang *et al*, 1994). Conflicting evidence comes from Scott *et al*, (1998), who have shown that microtubule polymerisation is equally stimulated in the presence of apoE E3 and E4. The interaction of apoE with the cytoskeleton may not only be crucial for neurite extension but also stabilization. It is suggested that apoE may bind to the microtubule-binding domain of tau and MAP-2c and protect their structure from hyperphosphorylation (Roses *et al*, 1996). The hyperphosphorylation of tau results in the

formation of paired helical filaments (neurofibrillary tangles). Lovestone *et al* (1996) have shown that the cellular distribution of apoE is dependent on the presence of tau, although it was also noted that neither apoE3 nor E4 altered the phosphorylation state, a finding confirmed in a subsequent study (Flaherty *et al*, 1999). In contrast, expression of apoE4 in neurons of transgenic mice results in hyperphosphorylation of tau (Tesseur *et al*, 2000). In this thesis it is suggested that cytoskeletal structure alterations after injury are *APOE* genotype dependent when apoE is expressed in neurons but not when expressed in astrocytes alone (as assessed in MAP-2 immunstained sections). This not only suggests that apoE is capable of modifying cytoskeletal proteins and that it is isoform dependent, but also highlights how the primary localisation of expression may be crucial to this process. This does not exclude the possibility that there may be ultrastructural differences in cytoskeletal structure in GFAP transgenics that could not be detected using the techniques employed. It has been shown that cells incubated with the apoE E4 isoform display a significantly greater degree of microtubule polymerisation (Nathan *et al*, 1995) when compared with apoE E3. ApoE promotes microtubule assembly and the rate of assembly has been found to be similar when incubated with apoE E3 and E4. However, one mechanism of how apoE may modulate the behaviour of cytoskeletal proteins is by differential binding to various cytoskeletal proteins. The binding of apoE isoforms to cytoskeletal proteins has previously been examined. These studies have found that, in general, the apoE E3 isoform binds with higher avidity to MAPs and tau when compared with apoE E4 (Huang *et al*, 1994; Flaherty *et al*, 1999). In Chapter VIII it was shown that apoE E4 protein was more greatly associated with microtubules than apoE E3. This finding differs from a previous study that found apoE E3 and E4 bound tubulin equally well (Fleming *et al*, 1996). However the apoE used in that study lacked an endogenous lipid source. In the present study, apoE was bound to HDL, which is more physiologically relevant considering apoE is always HDL bound in the CNS. The presence and type of lipoprotein to which the apolipoprotein is bound may have severe implications for the way in which the apolipoprotein interacts with the cytoskeleton and other proteins. This has been shown previously where the lipidation state of apoE affects the avidity with which it binds amyloid. In chapter VIII it was also shown that microtubules incubated with apoE E4 displayed an irregular structure. Processes were long and spindle-like and the number of processes radiating from the organising centre was reduced compared with microtubules incubated with apoE E3.

This suggests that apoE E4 has a detrimental effect on microtubule structure *in vitro*, and supports the finding of disarrayed dendritic processes *in vivo*.

9.4.4 Intracellular signalling pathways – from receptor to cytoskeleton

From the most recent data, it has become apparent that apoE binding to the LRP receptor may modulate plasticity via a cascade of intracellular signalling events (Herz *et al*, 2001). On binding to the NPxY cytoplasmic domain of the LRP receptor (Trommsdorf *et al*, 1998), FE65 and DAB1 (scaffold proteins) cause the assembly of a protein called Mena. Mena is a member of a family called Ena-Vasp proteins, which are enabled-vasodilator stimulated phosphoproteins. These proteins interact directly with the actin cytoskeleton but may also interact with other components such as tubulin and microtubule associated proteins. This process is thought to occur in the generation of neuritic processes. It has not been established as of yet however, whether there is an apoE isoform effect on the ability to stimulate this process. If for instance, apoE4 interacts differently at the receptor surface, this could result in differing intracellular signalling events. As can be seen from the diagram (Figure 9.2), the binding of apoE also influences the processing of APP through this pathway although the significance of this is unclear. However, FE65 binding to cytoplasmic tails does result in attenuation of the endocytosis signal, thus leaving APP extracellularly for α-secretase cleavage (Herz *et al*, 2000). Another pathway that has been implicated in reorganisation of the cytoskeleton is that mediated by the ApoER2 receptor. Via the reelin signalling pathway and other members of the scaffold family of proteins, apoE may cause cytoskeletal reorganisation, primarily through modifications of tau by MAP kinases. This has been shown to cause hyperphosphorylation of tau which leads to the production of neurofibrillary tangles in AD (Herz, 2001). Little is known at present of the precise function of apoER2 in the brain.

The LRP receptor has multiple ligands (up to 30 known) and each of these effect different actions intracellularly. One of these, α2 macroglobulin, binds to neuronal LRP receptors and induces calcium ion influx via NMDA receptors. The link between the LRP and NMDA receptor occurs via another scaffold protein, PSD-95. Entry of calcium due to LRP mediated activation of NMDA receptor channels may alter downstream signalling events and may modulate local synaptic plasticity alterations (Herz and

Strickland, 2001). Of interest in this thesis is also the finding that the LRP receptor binds an array of viruses and toxins. On binding, viruses may be internalised via the LRP receptor and thus this may be how HSV enters cells in the hippocampal slices in this thesis.

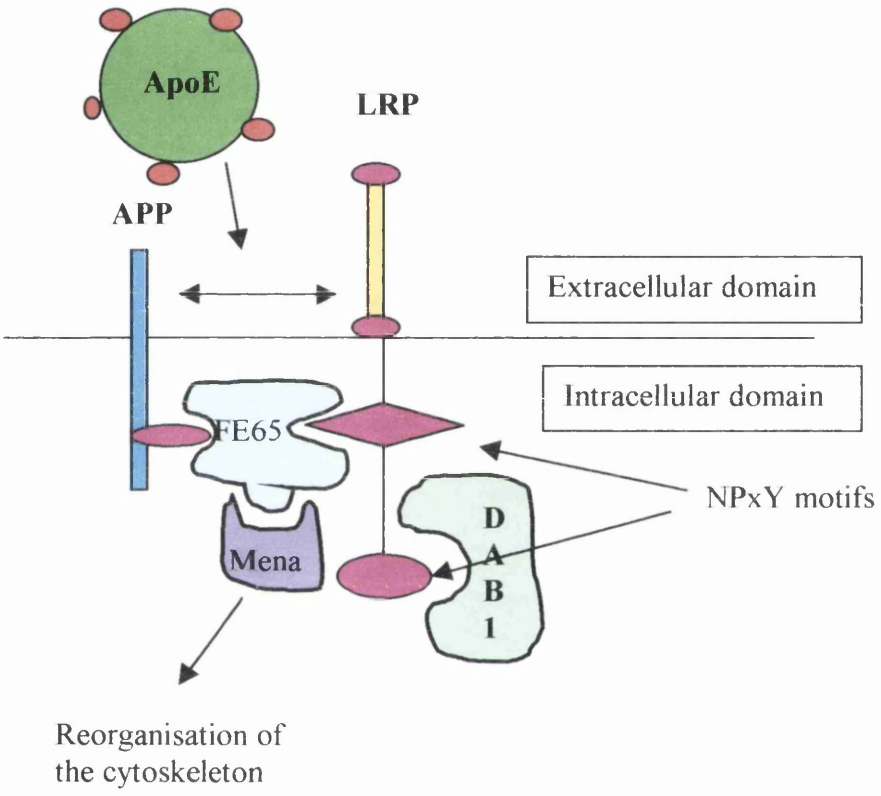

Figure 9.2 Intracellular signalling. The diagram illustrates the interactions of receptor neuronal adaptor proteins and cytoplasmic structural proteins. When apoE binds to the LRP receptor a cascade of intracellular events occur. The binding of DAB1 and FE65 molecules to the cytoplasmic tail of the receptor (NPxY) promotes the assembly of Mena and other proteins in the Ena-Vasp family. This in turn may act on the reorganization of the cytoskeleton (Derived from Herz *et al*, 2000).

9.4.5 *APOE* genotype, estrogen and sprouting

Estrogen has long since been known to be a strong influence on brain plasticity. Studies by Woolley and McEwan have shown that synaptic density increases in certain brain regions of the rat at stages of the estrus cycle when estrogen is most elevated. It was first discovered by Stone *et al* (1997), that in stages of the eostrus cycle, when estrogen was high, the brains of female rats expressed significantly greater levels of apoE mRNA within astrocytes and microglia. This was the first indication that estrogen may be neuroprotective, an effect that was mediated by increased apoE expression, due to actions via the α estrogen receptor pathway (Srivastiva *et al*, 1997). At present these pathways remain largely ambiguous. Estrogen has been shown to enhance compensatory sprouting, in response to entorhinal cortex lesion (Geddes *et al*, 1985) and that apoE is increased in the response (Stone *et al*, 2000). Using animal models, it has been confirmed that estrogen replacement in wild-type mice following ovariectomy, restores the sprouting response. In addition, estrogen replacement does not promote sprouting in *APOE* knockout mice (Stone *et al*, 1998; Teter *et al*, 1999). It remains undetermined if *APOE* isoforms can differentially modulate sprouting via estrogen mediated mechanisms and this is currently under investigation in our laboratory although there is some data from human studies suggesting that *APOE* genotype may influence this to a certain extent. It is suggested that estrogen is protective against AD and this is supported by statistics showing that AD is more prevalent in the human male population. Several papers have been published outlining the beneficial effects of hormone replacement therapy in human females in reducing the risk of developing AD (Tang *et al*, 1996; Yaffe *et al*, 1998; Slooter *et al*, 1999) and that the efficacy of these drugs may be genotype dependent. Cognitive decline is reduced in non-ε4 females with estrogen therapy but is not reduced in ε4 females.

9.5 Concluding remarks

This thesis has sought to establish an *in vivo* and *in vitro* animal model to assess brain plasticity and, using these models, the influence of *APOE* genotype on long-term plasticity changes following injury has been elucidated. It is evident, not only from the data contained in this thesis, but also a wide range of sources that the ε4 allele of the *APOE* gene is generally deleterious to brain plasticity. This does not only have implications for AD and head injury but also a great number of human diseases, with which *APOE* genotype influence has been linked. This thesis has also attempted to assess at least some of the mechanisms by which *APOE* isoforms may mediate their differential effects on plasticity. These mechanisms and others are represented schematically (Figure 9.3). This thesis is by no means a complete work but it has provided a basis for the direction of future studies. Now the important role of apoE in plasticity has been established it is important to investigate all pathways with which it may mediate its effects. This includes further analysis of cytoskeletal interactions (via various mechanisms) and elucidation of the role of estrogen in plasticity. Regardless of the mechanism by which the *APOE*ε4 allele imposes its deleterious effects, it is hoped in the future that an efficient therapy may be developed. Presently, the greatest hope for an apoE therapy in the treatment of CNS disease and injury lies with gene therapy. A study in this thesis has begun to evaluate the merits of gene therapy and it is hoped this work will be further developed in the future.

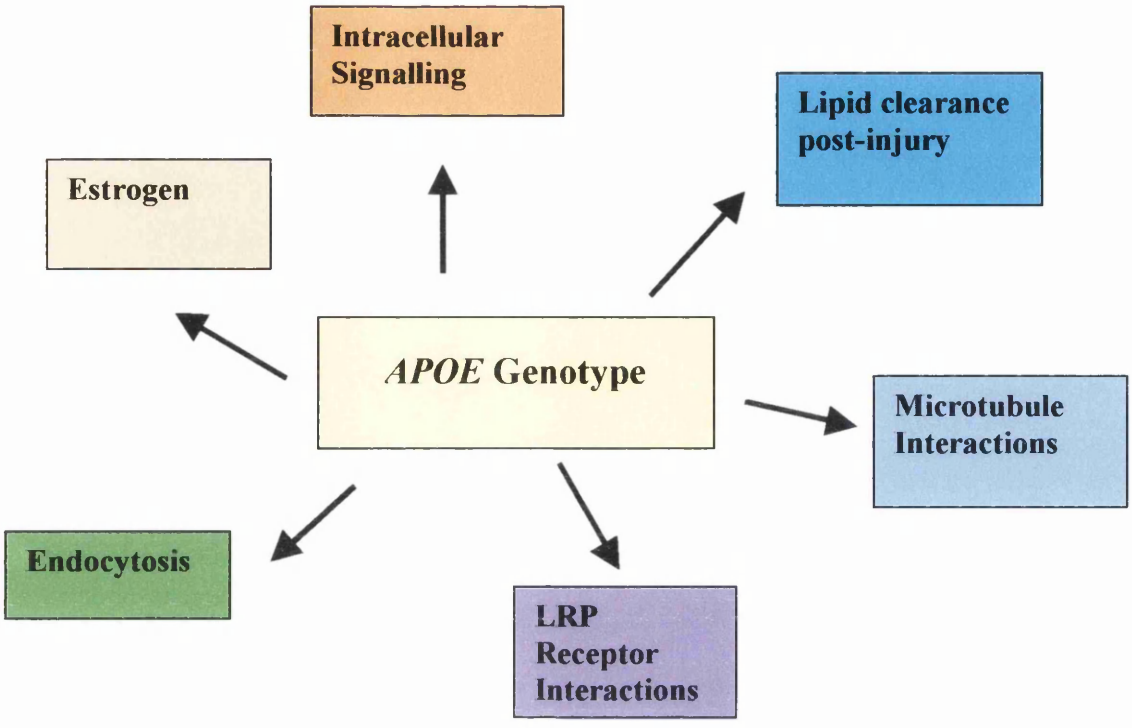

Figure 9.3 Schematic diagram illustrating pathways by which *APOE* genotype may influence the brains response to injury and disease.

References

Alberts MJ, Graffagnino C, McClenny C, DeLong D, Strittmatter W, Saunders AM and Roses AD. (1995) *APOE* genotype and survival from intracerebral haemorrhage. Lancet 346; p575.

Aleshkov S, Abraham CR and Zannis VI. (1997) Interaction of nascent apoE2, apoE3 and apoE4 isoforms expressed in mammalian cells with amyloid peptide β (1-40). Relevance to Alzheimer's disease. Biochemistry 36; p10571-80.

Ali SM, Dunn E, Oostveen JA, Hall ED and Carter DB (1996) Induction of apolipoprotein E mRNA in the hippocampus of the gerbil after transient global ischaemia. Molecular Brain Research 38: p37-44

Alonzo NC, Hyman BT, Rebeck GW and Greenberg SM. (1998) Progression of cerebral amyloid angiopathy – accumulation of amyloid-beta 40 in affected vessels. Journal of Neuropathology and Experimental Neurology 57; p353-359.

Alvarez J, Giuditta A, Koenig JA, Hall ED and Carter DB. (2000) Protein synthesis in axons and terminals: significance for maintenance, plasticity and regulation of phenotype with a critique of slow transport theory. Progress in Neurobiology 62; 1-62.

Anderson R, Barnes JC, Bliss TVP, Cain DP, Cambon K, Davies HA, Errington ML, Fellows LA, Gray RA, Hoh T, Stewart M, Large CH and Higgins GA. (1998) Behavioural, physiological and morphological analysis of a line of apolipoprotein E knockout mouse. Neuroscience 85; p93-110.

Arendt T, Marcova L and Bigl V (1991) Maintenance of neuronal plasticity in the reticular core and changes in the trophic activity in Alzheimer's disease. Annals of the New York Academy of Sciences 640; p210-214.

Arendt T, Schindler C, Bruckner MK, Eschrich K, Bigl V, Zedlick D and Marcova L. (1997) Plastic neuronal remodelling is impaired in patients with Alzheimer's disease carrying apolipoprotein ε4 allele. Journal of Neuroscience 17;p516-529

Arriagada PV, Growdon JH, Hedley-Whyte ET and Hyman BT (1992) Neurofibrillary tangles but not senile plaques parallel duration and severity of Alzheimer's disease. Neurology 42; p631-639

Arriagada PV, Marzloff K and Hyman BT. (1992) Distribution of Alzheimer-type pathologic changes in nondemented elderly individuals matches the pattern in Alzheimer's disease. Neurology 42; 1681-1688.

Aubert I, Poirier J, Gauthier S and Quirion R (1994) Multiple cholinergic markers are unexpectedly not altered in the rat dentate gyrus following entorhinal cortex lesions. Journal of Neuroscience 14; p2476-84.

Bales KR, Du Y, Holtzman DM, Cordell B, and Paul SM. (2000) Neuroinflammation and Alzheimer's disease: critical roles for cytokine/ Aβ-induced glial activation, NF-kB, and apolipoprotein E. Neurobiology of Ageing 21: p427-32

Barr and Keirnan (1993) The Human Nervous System: An Anatomical Viewpoint. Sixth Edition; JB Lippincott Company

Bart RD, Sheng H, Laskowitz DT, Pearlstein RD, and Warner DS. (1998) Regional CBF in apolipoprotein E-deficient and wild-type mice during focal cerebral ischaemia. Neuroreport 9: p2615-20

Baumann MH, Kallijarvi J, Lankinen H, Soto O and Haltia M. (2000) Apolipoprotein E includes a binding site which is recognised by several amyloidogenic peptides. Biochemical Journal 34: p977-84.

Bedlack RS, Strittmatter WJ and Morgenlander JC. (2000) Apolipoprotein E and neuromuscular disease: a critical review if the literature. Archives of Neurology 57: p1561-5

Beffert U and Poirier J. (1996) Apolipoprotein E, plaques, tangles and cholinergic dysfunction in Alzheimer's disease. Annal of the New York Academy of Sciences 777: p166-73.

Beffert U, Danik M, Krzywkowski P, Ramassamy C, Berrada F and Poirier J. (1998) The neurobiology of apolipoproteins and their receptors in the CNS and Alzheimer's disease. Brain Research Reviews 27: p119-42.

Beffert U, Cohn JS, Petit-Turcotte C, Tremblay M, Aumont N, Ramassamy C, Davignon J and Poirier J. (1999) Apolipoprotein E and β-amyloid levels in the hippocampus and frontal cortex of Alzheimer's disease subjects are disease-related and apolipoprotein E genotype dependent. Brain Research 84: p387-94

Bellosta S, Nathan BP, Orth M, Dong L, Mahley RW and Pitas RE. (1995) Stable expression and secretion of apolipoproteins E3 and E4 in mouse neuroblastoma cells produces differential effects on neurite outgrowth. Journal Biological Chemistry 27(45): 27063-71.

Bertrand P, Poirier J, Oda T, Finch CE and Pasinetti GM. (1995) Association of apolipoprotein E genotype with brain levels of apolipoprotein E and apolipoprotein J (clusterin) in Alzheimer's disease. Molecular Brain Research 33: p174-8.

Bigler ED, Lowry CM, Anderson CV, Johnson SC Terry J and Steed M. (2000) Dementia, quantitative neuroimaging and apolipoprotein E genotype. American Journal of Neuroradiology 21: p1857-68.

Bogdanovic N, Davidsson P, Volkmann I, Winblad B and Blennow K (2000) Growth-associated protein GAP-43 in the frontal cortex and in the hippocampus in Alzheimer's disease: an immunohistochemical and quantitative study. Journal of Neural Transmission 107(4): p463-478

Bolz J, Novak N, Gotz M and Bonhoeffer T (1990) Formation of target-specific neuronal projections in organotypic slice cultures from rat visual cortex. Nature 346(6282): p359-62

Borchelt DR, Thinakaran G, Eckman CB, Lee MK, Davenport F, Ratovitsky T, Prada CM, Kim G, Seekins S, Yager D. (1996) Familial Alzheimer's disease-linked presenilin 1 variants elevate Ab1-42/1-40 ration in vitro and in vivo. Neuron 17 : p1005-1013.

Boschert U, Merlo-Pich E, Higgins GA, Roses AD and Catsicus S. (1999) Apolipoprotein E expression by neurons surviving excitotoxic stress. Neurobiology of Disease 6: p508-14.

Boyles JK, Pitas RE, Wilson E, Mahley RW and Taylor JM (1985) Apolipoprotein E associated with astrocytic glia of the central nervous system and with non-myelinating glia of the peripheral nervous system. Journal of Clinical Investigation 76: p1501-13.

Boyles JK, Pitas RE, Wilson E, Mahley RW and Taylor JM (1989) A role for apolipoprotein E, apolipoprotein A-I, and low-density lipoprotein receptors in cholesterol transport during regeneration and remyelination of the rat sciatic nerve. Journal of Clinical Investigation 83: p1015-31

Braak H and Braak E (1991) Neuropathological stageing of Alzheimer-related changes. Acta Neuropathologica 82: p239-259

Bronfman F, Tesseur I, Hofker MH, Havekans LM and Van Leuven F (2000) No evidence for cholinergic problems in apolipoprotein E knockout and apolipoprotein E4 transgenic mice. Neuroscience 97(3): p411-7.

Bronge L, Femaeus S, Blomberg V, Ingelson M, Lannfelt L, Isberg B and Wahlund L. (1999) White matter lesions in Alzheimer patients are influenced by apolipoprotein E genotype. Dementia and Geriatric Cognitive Disorders 10: p89-96.

Brown MS and Goldstein JL (1986) A receptor-mediated pathway for cholesterol homeostasis. Science 232: p34-47.

Brown SM, Harland J, MacLean AR, Podlech J and Clement JB (1994) Cell type and cell state determine differential in vitro growth of non-neurovirulent ICP34.5 negative herpes simplex virus. Journal of Genetic Virology 75: p2367-77.

Bu G, Maksymovitch EA, Geuze H and Schwartz AL (1994) Subcellular localisation and endocytic function of low density lipoprotein receptor-related protein in human glioblastoma cells. Journal of Biological Chemistry 269: p29874-82.

Buttini M, Orth M, Bellosta S, Akeefe H, Pitas RE, Wyss-Coray T, Mucke L and Mahley RW (1999) Expression of human apolipoprotein E3 or E4 in the brains of apoE-/- mice: Isoform-specific effects on neurodegeneration. Journal of Neuroscience 19(12): p4867-80.

Buttini M, Akeefe H, Lin C, Mahley RW, Pitas RE, Wyss-Coray T and Mucke L (2000) Dominant negative effects of apolipoprotein E4 revealed in transgenic models of neurodegenerative diseases. Neuroscience 97(2): p207-210.

Calero M, Tokuda T, Rostagno A, Kumar A, Zlokovic BV, Frangione B and Ghiso J (1999) Functional and structural properties of lipid-associated apolipoprotein J (clusterin). Biochemical Journal 344: p375-83.

Cambon K, Davies HA and Stewart MG (2000) Synaptic loss is accompanied by an increase in synaptic area in the dentate gyrus of aged human apolipoprotein E4 transgenic mice. Neuroscience 97(4): 685-92.

Carlin C, Murray L, Graham D, Doyle D and Nicoll J (2000) Involvement of apolipoprotein E in multiple sclerosis: absence of remyelination associated with possession of the *APOE* epsilon 2 allele. Journal of Neuropathology and Experimental Neurology 59(5): p361-7.

Caroni P (1997) Intrinsic neuronal determinants that promote axonal sprouting and elongation. BioEssays 19: 767-74.

Cataldo AM, Hamilton DJ, Barnett JL, Paskevich PA and Nixon RA (1996) Properties of the endosomal-lysosomal system in the human central nervous system: disturbances mark most neurons in populations at risk to degenerate in Alzheimer's disease. Journal of Neuroscience 16: 186-99.

Cataldo AM, Peterhoff CM, Troncoso JC, Gomez-Isla T, Hyman BT and Nixon RA (2000) Endocytic pathway abnormalities precede amyloid β deposition in sporadic Alzheimer's disease and Down's syndrome. American Journal of Pathology 157: p277-86.

Chapman S, Sabo T, Roses AD and Michaelson DM (2000) Reversal of presynaptic deficits of apolipoprotein E-deficient mice in human apolipoprotein E transgenic mice. Neuroscience 97(3): p419-24.

Chapman J and Michaelson DM (1998) Specific neurochemical derangements of brain projecting neurons in apolipoprotein E-deficient mice. Journal of Neurochemistry 70: p708-14.

Chen Y, Lomnitski L, Michaelson DM and Shohami E (1997) Motor and cognitive deficits in apolipoprotein E-deficient mice after closed head injury. Neuroscience 80: p1255-62.

Cho YH and Jaffard R (1995) Spatial location learning in mice with ibotenate lesions of entorhinal cortex or subiculum. Neurobiology of Learning and Memory 64: 285-90.

Christie RH, Chung H, Rebeck GW, Strickland D and Hyman BT (1996) Expression of the very low density lipoprotein receptor (VLDL-r), an apolipoprotein E receptor, in the central nervous system and in Alzheimer's disease. Journal of Neuropathology and Experimental Neurology 55: p491-98.

Chung H, Roberts CT, Greenberg S, Rebeck GW, Christie R, Wallace R, Jacob HJ and Hyman BT (1996) Lack of association of trinucleotide repeat polymorphisms in very-low density lipoprotein receptor gene in Alzheimer's disease. American Journal of Pathology 148: p399-403.

Cioffi L, Sturtz FG, Witmer S, Barat B, Smith-Gbur J, Moore V, Gilligan B, Auerbach R and Gomez F (1999) A novel endothelial cell-based gene therapy platform for the *in vivo* delivery of apolipoprotein E. Gene Therapy 61: p153-9.

Clarke RF and Goate AM (1993) Molecular genetics of Alzheimer's disease. Archives of Neurology 50: p1164-72.

Clatworthy AE, Gomez-Isla T, Rebeck GW, Wallace RB and Hymna BT (1997) Lack of association of a polymorphism in the low-density lipoprotein receptor-related protein gene with Alzheimer disease. Archives of Neurology 54(10): p1289-92.

Cooper JA and Howell BW (1999) Lipoprotein receptors: Signalling functions in the brain? Cell 97: p671-4

Corbo RM and Scacchi R (1999) Apolipoprotein E (*APOE*) allele distribution in the world: is APOE*4 a "thrifty" allele? Annals of Human Genetics 63: p301-10

Corder EH, Saunders AM, Strittmatter WJ, Scmechel DE, Gaskell PC, Small GW, Roses AD, Haines JL and Pericak-Vance MA (1993) Gene dose of apolipoprotein E type 4 allele and the risk of Alzheimer's disease in late onset families. Science 261: p921-3

Corder EH, Robertson K, Lannfelt L, Bogdanovic N, Eggerston G, Wilkins J and Hall C (1998) HIV infected subjects with the E4 allele for *APOE* have excess dementia and peripheral neuropathy. Nature Medicine 4: p1182-4

Corey-Bloom J, Tiraboschi P, Hansen LA, Alford M, Schoos V, Sabbagh MN, Mas E and Thal LJ (2000) E4 allele dosage does not predict cholinergic activity or synapse loss in Alzheimer's disease. Neurology 54(2): p403-6

Corsellis JA, Bruton CJ and Freeman-Browne D (1973) The aftermath of boxing. Psychological Medicine 3(3): 270-303

Cotman CW and Nadler JV (1978) Reactive synaptogenesis in the hippocampus. In CW Cotman (ed): Neuronal Plasticity, New York: Raven Press: p227-71

Cotman CW (1976) Lesion-induced synaptogenesis in brain: A study of dynamic changes in neuronal membrane specializations. Journal of Supramolecular Structure 4: p319-27

Crook TH (1986) Developmental Neuropsychology 2: p261-76

Czech C, Forstl H, Hentschel F, Monning U, Besthorn C, Geigerkabisch C, Sattel H, - Masters C and Beyreuther K (1994) Apolipoprotein E4 gene dose in clinically diagnosed

Alzheimer's disease – prevalence, plasma cholesterol levels, and cerebrovascular change. European Archives of Psychiatry and Clinical Neuroscience 243: p291-2

Czekay RP, Orlando RA, Woodward L, Lundstrem M and Farquhar MG (1997) Endocytic trafficking of Megalin/RAP complexes in late endosomes. Molecular and Cellular Biology 8(3): p517-31

Danik M, Chabot JG, Hassan-Gonzalez D, Suh M and Quirion R (1993) Localization of sulphated glycoprotein-2/clusterin mRNA in the rat brain bi in situ hybridisation. Journal of Comparative Neurology 334(2): p209-27

Danik M and Poirier J (1998) Apolipoprotein E and neuronal plasticity following experimental de-afferentation and in Alzheimer's disease. Biochemical Society Transactions 26: p262-6

Davignon J, Gregg RE and Sing CF (1988) Apolipoprotein E polymorphism and atherosclerosis. Arteriosclerosis 8: p1-21

DeKroon RM and Armati PJ (2001) Synthesis and processing of apolipoprotein E in human brain cultures. Glia 33: p298-305

DeKroon M and Armati PJ (2001) The endosomal trafficking of apolipoprotein E3 and E4 in cultured human brain neurons and astrocytes. Neurobiology of Disease 8: p78-89

Deller T, Nitch R and Frotscher M (1996) Layer-specific sprouting of commissural fibres to the rat fascia dentate after unilateral entorhinal cortex lesion: A phaseolus vulgaris leucoagglutinin tracing study. Neuroscience 71: p651-60

Deller T and Frotscher M (1997) Lesion-induced plasticity of central neurons: Sprouting of single fibres in the rat hippocampus after unilateral entorhinal cortex lesion. Progress in Neurobiology 53: p687-727

Deller T, Frotscher M and Heimrich B (1997) Sprouting in the hippocampus is layer-specific. Trends in Neuroscience 20(5): p218-23

DeMattos RB, Curtiss LK and Williams DL (1998) A minimally lipidated form of cell-derived apolipoprotein E exhibits isoform-specific stimulation of neurite outgrowth in the absence of exogenous lipids or lipoproteins. Journal of Biological Chemistry 273(7): p4206-12

DeMattos RB, Thorngate FE and Williams DL (1999) A test of the cytosolic apolipoprotein E hypothesis fails to detect the escape of apolipoprotein E from the endocytic pathway into the cytosol and shows that direct expression of apolipoprotein E in the cytosol is cytotoxic. Journal of Neuroscience 24: p64-73

DeSilva H, Harmony J, Stuart W, Gil C and Robbins J (1990) Apolipoprotein J: Structure and tissue distribution. Biochemistry 29: p5380-89

DeSurmont C, Caillaud JM, Emmanuel F, Benoit P, Fruchart JC, Castro G, Branellec D, Heard JM and Duverger N (2000) Complete atherosclerosis regression after human *APOE* gene transfer in ApoE-deficient/nude mice. Arteriosclerosis, Thrombosis and Vascular Biology 20(2): p435-42

Dolan A, McKie EA, MacLean AR and McGeoch DJ (1972) Staus of the ICP 34.5 gene in herpes simplex virus strain 17. Journal of Genetic Virology 73: p971-3

Emilien G, Maloteaux J, Beyreuther K and Masters C (2000) Alzheimer's disease: Mouse models pave the way for therapeutic opportunities. Archives of Neurology 57(2): p176-81

Fagan A and Gage F (1994) Mechanisms of sprouting in the adult central nervous system: Cellular responses in areas of terminal degeneration and reinnervation in the rat hippocampus. Neuroscience 58: p705-25

Fagan A, Murphy BA, Patel SN, Kilbridge JF, Mobley WC, Bu G and Holtzman DM (1998) Evidence for normal ageing of the septo-hippocampal cholinergic system in ApoE (-/-) mice but impaired clearance of axonal degeneration products following injury. Experimental Neurology 151: p314-25

Fagan AM, Bu G, Sun Y, Daugherty A and Holtzman DM (1996) Apolipoprotein E-containing high density lipoprotein promotes neurite outgrowth and is a ligand for the low density lipoprotein receptor related protein. Journal of Biological Chemistry 27(47): p30121-5

Fagan AM and Holtzman DM (2000) Astrocyte lipoproteins, effects of apoE on neuronal function and role of apoE in amyloid-β deposition *in vivo*. Microscopy Research Techniques 50: p297-304

Farlow M, Lahiri D, Poirier J, Davignon J, Schneider L and Hui S (1998) Treatment outcome of tacrine therapy depends on apolipoprotein E genotype and gender of the subjects with Alzheimer's disease. Neurology 50: p669-77

Fazekas F, Strasser-Fuchs S, Schmidt H, Enzinger C, Ropele S, Lechner A, Flooh E, Schmidt R and Hartung H (2000) Apolipoprotein E genotype related differences in brain lesions of multiple sclerosis. Journal of Neurology, Neurosurgery and Psychiatry 69: p25-8

Fazio S, Linton MF and Swift LL (2000) The cell biology and physiologic relevance of ApoE recycling. TCM 10(1): p23-30

Fink RP and Heimer L (1967) Two methods for selective silver impregnation of degenerating axons and there synaptic endings in the central nervous system. Brain Research 4: p369-74

Flaherty D, Lu Q, Soria J and Wood JG (1999) Regulation of tau phosphorylation in microtubule fractions by apolipoprotein E. Journal of Neuroscience Research 56(3): p271-4

Fleming LM, Weisgraber KH, Strittmatter WJ, Troncoso JC and Johnson G (1996) Differential binding of apolipoprotein E isoforms to tau and other cytoskeletal proteins. Experimental Neurology 138: p252-260

Flory JD, Manuck SB, Ferrell RE, Ryan CM and Muldoon MF (2000) Memory performance and the apolipoprotein E polymorphism in a community sample of middle-aged adults. American Journal of Medical Genetics 96(6): p707-11

Forbes (1993) Cost of stroke. Scottish Medical Journal 38: p54-5

Friedman G, Froom P, Sazbon L, Grinblatt I, Shochira M, Tsenter J, Babaey S, Yehuda B and Grosswasser Z (1999) Apolipoprotein Eε4 genotype predicts a poor outcome in survivors of traumatic brain injury. Neurology 52: p244-8

Frotscher M, Heimrich B and Deller T (1997) Sprouting in the hippocampus is layer-specific. Trends in Neuroscience 20(5): p218-23

Fukuyama R, Mizuno T, Mori S, Yanagisawa K, Nakjima K and Fushi T (2000) Age-dependent decline in the apolipoprotein E level in cerebrospinal fluid from control subjects and its increase cerebrospinal fluid from patients with Alzheimer's disease. European Neurology 43(3): p161-9

Fullerton SM, Strittmatter WJ and Matthew WD (1998) Peripheral sensory nerve defects in apolipoprotein E knockout mice. Experimental Neurology 153: p156-63

Fullerton S, Clark AG, Weiss KM, Nickerson DA, Taylor SL, Stengara JH, SalomaaV, Vartainen E, Perola M, Boerwinkle E and Sng CF (2000) Apolipoprotein E variation at

the sequence haplotype level: implications for the origin and maintenance of a major human polymorphism. American Journal of Human Genetics 67: p881-900

Gahwiler BH (1981) Organotypic monolayer cultures of nervous tissue. Journal of Neuroscience Methods 4: p329-42

Gahwiler BH (1984) Development of the hippocampus *in vitro*: cell types, synapses and recpeotrs. Neuroscience 11: p751-760

Gahwiler BH, Capogna M, Debanne D, McKinney RA and Thompson SM (1997) Organotypic slice cultures: a technique has come of age. Trends in Neuroscience 20: p471-77

Gallyas F, Zaborszky L and Wolff JR (1980) Experimental studies of mechanisms involved in methods of demonstrating axonal and terminal degeneration. Stain Technology 55(5): p281-91

Gallyas F, Wolff JR, Bottcher H and Zaborszky L (1980) A reliable and sensitive method to localise terminal degeneration and lysosomes in the central nervous system. Stain Technology 55(5): p299-306

Games D, Adams D, Alessandri R, Barbour R, Bertheletto P, Blackwell C, Carr T, Clemens J, Donaldson T, Gillespie F et al (1995) Alzheimer-type neuropathology in transgenic mice overexpressing V717 β-amyloid precursor protein. Nature 373: p523-7

Geddes JW, Monaghan DT, Cotman CW, Lott IT, Kim RC and Chui HC (1985) Plasticity of hippocampal circuitry in Alzheimer's disease. Science 230(4730): p1179-81

Geddes JF,Vowles GH, Robinson SF and Sutcliffe JC (1996) Neurofibrillary tangles, but not Alzheimer-type pathology, in a young boxer. Neuropathology and Applied Neurobiology 22(1): p12-16

Gelman R and Euday L (1989) Biostatistical considerations for quality assessment of immunologic measurement used in clinical and longitudinal studies. Clinical Immunology and Immunopathology 52(1): p28.37

Genis I, Gordon I, Schayek E and Michaelson DM (1995) Phosphorylation of tau in apolipoprotein E-deficient mice. Neuroscience Letters 199: p5-8

Genis I, Fisher A and Michaelson DM (1999) Site-specific dephosphorylation of tau in apoE deficient and control mice by M1 muscarinic agonist treatment. Journal of Neurochemistry 72: p206-13

Genis L, Chen Y, Shohami E and Michaelson DM (2000) Tau hyperphosphorylation in apolipoprotein E-deficient and control mice after closed head injury. Journal of Neuroscience Research 60: p559-564

Gennarelli TA, Thibault LE, Adams JH, Graham DI, Thompson CJ and Marcincin RJ (1982) Diffuse axonal injury and traumatic coma in the primate. Annals of Neurology 12(6): p564-74

Gennarelli TA, Spielman GM, Langfitt TW, Gildenberg PL, Harrington T, Jane J, Marshall LF, Miller JD and Pitts LH (1982) Influence of the type of intracranial lesion in outcome from severe head injury. Journal of Neurosurgery 56(1): p26-32

Gentleman SM, Roberts GW, Gennarelli TA, Maxwell WL, Adams JH, Kerr S and Graham DI (1995) Axonal injury: a universal consequence of fatal closed head injury? Acta Neuropathologica 89: p537-543

Giannakopoulus P, Kovari E, French LE, Viard I, Hof PR and Bouras C (1998) Possible neuroprotective role of clusterin in Alzheimer's disease: A quantitative immunocytochemical study. Acta Neuropathologica 95: p386-94

Glenner GG and Wong CW (1984) Alzheimer's disease: initial report of the purification and characterization of a novel cerebrovascular amyloid protein. Biochemical and Biophysical Research Communications 120: p885-890

Gomez-Fernandez L (2000) Cortical plasticity and restoration of neuralgic functions: an update on this topic. Reviews in Neurology 31(8): p749-56

Gomez-Isla T, Price JL, McKeel DW, Morris JC, Growdon JH and Hyman BT (1996) Profound loss of layer II entorhinal cortex neurons occurs in very mild Alzheimer's disease. Journal of Neuroscience 16: p4491-4500

Gordon JW, Scangos GA, Plotkin DJ, Barbosa JA and Ruddle FH (1980) Genetic transformation of mouse embryo by microinjection of purifired DNA. Proceedings of the National Academy of Sciences 77: p7380-4

Gordon I, Grauer E, Genis I, Sehayek E and Michaelson DM (1995) Memory deficits and cholinergic impairments in apolipoprotein E-deficient mice. Neuroscience Letters 199: p1-4

Gotthardt M, Trommsdorff M, Nevitt MF, Shelton J, Richardson JA, Stockinger W, Nimpf J and Herz J (2000) Interactions of the low density lipoprotein receptor gene family with cytosolic adaptor and scaffold proteins suggest diverse biological functions in cellular communication and signal transduction. Journal of Biological Chemistry 275: p25616-25624

Grady MS, Jane JA and Steward O (1989) Synaptic reorganisation within the human central nervous system following injury. Journal of Neurosurgery 71: p534-7

Graham DI, McIntosh TK, Maxwell WL and Nicoll JAR (2000) Recent advances in neurotrauma. The Journal of Neuropathology and Experimental Neurology 59: p641-51

Graham DI, Adams JH, Nicool JA, Maxwell WL and Gennarelli TA (1995) The nature, distribution and causes of traumatic brain injury. Brain Pathology 5(4): p397-406

Graham DI and Gennarelli TA (1997) Trauma. Greenfields Neuropathology 6th Edition London, Arnold: p197-202

Greenberg SM, Rebeck GW, Vonsattel JP, Gomez-Isla T and Hyman BT (1995) Apolipoprotein Eε4 and cerebral haemorrhage associated with amyloid angiopathy. Annals of Neurology 38: p254-9

Guillaume D, Bertrand P, Dea D, Davignon J and Poirier J (1996) Apolipoprotein E and low-density lipoprotein binding and internalisation in primary cultures of rat astrocytes: isoform-specific alterations. Journal of Neurochemistry 66: p2410-8

Hall ED, Oostveen JA, Dunn E and Carter DB (1995) Increased amyloid protein precursor and apoliprotein E immunoreactivity in the selectively vulnerable hippocampus following transient forebrain ischaemia in gerbils. Experimental Neurology 135: p17-27

Han SH, Hulette C, Saunders AM, Einstein G, Pericak-Vance M, Strittmatter WJ, Roses AD and Schmechel DE (1994) Apolipoprotein E is present in hippocampal neurons without neurofibrillary tangles in Alzheimer's disease and in age-matched controls. Experimental Neurology 128: p13-26

Han SH, Einstein G, Weisgraber KH, Strittmater WJ, Saunders AM, Pericak-Vance M, Roses AD and Schmechel DE (1994) Apolipoprotein E is localised to the cytoplasm of human cortical neurons: a light and electron microscopy study. Journal of Neuropathology and Experimental Neurology 53: p535-44

Han SH and Chung SY (2000) Marked hippocampal neuronal damage without motor deficits after mild concussive-like brain injury in apolipoprotein E-deficient mice. Annals of the New York Academy of Sciences USA 903: p357-65

Handelman G, Boyles JK, Weisgraber KH, Mahley RW and Pitas RE (1992) Effects of apolipoprotein E, β-very low density lipoproteins and cholesterol on the extension of neuritis by rabbit dorsal root ganglion neurons in vitro. Journal of Lipid Research 33: p167-88

Hardman R, Evans DJ, Fellows L, Hayes B, Rupniak HT, Barnes JC and Higgins GA (1997) Evidence for recovery of spatial learning following entorhinal cortex lesions in mice. Brain Research 758: p187-200

Hardy J, Crook R, Perry R, Raghavan R and Roberts G (1994) *APOE* genotype, Down's syndrome and Alzheimer's disease. The Lancet 343(8903): p979-80

Hardy J, Duff K, Gwinn-Hardy K, Perez-Tur J and Hutton M (1998) Genetic dissection of Alzheimer's disease and related dementias: amyloid and its relationship to tau. Nature Neuroscience 1 (5): p355-360

Harr SD, Uint L, Hollister R, Hyman BT and Mendez AJ (1996) Brain expression of apolipoproteins E, J and A-I in Alzheimer's disease. Journal of Neurochemistry 66: p2429-35

Hartman RE, Wosniak DF, Nardi A, Olney JW, Sartorius L and Holtzman DM (2001) Behavioural phenotyping of GFAP-apoE3 and apoE4 transgenic mice: apoE4 mice show profound working memory impairments in the absence of Alzheimer's-like neuropathology. Experimental Neurology 170: p326-44

Hasty AH, Linton FM, Brandt SJ, Babaev VR, Gleaves LA and Fazio S (1999) Retroviral gene therapy in apoE-deficient mice: apoE expression in the artery wall reduces early foam cell lesion formation. Circulation 99(19): p2571-2576

Hayek T, Attias J, Smith J, Breslow JL and Keidar S (1998) Antiatherosclerotic and antioxidative effects of captopril in apoE-deficient mice. Journal of Cardiovascular Pharmacology 31: p540-4

Heikkinen AM, Niskanen L, Ryynanen M, Komulainen MH, Tuppurainen MT, Parviainen M and Saarikoski S (1999) Is the response of serum lipids and lipoproteins to post-menopausal replacement therapy modified by *APOE* genotype? Arteriosclerosis, Thrombosis and Vascular Biology 19(2): p402-7

Heimrich B, Frotscher M and Schwegler (1990) Plasticity of identified neurons in slice culture of hippocampus: Golgi/ electron microscopic and immunocytochemical study Progress in Brain Research 538: p263-8

Henderson Z, Harrison PS, Jagger E and Beeby JH (1998) Density of choline acetyltransferase immunoreactive terminals in the rat dentate gyrus after entorhinal cortex lesions: a quantitative light microscope study. Experimental Neurology 152: p50-63

Herz J, Kowal RC, Goldstein JL and Brown MS (1990) Proteolytic processing of the 600kDa low-density lipoproein receptor-related protein (LRP) occurs in a trans-Golgi compartment. EMBO 9: p1769-76

Herz J and Beffert U (2000) Apolipoprotein E receptors: linking brain development and Alzheimer's disease. Nature Reviews Neuroscience 1: p51-58

Herz J (2001) Lipoprotein receptors: beacons to neurons? Trends in Neuroscience 24(4): p193-5

Herz J (2001) The LDL receptor gene family: (un)expected signal transducers in the brain. Neuron 29: p571-581

Herz J and Strickland DK (2001) LRP: a multifunctional scavenger and signalling receptor. The Journal of Clinical Investigation 108(6): p779-84

Hesse C, Larsson H, Fredman P, Minthon L, Andreasen N, Davidsson K, Blennow K (2000) Measurement of apolipoprotein E (apoE) in cerebrospinal fluid. Neurochemical Research 25(4): p511-7

Hixson JE (1991) Apolipoprotein E polymorphisms affect atherosclerosis in young males, pathobiological determinants of atheosclerosis in youth. Arteriosclerosis, Thromobosis and Vascular Biology 11: p1237-44

Hogh P, Oturai A, Schrieber K, Blinkenberg M, Jorgensen OS, Ryder L, Paulsen OB, Sorensen PS, Knudsen GM (2000) Apolipoprotein E and multiple sclerosis: Impact of the epsilon 4 allele on susceptibility, clinical type and progression rate. Multiple Sclerosis 6(4): p226-30

Holden C (1998) Neuron growth and apoE. Science 280: p1013

Hollenbach E, Ackermann S, Hyman BT and Rebeck GW (1998) Conformation of an association between a polymorphism in exon 3 of the low-density lipoprotein recpeotr-related protein gene in Alzheimer's disease. Neurology 50(6): p1905-7

Holtzman DM, Pitas RE, Kilbridge J, Nathan B, Mahley RW, Bu G and Schwartz AL (1995) Low-density lipoprotein receptor-related protein mediates apolipoprotein E-dependent neurite outgrowth in a central nervous system-derived neuronal cell line. Proceedings of the National Academy of Science USA 92: p9480-4

Holtzman DM, Bales KR, Wu S, Batt P, Parsadanian M, Fagan AM, Chang LK, Sun Y and Paul SM (1999) Expression of human apolipoprotein E reduces amyloid-β deposition in mouse model of Alzheimer's disease. Journal of Clinical Investigation 103(6): pR15-R21

Holtzman DM, Bales KR, Tenkova T, Fagan AM, Parsadanian M, Sarotrius LJ, Mackey B, Olney J, McKeel D, Wasniak D and Paul SM (2000) Apolipoprotein E isoform-dependent amyloid deposition and neuritic degeneration in a mouse model of Alzheimer's disease. Proceedings of the National Academy of Sciences 97(6): p2892-97

Holtzman DM and Fagan AM (1998) Potential role of apoE in structural plasticity in the nervous system. Implications for disorders of the central nervous system. TCM 8(6): p250-55

Horsburgh K and Nicoll JAR (1996) Selective alterations in the cellular distribution of apolipoprotein E immunoreactivity following transient cerebral ischaemia in the rat. Neuropathology and Applied Neurobiology 22: p342-9

Horsburgh K, Fitzpatrick M, Nilsen M and Nicoll JAR (1997) Marked alterations in the cellular localisation and levels of apolipoprotein E following acute subdural haematoma in rat. Brain Research 763: p103-10

Horsburgh K, Graham DI, Stewarrt J and Nicoll JAR (1999) Influence of apoE genotype on neuronal damage and apoE immunoreactivity in human hippocampus following global ischaemia. Journal of Neuropathology and Experimental Neurology 58(3) p227-34

Horsburgh K, Keely S, McCulloch J, Higgins GA, Roses AD and Nicoll JAR (1999) Increased neuronal damage in apolipoprotein E-deficient mice following global ischaemia. Neuroreport 10: p837-41

Horsburgh K, McCulloch J, Nilsen M, Large C, Roses AD and Nicoll JAR (1999) Intraventricular infusion of apolipoprotein E (apoE) reduces neuronal damage in apoE-deficient mice following global ischaemia. Society for Neuroscience Abstract 236.3

Horsburgh K, Cole G, Yang F, Savage MJ, Greenberg BD, Gentleman SM, Graham DI and Nicoll JAR (2000) Beta-amyloid (Aβ)42(43), Aβ42, Aβ40 and apoE immunostaining of plaques in fatal head injury. Neuropathology and Applied Neurobiology 26: p124-32

Horsburgh K, McCulloch J, Nilsen M, Roses AD and Nicoll JAR (2000) Increased neuronal damage and apoE immunoreactivity in human apolipoprotein E, E4 isoform-specific, transgenic mice after global ischaemia. European Journal of Neuroscience 12: p4309-17

Horsburgh K, McCarron MO, White F and Nicoll JAR (2000) The role of apolipoprotein E in Alzheimer's disease, acute brain injury and cerebrovascular disease: Evidence of common mechanisms and utility of animal models. Neurobiology of Aging 21: p245-55

Howard MK, Kershaw T, Gibb B, Storey N, MacLean AR, Zeng B-Y, Tel BC, Jenner P, Brown SM, Woolf CJ, Anderson PN, Coffin RS and Latchman DS (1998) High efficiency gene transfer to the central nervous system of rodents and primates using herpes virus vectors lacking functional ICP27 and ICP34.5. Gene Therapy 5: p1137-47

Huang DY, Goedert M, Jakes R, Weisgraber KH, Garner CZ, Saunders AM, Pericak-Vance MA, Schmechel DE, Roses AD and Strittmatter WJ (1994) Isoform-specific interactions of apolipoprotein E with the microtubule-associated protein MAP-2c: implications for Alzheimer's disease. Neuroscience Letters 182: p55-8

Hyman BT, Van Hoeson GW, Damasion AR and Barnes CL (1984) Alzheimer's disease: cell-specific pathology isolates the hippocampal formation. Science 225: p1168-70

Hyman BT, Strickland DK and Rebeck GW (1994) Aplha-2-macroglobulin receptor/low-density lipoprotein receptor-related protein. Relationship to apolipoprotein E role in Alzheimer's disease senile plaques. Annals of the New York Academy of Science 737: p88-95

Hyman BT, Strickland D and Rebeck GW (2000) Role of the low-density lipoprotein receptor-related protein, β-amyloid metabolism and Alzheimer's disease. Archives of Neurology 57(5): p646-50

Igbavboa U, Avdulov, Chochina SV and Wood WG (1997) Transbilayer distribution of cholesterol is modified in brain synaptic plasma membranes of knockout mice deficient in the low-density lipoprotein receptor, apolipoprotein E, or both proteins. Journal of Neurochemistry 69(4): p1661-7

Ignatius MJ, Gebicke-Haerter PJ, Skene GHP, Schilling KH, Weisgraber KH, Mahley RW and Shooter EM (1986) Expression of apolipoprotein E during nerve degeneration and regeneration. Proceedings of the National Academy of Sciences USA 83: p1125-9

Ignatius MJ, Gebicke-Haerter PJ, Pitas RE and Shooter EM (1987) Apolipoprotein E in nerve injury and repair. Progress in Brain Research 71: p177-84

Ignatius MJ, Shooter EM, Pitas RE and Mahley RW (1987) Lipoprotein uptake in neuronal growth cones *in vitro*. Science 236: p959-962

Inzelberg R, Chapman J, Treves TA, Asherov A, Kipervasser S, Hilkewicz O, Verchovsky R, Climowitzky S and Korczyn AD (1998) Apolipoprotein E4 in Parkinson disease and dementia: New data and meta-analysis of published study. Alzheimers Disease and Associated Disorders 12(1): p45-8

Inzelberg R, Paleacu D, Chapman J and Korczyn AD (2000) Re: The apolipoprotein E epsilon 4 allele increases the risk of drug induced hallucinations in Parkinson's disease. Clinical Neuropharmacology 23(4): p230-1

Ishibashi S, Herz J, Maeda N, Goldstein JL and Brown MS (1994) The receptor model of lipoprotein clearance: tests of the hypothesis in knockout mice lacking the low-

density lipoprotein receptor, apolipoprotein E or both proteins. Proceedings of the National Academy of Science 91: p4431-5

Ivanco TL and Greenough WT (2000) Physiological consequences of morphologically detectable synaptic plasticity: potential uses for examining recovery following damage. Neuropharmacology 39(5): p765-76

Jackson-Beatty (1995) Principles of Behavioural Neuroscience

Jang M, Maestre G, Tsai W, Jui X, Feng L, Chung W, Schofield P, Stern Y, Tycko B et al (1996) Effects of age, ethnicity, and head injury on the association between APOE genotypes and Alzheimer's disease. Annals of the New York Academy of Science 802

Ji ZS, Pitas RE and Mahley RW (1998) Differential cellular accumulation/ retention of apolipoprotein E mediated by cell surface heparin sulphate proteoglycans. Journal of Biological Chemistry 273: p13452-60

Johnson SA, Young-Chan CS, Laping NJ and Finch CE (1996) Perforant path transection induces complement C9 deposition in hippocampus. Experimental Neurology 138(2): p198-205

Johnson JVW and Jope RS (1992) The role of microtubule-associated protein 2 (MAP-2) in neuronal growth, plasticity, and degeneration. Journal of Neuroscience Research 33: p505-12

Jolivalt C, Leininger-Muller B, Drozdz R, Naskalsky JW and Siest G (2000) Apolipoprotein E is highly susceptible to oxidation by myeloperoxidase an enzyme present in the brain. Neuroscience Letters 210: p61-4

Jordan BD, Relkin NR, Ravdin LD, Jacobs AR, Bennett A and Gandy S (1997) Apolipoprotein E epsilon 4 associated with chronic traumatic brain injury in boxing. JAMA 278(2): p136-40

Jordan-Starck T, Witte DP, Aronow B and Harmony J (1992) Apolipoprotein J: A membrane policeman? Current Opinion in Lipidology 3: p75-85

Kamboh MI, Harmony JAK, Sepehrnia B, Nwankwo M and Ferrell RE (1991) Genetic studies of human apolipoproteins. XX Genetic polymorphism of apolipoprotein J and it's impact on quantitative lipid traits in normolipidemic subjects. American Journal of Human Genetics 49: p1167-73

Kamboh MI (1995) Apolipoprotein E polymorphism and susceptibility to Alzheimer's disease. Human Biology 67: p195-215

Kang DE, Saitoh T, Chen X, Xia Y, Masliah E, Hansen LA, Thomas RG, Thal LJ and Katz R (1997) Genetic association of the low-density lipoprotein receptor-related protein gene (LRP), an apolipoprotein E receptor, with late-onset Alzheimer's disease. Neurology 49: p56-61

Kashyap VS, Santamarina-Fojo S, Brown DR, Parrott CL, Applebaum-Bowden D, Meyn S, Talley G, Paigan B, Maeda N and Brewer HB (1995) Apolipoprotein E deficiency in mice: gene replacement and prevention of atherosclerosis using adenovirus vectors. The Journal of Clinical Investigation 96(3): p1612-20

Kehoe P, Krawczak M, Harper PS, Owen MJ and Jones AL (1999) Age of onset in Huntington disease: Sex specific influence of apolipoprotein E genotype and normal CAG repeat length. Journal of Medical Genetics 36(2): p108-11

Kempermann G, Van Praag H and Gage FH (2000) Activity-dependent regulation of neuronal plasticity and self-repair. Progress in Brain Research 127: p35-48

Kerr ME and Kraus M (1998) Genetics and the central nervous system: apolipoprotein E and brain injury. AACN Clinical Issues 9: p524-30

Kida E, Pluta R, Lossinsky AS, Golabek AA, Choi-Miura NH, Wisnieski HM and Mossakowski MJ (1995) Complete cerebral ischaemia with short-term survival in rat induced by cardiac arrest II Extracellular and intracellular accumulation of apolipoprotein E and J in the brain. Brain Research 374: p341-6

Kida E, Choi-Miura MH and Wisniewski KE (1995) Depositon of apolipoproteins E and J in senile plaques is topographically determined in both Alzheimer's disease and Down's Syndrome brain. Brain Research 685: p211-6

Kounnas MZ, Haudenschild CC, Strickland DK and Argraves WS (1994) Immunological localisation of glycoprotein 330 low-density lipoprotein receptor-related protein and 39 kDa receptor-associated protein in embryonic mouse tissues. In Vivo 8: p343-352

Kruger R, Vieria-Saecker AM, Kuhn W, Berg D, Muller T, Kuhnl N, Fuchs GA, Storch A, Hungs M, Woitalla D, Przuntak H, Epplen JT, Schols L and Riess O (1999) Increased susceptibility to sporadic Parkinson's disease by certain combined alpha-synuclein/apolipoprotein E genotypes. Annals of Neurology 45(5): p611-7

Krzywkoski P, Ghribi O, Gagne J, Chabot C, Kar S, Rochford J, Massicotte G and Poirier J (1999) Cholinergic systems and long-term potentiation in memory impaired apolipoprotein E-deficient mice. Neuroscience 92(4): p1273-86

LaDu MJ, Falduto MT, Manelli AM, Reardon CA, Getz GS and Frail DE (1994) Isoform-specific binding of apolipoprotein E to β-amyloid. Journal of Biological Chemistry 270: p9030-42

Lampart-Etchells M, McNeill TH, Laping NJ, Zarow C, Finch CE and May P (1991) Sulphated glucoprotein 2 is increased in rat hippocampus following entorhinal cortex lesioning. Brain Research 563: p101-6

Laskowitz DT, Sheng H, Bart RD, Joyner KA, Roses AD and Warner DS (1997) Apolipoprotein E-deficient mice have increased susceptibility to focal cerebral ischaemia. Journal of Cerebral Blood Flow and Metabolism 17: p753-8

Laskowitz DT, Horsburgh K and Roses AD (1998) Apolipoprotein E and the CNS response to injury. Journal of Cerebral Blood Flow and Metabolism 18: p465-71

Laskowitz DT, Lee DM, Schmechel D and Staats HF (2000) Altered immune responses in apolipoprotein E-deficient mice. Journal of Lipid Research 41: p613-20

Laurer HL and McIntosh TK (1999) Experimental models of brain trauma. Current Opinion in Neurology 12: p715-21

Lee RJ and van Donkelaar P (1995) Mechanisms underlying functional recovery following stroke. Canadian Journal of Neurological Science 22(4): p257-63

Lehtovirta M, Laakso MP and Soininen H (1995) Volumes of hippocampus, amygdala and frontal lobe in Alzheimer patients with different apolipoprotein E genotypes. Neuroscience 67: p65-72

Lehtovirta M, Laakso MP, Frisoni GB and Soininen H (2000) How does the apolipoprotein E genotype modulate the brain in aging and in Alzheimer's disease? A review of neuroimaging studies. Neurobiology of Aging 21: p293-300

Lendon CL, Talbot CJ, Craddock NJ, Han SW, Wragg M, Morris JC and Coate AM (1997) Genetic association studies between dementia of the Alzheimer's type and three receptors for apolipoprotein E in a Caucasian population. Neuroscience Letters 222: p187-90

Li Y, Jaing N, Powers C and Chopp M (1998) Neuronal damage and plasticity identified by microtubule-associated protein-2, growth-associated protein –43 and cyclin D1 immunoreactivity after focal cerebral ischaemia in rats. Stroke 29: p1972-81

Lichtman SW, Seliger G, Tycko B and Marder K (2000) Apolipoprotein E and functional recovery from brain injury following postacute rehabilitation. Neurology 55(10): p1536-9

Lidstrom AM, Bogdanovic N, Hesse C, Volkman I, Davidsson P and Blennow K (1997) Clusterin (apolipoprotein J) protein levels are increased in hippocampus and in frontal cortex in Alzheimer's disease. Experimental Neurology 154: p511-21

Lie AA, Bluncke I, Beck H, Wiestler OD, Elgar CE and Schoen SW (1999) 5'-nucleotidase activity indicates sites of synaptic plasticity and reactive synaptogenesis in the human brain. Journal of Neuropathology and Experimental Neurology 58(5): p451-8

Lin L, Bock S, Carpenter K, Rose M and Norden JJ (1992) Synthesis and transport of GAP-43 in entorhinal cortex neurons and perforant pathway during lesion induced sprouting and reactive synaptogenesis. Molecular Brain Research 14: p147-53

Lindgren S and Rinder L (1966) Experimental studies in head injury. II. Pressure propogation in "percussion concussion". Biophysik 3(2): p174-80

Lomnitski L, Chapman S, Hochman A, Cohen R, Shohami E, Chen Y, Trembovler V and Michaelson DM (1999) Antooxidant mechanisms in apolipoprotein E deficient mice prior to and following closed head injury. Biochemica et Biophysica 1453: p359-68

Lomnitski L, Oron L, Sklan D and Michaelson DM (1999) Distinct alterations in phospholipid metabolism in brains of apolipoprotein E-deficient mice. Journal of Neuroscience Research 58: p586-92

Longa EZ, Weinstein PR, Carlson S and Cummins R (1989) Reversible middle cerebral artery occlusion without craniectomy in rats. Stroke 1: p84-91

Lopes MBS, Bogaev CA, Gonias SL and Vandenberg SR (1994) Expression of α2-macroglobulin receptor low-density lipoprotein receptor-related protein is increased in reactive and neoplastic glial cells. FEBS Letters 338: p301-5

Lovestone S, Anderton BH, Hartley C, Jensen TG and Jorgensen AL (1996) The intracellular fate of apolipoprotein E is tau-dependent and *APOE* allele-specific. Neuroreport 7 (5): p1005-8

Ma JJ, Yee A, Brewer HB, Das S and Potter H (1994) Amyloid-associated proteins alpha-1-antichymotrypsin and apolipoprotein E promotes assembly of Alzheimer β-proteins into filaments. Nature 372: p92-4

MacLean AR, Fareed MU, Robertson L, Harland J and Brown SM (1991) Herpes simplex virus type 1 deletion variants 1714 and 1716 pinpoint neurovirulence related sequences in Glasgow strain 17 between immediate early gene 1 and the α sequence. Journal of Genetic Virology 72: p631-9

Macrae IM, Robinson MJ, Graham DI, Reid JL and McCulloch JI (1993) Endothelin-1-induced reductions in cerebral blood flow: dose dependency, time-course, neuropathological consequences. Journal of Cerebral Blood Flow and Metabolism 2: p276-84

Mahley RW (1988) Apolipoprotein E: cholesterol transport protein with expanding role in cell biology. Science 240: p622-30

Mahley RW, Nathan BP, Bellosta S and Pitas RE (1995) Apolipoprrptein E: impact of cytoskeletal stability in neurons and the relationship to Alzheimer's disease. Current Opinion Lipidology 6: p86-91

Mahley RW and Ji ZS (1999) Remnant lipoprotein metabolism: key pathways involving cell surface heparin sulphate proteoglycans and apolipoprotein E. Journal of Lipid Research 40: p1-13

Masliah E, Mallory M, Hansen L, DeTeresa R, Alford M and Terry R (1990) Synaptic and neuritic alterations during the progression of Alzheimer's disease. Neuroscience Letters 174: p67-72

Masliah E, Fagan AM, Terry RD, DeTeresa R, Mallory M and Gage FH (1991) Reactive synapotgenesis assessed by synaptophysin immunoreactivity is associated with GAP-43 in the dentate gyrus of the adult rat. Experimental Neurology 113: p131-42

Masliah E, Mallory M, Hansen L, Alford M, Albright T, DeTeresa R, Terry R, Baudier J and Saitoh T (1991) Patterns of aberrant sprouting in Alzheimer's disease. Neuron 6(5): p729-39

Masliah E, Mallory M, Hansen L, Alford M, DeTeresa R, Terry R, Baudier J and Saitoh T (1992) Localization of amyloid precursor protein in GAP-43 immunoreactive aberrant sprouting neurites in Alzheimer's disease. Brain Research 574: p312-6

Masliah E, Mallory M, Ge N, Alford M, Veinberg I and Roses AD (1995) Neurodegeneration in the central nervous system of apoE deficient mice. Experimental Neurology 136: p107-22

Masliah E, Mallory M, Veinbergs I, Miller A and Samuel W (1996) Alterations in apolipoprotein E expression during aging and neurodegeneration. Progress in Neurobiology 50: p493-503

Masliah E, Samuel W, Veinbergs I, Mallory M, Mante M and Saitoh T (1997) Neurodegeneration and cognitive impairments in apoE-deficient mice is ameliorated by infusion of recombinant apoE. Brain Research 751: p307-14

Masliah E (1998) Mechanisms of synaptic pathology in Alzheimer's disease. Journal of Neural Transmission 531: p47-58

Mato M, Ookawara S, Mashiko T, Sakamoto A, Mato TK, Maeda N and Kodamo T (1999) Regional difference of lipid distribution in brain of apolipoprotein E-deficient mice. Anatomical Record 256: p165-76

Mattson MP, Cheng B, Cuwell AR, Esch FS, Lieberburg I and Rydel RE (1993) Evidence for excitoprotective and intraneuronal calcium-regulating roles for secreted forms of the β-amyloid precursor protein. Neuron 19: p243-254

Maxwell WL, Povlishock JT and Graham DL (1997) A mechanistic analysis of non-disruptive axonal injury: a review. Journal of Neurotrauma 7: p419-40

May PC, Lampert-Etchells M, Johnson SA, Poirier J, Masters JN and Finch CE (1990) Dynamics of gene expression for a hippocampal glycoprotein elevated in Alzheimer's disease and in response to experimental lesions in the rat. Neuron 5: p831-9

Mayeux R, Small SA, Tang M, Tycko B and Stern Y (1993) Memory performance in healthy elderly without Alzheimer's disease: effects of time and apolipoprotein E. Neurobiology of Aging 22: p683-9

McCarron MO and Nicoll JAR (1998) High frequency of apolipoprotein E ε2 allele is specific for patients with cerebral amyloid angiopathy-related haemorrhage. Neuroscience Letters 247: p45-8

McCarron MO, Muir KW, Weir CJ, Dyker AG, Bone I, Nicoll JA and Lees KR (1998) The apolipoprotein E ε4 allele and outcome in cerebrovascular disease. Stroke 29: p1882-7

McCarron MO, Hoffmann KL, DeLong DM, Gray L, Saunders AM and Alberts MJ (1999) Intracerebral haemorrhage outcome: *APOE*, haematoma and oedema volumes. Neurology 53(9): p2176-9

McCarron MO, DeLong D and Alberts MJ (1999) Meta-analysis of *APOE* genotype is ischaemic cerebrovascular disease. Neurology 53(6): p1308-11

McKie EA, Brown SM, MacLean AR and Graham DI (1998) Histopathological responses in the CNS following inoculation with a non-neurovirulent mutant (1716) of herpes simplex virus type 1 (HSV 1): relevance for gene and cancer therapy. Neuropathology and Applied Neurobiology 24: p367-72

Michel D, Chabot J, Moyse E, Danik M and Quirion R (1992) Possible functions of a new genetic marker in central nervous system: the sulphated glycoprotein-2 (SGP-2). Synapse 11: p105-11

Michel D, Chatelain G, North S and Brun G (1997) Stress-induced transcription of the clusterin/apoJ gene. Journal of Biochemistry 328: p45-50

Mielke R, Zerres K, Uhlhaas S, Kessler J and Heiss WD (1998) Apolipoprotein E polymorphism influences the cerebral metabolic pattern in Alzheimer's disease. Neuroscience Letters 254: p49-52

Miettinen R, Kotti T, Tuunanen J, Toppinen A, Reikkinen P and Halonen T (1998) Hippocampal damage after injection of kainic acid into the rat entorhinal cortex. Brain Research 813: p9-17

Mitchison T and Kirschner N (1988) Cytoskeletal dynamics and nerve growth. Neuron 1(9): p761-72

Moestrup S (1994) The α2-macroglobulin receptor and epithelial glycoprotein 330: two giant receptors mediating endocytosis of multiple ligands. Biochemica et Biophysica Acta 1197: p197-213

Montine TJ, Markesberry WR, Zackert W, Sanchez SC, Roberts LJ and Morrow J (1999) The magnitude of brain lipid peroxidation correlates with the extent of degeneration but not with density of neuritic plaques or neurofibrillary tangle or with *APOE* genotype in Alzheimer's disease patients. American Journal of Pathology 155: p863-8

Mortimer JA, van Duijn CM, Chandra V, Fratiglioni, Graves AB, Heyman A, Jorm AF, Kokmen E, Kondo K, Rocca WA *et al* (1991) Head trauma as a risk factor for Alzheimer's disease: a collaborative re-analysis of case-control studies. EURODEM Risk Factors Research Group. International Journal of Epidemiology 20: pS28-35

Mucke L, Masliah E, Johnson WB, Ruppe MD, Rockenstein EM, Forss-Petter S, Pietrapaolo M, Mallory M and Abraham CR (1994) Synaptotrophic effects of human amyloid β protein precursors in the cortex of transgenic mice. Brain Research 666: p151-67

Namba Y, Tomonaga M, Kawasaki H, Otoma E and Ikeda K (1991) Apolipoprotein E immunoreactivity in cerebral amyloid deposits and neurofibrillary tangles in Alzheimer's disease and kuru plaque amyloid in Creutzfeld-Jakob disease. Brain Research 264: p850-2

Narita M, Holtzman DM, Schwartz AL and Bu G (1997) Alpha 2-macroglobulin complexes with and mediates the endocytosis of beta-amyloid peptide via cell surface low-density lipoprotein receptor-related protein. Journal of Neurochemistry 69(5): p1904-11

Nathan BP, Bellosta S, Sanan DA, Weisgraber KH, Mahley RW and Pitas RE (1994) Differential effects of apolipoproteins E3 and E4 on neuronal growth *in vitro.* Science 264 (5160): p850-2

Nathan BP, Chang KC, Bellosta S and Brisch E (1995) The inhibitory effect of apolipoprotein E4 on neurite outgrowth is associated with microtubule depolymerization. Journal of Biological Chemistry 270: p19791-99

Neve RL, Coopersmith R, McPhie DL, Santeufemio C, Pratt KG, Murphy CJ and Lynn SD (1998) The neuronal growth-associated protein GAP-43 interacts with rabaptin 5 and participates in endocytosis. The Journal of Neuroscience 18(9): p7757-67

Newman MF, Crpughwell ND, Blumenthal JA, Lowry E, White W, Glower DD, Smith LR, Mahanna EP *et al* (1995) Predictors of cognitive decline after cardiac operation. Annals of Thoracic Surgery 59(5): p1326-30

Nicoll JAR, Roberts GW and Graham DI (1995) Apolipoprotein E epsilon 4 allele is associated with deposition of amyloid beta-protein following head injury. Nature Medicine 1: 135-7

Nicoll JAR, Roberts GW and Graham DI (1996) Amyloid beta-protein, *APOE* genotype and head injury. Annals of the New York Academy of Science 777: p271-5

Nicoll JAR, Burnett C, Love S, Graham DI, Ironside JW and Vinters HV (1997) High frequency of apolipoprotein E epsilon 2 in patients with cerebral amyloid angiopathy. Annals of Neurology 39: p682-3

Niemier A, Willnow T, Dieplinger H, Jacobsen C, Mayer N, Hilpert J and Beisiegel U (1999) Identification of megalin/gp330 as receptor for lipoprotein J *in vitro.* Arteriosclerosis, Thrombosis and Vascular Biology 19: p552-61

Nirkko AC, Rosler KM, Ozdoba C, Heid O, Schroch G and Hess TW (1997) Human cortical plasticity: functional recovery with mirror movements. Neurology 48(4) p1090-3

Ohara S, Tsukada M and Ikeda S (1999) On the occurrence of neuronal sprouting in the cortex of a patient with Down's syndrome. Acta Neuropathologica 97(1): p85-90

Oleson OF and Dago L (2000) High density lipoprotein inhibits assembly of amyloid β-peptides into fibrils. Biochemical and Biophysical Research Communications 270: p62-6

Olichney JM, Hansen LA, Galasko D, Saitoh T, Hofstetter CR, Katzman R and Thal LJ (1996) The apolipoprotein E epsilon 4 allele is associated with increased neuritic plaques and cerebral amyloid angiopathy in Alzheimer's disease and Lewy body variant. Neurology 47(1): p190-6

Oliveri RL, Nicoletti G, Cittadella R, Manna I, Branca D, Zappia M, Gambardella A, Caracciolo M and Quattrone A (1999) Apolipoprotein E polymorphisms and Parkinson's disease. Neuroscience Letters 277(2): p83-6

Ong WY, He Y, Suresh S and Patel SC (1997) Differential expression of apolipoprotein D and apolipoprotein E in the kainic acid-lesioned rat hippocampus. Neuroscience 79(2): p359-67

Page KJ, Hollister RD and Hyman BT (1998) Dissociation of apolipoprotein and apolipoprotein receptor response to lesion in the rat brain: an *in situ* hybridisation study. Neuroscience 85: p1161-71

Panckhurst GJ, Bennett CA and Easterbrook-Smith SB (1998) Characterisation of the heparin binding properties of human clusterin. Biochemistry 37: p4823-30

Pasinetti GM, Johnson SA, Oda T, Rozovsky I and Finch CE (1994) Clusterin (SGP-2): a multifunctional glycoprotein with regional expression in astrocytes and neurons of the adult rat brain. Journal of Comparative Neurology 339(3): p387-400

Perry EK, Perry RH, Blessed G and Tomlinson BE (1977) Neurotransmitter enzyme abnormalities in senile dementia: CAT and GAD activities in necropsy tissue. Journal of Neurological Science 34: p247-65

Perry EK, McKeith I and Thompson P (1991) Topography, extent, and clinical relevance of neurochemical deficits in dementia of Lewy body type, Parkinson's disease, and Alzheimer's disease. Annals of the New York Academy of Sciences 640: p197-202

Piedrahita JA, Zhang SH, Hagaman JR, Oliver PM and Maeda N (1992) Generation of mice carrying a mutant apolipoprotein E gene inactivated by gene targeting in embryonic stem cells. Proceedings of the National Academy of Sciences 89: p4471-5

Pitas RE, Ji ZS, Weisgraber KH and Mahley RW (1998) Role of apolipoprotein E in modulating neurite outgrowth: potential effect of intracellular apolipoprotein E. Biochemistry Society Transactions 26(2): p257-62

Plassman BL, Havlik RJ, Steffens DC, Helms MJ, Newman TN, Drosdick D, Philips C, Gau BA, Welsh-Bohmer KA, Burke JR, Guralnick JM and Brietner JC (2000) Documented head injury in early adulthood and risk of Alzheimer's disease and other dementias. Neurology 55(8): p1158-66

Poirier J, May PC, Osterburg HH, Geddes J, Cotman C and Finch CE (1990) Selective alterations of RNA in rat hippocampus after entorhinal cortex lesioning. Proceedings of the National Academy of Sciences USA 87: p303-7

Poirier J, Hess M, May PC and Finch CE (1991) Astrocytic apolipoprotein E mRNA and GFAP mRNA in hippocampus after entorhinal cortex lesioning. Molecular Brain Research 11: p97-106

Poirier J, Baccichet A, Dea D and Gauthier S (1993) Cholesterol synthesis and lipoprotein reuptake during synaptic remodelling in hippocampus in adult rats. Neuroscience 55: p81-90

Poirier J (1994) Apolipoprotein E in animal models of CNS injury and in Alzheimer's disease. Trends in Neuroscience 17(12): p525-530

Poirier J, Delisle MC, Quirion R, Aubert I, Farlow M, Lahiri D, Hui S, Bertrand P, Nalbantoglu J, Gilfix BM and Gauthier S (1995) Apolipoprotein E4 allele as a predictor of cholinergic deficits and treatment outcome in Alzheimer's disease. Proceedings of the National Academy of Sciences 92: p12260-64

Poirier J, Miinich A and Davignon J (1995) Apolipoprotein E, synaptic plasticity and Alzheimer's disease. Trends in Molecular Medicine 27: p663-70

Poirier J and Sevigny P (1998) Apolipoprotein E4, cholinergic integrity and the pharmacogenetics of Alzheimer's disease. Journal of Neural Transmission 53: p199-207

Pollard H, Khrestchatisky M, Moreau J, Ben-Ari Y and Represa A (1994) Correlation between reactive sprouting and microtubule protein expression in epileptic hippocampus. Neuroscience 61(4): p773-87

Povlishock JT and Christman CW (1995) The pathobiology of traumatically induced axonal injury in animals; humans; a review of current thoughts. Journal of Neurotrauma 4: p555-64

Posse de Chaves E, Rusinol A, Vance DE, Campenot RB and Vance JE (1997) Role of lipoproteins in the delivery of lipids to axons during axonal regeneration. Journal of Biological Chemistry 272: p30766-773

Raber J, Wong D, Buttini M, Orth M, Bellosta S, Pitas RE, Mahley RW and Mucke L (1998) Isoform-specific effects of human apolipoprotein E on brain function rvealed in apoE knockout mice. Increased susceptibility in females. Proceedings of the National Academy of Science 95(18): p10914-19

Raber J, Akana SF, Bhatnagar S, Dallman MF, Wong D and Mucke L (2000) Hypothalamic-pituitary-adrenal dysfunction in apoE-/- mice: possible role in behavioural and metabolic alterations. Journal of Neuroscience 20(5): p2064-71

Raisman G (1969) Neuronal plasticity in the septal nuclei of the adult rat. Brain Research 14: p25-48

Ramirez JL, McQuilkin M, Carrigan T, MacDonald K and Kelley MS (1996) Progressive entorhinal cortex lesions accelerate hippocampal sprouting and spare spatial memory in rats. Proceedings of the National Academy of Science USA 93: p11512-17

Rampling BP, Cruikshank G, MacLean AR and Brown SM (1998) Therapeutic replication competent herpes virus. Nature Medicine 2: p133

Randazzo EP, Kesery S, Gesser RM, Alsop D, Ford JC, Brown SM, MacLean A and Fraser NW (1995) Treatment of experimental intracranial murine melanoma with a neuroattenuated herpes simplex virus 1 mutant. Virology 211: p94-101

Rebeck GW, Reiter JS, Strickland DK and Hyman BT (1993) Apolipoprotein in Sporadic Alzheimer's disease: allelic variation and receptor interactions. Neuron 11: p575-80

Rebeck GW, Reiter JS, Strickland DK and Hyman BT (1993) Apolipoprotein E in sporadic Alzheimer's disease: allelic variation and receptor interactions. Neuron 11: p575-80

Reddick RL, Zhang SH and Maeda N (1994) Atherosclerosis in mice lacking apoE. Evaluation of lesional development and progression. Arteriosclerosis, Thrombosis and Vascular Biology 14: p141-47

Reiman EM, Caselli RJ, and Yun LS (1996) Preclinical evidence of Alzheimer's disease in persons homozygous for the ε4 allele for apolipoprotein E. New England Journal of Medicine 334: p752-58

Rensen PCM, Jong MC, Van Vark LC, Van der Boom H, Hendriks WL, Van Berkel TJC, Biessen EAL and Havekes LM (2000) Apolipoprotein E is resistant to intracellular degradation *in vitro* and *in vivo.* Journal of Biological Chemistry 275 (12): p8564-71

Roberts GW, Gentleman SM, Lynch A and Graham DI (1990) Beta A4 amyloid protein deposition in brain after head trauma. Lancet 338: p1422-23

Roberts GW, Gentleman SM, Lynch A, Murray L, Landon M and Graham DI (1994) Beta amyloid protein deposition in the brain after severe head injury: implications for the pathogenesis of Alzheimer's disease. Journal of Neurology, Neurosurgery and Psychiatry 57(4): p419-25

Robertson LM, MacLean AR and Brown SM(1992) Peripheral replication and latency reactivation kinetics of the non-virulent herpes simplex virus variant 1716. Journal of Genetic Virology 76: p967-70

Robertson IH and Murre JM (1999) Rehabilitation of brain damage: brain plasticity and principles of guided recovery. Psychology Bulletin 125(5): p544-75

Roses AD (1998) Apolipoprotein E and Alzheimer's disease. The tip of the susceptibility iceberg. Annals of the New York Academy of Sciences 855: p738-43

Roses AD (1996) Apolipoprotein E in neurology. Current Opinion in Neurology 9: p265-70

Roses AD, Einstein G, Gilbert J, Goedert M, Han SH, Huang D, Masliah E, Pericak-Vance MA, Saunders AM, Schmechel DE, Strittmatter WJ, Weisgraber KH and Xi PT (1996) Morphological, biochemical, and genetic support for an apolipoprotein E effect on microtubular metabolism. Annals of the New York Academy of Sciences 777: p146-57

Roses AD (1997) Apolipoprotein E, a gene with complex biological interactions in the aging brain. Neurobiology of Disease 4: p170-86

Roses AD, Gilbert J, Xu PT, Sullivan P, Popko B, Burkhart DS, Christian-Rothrock T, Saunders AM, Maeda N and Schmechel DE (1998) Cis-acting human apoE tissue expression element is associated with human pattern of intraneuronal apoE in transgenic mice. Neurobiology of Aging 19(15): p553-8

Russo C, Angelini G, Dapino D, Peccini A, Piombo G, Schettini G, Chen S, Teller JK, Zaccheo D, Gambetti P and Tabaton M (1998) Opposite roles of apolipoprotein E in normal brains and in Alzheimer's disease. Proceedings of the National Academy of Science USA 95(26): p15598-15602

Sabo T, Lomnitski L, Nyska A, Beni S, Maronpot R, Shohami E, Roses AD and Michaelson DM (2000) Susceptibility of transgenic mice expressing human apolipoprotein E to closed head injury : the allele E3 is neuroprotective whereas E4 increases fatalities. Neuroscience 101: p879-84

Samatovicz RA (2000) Genetics and brain injury: apolipoprotein E. Journal of Head Trauma and Rehabilitation 15: p869-74

Sanan DA, Wesigraber KH, Russell SJ, Mahley RW, Huang D, Saunders A, Schmechel D, Wisnieski T, Frangioni B and Roses AD (1994) Apolipoprotein E associates with beta amyloid peptide of Alzheimer's disease to form novel monofibrils isoform apoE4 associates more efficiently than apoE3. Journal of Clinical Invesigation 94: p860-9

Saunders AM, Strittmatter WJ, Schmechel D, George-Hysloop PH, Pericak-Vance MA, Joo SH, Rosi BL, Gusella JF, Crapper-MacLachlan DR, Alberts MJ, Hulette C, Crain B, Goldgaber D and Roses AD (1993) Association of apolipoprotein E allele epsilon 4 with late-onset familial and sporadic Alzheimer's disease. Neurology 43(8): p1467-72

Saunders AM, Trowers MK, Shimkets RA, Blakemore S, Crowther DJ, Mansefield TA, Wallace DM, Strittmatter WJ and Roses AD (2000) The role of apolipoprotein E in Alzheimer's disease: pharmacogenomic target selection. Biochemica et Biophysica 1502: p85-94

Scharfman HE, Goodman JH, Du F and Schwarcz R (1998) Chronic changes in synaptic responses of entorhinal and hippocampal neurons after amino-oxyacetic acid (AOAA) – induced entorhinal cortical neuron loss. Journal of Neurophysiology 80: p3031-46

Schmechel DE, Saunders AM, Strittmatter WJ, Crain BJ, Hulette CM, Joo SH, Pericak-Vance MA, Glodgaber D and Roses AD (1993) Increased amyloid beta-peptide deposition in cerebral cortex as a consequnce of apolipoprotein E genotype in late-onset Alzheimers disease. Proceedings of the National Academy of Science USA 90: p9649-53

Schmidt H, Schmidt R, Fazekas F (1996) Apolipoprotein Eε4 allele in the normal elderly: neuropsychologic and brain MRI correlates. Clinical Genetics 50: p293-9

Scott BL, Welch K, De Serrano V, Moss NC, Roses AD and Strittmatter WJ (1998) Human apolipoprotein E accelerates microtubule polymerisation *in vitro*. Neuroscience Letters 245: p105-8

Selkoe DJ (1994) Alzheimer's disease: a central role for amyloid. Journal of Neuropathology and Experimental Neurology 53(5): p438-47

Selkoe DJ (2001) Alzheimer's disease: Genes, proteins and therapy. Physiological Reviews 81 (2): p741-66

Shanmugaratnam J, Berg E, Kimerer L, Johnson RJ, Amaratunga A, Schreiber BM and Fine RE (1997) Retinal Muller glia secrete apolipoprotein E and J which are efficiently assembled into lipoprotein particles. Molecular Brain Research 50: p113-20

Sheng JG, Mrak RE and Griffin WST (1996) Apolipoprotein E distribution among different plaque types in Alzheimer's disease: implications for its role in plaque progression. Neuropathology and Applied Neurobiology 22: p334-41

Sheng H, Laskowitz DT, Bennett E, Schmechel DE, Bart RD, Saunders AM, Pearlstein RD, Roses AD and Warner DS (1998) Apolipoprotein E isoform–specific differences in outcome from focal ischaemia in transgenic mice. Journal of Cerebral Blood Flow and Metabolism 00: p00-00

Sheng H, Laskowitx DT, Mackensen GB, Kudo M, Pearlstein RD and Warner DS (1999) Apolipoprotein E deficiency worsens outcome from global cerebral ischaemia in the mouse. Stroke 30: p1118-1124

Shoji M, Golde TE, Ghiso J, Cheung TT, Estus S, Shaffer LM, Cai XD, McKay DM, Tintner R and Frangione B *et al* (1992) Production of the Alzheimer amyloid beta protein by normal proteolytic processing. Science 258: p126-9

Slooter AGC, Bronzova J, Witteman JCM, van Broeckhoven C, Hofman A and van Duijn CM (1999) Estrogen use and early onset Alzheimer's disease: a population based study. Journal of Neurosurgery and Psychiatry 67: p779-81

Small GW, Mazziotta JC and Collins MT (1995) Apolipoprotein E type 4 allele and cerebral glucose metabolism in relatives at risk for familial Alzheimer's disease. Journal of Neuroimaging 9: p2-9

Smith DH, Chen XH, Nonaka M (1995) Accumulation of amyloid beta and tau and the formation of neurofilament inclusions after diffuse braininjury in the pig. Journal of Neuropathology and Experimental Neurology 58: p982-92

Soininen HS and Reikkenen PJ (1996) ApolipoproteinE, memory and Alzheimer's disease. Trends in Neuroscience 19(6): p224-28

Sorbi S, Nacmias N, Piacentini S, Repice A, Latorraca, S, Forleo P and Amaucci L (1995) ApoE as a prognostic factor for post-traumatic coma. Nature Medicine 1: p852

Srivastava RAK, Bhasin N Srivastava N (1996) Apolipoprotein E gene expression in various tissue of mouse and regulation by estrogen. Biochemistry and Molecular Biology International 38(1): p91-101

Srivastava RAK, Srivastava N, Averna M, Lin RC, Korach KS, Lubahn DB and Schonfeld G (1997) Estrogen upregulates apolipoprotein E (apoE) gene expression by increasing apoE mRNA in the translating pool via the estrogen receptor α-mediated pathway. Journal of Biological Chemistry 272(52): p33360-66

Stevenson SC, Marshall-Neff J, Teng B, Lee CB, Roy S and McClelland A (1995) Phenotypic correction of hypercholesterolaemia in apoE-deficient mice by adenovirus mediated *in vivo* gene transfer. Arteriosclerosis, Thrombosis and Vascular Biology 15: p479-484

Steward O, Vinsant SL and Davis L (1988) The process of reinnervation in the dentate gyrus of adult rats: an ultrastructural study of changes in presynaptic terminals as a result of sprouting. Journal of Comparative Neurology 267: p203-10

Steward O (1976) Topographic organization of the projections from the entorhinal area to the hippocampal formation in the rat. Journal of Comparative Neurology 167: p285-314

Steward O and Vinsant SL (1983) The process of reinnervation in the dentate gyrus of the adult rat: a quantitative electron microscopic analysis of terminal proliferation and reactive synaptogenesis. The Journal of Comparative Neurology 214: p370-86

Stockinger W, Hengstschlager-Ottnad E, Novak S, Matus A, Huttinger M, Bohr J, Lassmann H, Schneider WJ and Nimpf J (1998) The low-density lipoprotein receptor gene family. Journal of Biological Chemistry 273: p32213-221

Stone DJ, Rozovsky I, Morgan TE, Anderson CP, Hajian H and Finch CE (1997) Astrocytes and microglia respond to estrogen with increased apoE mRNA *in vivo* and *in vitro*. Experimental Neurology 143(2): p313-8

Stone DJ, Rozivsky I, Morgan TE, Anderson CP and Finch CE (1998) Increased synaptic sprouting in response to estrogen via an apolipoprotein E dependent mechanism: implications for Alzheimer's disease. Journal of Neuroscience 18(9): p3180-85

Stone DJ, Rozovsky I, Morgan TE, Anderson CP, Lopez LM, Shick J and Finch CE (2000) Effects of age on gene expression during estrogen induced synaptic sprouting in the female rat. Experimental Neurology 165: p46-57

Stoppini L, Buchs P-A and Muller D (1991) A simple method for organotypic cultures of nervous tissue. Journal of Neuroscience Methods 37: p173-182

Stoppini L, Buch PA and Muller D (1993) Lesion-induced neurite sprouting and synapse formation in hippocampal organotypic cultures. Neuroscience 57(4): p985-94

Stoppini L, Parisi L, Oropesa C and Muller D (1997) Sprouting and functional recovery in co-cultures between old and young hippocampal organotypic slices. Neuroscience 80(4): p1127-36

Stroemer RP, Kent TA and Hulsebosch CE (1993) Acute increase in expression of growth-associated protein GAP-43 following ischaemia in rat. Neuroscience Letters 162: p51-54

Strickland D, Kuonnas M and Argraves W (1995) LDL-receptor-related protein: a multiligand receptor for lipoprotein and proteinase catabolism FASEB J 9: p890-898

Strittmatter WJ, Saunders AM, Schmechel, D, Pericak-Vance M, Enghild J, Salvesen GS and Roses AD (1993) Apolipoprotein E: high-avidity binding to beta-amyloid and increased frequency of type 4 allele in late-onset familial Alzheimer's disease. Proceedings of the National Academy of Science USA 90: p1977-81

Strittmatter WJ, Saunders AM, Goedart M, Weisgraber KH, Dong LM, Jakes R, Huang DY, Pericak-Vance M, Schmechel D and Roses AD (1994) Isoform-specific interactions of apolipoprotein E with microtubule-associated protein tau: implications for Alzheimer disease. Proceedings of the National Academy of Science USA 91: p11183-6

Stuart WD, Crol B, Jenkins SH and Harmony JAK (1992) Structure and stability of apolipoprotein J-containing high-density lipoproteins. Biochemistry 31: p8552-9

Sun Y, Wu S, Bu G, Onifade MK, Patel SM, LaDu MJ, Fagan AM and Holtzman DM (1998) Glial fibrillary acidic-protein-apolipoprotein E (apoE) transgenic mice: astrocyte-specific expression and differing biological effects of astrocyte-secreted apoE3 and apoE4 lipoproteins. The Journal of Neuroscience 18(9): p3261-72

Tamura A, Graham DI, McCulloch J and Teasdale GM (1981) Focal cerebral ischaemia in the rat. Description of technique and early neuropathological consequences following middle cerebral artery occlusion, Journal of Cerebral Blood Flow and Metabolism 1: p53-60

Tanaka S, Suzuki K, Watanabe M, Matsuda A, Tone S and Koike T (1998) Upregulation of a new microglial gene, mrf-1, in response to programmed cell death and degeneration. The Journal of Neuroscience 18(16): p6358-69

Tang MX, Jacobs D, Stern Y (1996) Effect of estrogen during menopause on risk and age at onset of Alzheimer's disease. Lancet 348: p429-32

Tao R and Aldskogius H (1999) Glial cell responses, complement and apolipoprotein J expression following axon injury in the neonatal rat. Journal of Neurocytology 28: p559-70

Tardiff B, Newman A and Saunders (1997) Apolipoprotein E allele frequency in patients with cognitive defects following cardiopulmonary bypass. Circulation 90: 1-20
Teasdale G, Nicoll JAR, Murray G and Fiddes M (1997) Association of apolipoprotein E polymorphism with outcome after head injury. Lancet 350: p1069-71

Teasdale GM, Murray G, Nicoll, JAR, Fiddes H, McLaughlin K, Dobson C, Swiatek S and Stewart E (2000) Effects of *APOE* genotype on outcome on head injury: relationship to age. British Journal of Neurosurgery Vol 14 No 5

Terrisse L, Poirier J, Bertrand P, Merched A, Visvikis S, Seist G, Milne R and Rassart E (1998) Increased levels of apolipoprotein D in cerebrospinal fluid and hippocampus of Alzheimer's patients. Journal of Neurochemistry 71: p1643-50

Terrisse L, Seguin D, Bertrand P, Poirier J, Milne R and Rassart E (1999) Modulation of apolipoprotein D and apolipoprotein E expression in rat hippocampus after entorhinal cortex lesion. Molecular Brain Research 70: p26-35

Terry RD and Wisniewski HM (1970) The ultrastructure of the neurofibrially tangle and the senile plaque. In: Wolstenholme GEW, O'Connor M (eds) Ciba Foundation Symposium in Alzheimer's disease and related conditions. Churchill, London p145-68

Tesseur I, Van Dorpe J, Spittaels K, Van den Haute C, Moeschars D and Van Leuven F (2000) Expression of human apolipoprotein E4 in neurons causes hyperphosphorylation of protein tau in the brain of transgenic mice. American Journal of Pathology 156 (3): p951-64

Tesseur I, van Dorpe J, Bruynseels K, Bronfman F, Sciot R, van Lommel A and van Leuven F (2000) Prominent axonpathy and disruption of axonal transport in transgenic mice expressing human apolipoprotein E4 in neurons of brain and spinal cord. American Journal of Pathology 157(5): p1495-1510

Teter B, Xu P-T, Gilbert JR, Roses AD, Galasko D and Cole GM (1999) Human apolipoprotein E isoform-specific differences in neuronal sprouting in organotypic hippocampal culture. Journal of Neurochemistry 73(6): p1-4

Teter B, Harris-White ME, Frautschy SA and Cole GM (1999) Role of apolipoprotein E and estrogen in mossy fibre sprouting in hippocampal slice cultures. Neuroscience 91(3): p1009-16

Tornqvist E, Liu L, Aldskogius H, Holst HV and Svensson M (1996) Complement and clusterin in the injured nervous system. Neurobiology of Aging 17 (5): p695-705

Trommsdorff M, Borg JP, Margolis B and Herz J (1998) Interaction of cytosolic adaptor proteins with neuronal apolipoprotein E receptors and the amyloid precursor protein. Journal Biological Chemistry 273: p33556-60

Trommsdorff M, Gotthardt M, Hiesberger T, Shelton J, Stockinger W, Nimpf J, Hammer RE, Richardson JA and Herz J (1999) Reeler/disabled-like disruption of neuronal migration in knockout mice lacking the VLDL receptor and apoE receptor 2. Cell 97: p689-701

Umans L, Overberg L, Serneels L, Tesseur I and van Leuven F (1999) Analysis of expression of genes involved in apolipoprotein E based lipoprotein metabolism in pregnant mice deficient in the receptor-associated protein, the low-density lipoprotein receptor and apolipoprotein E. Biology of Reproduction 61(5): p1216-25

Umans L, Serneels L, Lorent K, Dewachter I, Tesseur I, Moechars D and van Leuven F (1999) Lipoprotein receptor-related protein in brain and in cultured neurons of mice deficient in receptor associated protein and transgenic for apolipoprotein E4 or amyloid precursor protein. Neuroscience 94: p315-21

Van Leuven F, Stas L, Thiry E, Nelissen B and Miyake Y (1998) Strategy to sequence the 89 exons of the human LRP-1 gene coding for the lipoprotein receptor-related protein: identification of one expressed mutation among 48 polymorphisms. Genomics 52: p138-44

Van Lookeren Campagne M, Dotti CG, Verkleij AJ, Gispen WH and Oestreicher AB (1990) B-50/GAP-43 localisation on membranes of putative transport vesicles in the cell body, neuritis and growth cones of cultured hippocampal neurons. Neuroscience Letters 13: p129-32

Van Uden E, Sagara I, van Uden J, Orlando R, Mallory M, Rockstein E and Masliah E (2000) A protective role of the low-density lipoprotein receptor-related protein against amyloid β-protein toxicity. Journal of Biological Chemistry 275: p30525-530

Vance JE, Campenot, RB and Vance DE (2000) The synthesis and transport of lipids for axonal growth and nerve regeneration. Biochemica et Biophysica 1486: p84-96

Veinbergs I, Mallory M, Mante M, Rockenstein E, Gilbert JR and Masliah E (1999) Differential neurotrophic effects of apolipoprotein E in aged transgenic mice. Neuroscience Letters 265: p427-36

Weatherby SJ, Mann CL, Davies MB, Carthy D, Fryer AA, Boggild Young C, Strange RC, Ollier W and Hawkins CP (2000) Polymorphisms of apolipoprotein E; outcome and susceptibility in multiple sclerosis. Multiple Sclerosis 6(1): p32-6

Weisgraber KH, Rall SC and Mahley RW (1981) Human E apoprotein heterogeneity. Cysteine-arginine interchanges in the amino acid sequence of the apoE isoforms. Journal of Biological Chemistry 256: p9077-83

Weisgraber KH, Innerarity TL and Mahley RW (1982) Abnormal lipoprotein receptor niding activity of the human E apoprotein due to cysteine-arginine interchange at a single site. The Journal of Biological Chemistry 257: p2518-21

Weisgraber KH, Roses AD and Strittmatter WJ (1994) The role apolipoprotein E in the nervous system. Current Opinion in Lipidology 5: p110-16

Weisgraber KH and Dong LM (1996) Role of apolipoprotein E in Alzheimer's disease: clues from its structure. Apolipoprotein E in Alzheimer's disease: p11-19. Springer

White F, Nicoll JAR and Horsburgh K (2000) Alterations in apoE and apoJ in relation to degeneration and regeneration in a mouse model of entorhinal cortex lesion. Experimental Neurology 169: p307-18

White F, Nicoll JAR, Roses AD and Horsburgh K (2001) Impaired neuronal plasticity in transgenic mice expressing human apolipoprotein E4 compared to E3 in a model of entorhinal cortex lesion. Neurobiology of Disease 8: p611-25

Williams KR, Pye V, Saunders AM, Roses AD and Armatti PJ (1997) Apolipoprotein E uptake and low-density lipoprotein receptor-related protein expression by the Ntera2/D1 cell line: a cell culture model of relevance for late-onset Alzheimer's disease. Neurobiology of Disease 4: p58-67

Williams KR, Saunders AM, Roses AD and Armatti PJ (1998) Uptake and internalisation of exogenous apolipoprotein E3 by cultured human central nervous system neurons. Neurobiology of Disease 5: p271-9

Willnow TE, Hilpert J, Armstrong SA, Rohlmann A, Hammer RE, Strickland DK and Herz J (1996) Defective forebrain development in mice lacking gp330/ megalin. Proceedings of the National Academy of Sciences 93(16): p8460-4

Willnow TE (1999) The low-density lipoprotein receptor gene family: multiple roles in lipid metabolism. Journal of Molecular Medicine 77: p306-315

Wurtman RJ (1992) Choline metabolism as a basis for the selective vulnerability of cholinergic neurons. Trends in Neuroscience 15: p117-22

Xu PT, Schmechel D, Rothrock-Christian T, Burkhart DS, Qiu HL, Popko B, Sullivan P, Maeda N, Saunders AM, Roses AD and Gilbert JR (1996) Human apolipoprotein E2, E3 and E4 isoform-specific transgenic mice: human-like pattern of glial and neuronal

immunoreactivity in central nervous system not observed in wild-type mice. Neurobiology of Disease 3: p229-45

Xu PT, Gilbert JR, Qiu HL, Rothrock-Christian T, Settles DL, Roses AD and Schmechel DE (1998) Regionally specific neuronal expression of human *APOE* gene in transgenic mice. Neuroscience Letters 246: p65-8

Xu PT, Schmechel D, Qiu HL, Herbstreith M, Rothrock-Christian T, Eyster M, Roses AD and Gilbert JR (1999) Sialyated human apolipoprotein E (apoEs) is preferentially associated with neuron enriched cultures from apoE transgenic mice. Neurobiology of Disease 6: p63-75

Xu PT, Gilbert JR, Qiu HL, Ervin J, Rothrock-Christian TR, Hulette C and Schmechel DE (1999) Specific regional transcription of apolipoprotein E in human brain neurons. The American Journal of Pathology 154: p601-11

Yaffe K, Sawaya G, Lieberburg (1998) Estrogen therapy in postmenopausal women. Effects on cognitive function and dementia. JAMA 279: p688-95

Yamaguchi H, Hirai, Morimatso M, Sholi M and Ihara Y(1988) A variety of cerebral amyloid deposits in the brains of Alzheimer-type dementia demonstrated by β-protein immunostaining. Acta Neuropathologica 76: p541-49

Zarow C and Vitoroff J (1998) Increased apolipoprotein E mRNA in the hippocampus in Alzheimer's disease and in rats after entorhinal cortex lesioning. Experimental Neurology 149: p76-86

Zekraoui L, Lagarde JP, Raisonnier A, Gerard N, Aouizerate A, Lucotte G (1997) High frequency of the apolipoprotein E4 allele in African pygmies and of the African populations in sub-Saharan Africa. Human Biology 69(4): p575-81

Zhang SH, Reddick RL, Peidrahita JA and Maeda N (1992) Spontaneous hypercholesterolaemia and artery lesions in mice lacking apolipoprotein E. Science 258: p468-70

Zheng G, Bachinsky DR, Stamenkovic I, Strickland DK, Brown D, Andres G and McCluskey RT (1994) Organ distribution in rats of two members of the low-density lipoprotein receptor gene family, gp330 and LRP, and the receptor-associated protein. The Journal of Histochemistry and Cytochemistry 42: p531-42

Zlokovic BV (1996) Cerebrovascular transport of Alzheimer's amyloid and apolipopprotein J and E: possible anti-amyloidogenic role of the blood-brain barrier. Life Sciences 59(18): p1483-97

Zuliani G and Hobbs HH (1994) Tetranucleotide length polymorphism 5' of the α2-macroglobulin receptor/ LDL receptor-related protein (LRP) gene. Human Molecular Genetics 3: p215

Publications

Papers

White F, Nicoll JAR and Horsburgh K (2001) Alterations in apoE and apoJ in relation to degeneration and regeneration in a mouse model of entorhinal cortex lesion. Experimental Neurology 169: p307-18

White F, Nicoll JAR, Roses AD and Horsburgh K (2001) Impaired neuronal plasticity in transgenic mice expressing human apolipoprotein E4 compared to E3 in a model of entorhinal cortex lesion. Neurobiology of Disease 8: p611-25

Horsburgh K, McCarron MO, **White F** and Nicoll JAR (2000) The role of apolipoprotein E in Alzheimer's disease, acute brain injury and cerebrovascular disease: evidence of common mechanisms and utility of animal models. Neurobiology of Ageing 21: p245-255

McCulloch (White) F and Breckenridge L (1999) Effects of target tissue on growth of snail neurons in collagen gel culture. Neuroreport 9: p2391-7

White F, Nicoll JAR, Holtzman DM and Horsburgh K. *APOE* genotype influence on long-term neuronal repair processes in *APOE* knockout, ε3 and ε4 transgenic mice (GFAP promoter) after entorhinal cortex lesion. Neurobiology of Disease (in preparation)

White F, Nicoll JAR, Holtzman DM and Horsburgh K. The influence of *APOE* genotype on neuronal plasticity in the aged *APOE* transgenic mouse hippocampus. Neuroscience Letters (in preparation)

Abstracts

White F, Nicoll JAR and Horsburgh K Alterations in apoE and apoJ in relation to synaptic degeneration and regeneration in a mouse model of entorhinal cortex lesion (1999). XIVth International Congress of Neuropathology. Brain Pathology 10(4) C58-09

White F, Nicoll JAR, Roses AD and Horsburgh K (2000) Impaired long-term recovery from brain injury in transgenic mice expressing mice expressing human apolipoprotein E4 compared to E3. Journal of Neurotrauma 17(10) poster J1

White F, Nicoll JAR, Roses AD and Horsburgh K (2000) Impaired neuronal plasticity in transgenic mice expressing human apolipoprotein E4 compared to E3 after entorhinal cortex lesion. Society for Neuroscience 30th annual meeting, poster 665.6

White F, Nicoll JAR, Roses AD and Horsburgh K (2001) Human apolipoprotein E4 mice have an impaired reparative capacity after hippocampal denervation. British Neuroscience Association 16th annual meeting, poster 6.15

Awards

Winner of the Women in Neurotrauma Research award 2001. Awarded at the International Neurotrauma Symposium, New Orleans.

Appendix 1 Staining protocols and perfusion

A1.1 Haematoxylin and Eosin histological staining on paraffin sections

1. Dewax in histoclear (10mins)
2. Absolute alcohol (2mins)
3. Methylated spirit (1min)
4. Wash in water (couple of mins)
5. Hematoxylin (1-10mins depending on section thickness and desired staining intensity)
6. Differentiate in methanol containing 1% HCl
7. Wash in water
8. Scot's tap water substitute (1min)
9. Wash in water
10. Aqueous eosin (3mins)
11. Wash sections thoroughly in water (10-20mins)
12. Dehydrate through a graded series of alcohols (70%, 90% 100%x2)
13. Clear in histoclear (5mins)
14. Mount coverslips with histomount

A1.2 Fink Heimer Silver staining

A. *Potassium permanganate* ($KMNO_4$):- 0.1% in dH2O

B. *Decolourizing solution*:- Mix equal volumes of 1% hydroquinone and 1% oxalic acid. This solution should be prepared immediately before use. This compound is quite unstable.

C. *Uranyl nitrate*:- $UO_2(NO_3)_2 \cdot H_2O$ 0.5% in dH_2O

D. *Silver nitrate*:- $AgNO_3$ 2.5% in dH_2O

E. *Sodium hydroxide*:- NaOH 2.5% in dH_2O

F. *Ammonical silver nitrate solution*:- 20ml silver nitrate solution, 1ml concentrated ammonia (28%), 1.8ml sodium hydroxide

G. *Nauta-Gygax reducer*:- 27ml 10% formalin, 27ml 1% citric acid, 90ml 90% alcohol, 910ml H_2O

H. *Fixing solution*:- sodium thiosulphate ($Na_2S_2O_3.5H_2O$) 0.5% in dH_2O

Staining protocol (Staining Procedures Fourth Edition, Williams and Wilkins)

1. Rinse sections in water
2. Solution A (5-10mins)
3. Rinse in water
4. Decolourize in solution B
5. Rinse thoroughly
6. Solution C(10ml), Solution D(10ml), H_2O(30ml) for 30-60mins
7. SolutionC(15ml), Solution D(35ml) for 30-40mins
8. Rinse thoroughly in water
9. Solution F (1-5mins)
10. Directly to reducer (Solution G) change after 30 secs, total period of 1-2mins
11. Solution H 1min
12. Rinse, dehydrate, clear and coverslip.

Background can be of variable tones of orange/yellow depending on the degree of fixation however the degeneration products always appear strikingly as black punctate neuropil staining.

A1.3 Transcardiac Perfusion of Mouse

Mice were halothane anaesthetised and fixed into a face mask and anaesthesia maintained throughout the procedure. The chest cavity was exposed by 2 incisions into the chest wall and the diaphragm removed to completely expose the heart. A perfusion needle was inserted into the left ventricle and clamped into place. Heparinised saline (10ml) was then administered using a constant infusion pump (3.33ml/min) and the right atria immediately snipped using scissors. 20mls of 4% paraformaldehyde was then delivered using the constant infusion pump. The head was then removed and placed in fixative overnight.

Appendix II Solutions and Sources

ABC	Vector
Anti-mouse IgG HRP	Promega
Anti-goat/sheep HRP	Scottish health board
Ammonium persulphate	Promega
Bovine serum albumin (fracion V)	Sigma
DAB	Vector
ECL	Amersham
Geys balanced salt solution	GIBCO
Glutamax I	GIBCO
Hydrogen peroxide	Sigma
Hydroquinone	Sigma
Ibotenic acid	Sigma
Kaleidoscope molecular weight marker	Bio-Rad
Membrane inserts (0.4μm pore size)	Becton Dickinson
Microtubule associated protein spin-down assay	Cytoskeleton Inc
Microtubule fluorescence motility kit	Cytoskeleton Inc
Minimal essential medium	GIBCO
Normal horse/goat serum	Vector
Oxalic acid	Sigma
PBS	Oxoid
Protogel	National Diagnostics
PVDF membrane	Amersham
SDS	Sigma
SG	Vector
Silver nitrate	Sigma
Streptomycin/ penicillin	GIBCO
TCM serum replacement	ICN Biomedicals
TEMED	Amersham
Tris	Sigma
Uranyl nitrate	TAAB

A1.4 4% Paraformaldehyde

2 litres:-

1. Heat 1800ml of 50mM PB to 65^0C
2. Add 80g of paraformaldehyde to the heated PB in fumehood
3. Make up to 2L with 200ml of PB
4. Filter
5. Store in fridge (use for upto 2 weeks)

A 1.5 Ibotenic acid

Purchased from Sigma in 1mg powder form. This should be diluted at 10mg/ml in PBS (100µl), aliquoted and stored at 4^0C. This compound precipitates once defrosted and therefore should be thawed immediately before commencement of surgery.

A1.6 PCR Analysis

Proteinase K digest mix:- 178µl water, 20µl buffer (Amplitaq Gold PCR 15mM MgCl), 2µl proteinase K (10mg/ml) (final proteinase K concentration 100µg/ml)

Master Mix:-

Analar water	9.025µl
Amplitaq buffer	1.5µl
dNTPs(2mM)	1.5µl
Primer L3(10mm)	0.3µl
Primer R3+(10mm)	0.3µl
DMSO (Di Methyl Sulphoxide)	1.5µl
Amplitaq Gold polymerase	0.075µl
Total	14.2µl

To this master mix 0.8µl of target DNA must be added.

A1.7 Immunohistochemistry

50mM Phosphate buffer(PB) To make 2L: 95ml (A) Sodium dihydrogen ortho posphate ($NaH_2PO_42H_2O$)(24g/L)
405ml (B)Disodium hydrogen orthophosphate (Na_2HPO_4)(28.5g/L)

To make phosphate buffered add 9g NaCl/L to the above mixture

PBS: 50ml of liquid PBS to 1L of distilled water

Bovine Serum Albumin (BSA) 10% BSA Fraction V (Sigma) in PBS

ABC complex: 1 drop of reagent A + 1 drop of reagent B in 5mls PBS

DAB: 2 drops buffer solution + 4 drops of DAB solution + 2 drops of hydrogen peroxide solution in 5mls distilled water

A1.8 Western Blotting

1. *Homogenisation Buffer*:- 25mM Tris-HCl (pH6), 3mM $MgCl_2$, 100mM NaCl
3.0275g + 0.6099g + 5.844g

Made up in 1L of distilled water

2. *Samples*: each tissue sample was weighed and the weight matched in volume of homogenisation buffer. Homogenates were then produced using a hand held homogeniser. The samples were then centrifuged for 15mins and the supernatant removed. Following protein content determination defined amounts of supernatant were diluted in water (X5 volume) and Laemmli buffer added to the final samples such that 40µl of sample contained 10µg of protein.

3. *SDS 10%:* Dissolve 10g of sodium dodecyl sulphate in 100ml of water. Solution should be coulourless. If necessary heat to dissolve.
Ammonium persulphate 10%: Dissolve 0.1g APS in 1ml water immediately before to use.

Buffer 1: 18.15g Tris (1.5M), pH8.8 with HCl, 4ml 10% SDS, 100ml total volume with water

Buffer 2: 6g Tris (0.5M), pH6.8 with HCl, 4ml 10% SDS, 100ml total volume with water.

Running Buffer: 72g glycine, 15g Tris, 50ml 10% SDS (made up to 5L with distilled water and precooled to 4^0C.

Blotting Buffer: 72g glycine, 15g Tris, 1L methanol (made up to 5L with water)

2XTBS: 116.9g NaCl, 40ml 2M Tris (9.68g Tris in 40ml)/HCl pH7.5 made up to 2L with distilled water.

TTBS: 1XTBS + 250µl Tween 20

Laemlli Buffer: 0.1M Tris HCl pH8, 0.1% bromophenol blue, 5M urea, 5%DDT, 5%SDS. Separate into aliquots and store at -20^0C.

Table 10 Gel Preparations

Resolving Gel	12.5%	X2	10%	X2
H_2O	8.6ml	17.2ml	13.2ml	26.4ml
Buffer 1	12ml	24ml	12ml	24ml
Protogel	23ml	26ml	18.4ml	36.8ml
Glycerol 50%	4ml	8ml	4ml	8ml
APS 10%	320µl	640µl	320µl	640µl
Temed	50µl	100µl	50µl	100µl

Stacking Gel	X1	X2
H_2O	8.55ml	17.1ml
Buffer 2	3.75ml	7.5ml
Protogel	2.7ml	5.4ml
APS 10%	150µl	300µl
Temed	20µl	40µl

Temed should be added to the mixture last as this stimulates polymerisation.

A1.9 Organotypic Hippocampal Slice Culture

Medium:- 96% essential medium (containing Hanks salt solution)

0.5% glutamax I supplement

50U/ml streptomycin/penicillin

1% glucose

2% TCM (serum replacement)

Medium should be prepared under sterile conditions in a culture hood. The medium should be stored at 4^0C and should be heated to 37^0C before addition to cultures. Prepared medium should not be used after 7 days.

Geys balanced salt solution (for slides):- This should be chilled before used but stored at 4^0C.

Appendix III

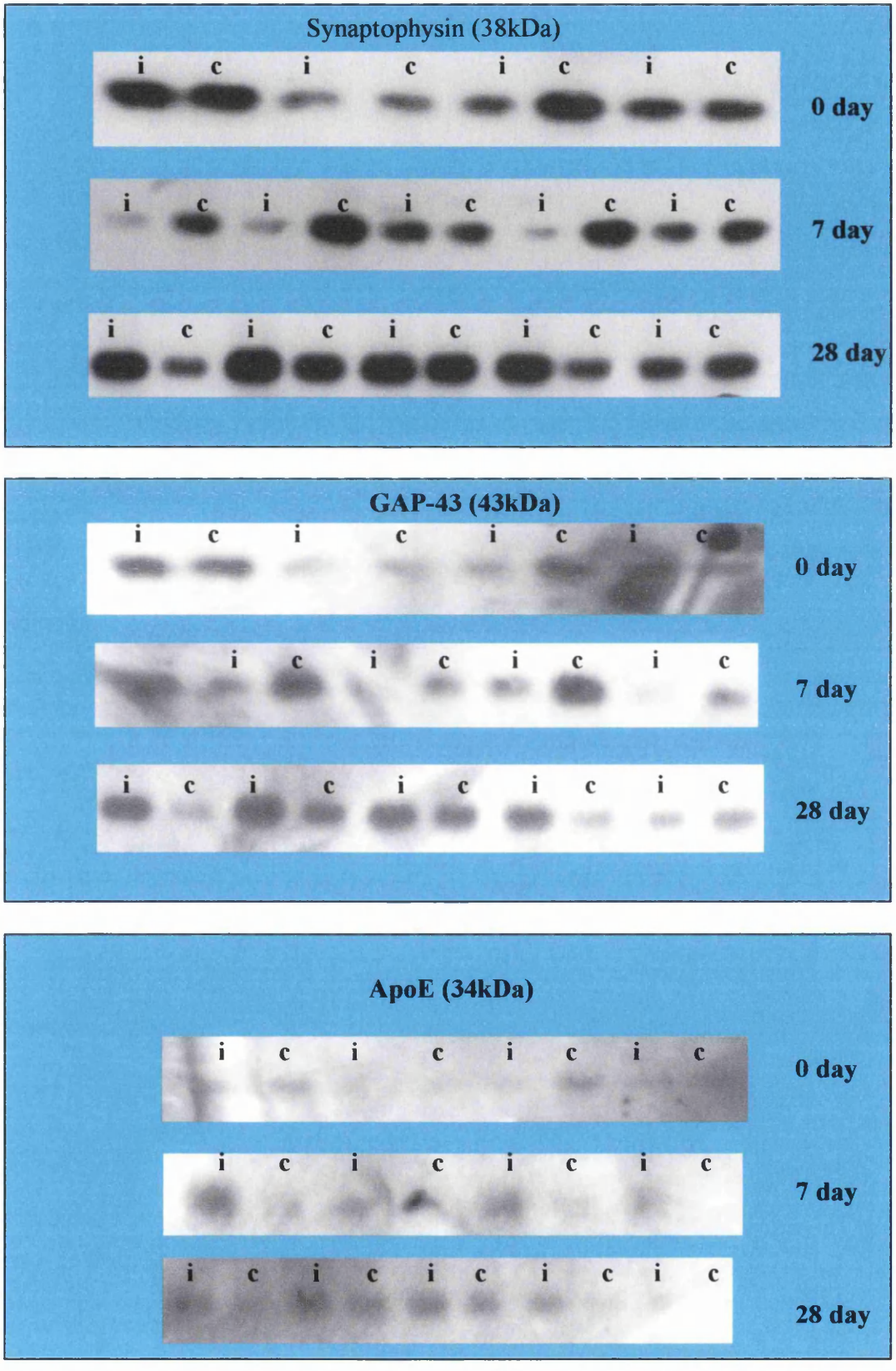

Figure A3.1 Western blotting bands from the hippocampus of C57 BL/6J mice at day 0, 7 and 28 post-ECL. The blots were incubated with antibodies to synaptophysin, GAP-43 and apoE. i- ipsilateral, c- contralateral

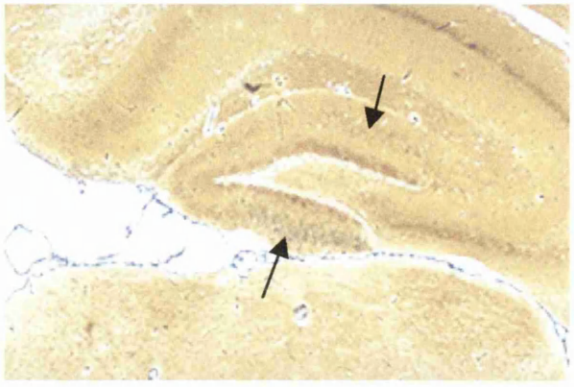

Figure A3.2 **Silver staining in a 3 day control section**

Illustrative example of the presence of silver labelled degeneration products in the molecular layers of the dentate gyrus. This section was run in parallel with sections from chapter VI to ensure the accuracy of staining since no 3 day timepoint was included in that study.

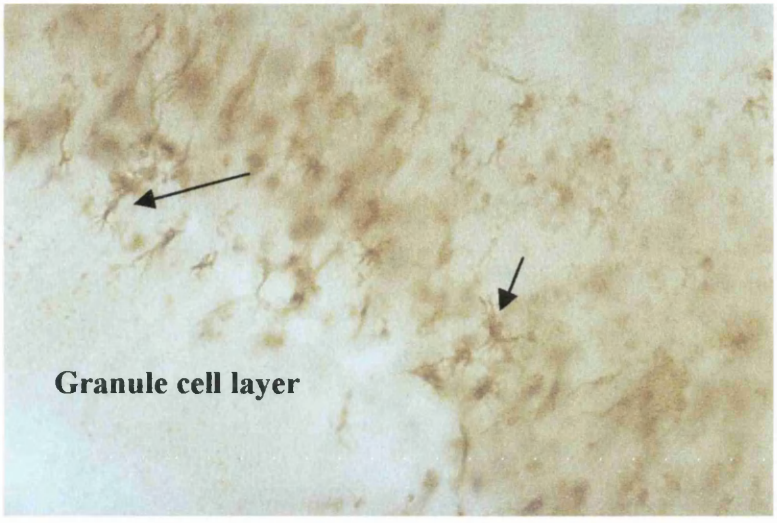

Figure A3.3 **Astrocyte proliferation in the molecular layers of the hippocampal dentate gyrus post-culture**

Illustrative example of astrocyte proliferation post-culture in hippocampal slices. The molecular layers are densely populated with reactive astrocytes by day 7 *in vitro*. x200 magnification

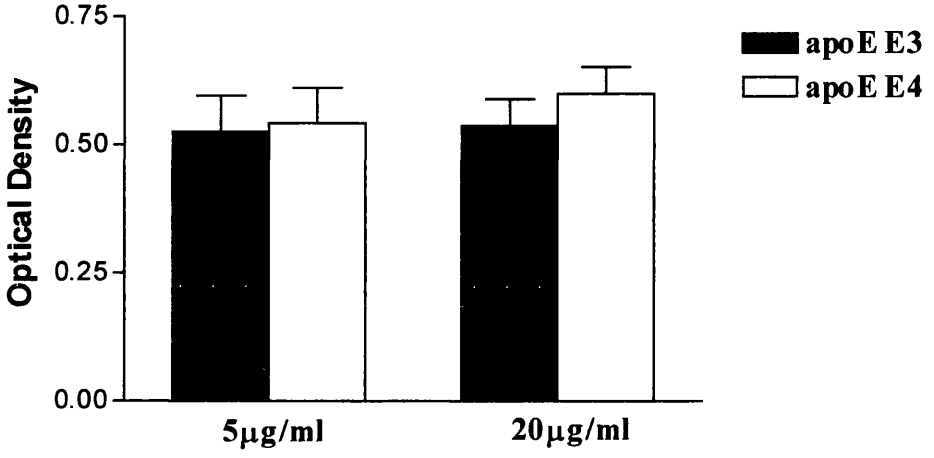

Figure A3.4 Graph illustrating tubulin levels in each reaction

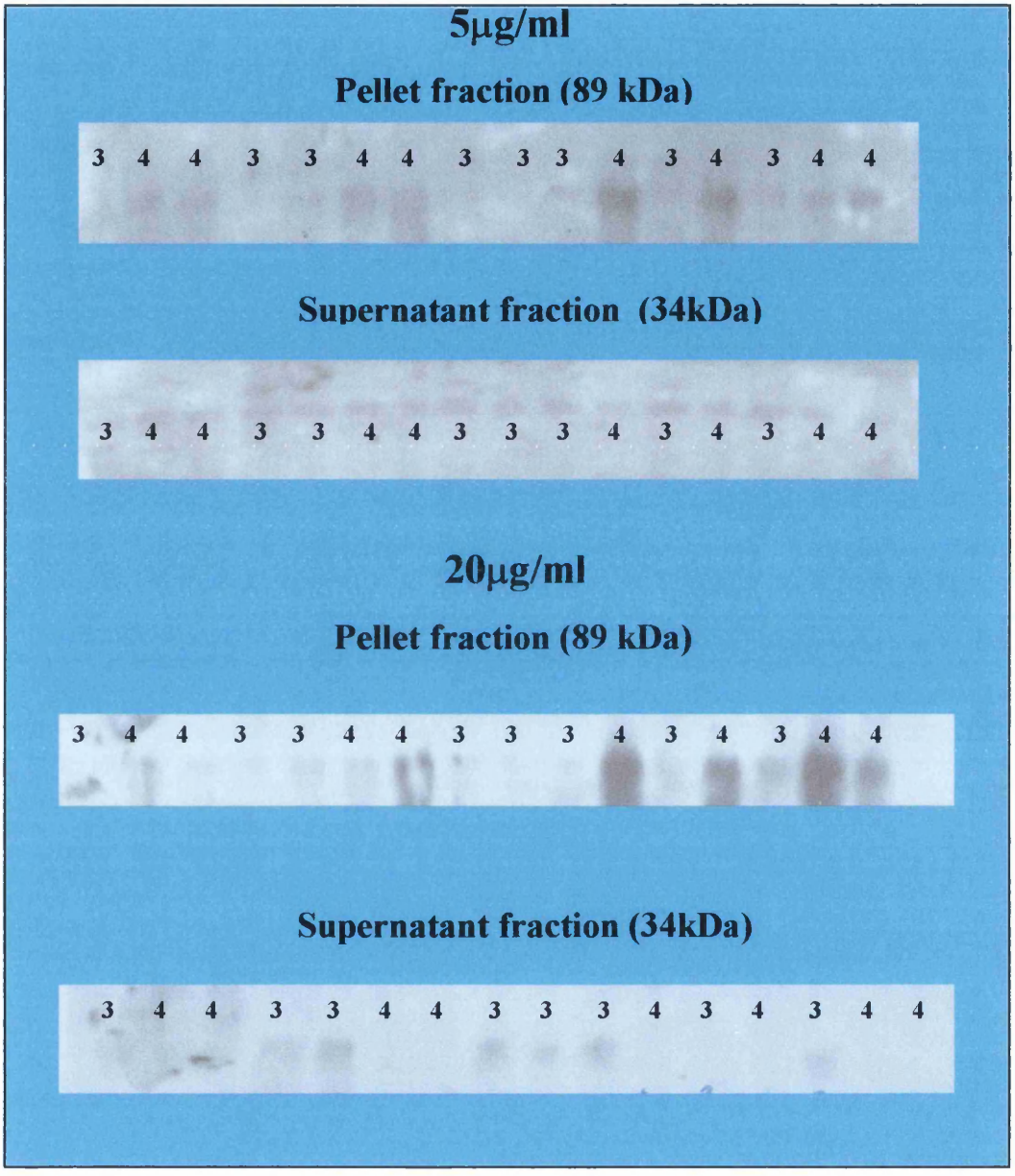

Figure A3.5 **Microtubule binding of apoE E3 and E4 at apoE concentrations of 5µg/ml and 20 µg/ml**

Illustrative examples of apoE immunoblotting. At both concentrations apoE E4 was found to be greater in the pellet fraction. In the pellet fraction the apoE is microtubule bound and is present in a band at approximately 89kDa (apoE 34kDa + tubulin 55kDa). In the pellet fraction apoE E3 was found to greater compared to apoE E4.